# Arylation Reactions Using Diaryliodonium Salts


**Zhengguang Xiao**

Doctor of Philosophy

School of Natural and Environmental Sciences

Newcastle University

June 2020

**Acknowledgments**

I would like to acknowledge foremost my supervisor Dr Michael A. Carroll for his invaluable guidance, support and encouragement during this research, and patient modifications for my report. I would also like to thank all the people in the same research group. I would like to thank my family who funded me and supported me to finish my PhD degree.

I would also like to thank Dr Corinne Y. Wills for NMR spectroscopy, Dr Paul G. Waddell for their help with X-ray crystallography, Dr Elizabeth Gibson for the help of DSC-TGA, Dr Emma Richards for the EPR and Dr Agnieszka Bronowska for guiding me through the computational calculations.

Finally I would thank my friends for their relentless love and support.

**Abstract**

Diaryliodonium salts have been widely used in organic chemistry, in particular as oxidizing agents and more recently as arylation reagents. The work presented in this thesis considers both the metal-free and copper catalysed processes for *N*-, *O*-arylation and fluorination using diaryliodonium salts, in particular how the control and selectivity of the transformation is influenced by the nature of various substitution patterns and typical reaction conditions.

During this study, a range of diaryliodonium salts with different substituent patterns and counter-ions have been synthesized in order to determine their chemical and physical properties and the resultant selectivity of the arylation process as this variation of functionality allows exploration of the impact of both steric and electronic factors. A novel diaryliodonium copper complex was discovered. By using DSC-TGA analysis, the thermal decomposition of different diaryliodonium salts has been determined. Some decompose rather than melt at these temperatures suggesting limits on the temperatures that may be employed in their subsequent reactions. This study has also shown that when the arylation reaction is conducted metal-free (i.e. without a catalyst), the selectivity of fluorination and both *N*- and *O*-arylation is mostly determined by the electronic nature of the relevant groups (the most electron-deficient arene is transferred) whereas when the reaction was conducted in the presence of a copper catalyst, the selectivity was mostly influenced by extreme steric factors (the least hindered arene was transferred) although electronic control was still evident but to a lesser extent. According to introducing a fluorous target into diaryliodonium salts and using F-SPE method, product and by-products could be easily separated.

In summary, it was found that:

- A range of diaryliodonium salts could be readily prepared using a range of synthetic methods.
- The thermal stability of diaryliodonium salts was affected by the choice of counter-ion.
- When the reaction was conducted under copper catalysis good selectivity (transfer of the

least hindered arene) could be achieved for fluorination and both *N*- and *O*-arylation reactions

- A novel diaryliodonium copper complex was discovered having a unique iodine (III) copper interaction.
- A range of fluorous diaryliodonium salts have been prepared and in association with F-SPE enabled rapid separation of the desired arylated product from the arene by-products and any unreacted diaryliodonium salt.

## Abbrebiations

| | |
|---|---|
| **Ac** | Acetyl |
| **ASAP** | Atmospheric Solids Analysis Probe |
| **ACCN** | 1,1′-Azobis(cyclohexanecarbonitrile) |
| **°C** | Degrees Celsius |
| **CCDC** | Cambridge Crystallographic Data Centre |
| **DBU** | 1,8-Diazabicyclo[5.4.0]-undec-7-ene |
| **DCM** | Dichloromethane |
| **DFT** | Density functional theory |
| **DMF** | *N,N*-dimethylformamide |
| **DMP** | Dess–Martin periodinane |
| **DMSO** | Dimethyl sulfoxide |
| **DSC** | Differential scanning calorimetry |
| **Eq.** | Equivalents |
| **EPR** | Electron Paramagnetic Resonance |
| **EDG** | Electron-donating groups |
| **EWG** | Electron-withdrawing groups |
| **Et** | Ethyl |
| **ESI** | Electrospray ionization |
| **F-SPE** | Fluorous Solid-Phase Extraction |
| **FTIR** | Fourier Transform Infra-Red |
| **GC** | Gas chromatograph |
| **HPLC** | High Pressure Liquid Chromatography |
| **Hz** | Hertz |
| **IBX** | 2-Iodoxybenzoic acid |
| **IUPAC** | International Union of Pure and Applied Chemistry |
| ***J*** | Coupling constant |

| | |
|---|---|
| **$K_{222}$** | Kryptofix 222® |
| ***m*-CPBA** | *Meta*-chloroperoxybenzoic acid |
| **mmol** | Millimole |
| **mL** | Millilitre |
| **NSI** | Nanospray ionization |
| **NMR** | Nuclear magnetic resonance |
| **Nu** | Nucleophile |
| ***o-*** | *Ortho-* |
| ***p-*** | *Para-* |
| **PTFE** | Polytetrafluoroethylene |
| **PET** | Positron Emission Tomography |
| **ppm** | Parts per million |
| **SPE** | Solid phase extraction |
| **TFA** | Trifluoroacetic acid/ Trifluoroacetate |
| **TEGOH** | Triethylene glycol monomethyl ether |
| **TfOH** | Trifluoromethanesulfonic acid |
| **TsO** | Tosylate |
| **THF** | Tetrahydrofuran |
| **TEMPO** | (2,2,6,6-Tetramethylpiperidin-1-yl)oxyl radical |
| **TGA** | Thermogravimetric analysis |

# Table of Contents

# Chapter 1. Introduction

## 1.1 Hypervalent Iodine

Generally, the valency of iodine is -1 which is the same as the other halogens (F, Cl, Br). Since the atomic radius and the polarizability of iodine are relatively large, it is capable of forming stable high-valency compounds. Since 1886, Willgerodt reported the first high valency organic iodine (III) compound dichloroiodobenzene ($PhICl_2$)[1] was synthesized from iodobenzene and chlorine gas, it reacted with ethanol to give acetic acid and hydrochloride. Then Willgerodt used iodosobenzene **8** (Figure 4) under acid conditions to afford iodobenzene diacetate.[2] Subsequently, Hartmann and Meyer have synthesized the iodine (V) compound 2-iodoxybenzoic acid (IBX)[3] **7** (Figure 4) and the iodine (III) reagents diaryliodonium salts.[4] Hypervalent molecules are defined as having one or more atoms containing more than eight electrons in the valence shell. Usually the atoms are from the group 15-18 of the Periodic Table.[5]

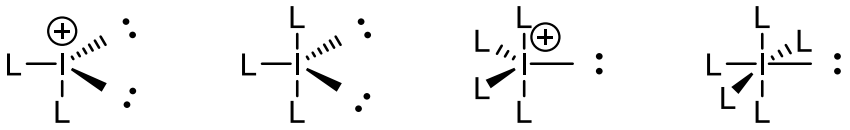


**Figure 1. Structure of hypervalent iodine compounds**

Using the Martin-Arduengo N-X-L (number of valence electrons-centre atom-number of ligands) designation, the electrons (N) surrounding iodine and the ligands (L) suggest iodine is hypervalent (Figure 1).[6] There are different hypervalent iodine states, according to IUPAC, iodine (III) compounds are also named $\lambda^3$-iodanes (**1, 2**) and iodine (V) compounds are named $\lambda^5$-iodanes (**3, 4**). Structure **2** is the most common example of a hypervalent iodine (III) compound, it has a T-shaped molecular structure with respect to the L groups and is often

referred to as a pseudotrigonal bipyramid structure with respect to electrons, with the iodine atom at the centre, one ligand and two lone pairs of electrons evenly distributed in the plane and two ligands which are perpendicular to this plane.

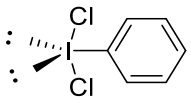


**5**

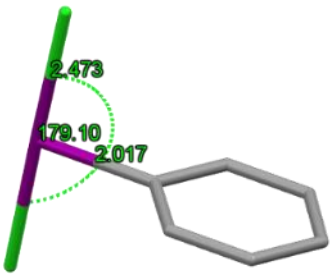


**Cl-I-C = 89.55°**

**Cl-I-Cl = 179.10°**

**I-Cl = 2.473 Å**

**I-C = 2.017 Å**

**Figure 2. X-ray Diffraction structure of dichloroiodobenzene 5**[7]

In 1953 the crystal structure of dichloroiodobenzene **5** was determined[7] and it was found that the angle between the two chlorines is 179.10 ° which may be considered a slight distortion of the T-shape. This might be because the lone pairs of the hypervalent iodine atom make the electron density close to the iodine than the bonding pairs of electrons and thus push the two counterions forward (Figure 2). The linear L-I-L is a 3c-4e (three-centre four-electron)[8] bond which is not as strong a bond when compared to a covalent bond. In 2019, a calculation based on the $\lambda_3$-iodanes showed that the energy of the 2c–2e F-I bonds are shorter and stronger than 3c–4e F-I bonds ($IF_3$, $PhIF_2$). The linear Cl-I bond distance in the crystal structure of dichloroiodobenzene **5** is 2.473 Å and the I-C bond is 2.017 Å.

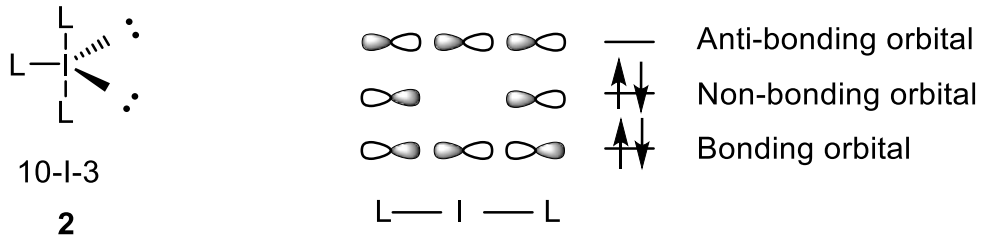


**Figure 3. Three-centre-four-electron bond model**

The 3c-4e (three-centre four-electron) bond model is shown in Figure 3 with the iodine atom at its centre and three ligands surrounding the iodine atom. Three bonding orbitals are formed from three atomic orbitals: the iodine atom filled 5p orbital with the ligands providing two unpaired electrons. Overall two electrons occupy the bonding orbital and two electrons occupy the non-bonding orbital, which the node at the iodine centre, hence the iodine has the positive charge.[8]

Hypervalent iodine (V) compounds such as 2-iodoxybenzoicacid (IBX) **7**[1] and Dess–Martin periodinane (DMP) **6**[9, 10] and iodylbenzene **8**[11] are often used in oxidation reactions in organic synthesis.

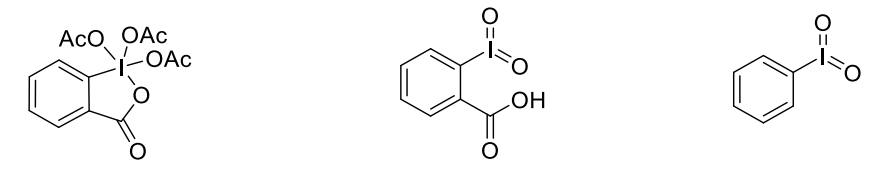


**Figure 4. Samples of iodine (V) organic compounds**

These compounds oxidise 1,2-diols to α-ketols or α-diketones,[12] primary alcohols to aldehydes, and secondary alcohols to ketones in good yields.[9, 10]

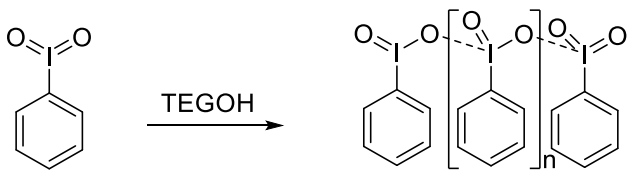


8 9

**Scheme 1. Synthesis of $PhIO_2$ nanoparticles**

Recently, iodylbenzenes (**8**) have also found application as nanostructure synthesis reagents when in the presence of triethylene glycol monomethyl ether (TEGOH) and generated the $PhIO_2$ nanoparticles **9**.[13, 14]

However, to synthesize iodine (V) compounds, a strong oxidant such as periodate, hypochlorite, dimethyl dioxirane, oxone or dioxygen is usually used.[15-17] And because of iodylalkanes are extremely unstable and can exist only at very low temperatures,[18] iodine (V) compounds still have not found widespread use in organic synthesis beyond their use as selective oxidizing agents.

Generally, iodine (III) organic compounds are more stable than iodine (V) compounds except iodosobenzene **7**. Iodine (III) compounds are generally divided into two types: $RIL_2$ and $R_2IL$, because of the weak bond between the iodine (III) centre and the R/L groups there is a weak electrophilic centre at the iodine atom. These compounds are widely used in reactions with nucleophiles (such as nitrogen, oxygen and halides).[19-21]

### *1.1.1 $RIL_2$-Type*

In the $RIL_2$-type, the structure is also T-shaped, where the iodine atom in the centre and the two ligands share a 3c-4e bond which are weaker and longer than the R-I bond and the ligands may be easily exchanged.

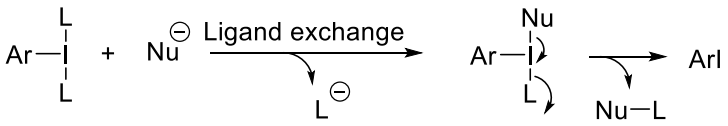


**Scheme 2. Reaction of $RIL_2$-type with nucleophiles**

Usually in $RIL_2$-type hypervalent iodine, R is an aromatic ring, and with two halide ligands or acetoxy ligands. In the reaction of $ArIL_2$-type hypervalent iodine compounds, the nucleophile and one ligand are exchanged, followed by ArI (iodine (I)) and NuL generation (Scheme 2).

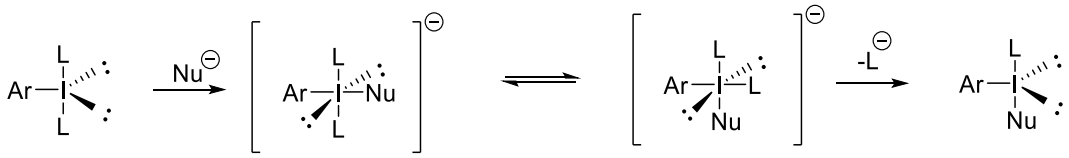


Associative pathway

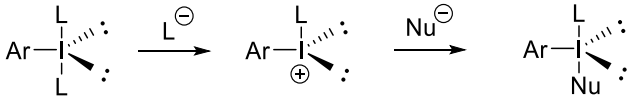


Dissociative pathway

**Scheme 3. Associative and dissociative pathway of $ArIL_2$-type**

There are two main mechanistic pathways to explain this typical ligand exchange reaction: an associative pathway[22] and a dissociative pathway (Scheme 3).[23] In the associative pathway, the nucleophile is added to the central iodine atom of the $\lambda^3$-iodane forming a planar quadrangular with respect to the ligands. The intermediate could exchange the ligands and nucleophile to generate a *cis* planar quadrangular via Berry pseudorotation. Then one of the ligands leaves the intermediate and forms ArINuL.

In the dissociative pathway, one of the ligands leaves first to form an iodonium ion, with which the nucleophile reacts with and generates ArINuL. This general process occurs widely and in a range of different reactions such as carbon-carbon bond forming reactions,[24] nucleophilic

substitution of alkyl iodides via oxidative ligand transfer,[25] halogenation (such as chloride as ligand in $RIL_2$-type reagents) of aromatic compounds[26] and addition of a ligand to double bonds.[27, 28] For example, $RIL_2$-type $\lambda^3$-iodane reagents also provide selective syn diacetoxylations of alkenes in the presence of water (Scheme 4).[29]

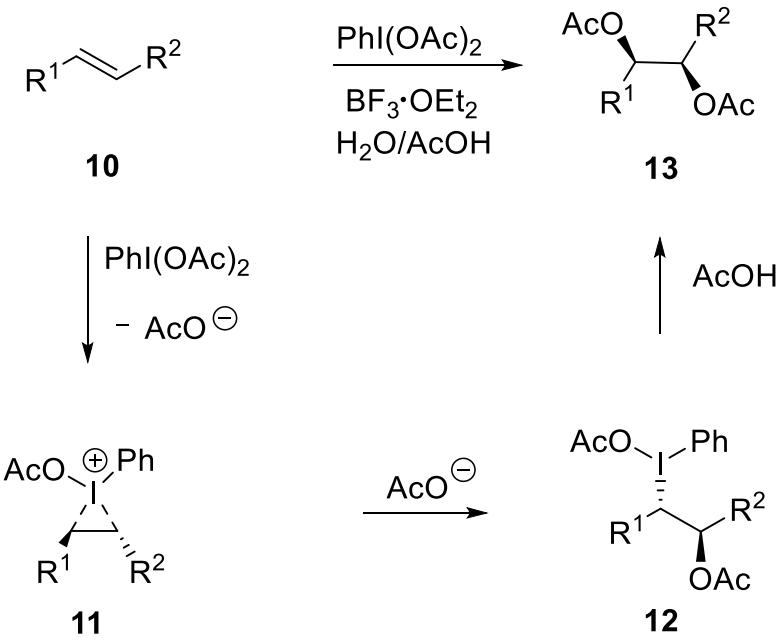


**Scheme 4. Proposed mechanism for oxidiation of alkenes**

Diacetoxyiodobenzene (PIDA) is the most widespread reagent of the $RIL_2$-type and was first synthesised by Willgerodt in 1892[30] from iodobenzene, acetic acid and peracetic acid. PIDA is used as a mild oxidising agent in a wide range of different kinds of organic reaction especially in the oxidiation of alkenes.[29, 31] As shown in Scheme 4, for this reaction $BF_3 \cdot OEt_2$/AcOH system is a strong Brønsted acid catalyst used to activate the PIDA, with the weak hypervalent bond between the acetate ligand and the iodine atom. The iodine atom is an electrophilic centre and reacts with the double bond to form a cyclic iodonium intermediate **11**, followed by acetate promoted ring opening using a $S_N2$ mechanism and thus generating compound **12**. A further $S_N2$ reaction displaces the iodine fragment (as PhI and $AcO^{\ominus}$) to give 1,2-diacetoxy species **13**.

### *1.1.2 $R_2$IL-Type*

Diaryliodonium salts have been considered as versatile reagents in organic synthesis because they are non-toxic and tolerate mild reaction conditions, thus diaryliodonium salts are the most widely used reagents of the $R_2$IL-type.

Diaryliodonium salts are now an important part of hypervalent iodine chemistry, but surprisingly did not attract much attention after their initial synthesis. In 1953, Beringer, *et al*.,[32] on the basis of previous work, reported the nucleophilic substitution reaction of diaryliodonium salts with organic and inorganic bases, and found diaryliodonium salts could react with carbon, oxygen, sulfur, nitrogen, phosphorus, selenium, arsenic, antimony and halogen-based nucleophiles generating arylation products.

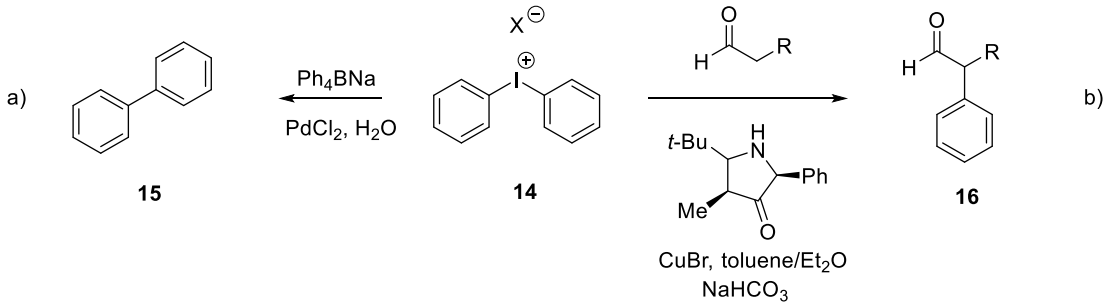


**Scheme 5 The coupling reaction and the arylation of the α-position of carbonyl groups using diaryliodonium salts**

In this regard, diaryliodonium salts were expected to become universal arylation reagents, later studies confirmed the Beringer forecast. Diaryliodonium salts have also been widely used in coupling reactions (Scheme 5a)[33] and as reagents for the arylation of the α-position of carbonyl groups (Scheme 5b).[34]

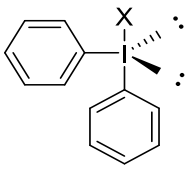

14

**Figure 5. Structure of a diaryliodonium salt**

X-ray single crystal diffraction studies show, diaryliodonium salts are not ionic salts, but have a T-shaped molecular structure (Figure 5) which is similar like $RIL_2$-type.[35] From the three-dimensional view it is a pseudotrigonal bipyramid structure with respect to the electrons with the iodine atom at the centre, an aryl group, and two lone pairs of electrons evenly distributed in the plane and two ligands which are perpendicular to this plane. The diaryliodonium salt structure in solution is still controversial[36], as it is affected by the counter anion ($X^{\ominus}$), the solvent and the nature of the aromatic rings.

Usually in the reaction of diaryliodonium salts, the iodine atom is a weak electrophilic centre, which can react with a nucleophile as shown in Scheme 6(a). In addition, diaryliodonium salts can arylate transition metals to generate highly electrophilic metal arylates. Metal arylate cross-coupling reactions can thus occur and react subsequently with nucleophiles as shown in Scheme 6(b).

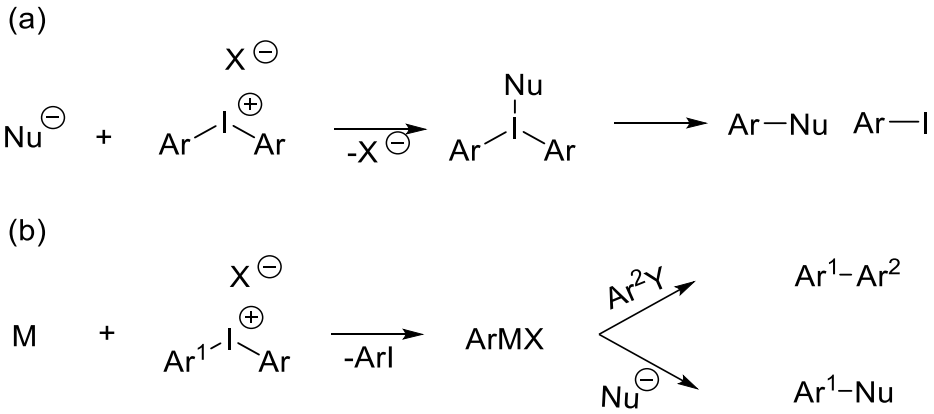


**Scheme 6. The typical reaction of diaryliodonium salts**

As stated, the solubility and reactivity of the diaryliodonium salts are affected by the anion ligands ($X^{\ominus}$). When the anion is halide, the diaryliodonium salt is poorly soluble in most organic solvents. In addition, because the halogen ions are weakly nucleophilic, it may lead to some side reactions such as the generation of ArX. In many applications, researchers choose the trifluoromethanesulfonate anion, tetrafluoroborate anion, trifluoroacetate anion or other non-nucleophilic anions to address this issue.[37]

## 1.2 Synthesis of Diaryliodonium Salts

Since diaryliodonium salts were synthesized for the first time, many subsequent preparation methods have been developed. The distinction between the different approaches is the use of different oxidizing agents, acids and metal reagents and whether intermediates are isolated or not.[38] Preparation of diaryliodonium salts generally takes two to three steps: the first step is the preparation of a trivalent iodine intermediate, which can be synthesised by oxidizing an aryl iodide, the second step depending on the reaction mechanism, can be roughly divided into two approaches: with electron-rich aromatic systems undergoing direct electrophilic aromatic substitution reactions, Scheme 7(a), and an aryl-metal reagent in the metal-iodine exchange reaction, Scheme 7(b). The diaryliodonium salts may also need an anion exchange reaction step, in order to obtain a specific ligand anion.

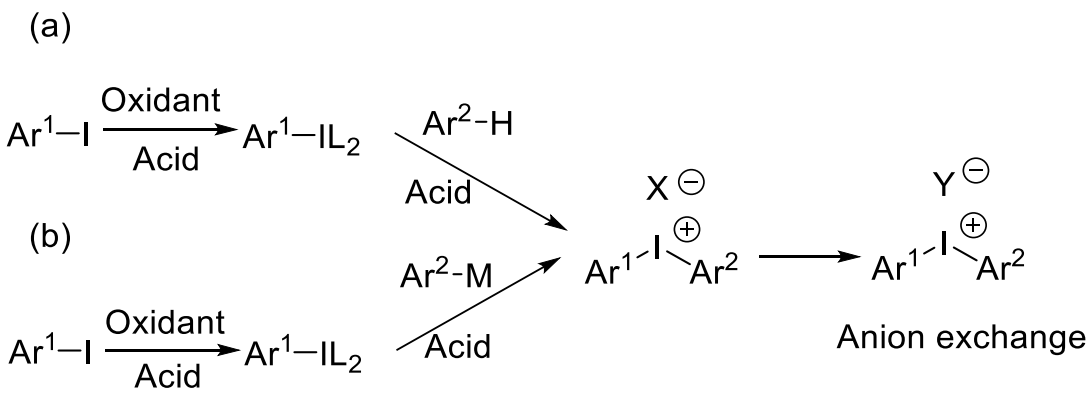


**Scheme 7. The typical synthetic route to diaryliodonium salts**

At present, a widely used method is from the Olofsson group[39,40] and is a "one-pot" synthesis: aromatic **18** and aromatic iodide **17** are mixed at room temperature, in the presence of trifluoromethanesulfonic acid with *m*-CPBA as oxidant, the reaction can be complete within a few hours. This method has a good adaptability to the substrate, mild reaction conditions, high yield, and post-processing is simple. If this method is used to synthesis symmetrical diaryliodonium salts ($R^1$=$R^2$), it can directly use aromatics as raw materials and inject iodine directly which would also make the C-I bond.

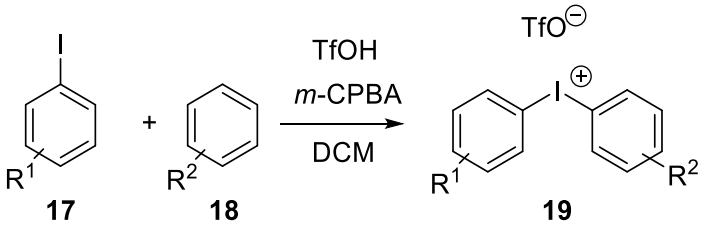


**Scheme 8. One-pot synthetic route of diaryliodonium salts**

The method was developed for making diaryliodonium triflates, the reaction occurs at room temperature in 10 min, results in a high yield and can be applied to various substitution patterns (38 examples, 54% to 94% yield).[39]

However, there are significant limitations to the above-described method for selective preparation of diaryliodonium salts, which is when the aromatic hydrocarbon group has substituents present which may affect the outcome of the reaction. As the reaction is an electrophilic aromatic substitution, electron-donating groups (EDG) on the arene lacking iodine benefit the reaction, but these electron-donating groups may direct to specific positions which may not be the wanted one and also the separation of these different diaryliodonium salts from a mixture can be difficult. Electron-withdrawing groups (EWG) also direct substitution, but because of low reactivity, the reaction is less likely to proceed (Scheme 9).

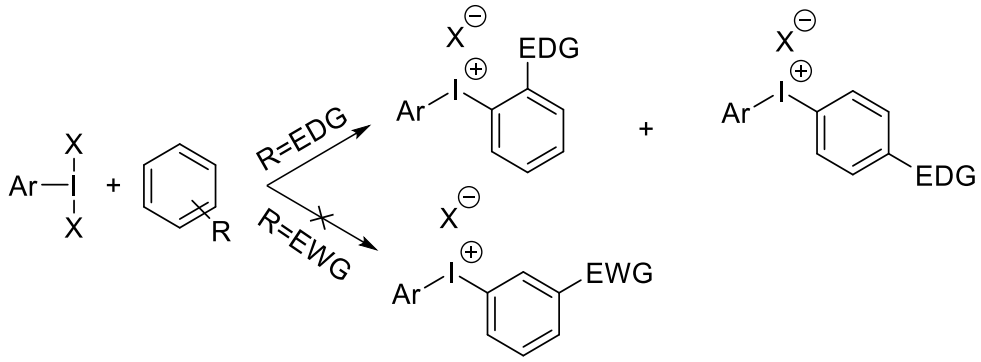


**Scheme 9. Formation of diaryliodonium salts**

Koser *et al.*,[41] using an aryl silane and [hydroxy(tosyloxy)iodo]benzene first realized the regiospecific synthesis of diaryliodonium salts (Scheme 10).

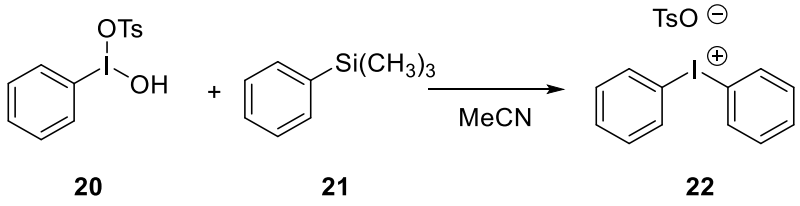


**Scheme 10. Synthesis of diaryliodonium tosylate by Koser's reagent**

Then it was showed that aryltributylstannanes[42] and arylboronic acids[43] could achieve a similar transformation. Then various methods were used for diaryliodonium salts, trifluoromethanesulfonic acid (TfOH) and trifluoroacetic acid (TFA) were both widely used, because they give non-nucleophilic counter-ions and they provide good solubility in organic

solvents. Kitamural, *et al.*, developed the method, in which diaryliodonium triflates were synthesized from diacetoxyiodobenzene and TfOH.[44] This method provides the diaryliodonium salts in a good yield, and it tends to give *para* selectivity, when the arenes with EDG, which is useful if the reactant would generate both *para*- and *ortho*-substituted compounds.

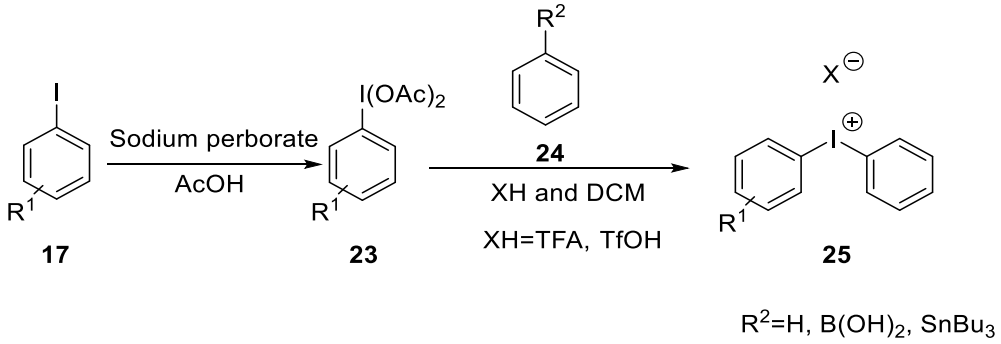


**Scheme 11. Synthesis pathway of diaryliodonium salts using sodium perborate**

This method was then adapted by McKillop[45] and developed by Pike and Widdowson,[46] who oxidized the iodobenzene using sodium perborate, which is a solid compound with exceptional storage stability and no shock sensitivity,[47, 48] to generate **23** which was then reacted with another arene on the presence of TFA (Scheme 11).

Recently, more methods for the one-pot syntheses of diaryliodonium salts have been developed.

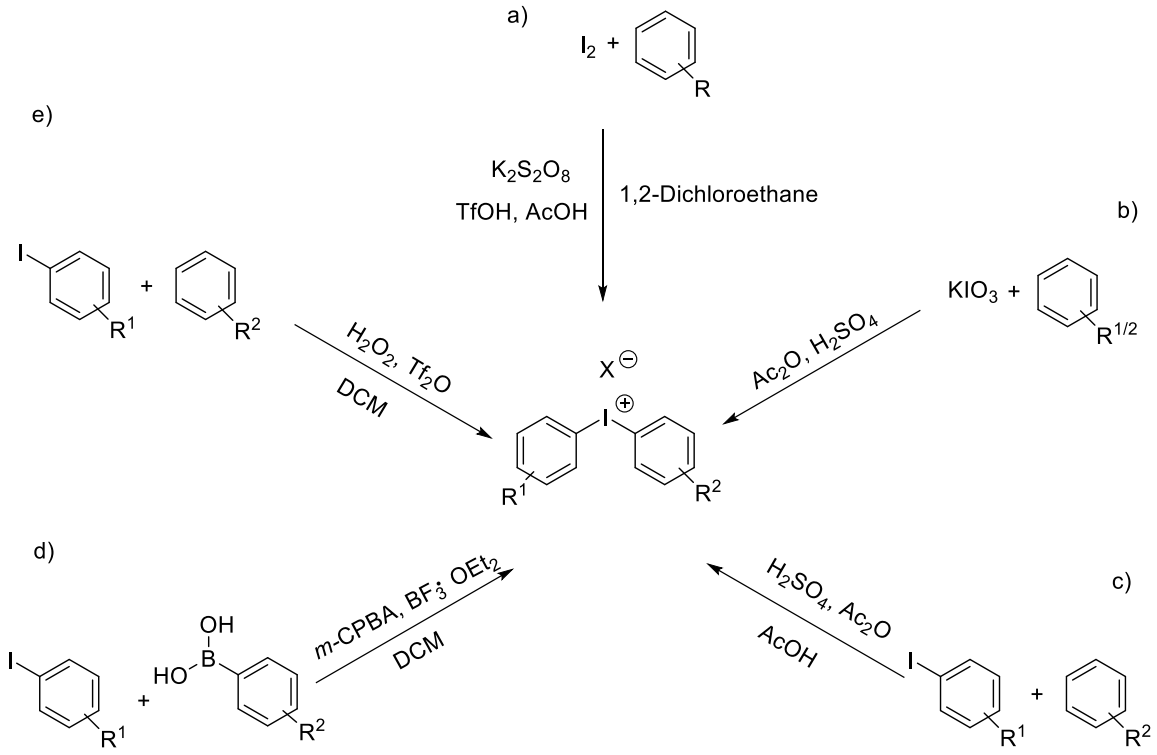


**Scheme 12. One-pot synthesis of diaryliodonium salts.[40, 49-52]**

The yields from these methods all provided the product in a good yield on a small scale, however, these methods generated lower yields and faced some problems on a larger scale and some of them such as the methods given in Scheme 12 a)[50] and b)[51], only result in symmetrical diaryliodonium salts.

### 1.3 Nucleophilic Substitution of Diaryliodonium Salts

Because of their unique reactivity, diaryliodonium salts have been widely used in arylation, such as transition metal-catalysed, metal-free C-H bond arylation, and arylation of heteroatom nucleophiles, especially in areas such as the production of *N*- and *O*-arylated products. In the 1950s, Beringer reported the synthesis[32] and reactivity of diaryliodonium salts with a range of nucleophiles such as phenoxides, sulfonamides, amines, hydroxides in refluxing solvents.[53-55] In the 1970s, McEwen reported other nucleophiles including nitrite, aliphatic alcohols and

thiocyanate as substrates for arylations by diaryliodonium salts.[56-59]

Due to diaryliodonium salts being electron-deficient and iodobenzene in the diaryliodonium salts being a good leaving group which is ~$10^6$ times better than triflate and ~$10^{17}$ times better than dimethylsulfide as a leaving group (Table 1),[60] even in the absence of transition metal catalyst, they can be effectively used as reagents in arylation reactions.

**Table 1. Leaving group relative leaving ability**

| **Nucleofuge** | **Relative leaving ability (vs $TfO^{\ominus}$)** | **Relative leaving ability (vs $Me_2S^{\oplus}$)** |
|---|---|---|
| $PhI^{\oplus}$ | $8 \times 10^5$ | $5 \times 10^{17}$ |
| $TfO^{\ominus}$ | 1 | $6 \times 10^{11}$ |
| $TsO^{\ominus}$ | $1.2 \times 10^{-6}$ | $5 \times 10^{17}$ |
| $Me_2S^{\oplus}$ | $1.6 \times 10^{-12}$ | 1 |

It is widely believed the reaction between diaryliodonium salts and nucleophiles, under metal-free conditions, gives via a trigonal bipyramidal intermediates (Scheme 13, **26** and **27**). [61]

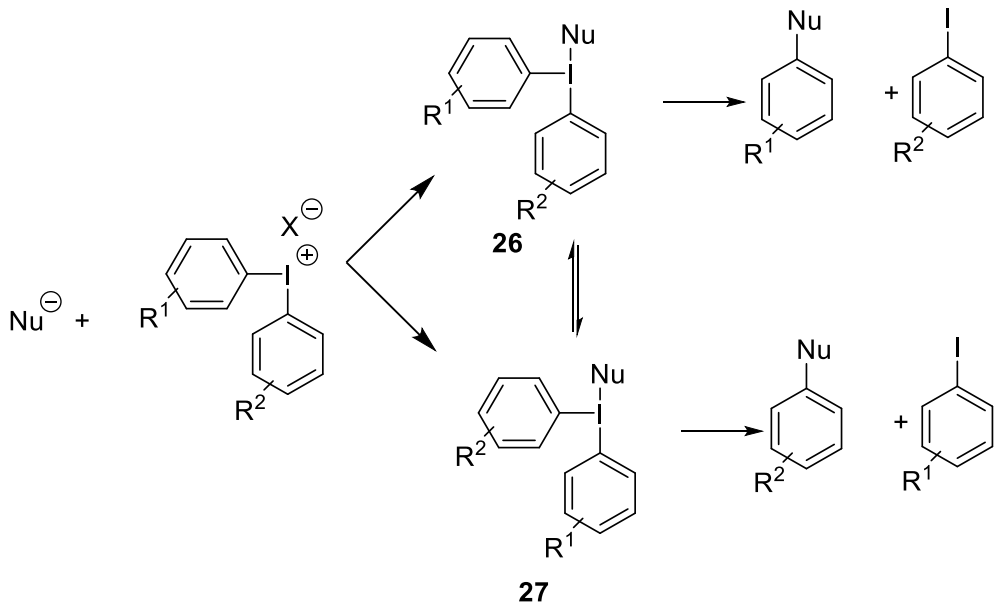


**Scheme 13. Metal-free arylation of nucleophiles**

While some researchers also discuss the probable mechanism, Yu *et al.*[62] used the method, without a metal catalyst, to achieve a diaryliodonium salt and nitrogen-containing heterocyclic arylation coupling reaction, the reaction can be carried out simply under alkaline conditions. They conducted a preliminary study of the reaction mechanism, after the free radical inhibitor TEMPO was added, the reaction hardly proceeds, indicating that the reaction is probably a radical nucleophilic substitution reaction, rather than the usual two-electron process of nucleophilic substitution.

Due to diaryliodonium salts having two aromatic rings which can both react with nucleophiles, the product is often generated as part of a mixture and therefore it may be hard to separate the various compounds as they have similar properties. Therefore, the way to improve the chemical selectivity of this process is important with Carroll and Wood,[63] Malmgren,[61] and Gonda and Novak[64] investigating ways of controlling the outcome.

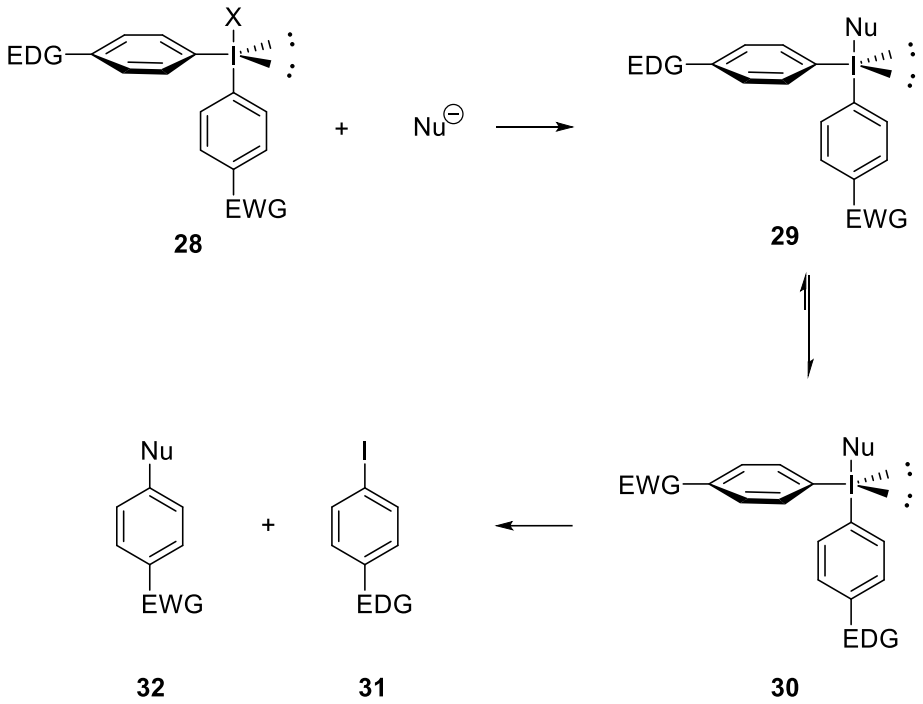


**Scheme 14. Electronic effect in the nucleophilic substitution of diaryliodonium salts**

Under metal-free conditions, the nucleophiles replace the ligand/anion from the diaryliodonium salt generating T-shape intermediates, these have two possible conformers **28** and **29** which may interconvert by Berry *pseudo*-rotation, then the nucleophiles tend to react with the more electron-deficient group, this is considered the electronic effect. Due to the 3c-4e bond, the most electron-rich group prefers the *pseudo* axial position meaning the nucleophile is adjacent to the most electron-deficient ring and hence reacts preferentially with this ring (Scheme 14).

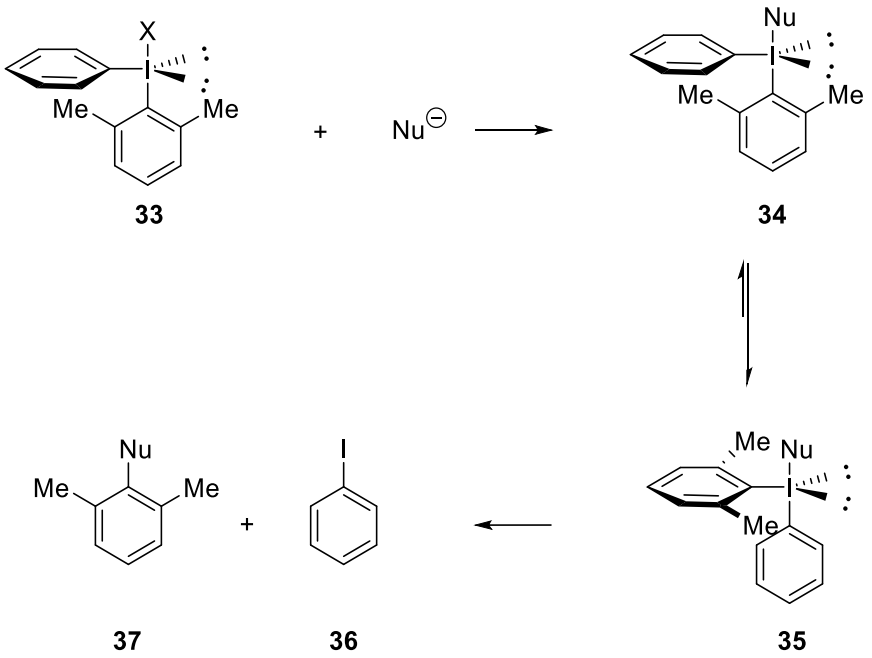


**Scheme 15. Steric effects in the nucleophilic substitution of diaryliodonium salts**

Meanwhile the steric effects on the outcome of the reaction (often called the '*ortho*-effect') also plays an important part, if the aromatic ring has one or two substituent groups, such as methyl groups, in the *ortho* position, e.g. **33**, nucleophiles prefer to react with the arene with the *ortho* substitutions. This is because when the arene with increased steric hindrance occupies the apical position (intermediate **34**), the bulky groups are more crowded, thus this arene prefers to occupy the equational position in the trigonal bipyramidal structure to form the intermediate **35**.[65] Both electronic and steric effects influence the selectivity of the reactions of diaryliodonium salts.

Under metal-free conditions, the electronic effect is much more important unless both *ortho*-positions are occupied by very large groups (Scheme 15).

However, when the reaction is in the presence of a metal catalyst such as copper, the steric effect becomes the most important factor in determining the selectivity of diaryliodonium salts reactions.

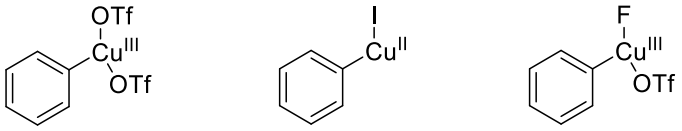


**38** **39** **40**

**Figure 6. Examples of proposed intermediates in copper catalysed reactions [66-70]**

It has been proposed that there are various intermediates for example **38**, **39** and **40**, in the mechanism for the copper catalysed reaction. All of them exhibit steric control over the reaction due to the large size of the copper atom which prevents the copper attacking the sterically

demanding ring (Figure 6, Scheme 16).[66-70]

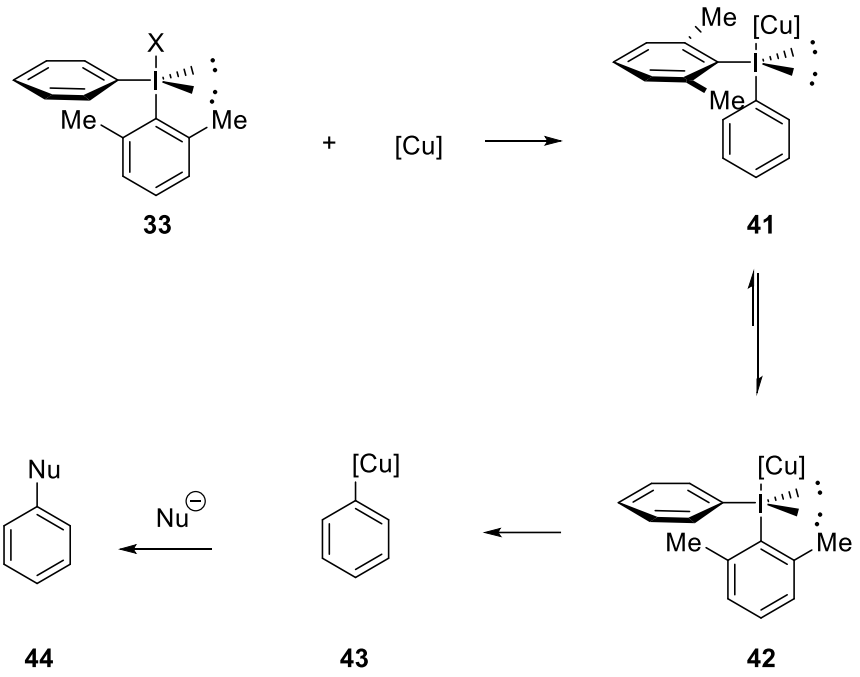


**Scheme 16. Steric effect of copper catalysed diaryliodonium salts reaction**

The diaryliodonium salts reaction in the presence of copper might be separated into three processes, first the copper reacts with the diaryliodonium salt displacing the counter-ion X. Due to the large size of the copper atom and the bulky groups, when the arene with the most steric hindrance occupies the equational position, it is much more crowded, thus this arene prefers to occupy the apical position in the trigonal bipyramidal structure, which is opposite to that observed for the metal-free process. The next step is the copper reacting with the less sterically demanding ring, following by the nucleophiles reacting with the aryl copper species which was generated (Scheme 16).

### *1.3.1 N-Arylation*

Arylamines, as an *N*-arylation product, are widely used medically as analgesic[71,72] and antibacterial drugs.[73] In addition imidazole, benzimidazole, benzotriazole, pyrazole and carbazole are important structural components in drug chemistry and these and other *N*-

heterocyclic moieties are also present in many biologically active natural products. Therefore, formation of C-N bonds and the synthesis of these compounds has received much attention over recent years with most *N*-arylation processes also preferring a copper-catalysed process.

For example, the Chan-Lam Coupling and Ullmann Reaction are the major synthetic methods used for *N*-arylation reactions. Transition metal catalysed carbon-heteroatom cross-coupling reactions have seen a recent increase in organic synthesis as they have a wide range of applications.

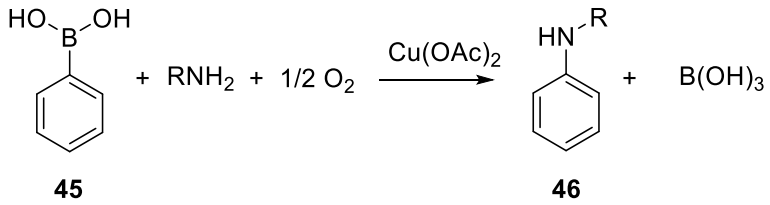


**Scheme 17. An example of a Chan-Lam coupling synthesis**

In 1998 Chan, Evans, and Lam first reported the coupling of amines with benzeneboronic acid **45** using copper(II) acetate.[74-76] In the following years, Chan-Lam coupling was developed and different copper catalysts, such as copper (I) iodide and copper (II) oxide, were also used in the *N*-arylation reactions.[77-79] Because of the structural diversity tolerances, Chan-Lam coupling is still widely used in the arylation of nitrogen nucleophiles. However, the other methods using diaryliodonium salts for *N*-arylation were developed.

#### 1.3.1.1 Metal-Free *N*-arylation Using Diaryliodonium Salts

As hypervalent iodine compounds have been made, methods of *N*-arylation using diaryliodonium salts were reported. McEwen[57] found that diaryliodonium salts could react with inorganic anions and allowed the formation of C-N bonds, such as sodium nitrite, and the reaction with sodium azide to generate arylazides in a good yield, which was around 99%.

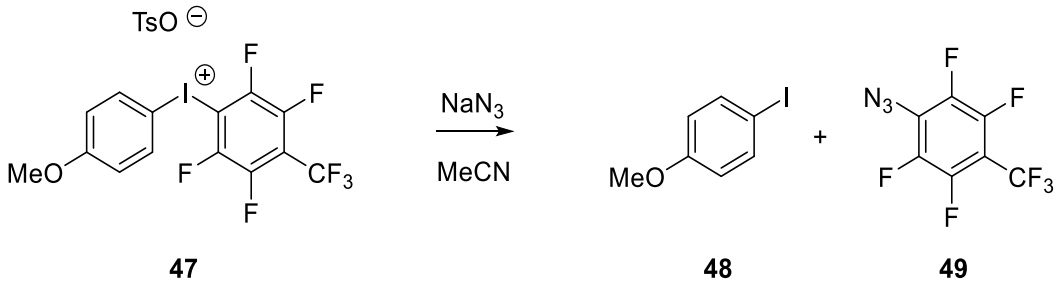


**47** **48** **49**

**Scheme 18. The formation of arylazides using diaryliodonium salts**

The selectivity of arylazides using asymmetric diaryliodonium salts has been improved in 2010 by introducing the electron-rich non-participating ring 4-methoxyphenyl for example in the formation of product **49** in a 64% yield.[80]

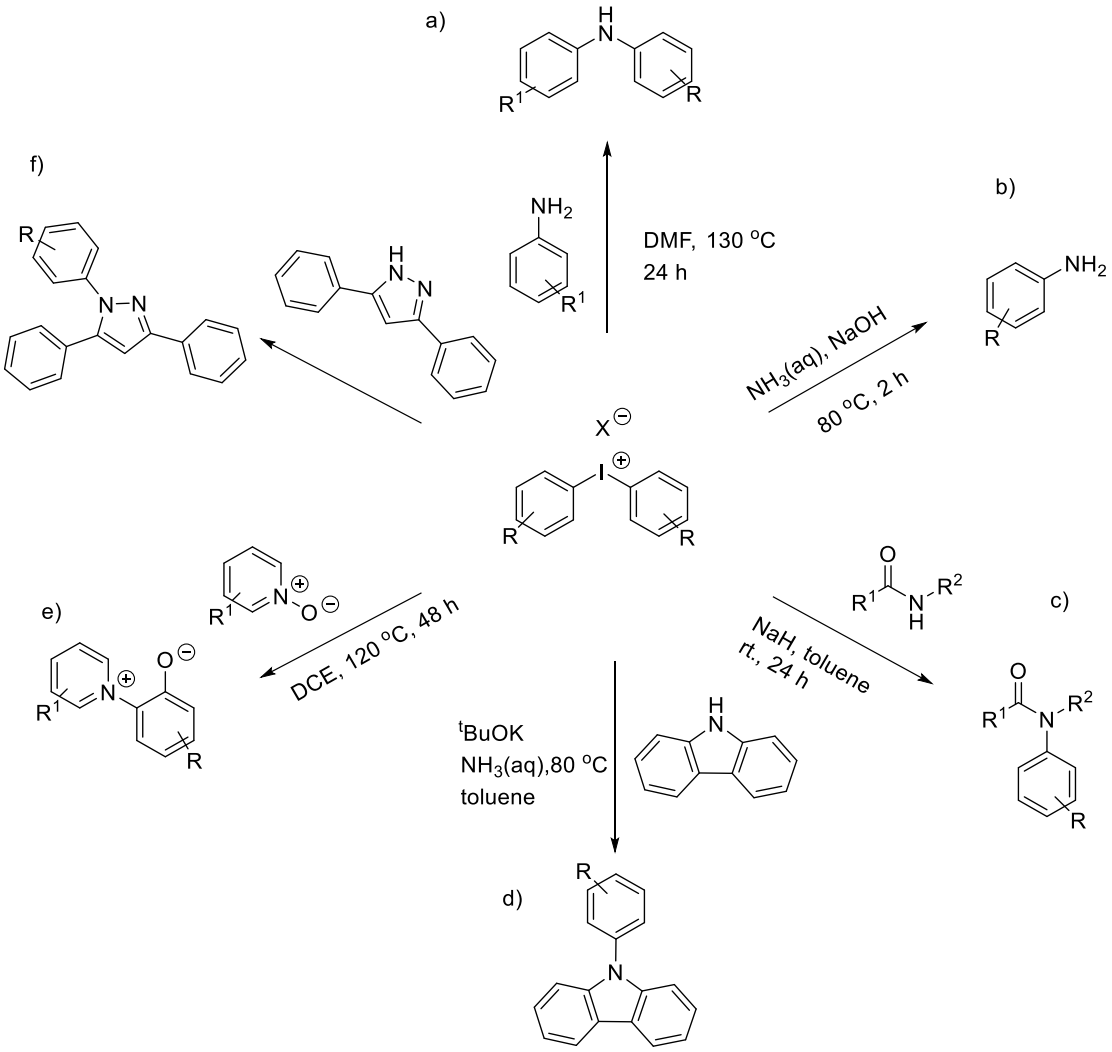


**Scheme 19. Examples of *N*-arylation reactions using diaryliodonium salts**

Carroll and Wood reported a metal-free *N*-arylation of aniline with diaryliodonium salts in DMF (Scheme 19a) and noted that the electronic control is more important than steric control in this transformation.[63]

**Table 2. The selectivity of *N*-Arylation using diaryliodonium salts**

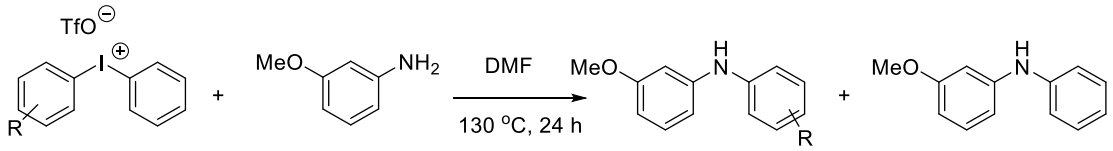


**50** R=4-Me
**51** R=2-Me
**52** R=2-OMe
**53** R=2,6-$OMe_2$
**54** R=2,4,6-$OMe_3$

**55**

**56** R=4-Me
**57** R=2-Me
**58** R=2-OMe
**59** R=2,6-$OMe_2$
**60** R=2,4,6-$OMe_3$

**61**

| Iodonium salt | Ratio **61** : (**56**-**60**)[a] | Yields[b] |
|---|---|---|
| **50** | 1.4 : 1 | 53 |
| **51** | 1.4 : 1 | 40 |
| **52** | 3 : 1 | 62 |
| **53** | 1 : 0 | 70 |
| **54** | 1 : 0 | 45 |

[a]Product ratios are taken from 1H NMR spectroscopy of the combined isolated products [b]Combined yields of the isolated products.

Olofsson expounded on this suggestion and demonstrated that the trimethoxyphenyl and dimethoxyphenyl are suitable for controlling the selectivity in *N*-arylation as it only generates the desired product, it also appears that the *ortho* effect in *N*-arylation reaction is reversed as *m*-anisidine prefers to react with the ring having lower steric requirements (Table 2).[61]

Jian Liu reported an effective and simple method for synthesis of anilines by using diaryliodonium salts in aqueous ammonia at 80 °C with high yields (62% to 96% with 19 examples) (Scheme 19b).[81] The synthesis of aryl amides has received considerable attention, and in 2015, a synthetic route to aryl amides using diaryliodonium salts was reported. It provided a metal-free *N*-arylation process in the presence of NaH in toluene at room temperature resulting in around 80% yields with diphenyliodonium salts, however when using asymmetric diaryliodonium salts, selectivity was now an issue, with the electron-rich non-participating arene still providing some control with 45% of desired product being generated (Scheme 19c).[82] Carbazoles are also important medical materials and were effectively arylated

by using diphenyliodonium salts with $^{t}$BuOK as the base in toluene to generate 86% of the product (Scheme 19d).[83]

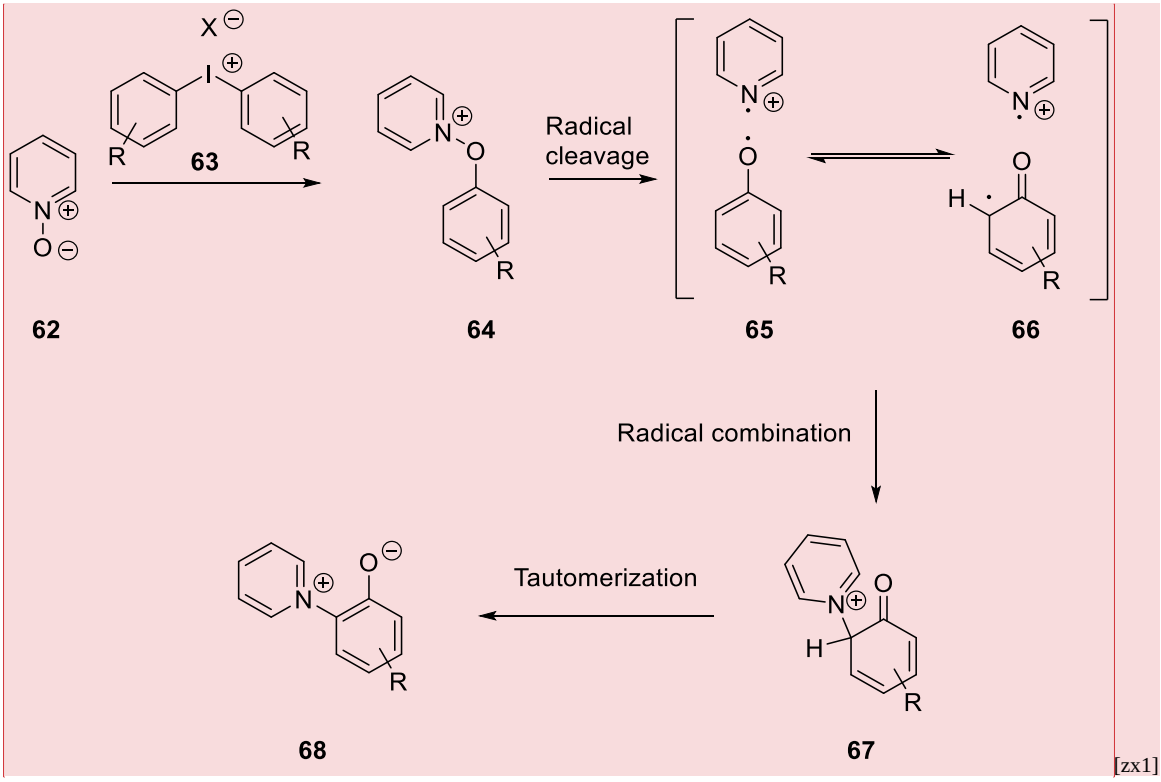


**Scheme 20. Proposed mechanism of the vicinal substitution of diaryliodonium with pyridine *N*-oxides**

The arylation of pyridine *N*-oxide **62** was reported in 2013, shown in Scheme 18, the method underwent *O*-arylation first, followed by a 1,3-radical rearrangement, and then arylation of the radical intermediate to give the product (Scheme 19e).[84] Diaryliodonium salts could also be used for the synthesis of *N*-arylated pyrazoles under metal-free conditions with a good selectivity, however both the electronic effect and the steric effect were important in determining the selectivity of the reaction, however when using the heterocyclic ring thiophene as the non-participating arene, the electron-rich ring was also transferred (Scheme 19f).[64]

### 1.3.1.2 Metal Catalysed *N*-Arylation Using Diaryliodonium Salts

Transition metal catalysts, especially Pd, Ru and Cu based catalysts, are important in organic syntheses,[85-87] the use of metal catalysts has also been considered with diaryliodonium salts in the *N*-arylation reaction.

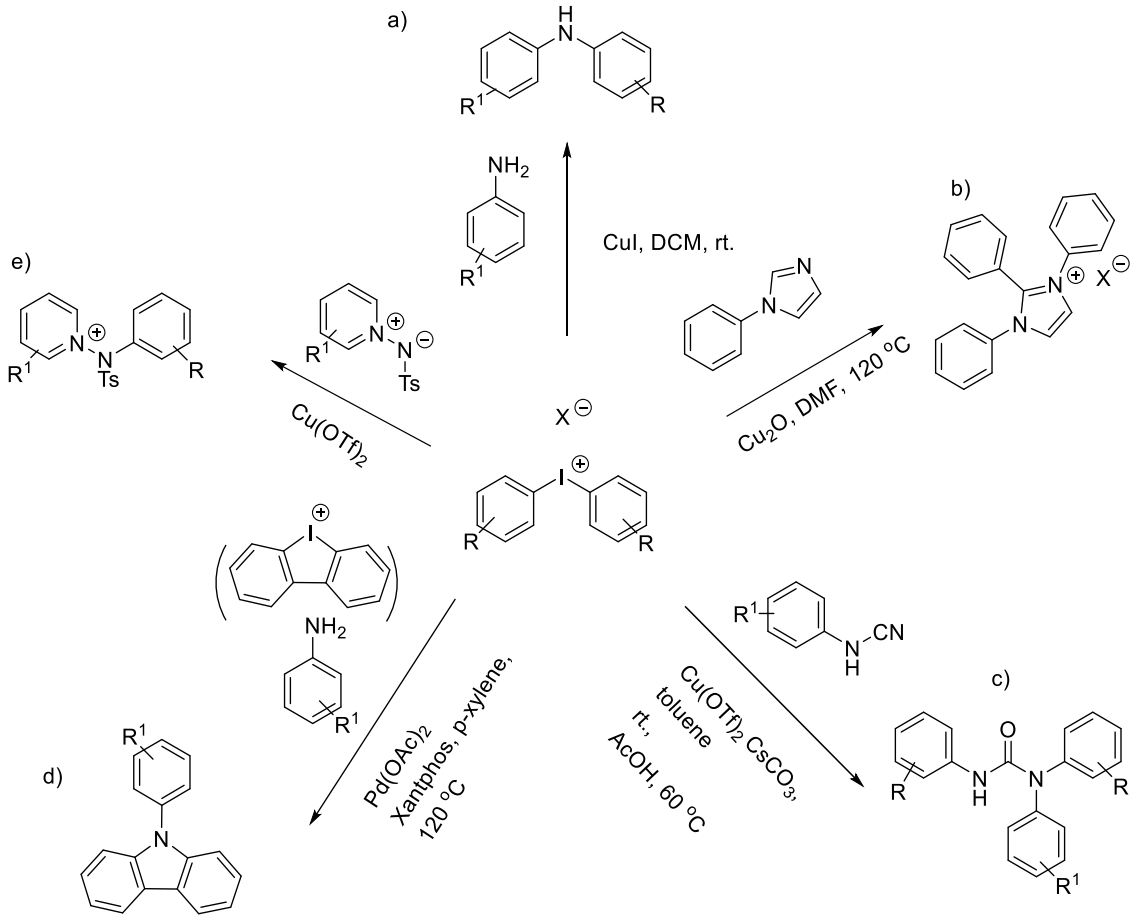


**Scheme 21. Examples of metal catalysed *N*-arylation using diaryliodonium salts**

In 1996, Kang first reported a method using a metal catalyst and developed a series of metal catalysed *N*-arylation reactions using diaryliodonium salts, including the Pd-catalysed synthesis of arylamines at room temperature and the Cu-catalysed arylation of aromatic amines, secondary aliphatic amines, amides and triazoles in 30% to 83% yields (Scheme 21a). [88, 89]

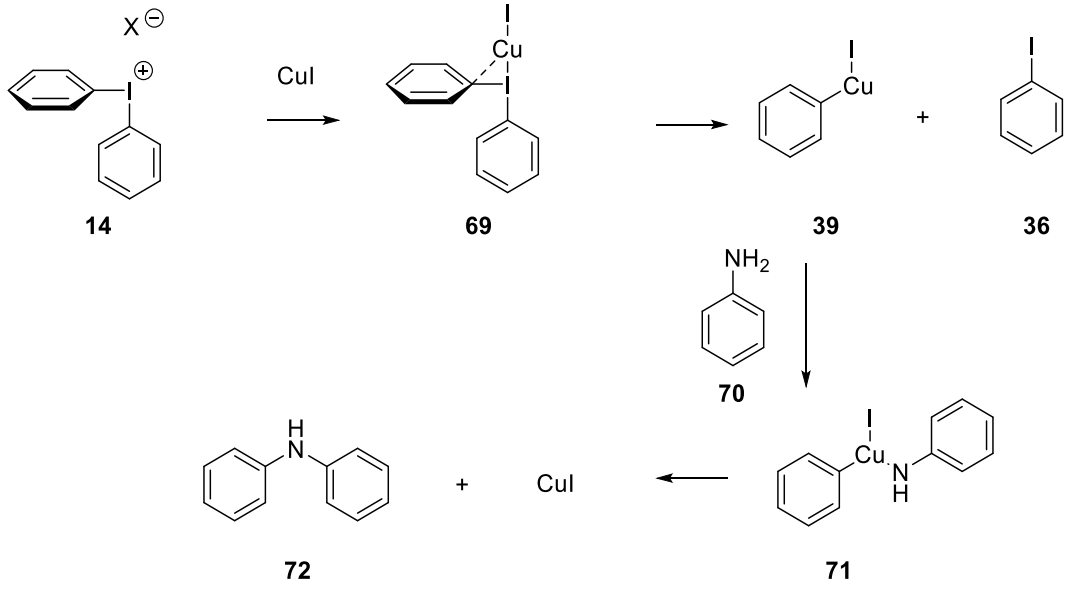


**Scheme 22. Proposed mechanism for the copper catalysed *N*-arylation reaction**

As Scheme 22 shows, copper generates complex **69** from the diphenyliodonium salt **14** and the iodobenzene leaves to form aryl copper **39** which then reacts with aniline,[89] the addition of the catalyst allows the reaction to proceed at room temperature.[90]

In 2019, a novel method for domino di-/triarylation reaction of imidazoles was reported, which was effective in obtaining a di-/triaryl imidazolium salt in one step by using diaryliodonium salts. Controlling the amount of the copper catalyst added determined the degree of arylation, fortunately the generation of diarylation imidazolium and the triarylation imidazolium could be easily controlled, for example 5 mol% $Cu_2O$ generated the diarylation imidazolium whereas 100 mol% $Cu_2O$ only generated triarylation imidazoles.[91] This method to directly quaternize the *N*-substituted imidazole using diaryliodonium salts provided an efficient route for the introduction of a series of functional groups to *N*-substituted imidazoles (Scheme 21b).[92] A synthetic route to *N,N,N*-triarylureas was also developed recently by using *N*-arylcyanamide with diaryliodonium salts, which provided a one-pot synthesis in the presence of base and a copper catalyst resulting in 52% to 88% yields (Scheme 21c).[69]

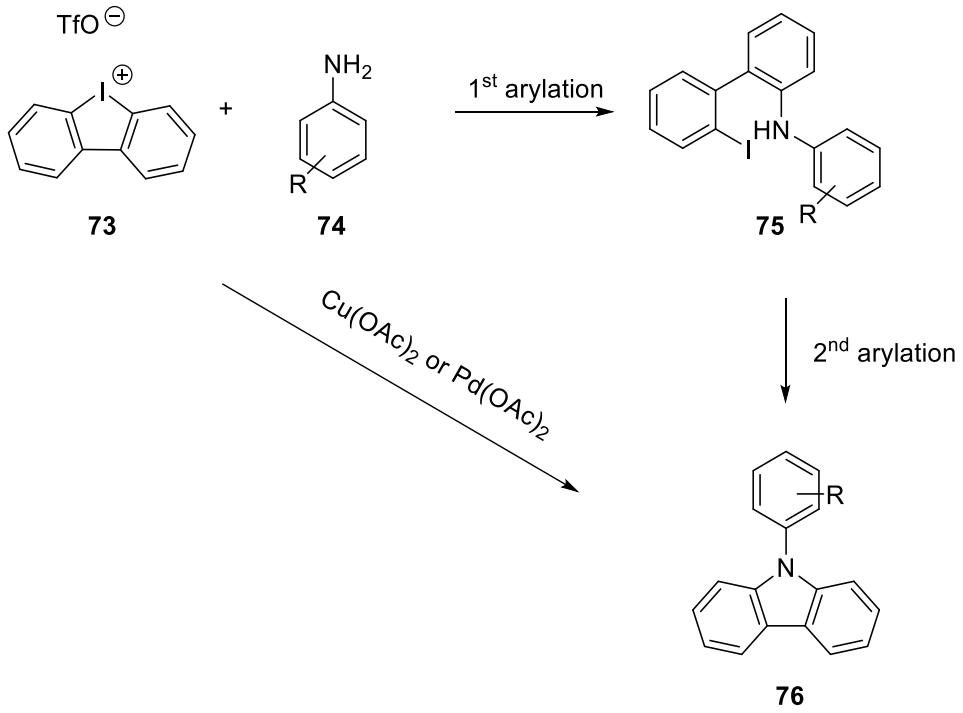


**Scheme 23. Synthetic route to *N*-aryl carbazoles**

Synthesis of carbazole **76** using diaryliodonium salts was reported under metal-free conditions,[83] but the addition of a metal catalyst would make it easier and in only one step (Scheme 21d).[93] In the metal-free arylation, the product needs a two-step arylation process which generates **75** first and then **76**, while in the metal catalysed process it can be done in a one-pot process. Both copper catalyst[94] and palladium catalyst[95, 96] provide good yields which are all around 90% (Scheme 23).

The synthesis of *N*-pyridinium sulfonamidates was demonstrated by using diaryliodonium salts with a copper catalyst and the product was similar to using pyridine *N*-oxides as it could undergo a radical rearrangement (Scheme 21d).[84, 97]

### *1.3.2 O-Arylation*

The diaryl ether group is widely used in organic synthesis and the polymer industry,[98] and some diaryl ethers are reported to possess pharmaceutical activity. [86, 87,99, 100] Diaryl ethers can be synthesized by different methods and the most common method is the copper-catalysed Ullmann coupling. The classical method for the preparation of diaryl ether usually uses a phenol and aryl halides under Ullmann's procedure, but it requires high temperatures around 120 ℃ (Scheme 24).[101, 102]

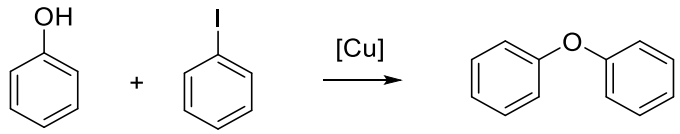


**77** **36** **78**

**Scheme 24. An example of copper-catalysed Ullmann diaryl ether synthesis**

Recently, many other catalysts have been developed, such as copper complexes,[103] palladium complexes,[104, 105] Pd/ZnO nanoparticle[106] and others.[107] But all of these methods still need 90 ℃ to 110 ℃ to carry out the reaction which is not suitable if the substrates and/or products are temperature sensitive compounds.

### 1.3.2.1 Metal-Free *O*-Arylation Using Diaryliodonium Salts

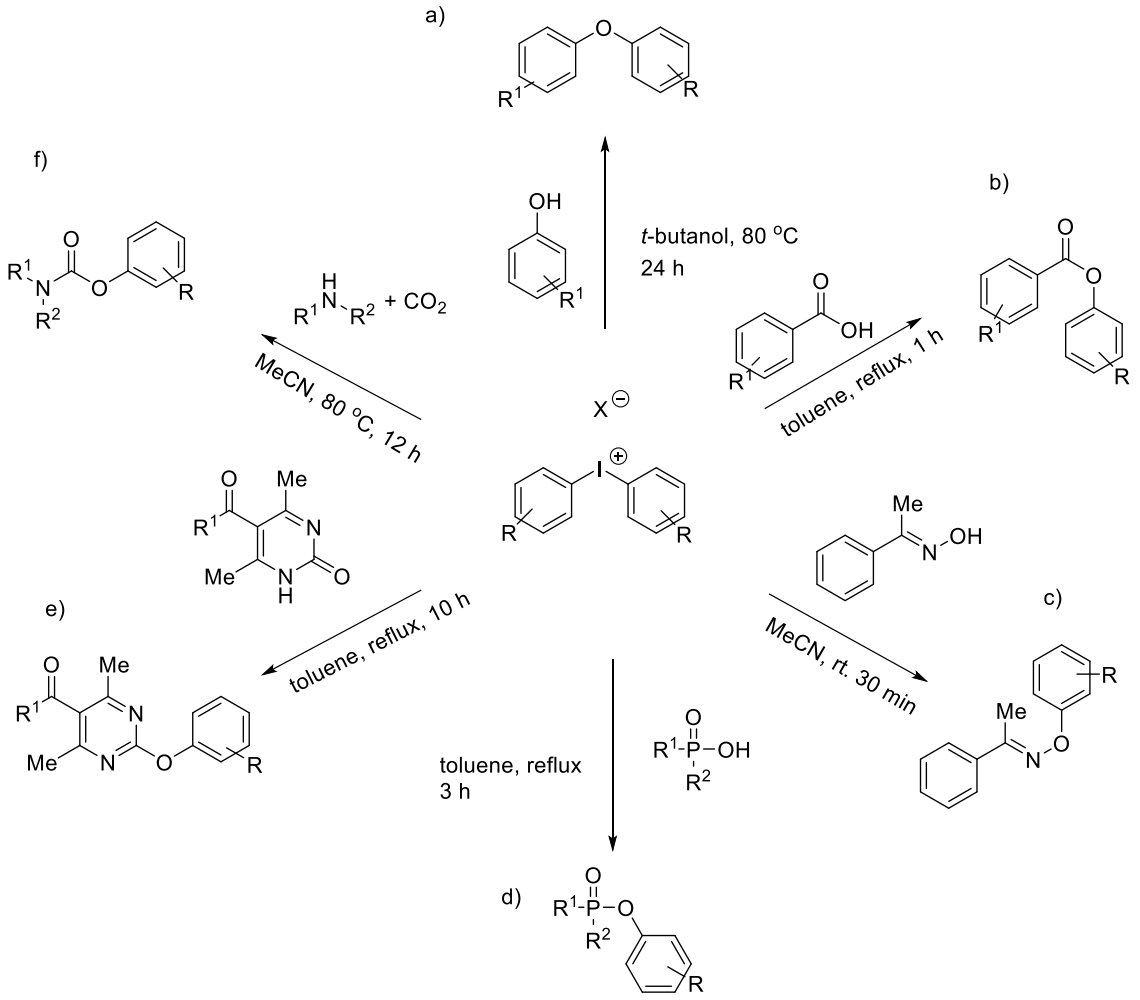


**Scheme 25. Examples of *O*-arylation reaction using diaryliodonium salts**

In 1963, Jorgensen reported *O*-arylation using diaryliodonium salts in *t*-butanol and formed a range of diarylethers, however the yields were only 20% to 66% (Scheme 25a).[108] The Olofsson group also provided a synthetic route to diarylethers using diaryliodonium salts, which allowed the reaction to be carried out at room temperature or 40 °C and also allowed the formation of complex products in >90% yields. However the selectivity is different to compare with *N*-arylation, when the reaction used **51**, the ratio of by-product and product is 1:2.4, which in *N*-arylation is 1.4:1, suggesting that the *ortho*-effect influence the selectivity in *O*-arylation, **79** preferred to react with the most sterically hindered ring (Table 3).[109]

**Table 3. The selectivity of *O*-Arylation using diaryliodonium salts**

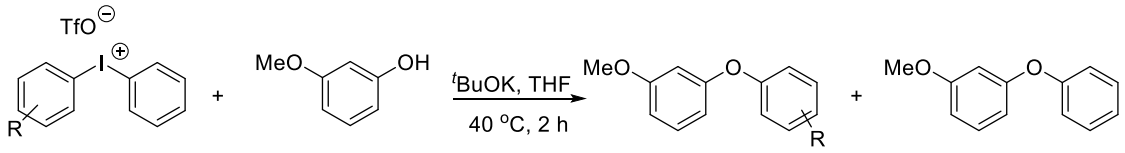


**50** R=4-Me
**51** R=2-Me
**52** R=2-OMe
**53** R=2,6-$OMe_2$
**54** R=2,4,6-$OMe_3$

**79**

**80** R=4-Me
**81** R=2-Me
**82** R=2-OMe
**83** R=2,6-$OMe_2$
**84** R=2,4,6-$OMe_3$

**85**

| Iodonium salt | Ratio **85** : (**80**-**84**)[a] | Yields[b] |
|---|---|---|
| **50** | 2.9:1 | 78 |
| **51** | 1:2.4 | 98 |
| **52** | 1:0 | 93 |
| **53** | 1:0 | 99 |
| **54** | 1:0 | 85 |

[a]Product ratios are taken from $^1$H NMR spectroscopy of the combined isolated products [b]Combined yields of the isolated products.

However, when the nucleophile is a weak nucleophile such as carboxylate, the reaction requires a higher temperature such as refluxing toluene (Scheme 25b).[97, 98] Arylated hydroxylamines could also be prepared by this method allowing the formation of complex pharmaceutical intermediates, this is achieved in the presence of base and toluene as the solvent at room temperature, the selectivity was similar to the *N*-arylation, the electronic control was the most important factor in the reaction, but the *ortho*-effect also has some influence on the reaction selectivity, as the oxygen in hydroxylamines preferred to react with the most sterically hindered ring (Scheme 25c).[110, 111] Organophosphorus compounds can also be synthesised using diaryliodonium salts, for example in 2014, a method using diaryliodonium salts for the *O*-arylation of P(O)−OH compounds was reported, however, it also required elevated temperatures (110 °C) and resulted in 87% to 96% yields (Scheme 25d). [112]

The reaction of pyrimidinone with diaryliodonium salts faced a problem as the diaryliodonium salts prefer *N*-arylation over *O*-arylation.[113, 114] In 2014, a direct synthetic method using the Biginelli reaction gave 4-aryl-6-methyl-pyrimidine-2(1H)-ones, in which, due to the steric hindrance in the pyrimidinone compound, the diaryliodonium salts only gave *O*-arylation to afford 2-aryloxy pyrimidines and this was achieved in good yield, 53% to 74% (Scheme 25e).[115]

In 2015, a one-pot three-component coupling approach to carbamates was reported using diaryliodonium salts, an amine and carbon dioxide at 80 °C, this was an efficient process and gave the product in 90% yield (Scheme 25f).[116]

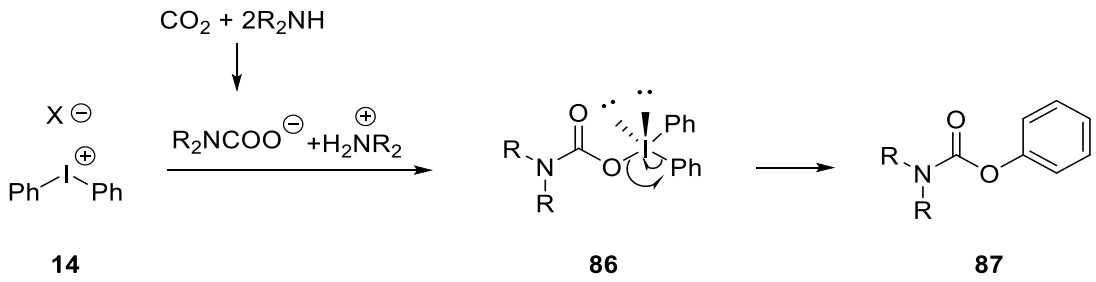


**14** **86** **87**

**Scheme 26. The synthetic route of *O*-aryl carbamates**

The proposed mechanism might be that initially, the carbamic acid ammonium salt could be formed from the amine and carbon dioxide in the presence of 2 equivalents of 1,8-diazabicyclo[5.4.0]-undec-7-ene (DBU), other organic or inorganic bases lowered the product yield, followed by the carbamate anion attacking the diphenyliodonium salt **14** and then aryl transfer to the oxygen and elimination of PhI to form the product **87** (Scheme 26).

### 1.3.2.2 Metal Catalysed *O*-Arylation Using Diaryliodonium Salts

The metal catalysed *O*-arylation has also been reported. Most *O*-arylation reactions are in the presence of copper and are carried out under mild conditions.

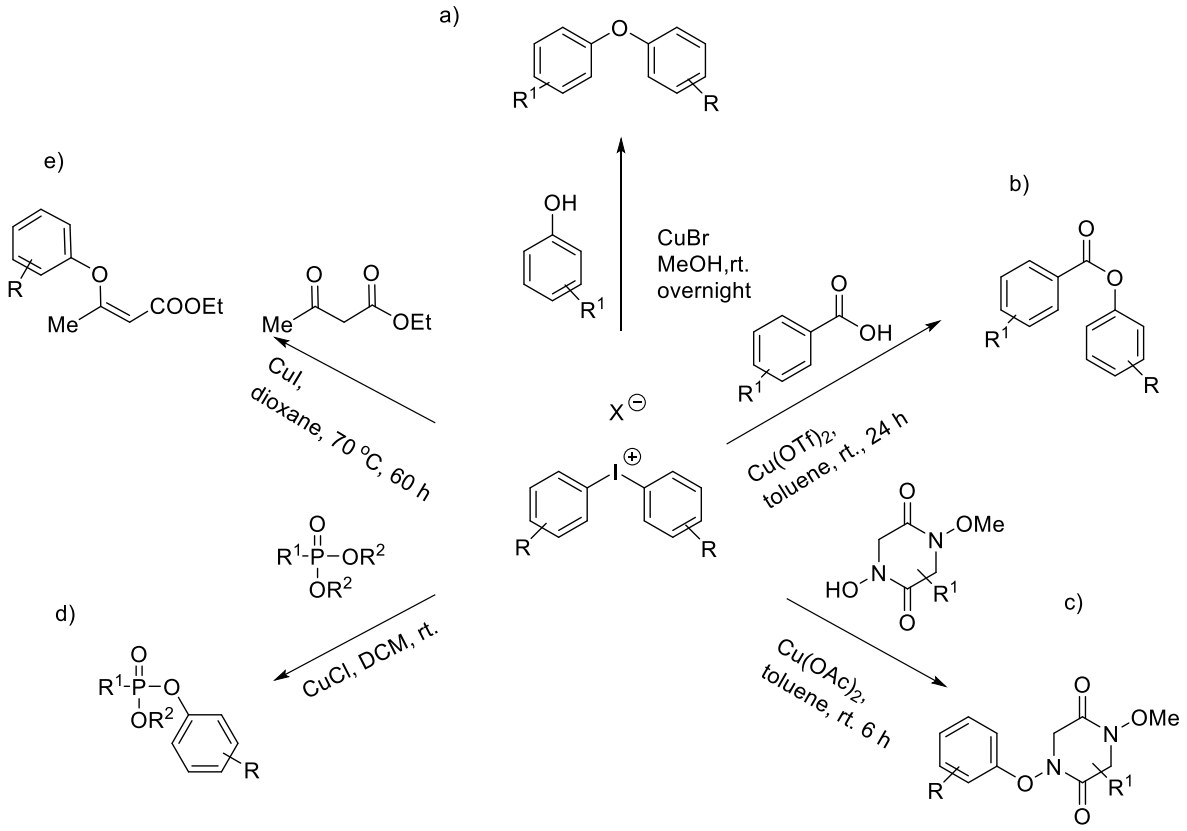


**Scheme 27. Examples of metal catalysed *O*-arylation using diaryliodonium salts**

A method of *O*-arylation using diaryliodonium salts at room temperature was reported in the presence of copper(I) bromide which gave a 55% yield of the product at room temperature (Scheme 27a).[117] Due to the presence of a copper catalyst, the weak nucleophile carboxylate could react with the diaryliodonium salts at room temperature over 24 h instead of at high temperature and resulted in 85% of the product (Scheme 27b).[118] Copper-catalysed arylation of hydroxamic acids was also reported and allowed the formation of complex compounds as intermediates in the total synthesis of some natural products and the yields varied from 36% to 74% and were higher than those obtained using Chan-Lam conditions with arylboronic acids (45% to 51%) (Scheme 27c).[119, 120] Using diaryliodonium salts and a copper catalyst also allowed arylation at room temperature to form alkyl aryl phosphonates in one-step and about 90% yield (Scheme 27d).[121]

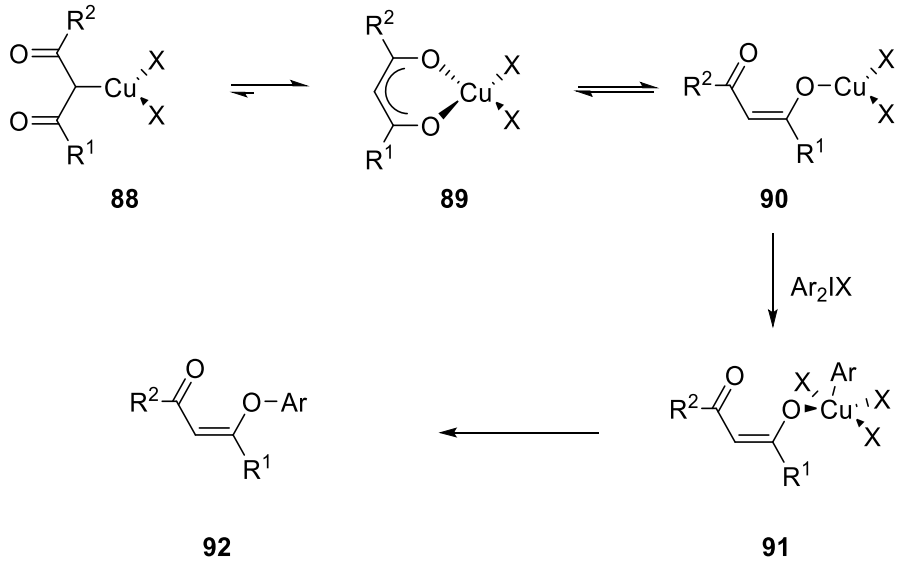


**Scheme 28. Proposed mechanism for copper catalysed *O*-arylation of enolates**

A method of copper catalysed *O*-arylation of ethyl acetoacetate using diaryliodonium salts was also reported and interestingly the reaction only resulted in the Z-configuration of the product (Scheme 27e).[122] A possibile process for controlling the selectivity is shown in Scheme 28, the copper catalyst is bound to both oxygens first to form complex **89,** which then rearranges to give **90** and then the diaryliodonium salt was added followed by elimination of ArI to form the product **92** (Scheme 28).

As mentioned before in the copper catalysed *N*-arylation reactions, copper catalysed *O*-arylation can also be carried out under mild conditions with most reactions done at room temperature.

### *1.3.3 Fluorination*

Fluorination using diaryliodonium salts has been considered as an important method for fluorine-18 ($^{18}F$) nucleophilic aromatic substitutions due to the short-lived of $^{18}F$ ($t_{1/2}$=109.6 min).[123] The $S_NAr$ process usually requires a high temperature (around 100 °C) and 24 h to generate the fluorination product which is not suitable for $^{18}F$.[124]

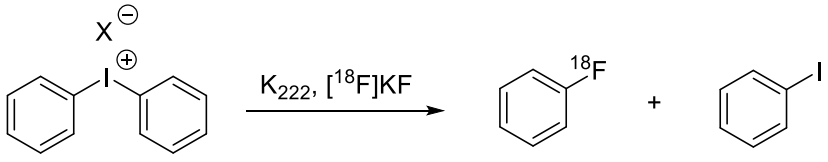


**14** **93** **36**

**Scheme 29. Preparation of [$^{18}F$] fluorobenzene using diphenyliodonium salts**

In 1982, the first method of fluorination using diaryliodonium salts was reported by Michael van der Puy, using KF as the fluorination reagent in DMF.[125] But due to the poor solubility of KF in organic solvents, the reaction yields were only around 50%. A method using Kryptofix 222® ($K_{222}$) and [$^{18}F$]KF was developed in 1995 which improved the yield up to 88% (Scheme 29). [120, 121] This study also provided a method for preparation of PET (Positron Emission Tomography) imaging radiotracers by using diaryliodonium salts, it was also found that when the reaction was carried out in microreactors it provided a fast and effective method for synthesis of radiofluorinated arenes.

In 2007, a method using 4-methoxyphenyl as the non-participating arene in the radiosynthesis of 3-[$^{18}F$]fluoropyridine and 3-[$^{18}F$]fluoroquinoline was reported to have good selectivity and resulted good yields.[126] In the same year, the effect of adding TEMPO was reported and the product yields and reproducibility of the process were improved for certain types of substrates.[127]

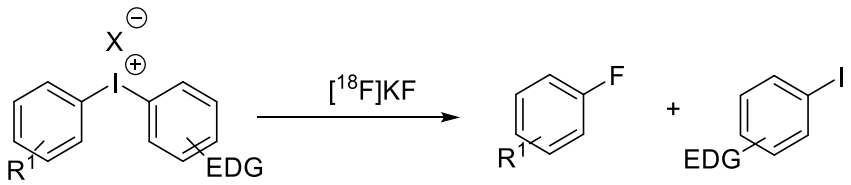


**94** **95** **96**

**Scheme 30. Electronic effect in the fluorination of diaryliodonium salts**

The electronic nature of the substrate was found to have the major effect on the selectivity of fluorination when using diaryliodonium salts **94**, with highly electron-rich arenes acting as a dummy group and thus the other aromatic was transferred forming the fluoroarene **95**.[128, 129]

Most fluorinations were under metal-free conditions, however in 2013, a method using copper catalysis for selective fluorination using diaryliodonium salts was developed.[67]

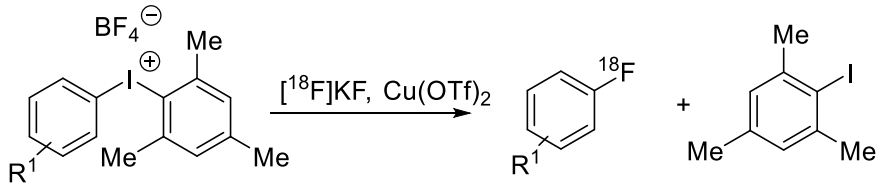


**97** **95** **98**

**Scheme 31. Selective fluorination using diaryliodonium salts**

It was found that the *ortho*-effect (where the nucleophile prefers to attack the *ipso* carbon of the most hindered arene in diaryliodonium salts[130, 131]) was no longer a control element with the addition of copper catalyst. It was noticed that the selectivity of the reaction was opposite to the metal-free reaction, the fluoride now preferred to attack the less sterically hindered ring, and therefore mesitylene is often used as the dummy group.

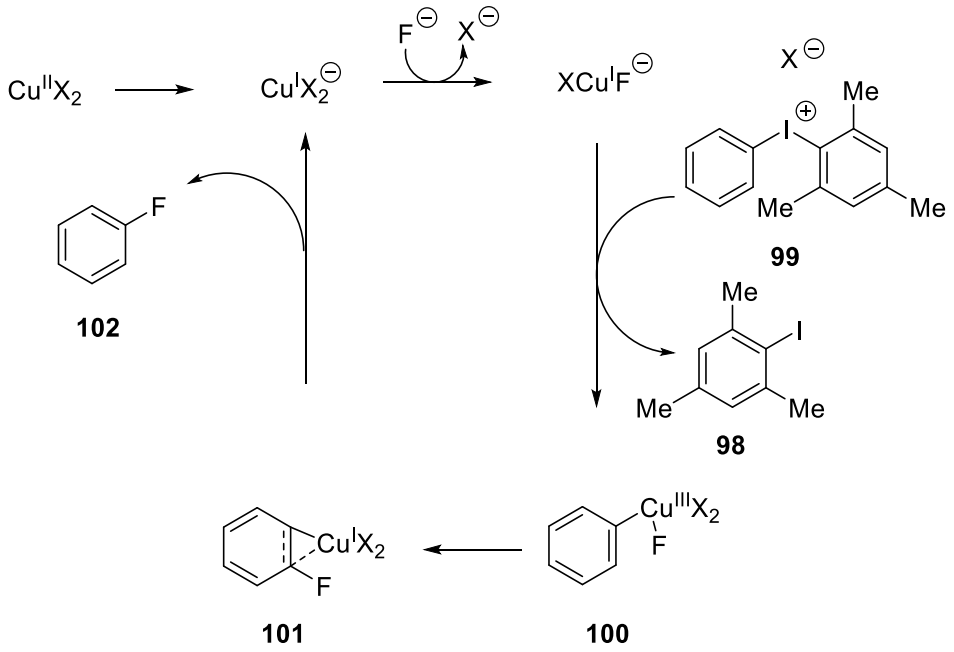


**Scheme 32. Proposed mechanism of copper catalysed fluorination using diaryliodonium salts**

The proposed mechanism was suggested following computational calculations using DFT methods and suggested that the copper catalyst facilitates the formation fluorobenzene via an aryl copper intermediate **101** (Scheme 32).[132, 133] Later, the method was developed and used in the synthesis of clinically relevant PET-tracers and resulted in good radiochemical yields.

## 1.4 Fluorous Compounds in Organic Chemistry

Fluorous chemistry involves the use of perfluorinated compounds or compounds having perfluorinated substituents and the amount of fluorous compounds used in science and in daily life increases year by year. Due to the fluorine having the smallest atomic radius of the Period 2 elements and the highest electronegativity, the C–F bond is one of the strongest in organic chemistry (105.4 kcal/mol),[134] thus fluorous compounds have high thermal and oxidative stability, low polarity, weak inter-molecular interactions and surface tension, and are therefore widely used in plastics, dyes, surfactants, drugs and pesticides.[135]

### *1.4.1 Fluorous Silica Gel*

Fluorous silica gel has been prepared by bonding silanes with perfluoroalkyl groups, which is similar to the preparation of reverse phase silica gel with long alkyl chains. In 1978, Berendsen, Pikaart and de Galan[136] introduced silica gel with a fluorocarbon bonded phase, their method used (heptadecafluorodecyl)dimethylsilyl chloride ($C_8F_{17}CH_2CH_2Si(Me)_2Cl$) **104** and silica **103** and was later widely adopted in the preparation of different kinds of fluorous silica gel.

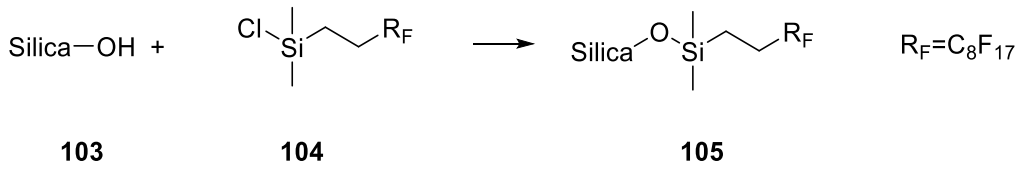


**Scheme 33. Preparation of fluorous silica gel**

Recently, this original fluorous silica gel, with different fluorocarbon-bonded phases, has been used exclusively as a stationary phase for analysis and HPLC applications. This fluorocarbon-bonded silica gel has a lower ability to absorb non-fluorous organic compounds than fluorous compounds. Non-fluorous organic compounds can quickly pass through this silica gel column, whereas fluorous compounds will remain in the column they may then be eluted with a

fluorophilic solvent.[137]

Fluorous silica gel incorporates perfluoroalkyl ($R_F$) groups, which are important for separating fluorous compounds and non-fluorous compounds. It has been shown that the longer fluorous chains are more beneficial in retaining the fluorous compound, it is common to use the $C_8F_{17}$ group, which can also provide favourable separation for different fluorous substrates.

### *1.4.2 Fluorous Solid-Phase Extraction*

SPE technology is originally a sample pre-treatment method, which was developed from the mid-1980s and is based on liquid-solid phase chromatography theory, it is mainly used for sample separation, purification and enrichment, which can reduce sample matrix interferences and improve detection sensitivity.[138, 139]

SPE uses the liquid chromatography separation principles of selective adsorption and selective elution. The more commonly used method is to pass the liquid sample through the absorber, which retains the test substance, allowing removal of the impurities, the stationary phase is then eluted with a small amount of appropriate solvent to rapidly elute the test substance, to achieve the purpose of rapid separation and purification of the sample. It is also possible to selectively absorb the impurities and let the test substance pass straight through; or simultaneous adsorption of impurities and the test substance, and then using a suitable solvent system to selectively elute the components.

Once fluorous silica gel was prepared, the research into fluorous solid-phase extraction (F-SPE) commenced. Standard F-SPE was introduced in 1997[140] and used a fluorophilic (but not fluorous) solvent for elution. Fluorous silica gel provides a convenient stationary phase for F-SPE where fluorous compounds could easily interact. There are two main methods for F-SPE, reverse F-SPE and normal F-SPE.

The normal F-SPE technique uses fluorous silica gel, in combination with a fluorophobic solvent like 70–80% MeOH–$H_2O$, 50–60% $CH_3CN$–$H_2O$, 80–90% DMF–$H_2O$, or 100% DMSO as the elution solvent. Non-fluorous compounds (organic) are eluted and the fluorous compounds retained which can then be easily eluted by a change to a fluorophilic solvent such as water-free MeOH or $CH_3CN$.[141]

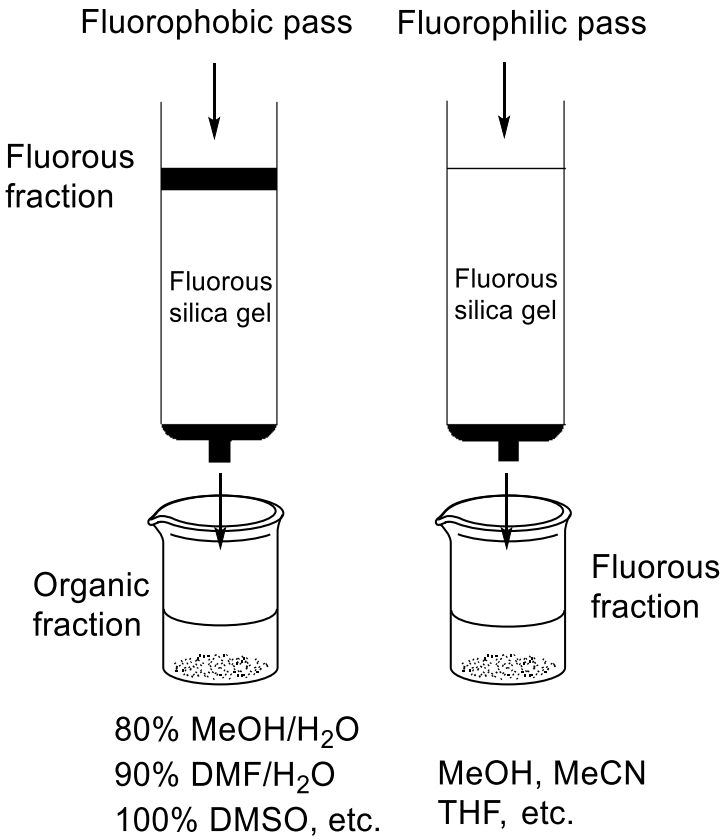


**Figure 7. Operation of normal F-SPE**

This method is simple and reliable and has been widely used in different areas. But it is important to note that it does not seem to be very sensitive to the polarity of the fluorous or organic components. Therefore, normal F-SPE could not be used to separate fluorous compounds bearing different fluorous groups or a mixture of non-fluorous compounds.

In this situation, reverse F-SPE was developed for the separation of fluorous compounds from

a mixture of non-fluorous compounds in a single process. After using this method, non-fluorous products could easily be separated by standard liquid chromatography in the same column. [142]

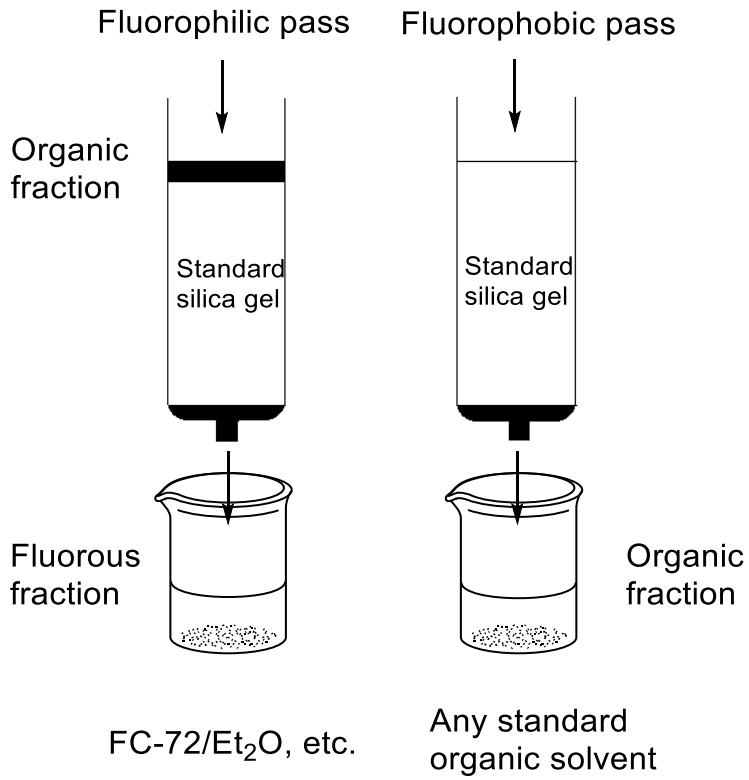


**Figure 8. Operation of reverse F-SPE**

Reverse F-SPE uses standard silica gel and perfluorohexanes and ether as the eluent.[142] Fluorous and non-fluorous components are loaded onto a standard silica gel column, and then the silica is eluted with perfluorohexanes to remove the fluorous fraction. Because this method uses standard silica gel, the reverse F-SPE method could also separate non-fluorous compounds with different polarity. Hence, silica chromatography is only needed once to separate both the organic compounds and fluorous compounds, which could save a lot of time and solvent compared with normal F-SPE. However, due to the price of perfluorohexanes, this method is more suitable for removing fluorous catalysts, which are often present only on a small scale.

### *1.4.3 The Method to Introduce Fluorous into Aromatic*

F-SPE method could provide a rapid separation method. Thus, the diaryliodonium salts with a fluorous target could improve the separation method of reaction using diaryliodonium salts.

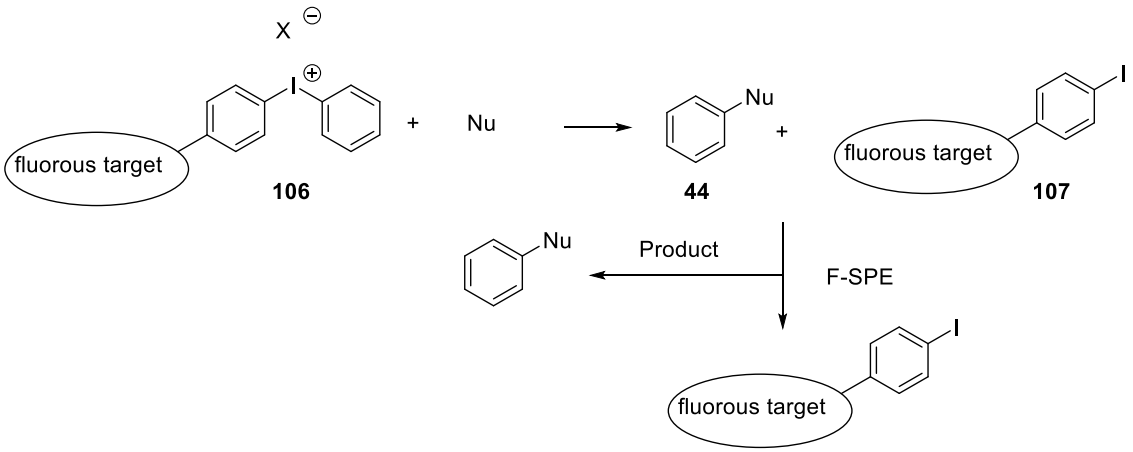


**Scheme 34. The proposed reaction and separation route of reaction using fluorous diaryliodonium salts**

After introducing the fluorous target into diaryliodonium salts, the reaction could be separated rapidly. The product and by-product could be easily separated by F-SPE. There were different methods for introducing a fluorous target into aromatics (Scheme 34).

Transition metal-catalysed reactions, especially those using noble metals such as platinum or ruthenium could achieve the introduction of perfluoroalkyl groups into alkenes and benzene. Von Werner[143] found that iodoperfluoroalkanes **107** could react with alkenes **108** in the presence of transition metal-catalysts, and also transfer the perfluoroalkyl group from **107** to benzene **110,** forming **111**. Since then there have been lots of publications reporting the introduction of perfluoroalkyl groups into benzene using perfluoroalkyliodides.[144-149]

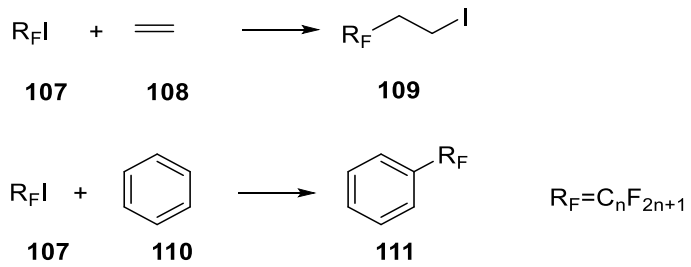


**Scheme 35. Preparation of perfluoroalkyl ethyl iodide and perfluoroalkylbenzene**

There are several other ways to introduce perfluoroalkyl groups into benzene. Sawada, *et al*.,[150] first reported the reaction of iodobenzene **36** or 1-iodonaphthalene with 1-iodoperfluoro-*n*-heptane or 1-iodoperfluoro-*n*-octane **107** in the presence of copper bronze using DMSO as solvent. Paciorek, *et al*.,[151] and Xiao, *et al*.,[152] used iodoperfluoroalkanes **107** and iodobenzene **36** to synthesis perfluoroalkylbenzene **111**.

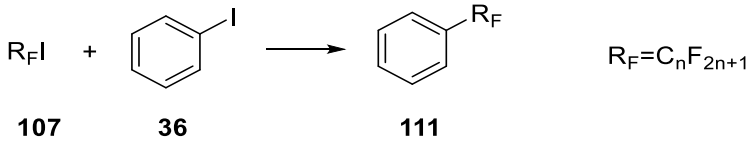


**Scheme 36. The synthesis of perfluoroalkylbenzene 111**

Paciorek,[151] followed this protocol and achieved the products in 78% to 89% yields, Xiao[152] carried out the synthesis at room-temperature in an ionic liquid, as it was hoped this would improve the copper-catalysed reactions and also could also be recycled easily, yields of 84% to 92% were achieved and yields of at least 85% of products were still obtained over five cycles by re-using the catalyst system.

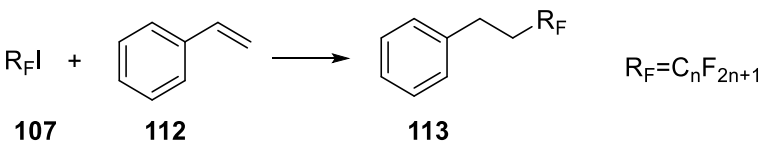


**Scheme 37. The synthesis of perfluoro(ethyl)benzene 11**

Styrene **112** is an important chemical raw material, thus finding out a route for the introduction

of perfluoroalkanes groups into benzene using this substrate could be useful. Guo and Chen,[153] Ignatowska and Dmowski,[154] Barata-Vallejo and Postigo,[155] Takagi and Kanamori,[156] Mikhaylov, [149] and Choi,[157] have all investigated this reaction but with different catalysts.

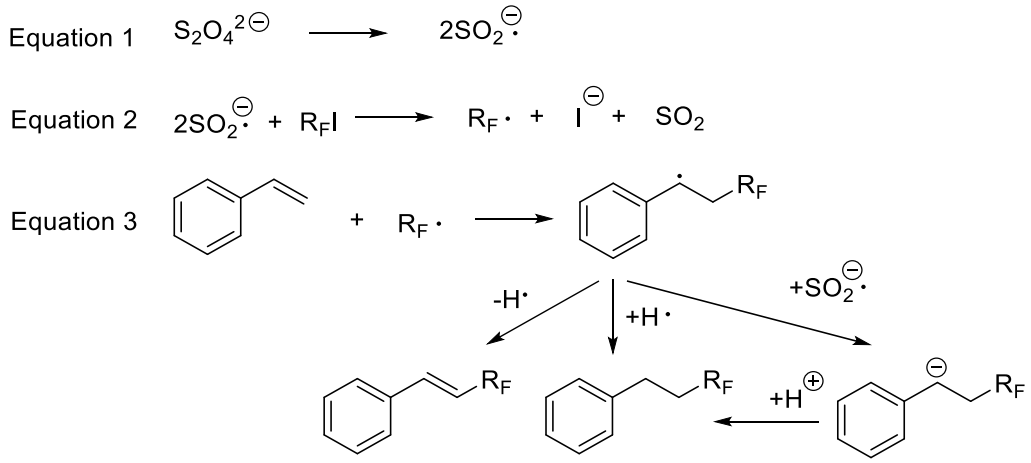


**Scheme 38. The mechanism of sulfinatodehalogenation method**

Guo and Chen[153] used a different system, made up of an oxidant (i.e. $Ce(SO_4)_2 \cdot 4H_2O$), a metal under redox conditions (i.e. $(NH_4)_2S_2O_8/HCO_2Na$), and tried to get the reaction to proceed, but only the sulfinatodehalogenation method gave the product. The mechanism of this reaction may be that dithionite is broken down into the radical anion of sulfur dioxide which could then transfer its electron to get $R_F$· which reacted with the styrene (Scheme 38).

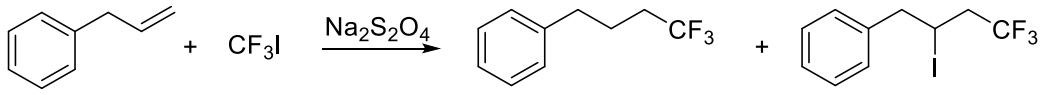


**114** **115** **116** **117**

**Scheme 39. The synthesis of (4,4,4-trifluoro-2-iodobutyl)benzene 117 and (4,4,4-trifluorobutyl)benzene 116**

Ignatowska and Dmowski [154] then used this method to generate the fluorous derivative of allylbenzene. The reactions of trifluoroiodomethane with allylbenzenes, were carried out in a

closed system (pressure glass ampoule) to get 57% of (4,4,4-trifluoro-2-iodobutyl)-benzene **117** and less than 6% of (4,4,4-trifluorobutyl)-benzene **116**, however, these reactions do not provide high yields (Scheme 39). Barata-Vallejo and Postigo[155] increased the yields to over 80% by using the radical initiator 1,1′-azobis(cyclohexanecarbonitrile) (ACCN) with $(Me_3Si)_3SiH$ in water. The experimental method provided a simple and versatile way to achieve the introduction of perfluoroalkyl groups into benzene.

Transition metal-catalysts such as platinum[158] or indium,[156] and metal complexes such as $[Ca_2N]^+$ could also achieve it and provide high yields,[157] but these catalysts are exorbitant for reactions to be carried out on a large scale.

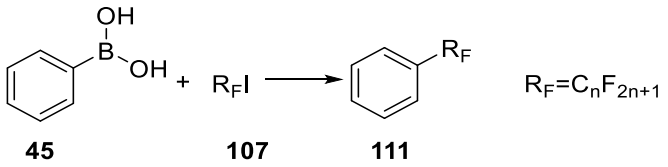


**Scheme 40. The synthesis of perfluoroalkylbenzene 111**

Phenylboronic acid and its derivatives have also attracted interest, in organic synthesis, catalysis, supramolecular chemistry, materials engineering, and also have new applications, in biology and medicine. It has been reported that the perfluoro derivative could be synthesised by using Cu-mediated, process using iodoperfluoroalkane **107** and arylboronic acids **45** under mild conditions.[159] This Suzuki cross-coupling reaction is not sensitive to water and the product **111** could be simply synthesized on a multi-gram scale in good yield.

Since Grignard reagents were developed, they have been widely used in various reactions, because the reaction conversion rate is high, and the reagent is relatively easy to prepare. In 1996, it was reported that it could be used to introduce the perfluoroalkyl group into benzene.[160] They introduced heptadecafluoro-1-iododecane **109** into benzene by copper-catalysis cross-couplings of Grignard reagents **118**.

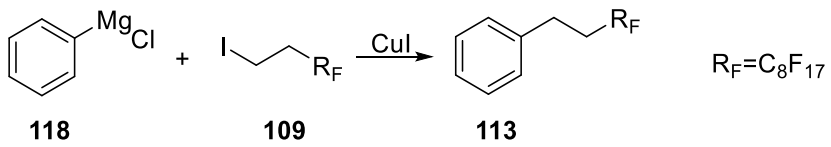


**Scheme 41. The synthesis of perfluoro(ethyl)benzene 113**

They found that palladium- and nickel-phosphine complexes were not as effective and only provided the product in about 20% yield. But the addition of Cu(I) or Cu(II) salts as well as a Cu(I) complex was quite effective, and this could provide the target compound in more than 80%, hence this reaction is suitable for introduction of the perfluoroalkyl groups into benzene. In 2003, Wende, used this method to get 95% of which prodcut.[161]

## 1.5 Aims and Objectives

As discussed in the introduction, diaryliodonium salts have been widely used in various organic synthesis such as *N*-, *O*-arylation and fluorination. However, the selectivity and separation still are the main problem when using the diaryliodonium salts, and the intermedia of copper catalysed reaction has not been found. Therefore, this project intended to discovery the selective metal-free and copper catalysed processes for *N*-, *O*-arylation and fluorination using diaryliodonium salts. The rapid separation can be achieved by introducing fluorous chains into diaryliodonium salts and the use of fluorous solid-phase extraction (F-SPE), the organic compounds (desired products) and fluorous compounds (by-products) can be easily separated.

Therefore, in this thesis I will attempt to:

- Prepare a range of diaryliodonium salts with different ligands and substitution groups.
- Prepare and identify the structure of diaryliodonium salts and the copper complexes and figure out the week interaction between copper and iodine in the copper complexes.
- Figure out the thermal stability of diaryliodonium salts and provide the reaction temperature range.
- Improve the selectivity of diaryliodonium salts *N*-, *O*-arylation and fluorination, and figure out the best reaction conditions.
- Generate the selective rapid separation methods by using fluorous diaryliodonium salts in *N*-, *O*-arylation and fluorination.

# Chapter 2. Results and Discussions

## 2.1 Synthesis of Diaryliodonium Salts

As mentioned in the Introduction, there are several methods for the synthesis of diaryliodonium salts all of which have limitations on the substituents and possible counter-ion combinations. In this research, the general process used starts by the synthesis of an aryliodobis(acetate), the next step is counter-ion exchange. Treatment of this product, $ArIX_2$, with an arylstannane such as tributylphenylstannane or an arylboronic acid such as phenylboronic acid gives the target diaryliodonium salt. For diaryliodonium tosylate salts, the Koser's Reagent is prepared by the addition of p-toluenesulfonic acid to the aryliodobis(acetate), followed by the same procedure of adding an arylstannane or an arylboronic acid to form the target diaryliodonium tosylate salt.

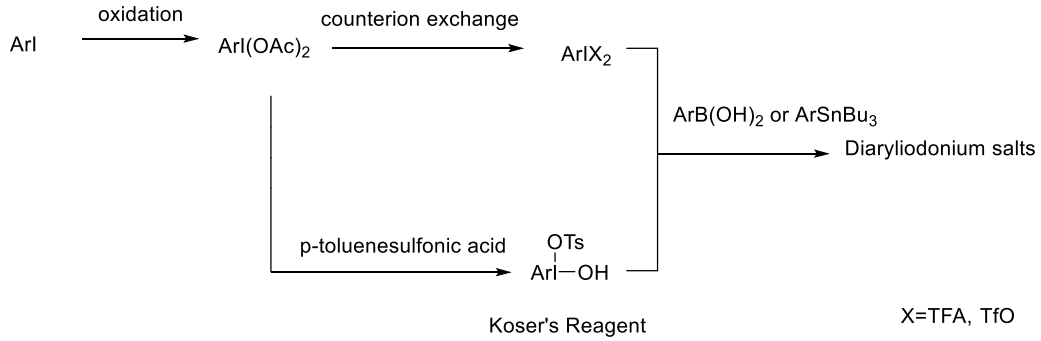


**Scheme 42. Synthetic routes to diaryliodonium salts**

Due to the different polarity of the diaryliodonium salt and the other by-products and starting materials, the diaryliodonium salts can often be easily separated from the reaction mixture by recrystallisation rather than column chromatography.

### *2.1.1 Preparation of Aryliodobis(acetate)*

In 1963, the synthesis of aryliodobis(acetate) was reported by using acetic acid and peracetic acid[162] which is a hazardous oxidation reagent (it can explode at 110℃) and gave the product in a high yield. Recently many research groups have issued a series of strategies that allow the oxidation of iodoaromatics to aryliodobis(acetate) under mild conditions. Given that the procedure using sodium perborate is under mild conditions, it is useful for the synthesis aryliodobis(acetate)s.[45] A series of aryliodobis(acetate)s were prepared having different substitution patterns to allow a study of both electronic and steric effects in the subsequent reactions.

**Table 4. Aryliodobis(acetate)s prepared from iodoaromatics**

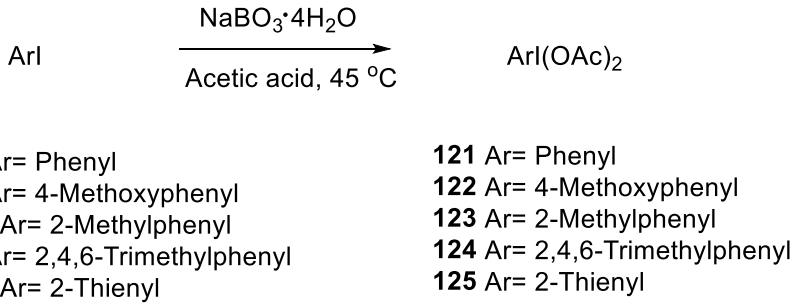


| Aryliodobis(acetate) | **121** | **122** | **123** | **124** | **125** |
|---|---|---|---|---|---|
| Isolated yield (%)[a] | 76% | 52% | 63% | 53% | 23% |

[a]Isolated yield was the average yield of the reaction

As the Table 4 shows, the most electron-deficient arene **32** has the highest yield and the more electron-rich aromatics have lower yields. In particular, 2-iodothiophene **120** only gave a 23% yield of the product. It was found that the drop time of sodium perborate tetrahydrate was important in this reaction. Usually sodium perborate tetrahydrate need to be added for 30 min. Especially for the synthesis of 2-thienyl iodobis(acetate) **125**, if sodium perborate tetrahydrate was added for 15 min, the product yield was dropped to 12%. The recrystallization could use

DCM-petrol system to afford the product, but due to the different of polarity, some unwanted oil was found in the mixture, the adding of ether before petrol could avoid this, therefore the DCM-ether-petrol system was used in the recrystallization.

Sodium perborate tetrahydrate is usually recognized as a weak oxidation reagent, and it is not just an adduct with hydrogen peroxide.[163] McKillop and Sanderson reported the proposal mechanism for this reaction in which sodium perborate tetrahydrate with acetic acid generates the active oxidative species peracetic acid *in situ*.[48]

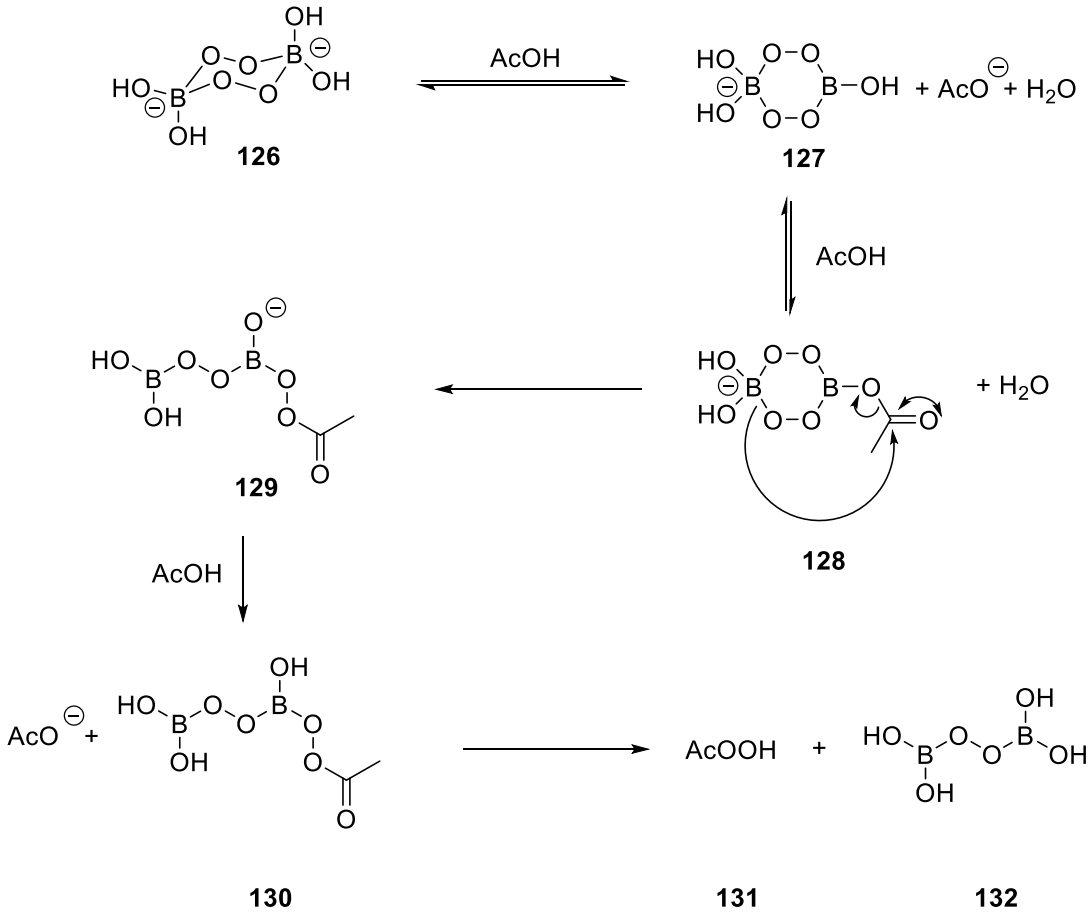


**Scheme 43. Formation of reactive peracetoxyboron species and peracetic acid**

As Scheme 43 shows, when sodium perborate tetrahydrate **126** is in treated acetic acid, there might be an intermediate solvolysis of B-O-O-B linkage **128** is proposed after acetylation. This generates species **130** which contain a B-O-OAc, which could also be used directly as the

oxidizing agent for this reaction in addition to the peracetic acid generated.[48]

But due to the peroxide compounds were formed in the reaction mixture, when removed the solvent, the temperature should be below 30 °C, and some DCM should be left in the reaction mixture at the end to decrease the risk of this reaction.

### *2.1.2 Preparation of Arylstannanes*

There are several routes to prepare arylstannanes from aryl halides; palladium mediated stannylation, cobalt mediated stannylation and stannylation of an aryl lithium intermediate are the most traditional.

For this research, halogen-lithium exchange followed by reaction with tributyltin chloride was the simplest way to prepare the arylstannanes.

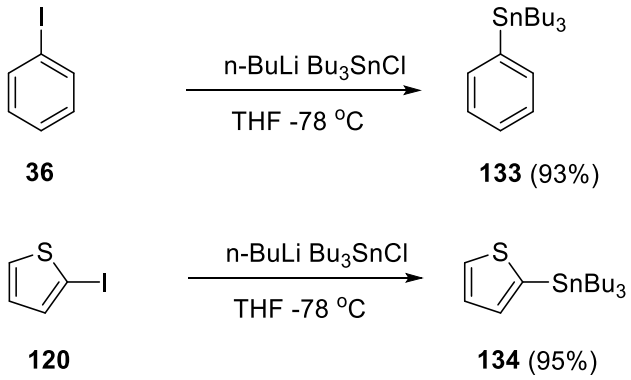


**Scheme 44. Preparation od arylstannanes**

Scheme 41 shows, the reactions were carried out using a standard lithiation procedure and provided greater than 90% of the product for both tributylphenylstannane **133** and 2-(tributylstannyl)thiophene **134** after chromatography.

### *2.1.3 Preparation of Diaryliodonium Salts*

A range of diaryliodonium salts with different substituent patterns and counter-ions needed to be synthesis in order to determine their chemical and physical properties and the resultant selectivity of the arylation process as this variation of functionality allows exploration of the impact of both steric and electronic factors. Therefore, four methods were used in the preparation for different diaryliodonium salts.

**Method A**

It has been mentioned earlier, there are a number of diverse routes for the synthesis of diaryliodonium salts. The method we used is that dropwise addition of acid (2 equivalents of TFA, TfOH) to a cold solution of the aryliodobis(acetate) to generate the more reactive $ArIX_2$ species to which the arylstannane was then added. The diaryliodonium salt was then purified by recrystallisation rather than chromatography although this can be used as an initial purification step if the direct recrystallisation does not give pure material. [164, 165]

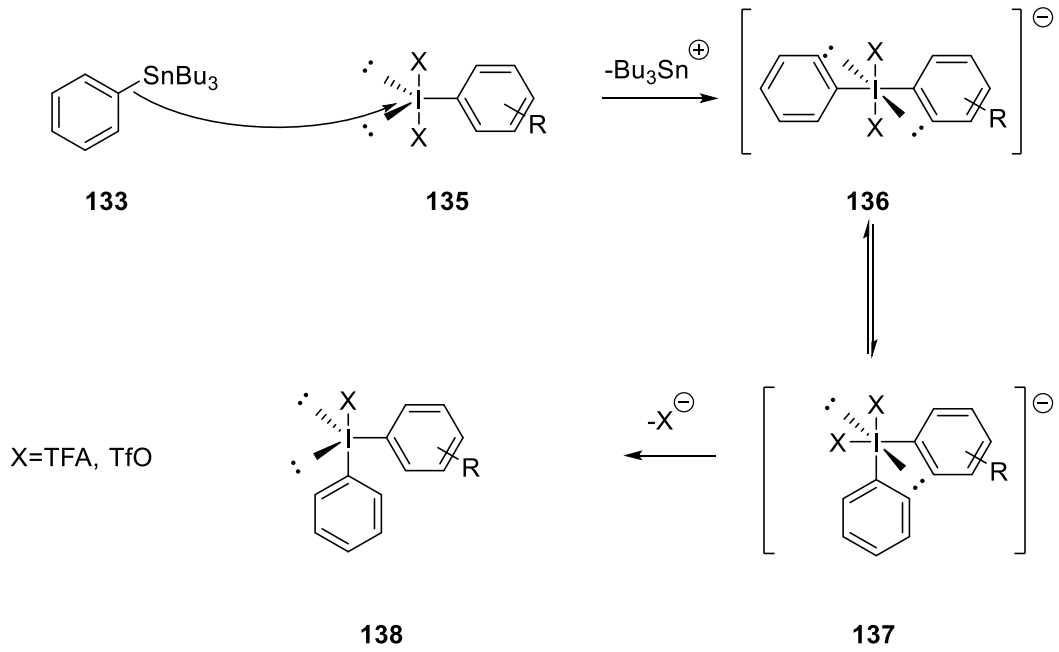


**Scheme 45. Proposed mechanism of the formation of diaryliodonium salts**

The proposed mechanism is shown in Scheme 45, in which the C-Sn bond attacks the hypervalent iodine centre, the intermediate **136** rearranges to **137,** and then one counter-ion leaves the iodine forming the diaryliodonium salt.

**Table 5. Diaryliodonium salts prepared from tributylphenylstannane and aryliodobis(acetate)s**

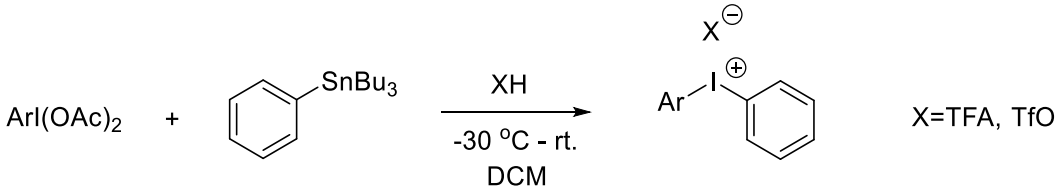


**121** Ar= Phenyl
**122** Ar= 4-Methoxyphenyl
**123** Ar= 2-Methylphenyl
**124** Ar= 2,4,6-Trimethylphenyl

**139** Ar= Phenyl (TFA)
**140** Ar= Phenyl (TfO)
**141** Ar= 4-Methoxyphenyl (TFA)
**142** Ar= 4-Methoxyphenyl (TfO)
**143** Ar= 2-Methylphenyl (TFA)
**144** Ar= 2,4,6-Trimethylphenyl (TFA)

| | **Ar** | **X** | **Isolated yield (%)** |
|---|---|---|---|
| **139** | Phenyl | TFA | 67[a] |
| **140** | Phenyl | TfO | 75[a] |
| **141** | 4-Methoxyphenyl | TFA | 45[a] |
| **142** | 4-Methoxyphenyl | TfO | 50[a] |
| **143** | 2-Methylphenyl | TFA | 43 |
| **144** | 2,4,6-Trimethylphenyl | TFA | 45 |

[a]Isolated yield was the average yield of the reaction

As shown in Table 3, when the aromatic ring was electron-rich ring such as **91**, the yield was lower than when using an electron-deficient arene, which was also found in the preparation of aryliodobis(acetate)s. The yields for substrates with increased steric hindrance such as **143**, **144** were also lower than using just phenyl. This reaction results in good yields of both TFA and TfOH diaryliodonium salts, with triflate salts giving the better yield as the $PhI(OTf)_2$ is a more electrophilic reagent than $PhI(TFA)_2$. In the recrystallization, the diaryliodonium triflates are more easily to form the crystal than diaryliodonium trifluoroacetates, because of the poor dissolvability of diaryliodonium triflates in DCM.

**Table 6. Diaryliodonium salts prepared from 2-(tributylstannyl)thiophene and aryliodobis(acetate)s**

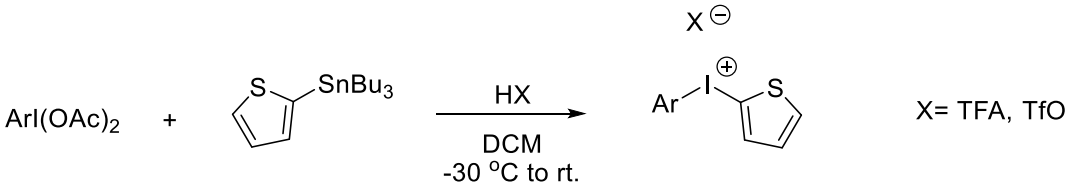


**121** Ar= Phenyl
**122** Ar= 4-Methoxyphenyl
**123** Ar= 2-Methylphenyl
**124** Ar= 2,4,6-Trimethylphenyl

**145** Ar= Phenyl (TFA)
**146** Ar= Phenyl (TfO)
**147** Ar= 4-Methoxyphenyl (TFA)
**148** Ar= 2-Methylphenyl (TFA)
**149** Ar= 2,4,6-Trimethylphenyl (TFA)

| | **Ar** | **X** | **Isolated yield (%)** |
|---|---|---|---|
| **145** | Phenyl | TFA | 23[a] |
| **146** | Phenyl | TfO | 30[a] |
| **147** | 4-Methoxyphenyl | TFA | 18 |
| **148** | 2-Methylphenyl | TFA | 19 |
| **149** | 2,4,6-Trimethylphenyl | TFA | 26 |

[a]Isolated yield was the average yield of the reaction

The synthesis of 2-thienyliodonium salts was similar but when the aryl group is 2-thienyl, the formation of TFA salts and TfO salts gave yields less than 30%. All the 2-thienyliodonium salts would change colour from white crystals to yellow crystals when stored at room temperature in less than two weeks, especially the dithienyliodonium trifluoroacetate salts which would decompose and become black crystals at room temperature within one week (due to the poor stability, this compound was not used in the reaction).

**Method B**

This method could also use an arylboronic acid to replace the arylstannane. The mechanism of preparation of diaryliodonium salts using arylboronic acids is similar.

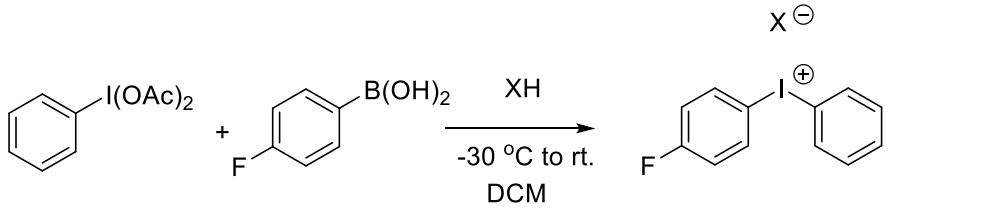


**150** X= TFA (67%)
**151** X= TfO (72%)

**Scheme 46. Diaryliodonium salts prepared from 4-fluorobenzene boronic and aryliodobis(acetate)s**

As the 4-fluorobenzene boronic acid is a commercial product, it was used instead of the arylstannane for the synthesis 4-fluorophenyl(phenyl) iodonium salts.[166] Both TFA, TfOH salts provided around 70% yields. It also provided a label, the $^{19}F$, to monitor the subsequent reactions by NMR (Scheme 46).

**Method C**

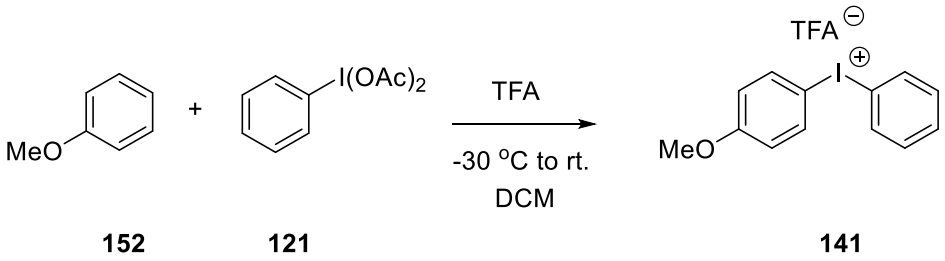


**152** **121** **141**

**Scheme 47 An example of the synthetic route of method C**

Pike reported a direct method using arenes,[167, 168] specifically for those with electron-rich groups, such as anisole instead of using the arylstannane to react with aryliodobis(acetate)s to form diaryliodonium salts. As Scheme 44 shows, the aryliodobis(acetate) only reacts at the *para* position of **152** to generate **141**. This method is also suitable for reactions with sterically large aromatic groups, for example in the case of mesitylene, albeit in a low yield (10%).

**Table 7. Diaryliodonium salts prepared from arenes and arylstannane**

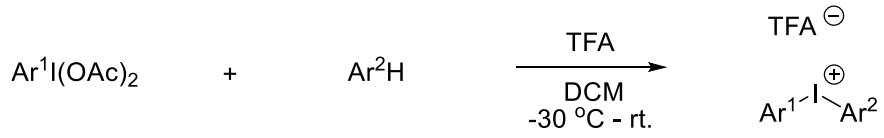


**121** $Ar^1$= Phenyl
**125** $Ar^1$= 2-Thienyl

**152** $Ar^2$= 4-Methoxyphenyl
**153** $Ar^2$= 2-Methyl-4-methoxyphenyl
**154** $Ar^2$= 2-*n*-Butyl-4-methoxyphenyl
**155** $Ar^2$= 2,6-Dimethyl-4-methoxyphenyl
**156** $Ar^2$= 2,4,6-Trimethylphenyl

**141** $Ar^1$= **121** $Ar^2$= **152**
**157** $Ar^1$= **121** $Ar^2$= **153**
**158** $Ar^1$= **121** $Ar^2$= **154**
**159** $Ar^1$= **121** $Ar^2$= **155**
**144** $Ar^1$= **121** $Ar^2$= **156**
**147** $Ar^1$= **125** $Ar^2$= **152**
**160** $Ar^1$= **125** $Ar^2$= **153**
**161** $Ar^1$= **125** $Ar^2$= **155**

| | **$Ar^1$** | **$Ar^2$** | **Isolated yield (%)** |
|---|---|---|---|
| **141** | Phenyl | 4-Methoxyphenyl | 58[a] |
| **157** | Phenyl | 2-Methyl-4-methoxyphenyl | 67 |
| **158** | Phenyl | 2-*n*-Butyl-4-methoxyphenyl | 15 |
| **159** | Phenyl | 2,6-Dimethyl-4-methoxyphenyl | 82[a] |
| **144** | Phenyl | 2,4,6-Trimethylphenyl | 10[a] |
| **147** | 2-Thienyl | 4-Methoxyphenyl | 45 |
| **160** | 2-Thienyl | 2-Methyl-4-methoxyphenyl | 55 |
| **161** | 2-Thienyl | 2,6-Dimethyl-4-methoxyphenyl | 48 |

[a]Isolated yield was the average yield of the reaction

When using an electron-rich ring as one of the arenes in the diaryliodonium salts, especially the 4-methoxyphenyl group, this method provided good yields compared with other methods. But due to the steric hindrance of compounds **158** and **144** less than 20% of the products were obtained. The method was also suitable for the synthesis of 2-thienyliodonium salts **147**, **160** and **161**.

**Method D**

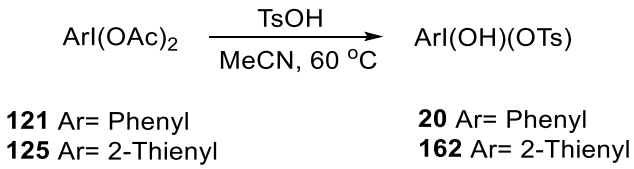


**Scheme 48. Synthesis of Koser's Reagent**

Koser's Reagent is prepared by the addition of *p*-toluenesulfonic acid to a solution of aryliodobis(acetate). The addition of the arylstannane to a DCM solution of Koser's Reagent generates the diaryliodonium tosylates.

**Table 8. Preparation of diaryliodonium tosylate salts**

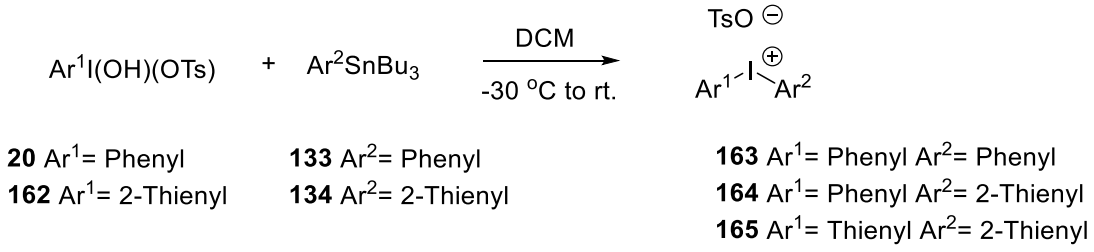


| **Compound number** | **$Ar^1$** | **$Ar^2$** | **Yields (%)** |
|---|---|---|---|
| **163** | Phenyl | Phenyl | 59 |
| **164** | Phenyl | 2-Thienyl | 30 |
| **165** | 2-Thienyl | 2-Thienyl | 30 |

The tosylate salts were prepared in practical yields, although this could be improved. It should be noted that the di(2-thienyl)iodonium salt **165** was more stable than the corresponding TFA salt.

## 2.2 The Structure of Diaryliodonium Salts

X-ray single crystal Diffraction is a non-destructive technique to provide the structure of crystal. According to this technician, we found a novel linear structure diaryliodonium salt in solid state which is different to compare with other diaryliodonium salts.

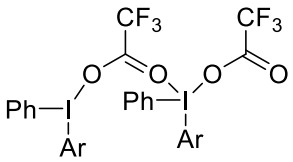


Linear

**166**

O-I distance: 2.804 Å and 2.721 Å

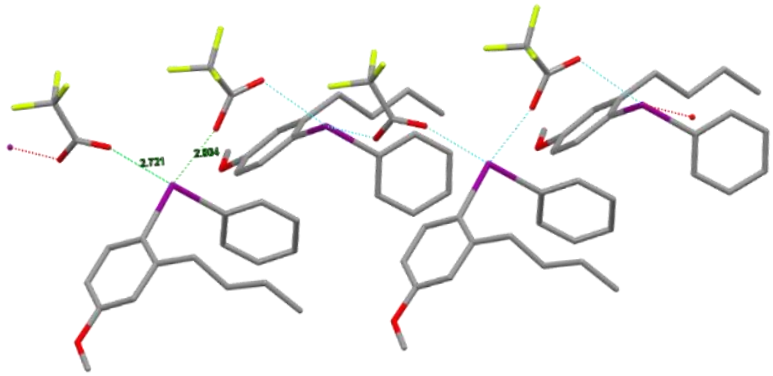


**Figure 9. Linear structure of diaryliodnoium salt**

The recrystallization used DCM-petrol solvent system. The diaryliodonium salt (0.020g) was dissolved in DCM (5 mL) and petrol (1 mL). The clear solution was stored in the fridge for 48 h to form the crystal.

It has been mentioned that there are many reactions using diaryliodonium salts with copper catalysts, however, there is no evidence showing the structures of the copper complexes. After recrystallization, we found three different diaryliodonium salts copper complexes.

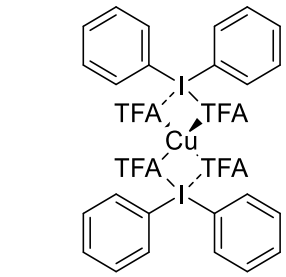


167

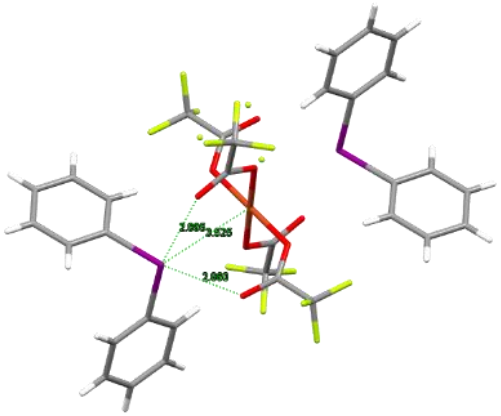

167

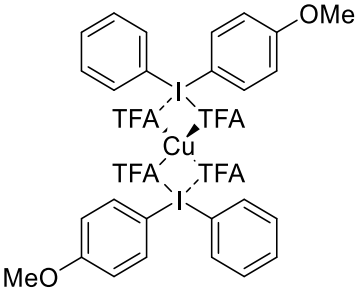


168

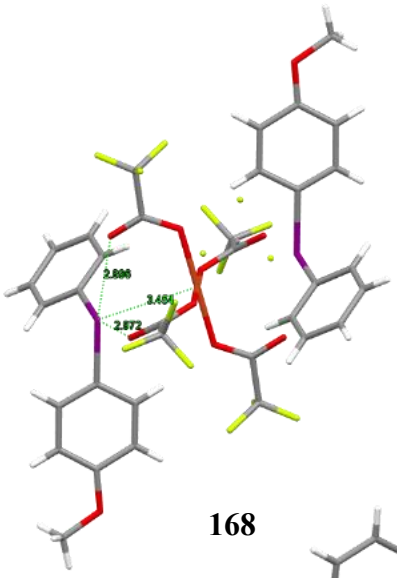

168

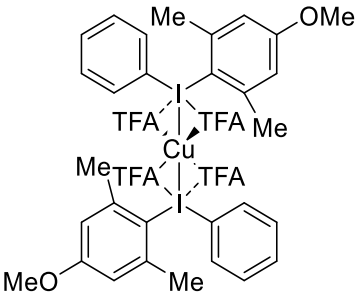


169

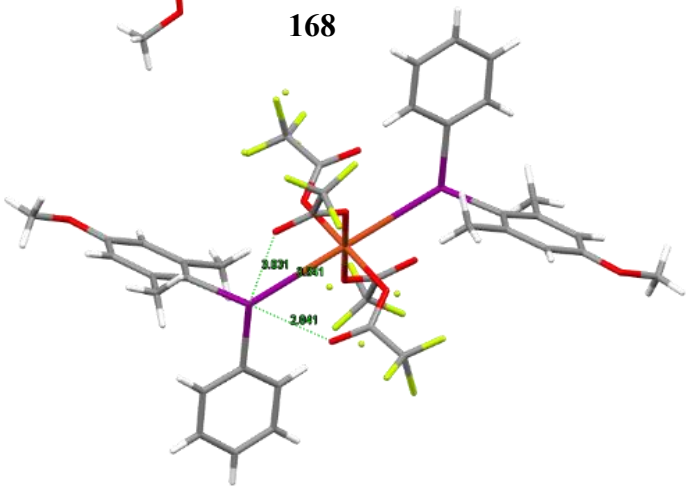

169

**Figure 10. The structure of three different diaryliodonium salts copper complexes**

The recrystallization of the diaryliodonium salts copper complexes used acetonitrile as the solvent. The diaryliodonium salt (0.01 mmol) and copper(II) trifluoroacetate (0.005 mmol) was

dissolved in acetonitrile (5 mL). The clear solution was stored in the fridge for 4 days to form the crystal.

**Table 9. The formation of diaryliodonium salts copper complexes**

| | Diaryliodonium trifluoroacetate | Diaryliodonium triflate | Diaryliodonium tosylate |
|---|---|---|---|
| $Cu(TFA)_2$ | Formed crystal | N/A | N/A |
| $Cu(OTf)_2$ | N/A | N/A | N/A |
| $Cu(OAc)_2$ | N/A | N/A | N/A |

It was found that only diaryliodonium trifluoroacetates with copper(II) trifluoroacetate could form the crystal (Table 9). The diaryliodonium salts copper complexes need to be stored in fridge. It was found that the complexes could decompose at room temperature for 24 h.

In this chapter, we discussed the basic structure of diaryliodonium salts, the navel linear structure and the diaryliodonium salts copper complexes. The EPR and computational studies were used to understand the week interaction between copper and iodine in the copper complexes.

### *2.2.1 Basic Structure of Diaryliodonium Salts*

Much of the research on the understanding of the mechanisms of diaryliodonium salt reactions has been based on the monomeric structure only. In 1977, N. W. Alcock reported the first structure of iodonium salts, and discovered that the diphenyliodonium chloride salts were dimeric structures in the solid state rather than the expectedmonomeric structure (Figure 11) .[169]

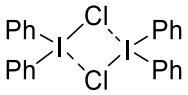


Dimer

**170**

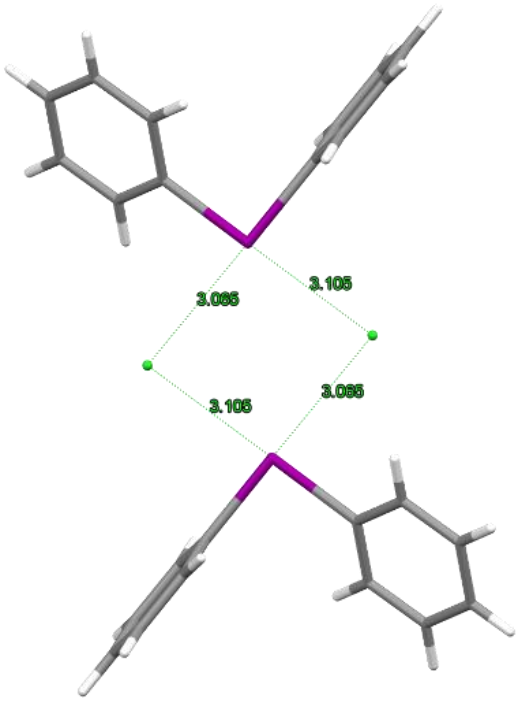


**170**

**Figure 11. Structure of diphenyliodonium chloride**

As shown in Figure 11, the structure of diphenyliodonium chloride salt could be considered a trigonal bipyramid (the monomer), but in the dimer a second counter-ion has a similar distance to the central iodine, which could be described as a secondary interaction.

While in solution, the diphenyliodonium chloride salt dimer **171** might easily fragment to give the monomeric structure **172**, and then dissociate further to give the free diaryliodonium cation (Scheme 49).

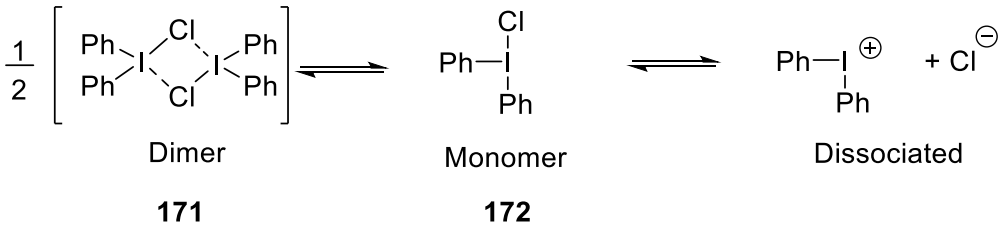


**Scheme 49. Proposed transfer pathway from dimer to monomer**

However, when the aromatic groups are different in the diaryliodonium salt, and because of the similar distances between these two counter-ions and the central iodine the monomers might exist in two isomeric forms such as **173** and **174** in which the relative positions of the aromatic groups would be different, when the diaryliodonium salts transfer to the monomeric forms **175**, **176** this may be retained and could effect the subsequent reaction selectivity (Scheme 50).

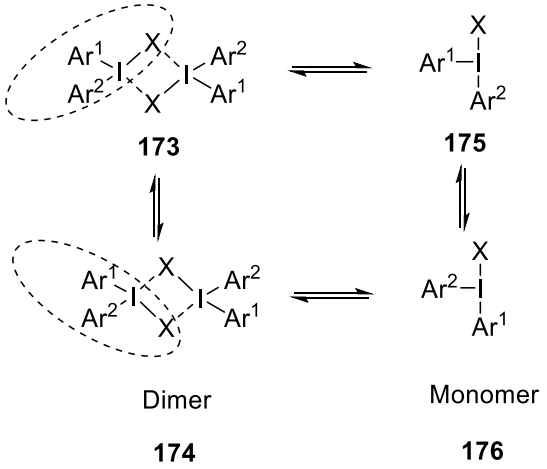


**Scheme 50. Proposed pathway from dimer to monomer in solution**

It has been suggested that these two monomers could easily be interconverted by Berry pseudo rotation, however this lower energy pathway which would result in the same outcome, and the substituent effects in these transition states are almost completely additive compared to the monomers.[36]

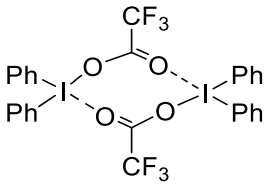


Dimer

**177**

O-I distance: 2.865 Å and 2.832 Å

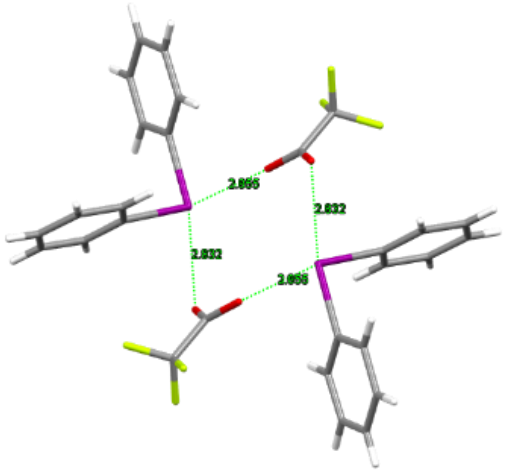


**177**

**Figure 12. Structure of diphenyliodonium triflate**

Diaryliodonium salt dimers are not only possible with mono atomic counter-ions such as $Cl^-$, $Br^-$ and $I^-$,[169, 170] but also for more complex counter-ions,[171, 172] It was found that the diphenyliodonium salts with complex counter-ions such as trifluoroacetate **177**, tosylate **178** and triflate **179** (Figure 13) also form dimers in solid state (X-ray structures were determined by previous group members).

As Figure 12 shows, the compound **177** is different from the monomer, the two oxygen atoms in the trifluoroacetate connect with different iodines to form an eight membered ring.

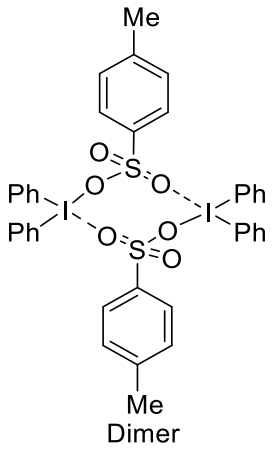


**178**

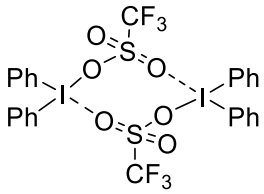


**179**

O-I distance: 2.915 Å and 2.876 Å

O-I distance: 2.887 Å and 2.846 Å

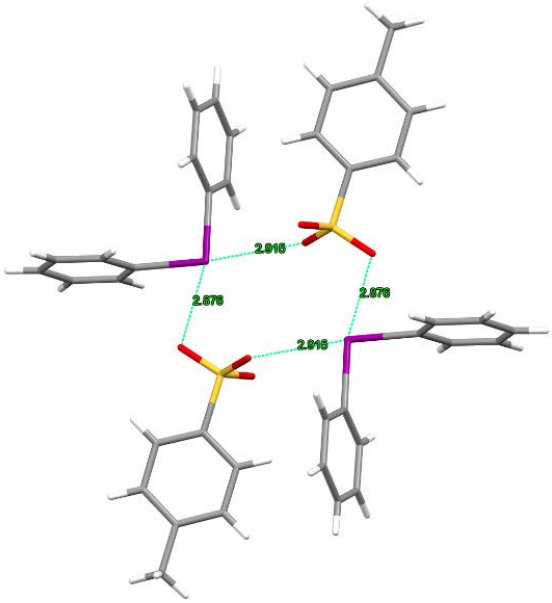


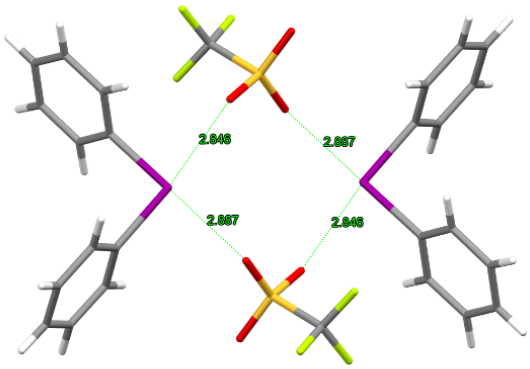


**178** **179**

**Figure 13. Structure of diphenyliodonium tosylate[173] and triflate[171]**

In the structure of diphenyliodonium tosylate **178** and triflate **179**, both the tosylate and the triflate groups contain three oxygens which suggests it might be three weak I-O interactions, however, according to the X-Ray structures, both of them are similar to the diphenyliodonium trifluoroacetate **177**, with two of three oxygen atoms connecting with each of the iodines to form an eight member ring (Figure 11).

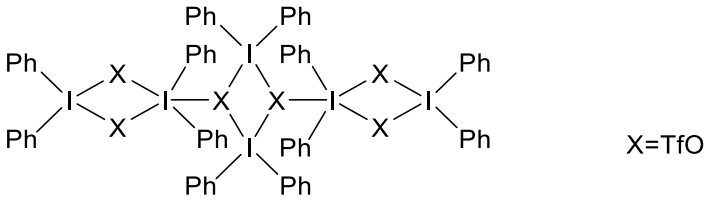


**180**

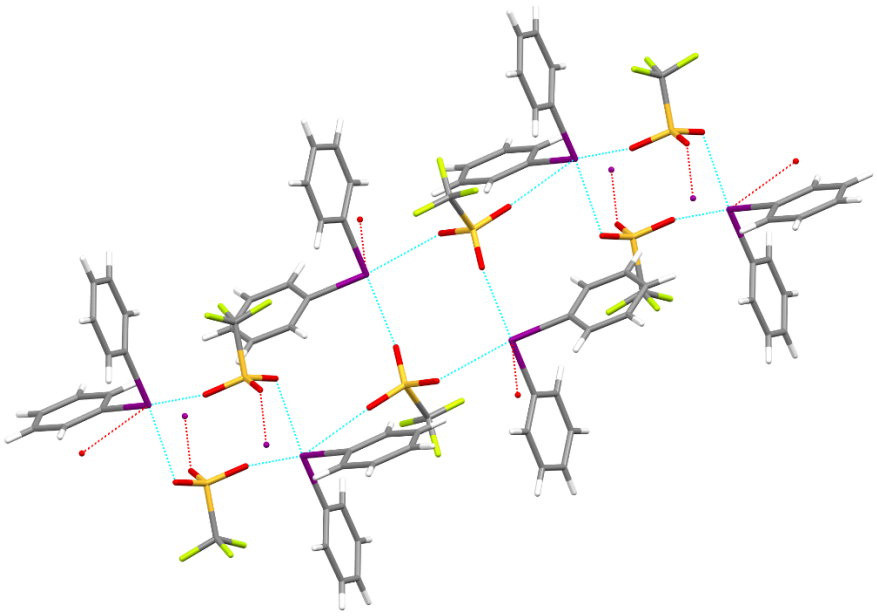

**180**

**Figure 14. Network structure of diphenyliodonium triflate**

Diphenyliodonium tosylate **178** is a single dimer in the crystal, however, diphenyliodonium triflate **180** is different, these three oxygen atoms have interactions with three different iodine atoms. As Figure 14 shows, the triflate counter-ions connect different dimers to form a network structure in the crystal, and the dimers are alternately linked together.

The dimeric structure is the most common structure in diaryliodonium salts, although different counter-ions containing different number of atoms have the chance to form further interactions with iodine such as the oxygens in TFA (two oxygens) and TfO (three oxygens). There may also be interactions between the counter-ions, the iodine and any functionality on the aromatic rings. For example in 2003, an iodonium zwitterion was reported that formed linear structure.[174]

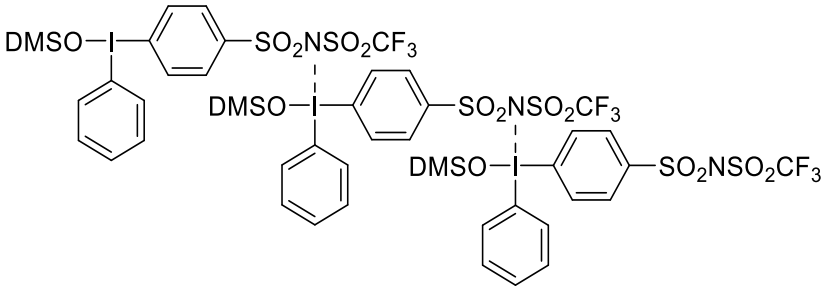


Linear

**181**

O-I distance: 2.691 Å  N-O distance: 2.949 Å

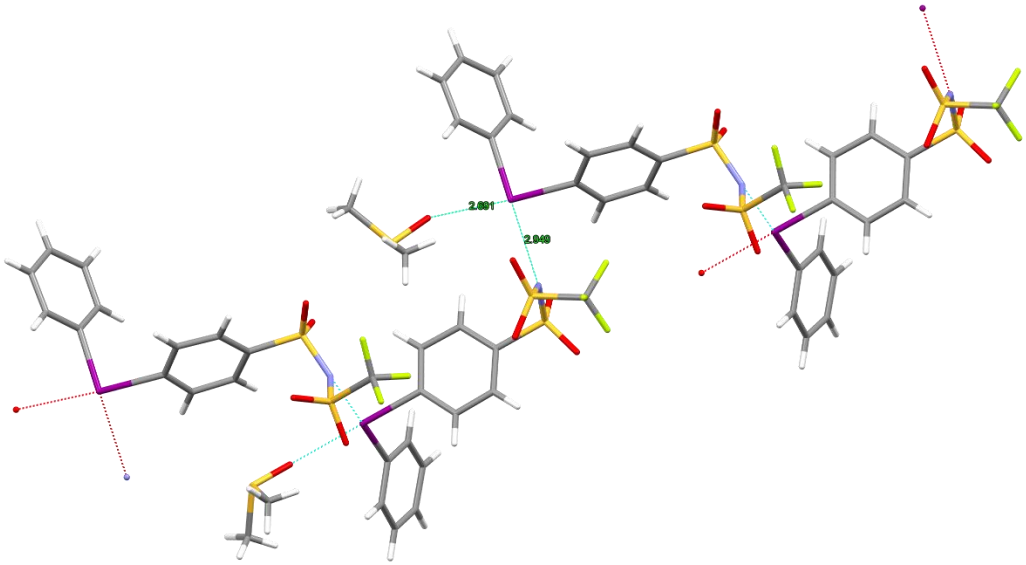


**181**

**Figure 15. Linear structure of iodonium zwitterions**

The iodonium zwitterions with DMSO **181** form a linear structure, which is different from other diaryliodonium salts, the iodine is coordinating to the nitrogen atom of the aryl substituent which results in the linear structure.

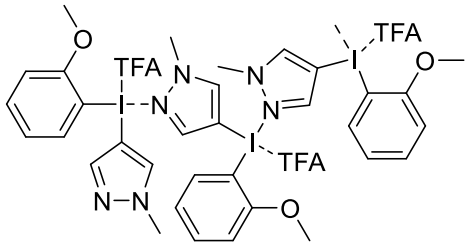


**182**

O-I distance: 2.656 Å  N-O distance: 3.060 Å

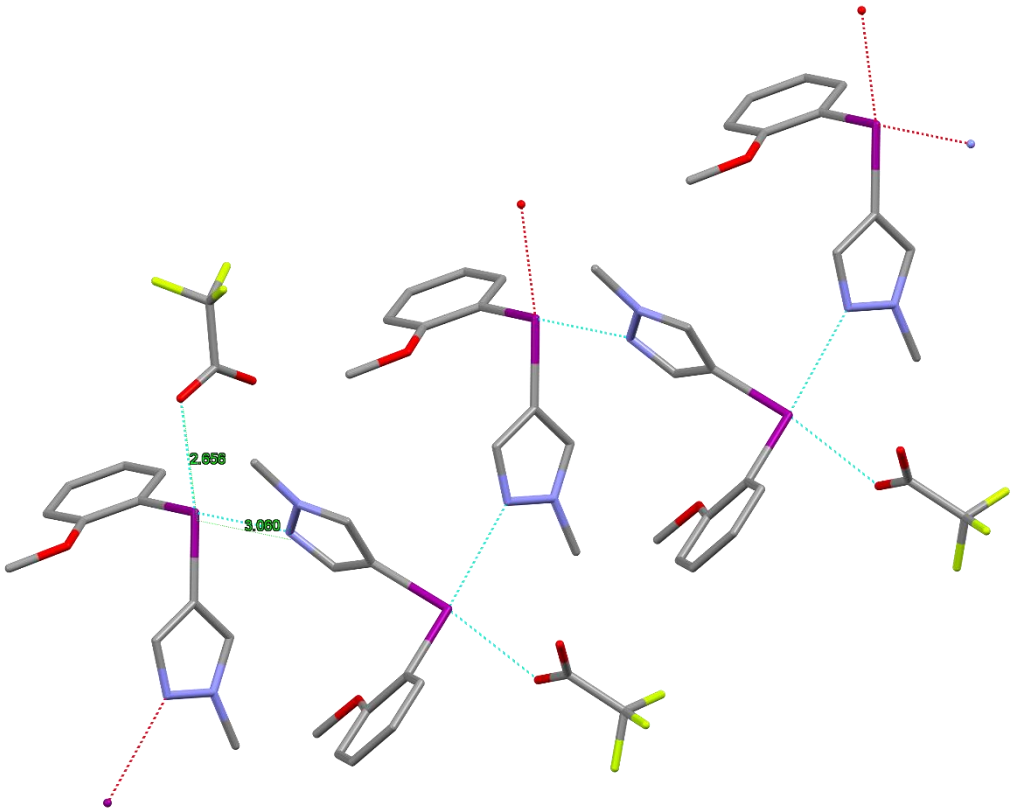


**182**

**Figure 16. X-Ray crystal structure of linear structure diaryliodonium salt**

It was found by John L Woodcraft that this analogue also formed a linear structure. The nitrogen in the pyrazole coordinates the iodine in another diaryliodonium salt to form the linear structure.[175]

To the best of our knowledge, there is no reported linear structure linked just by the counter-ions in diaryliodonium salts. The X-Ray crystal structure of diaryliodonium salt **166** appears to be the first example of a linear structure instead of the more usual dimers. (Figure 15)

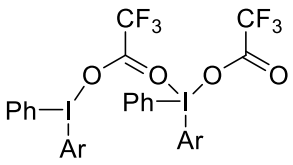


Linear

**166**

O-I distance: 2.804 Å and 2.721 Å

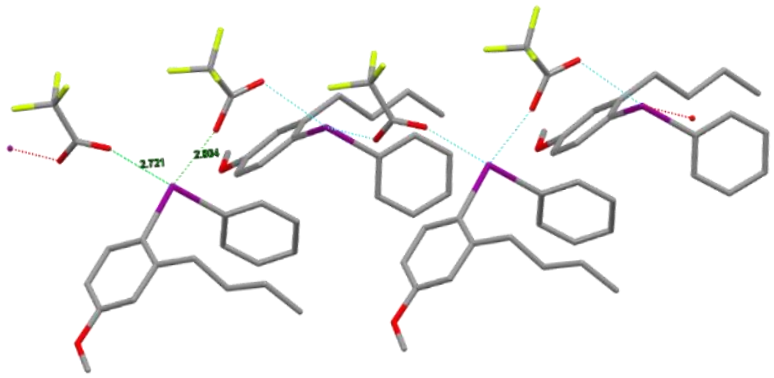


**Figure 17. Linear structure of diaryliodnoium salt**

We propose that the *n*-Butyl group generates efficient steric hindrance which pushes the second diaryliodonium fragment further away. The distances of these two counter-ions to the hypervalent iodine are 2.721 Å and 2.804 Å, the difference is 0.083 Å. To compare this with diphenyliodonium trifluoroacetate **170** in which the difference in the distances for counter-ions is only 0.017 Å.

As most of the diaryliodonium salts exist as a dimeric structure, the structure of diaryliodonium salt **166** is different to the others and may be considered to be 'monomeric' in reactions.

### *2.2.2 Structure of Diaryliodonium Salt Copper Complexes*

It has been shown in introduction that there are various mechanisms proposed for the copper catalysed arylation reaction using diaryliodonium salts.

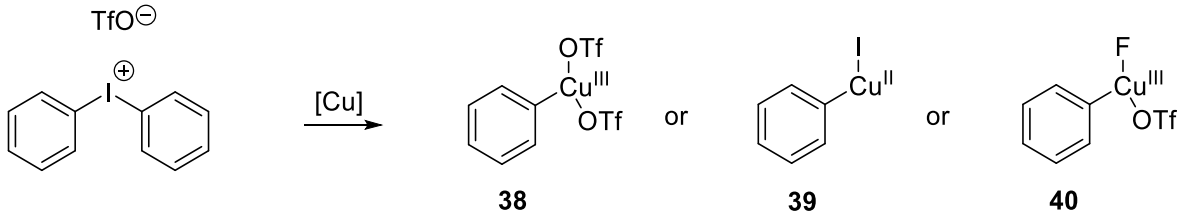


**Scheme 51. The intermediates of copper catalyst reaction**

In these mechanisms the proposed intermediates were reported and some of them have also been studied by computational methods (Scheme 48 **38**, **40**).[176] Unfortunately the intermediates have no XRD or other data to support these structures.

In order to explain the mechanism of the copper cataylsed reaction the isolation of the intermediates was attempted and the isolated compounds subjected to X-Ray crystal analysis. Diaryliodonium salts with different counter-ions have allowed a series of copper complexes to be prepared using this procedure and it was found that only the combination of diaryliodonium trifluoroacetates and copper (II) trifluoroacetate gave a new type of material with triflates and tosylates resulting in no change.

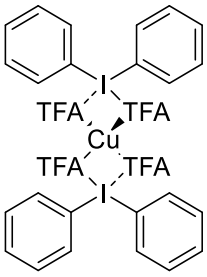


**167**

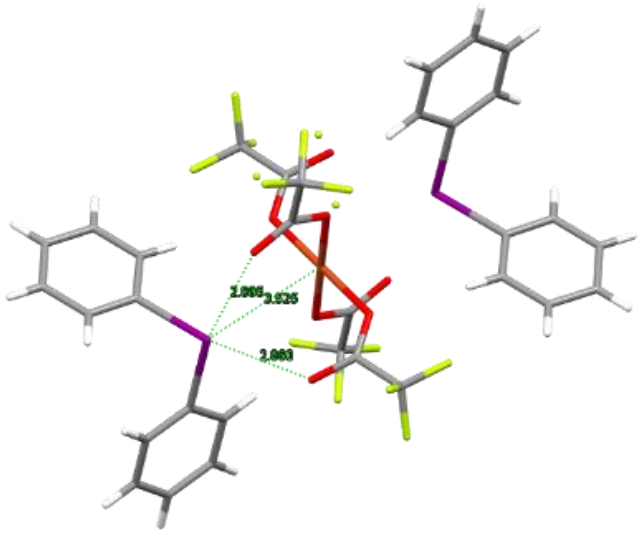

**167**

**Figure 18. Structure of diphenyliodonium copper tetratifluoroacetate complex, 167**

The bis(diphenyliodonium) copper tetratrifluoroacetate complex **167** had some structural features similar to the diphenyliodonium salt dimer structure **170** in which the distances from the counter-ions to the hypervalent iodine and the angle between two phenyl groups is similar.

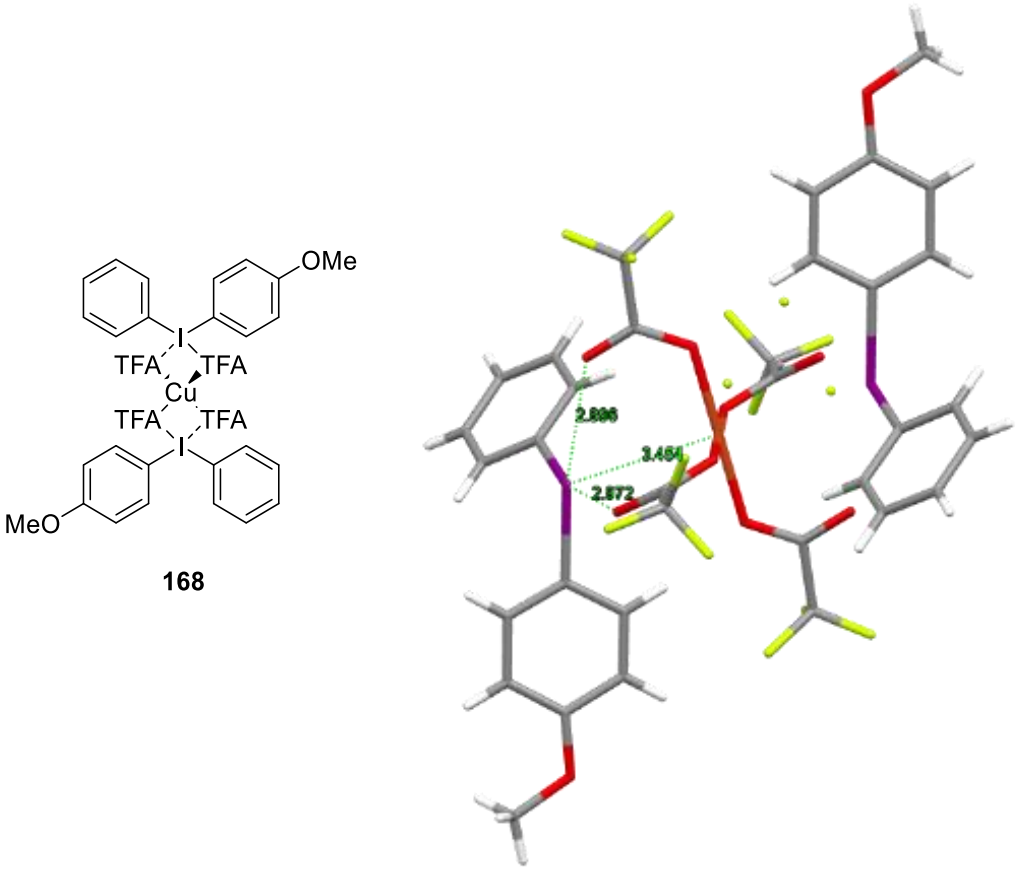


**Figure 19. Structure of diaryliodonium (141) copper tetratifluoroacetate complex 168**

As Figure 17 shows that the 4-methoxyphenyl(phenyl)iodonium trifluoroacetate salt **141** also forms the corresponding copper complex **168**. The difference in distance between the two counter-ions and the hypervalent iodine is about 0.076 Å. This structure is similar to the bis(diphenyliodonium) copper tetratrifluoroacetate complex, the angle between the two phenyl groups is also similar, which suggests that the addition of an electron-donating group to one ring dose not change a lot in the structure of the copper complex.

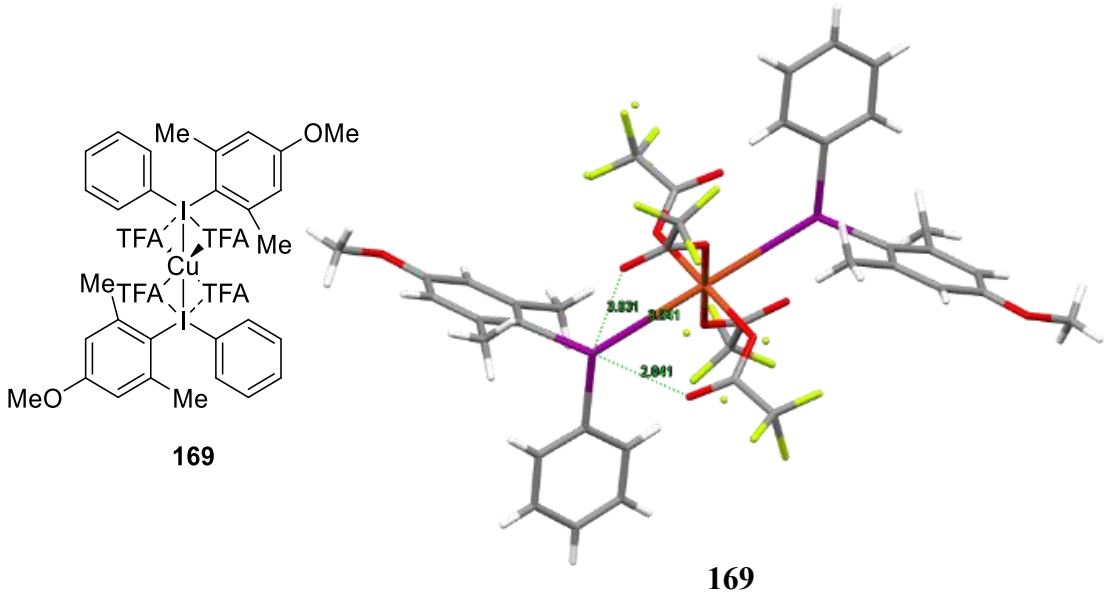


**Figure 20. Structure of diaryliodonium (144) copper tetratrifluoroacetate complex 169**

However when the diaryliodonium salt **144** forms the copper complex **169**, the basic structure is the same however with one critical difference. The distance from the counter-ions to the hypervalent iodine are now 3.031 Å and 2.841 Å, with the difference now increasing to 0.090 Å. The angle between the aryl groups has also been changed which could suggest that steric hindrance is now an important factor in the structure of the copper complex.

**Table 10. The distance from different copper complexes**

| Compound | Distances between the counter-ions and the iodine (Å) | | The difference distance (Å) | Distances between the copper and the iodine (Å) |
|---|---|---|---|---|
| | Shorter | Longer | | |
| **167** | 2.860 | 2.895 | 0.035 | 3.525 |
| **168** | 2.896 | 2.972 | 0.076 | 3.454 |
| **169** | 2.841 | 3.031 | 0.190 | 3.341 |

In the literature it has been suggested that the steric effect resulting in the selectivity was because the copper atom is a large atom and this is pushed away from the large ring. But in Table 10, the diaryliodonium copper complex **169** has the shortest distance between copper and hypervalent iodine which is 3.341 Å, this is now below the combined van der Waals radii (1.40+1.98=3.38 Å) and suggests a Cu-I(III) interaction. It also shows that one methyl group of the trisubstituted arene sits in between the two counter-ions.

The centre of the diaryliodonium copper complex is the same in these three compounds, but the postion of diaryliodonium salts and the distance between the counter-ions and the iodine are different which could suggest that it might be because of the steric hindrance influenced the position of this ring. In order to have the lowest energy in this system, one of the two methyl groups has to be in the middle of two counterions, and this also suggests if there is only a single 2-position substituent, then this group could be positioned away from the two counter-ions which could not provide the good selectivity like 2,6-disubstitution.

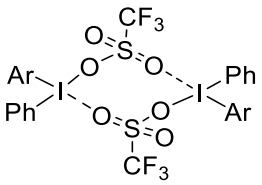


Dimer

**183**

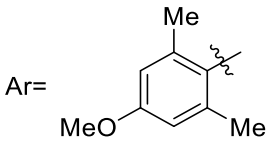


O-I distance: 3.048 Å and 2.827 Å

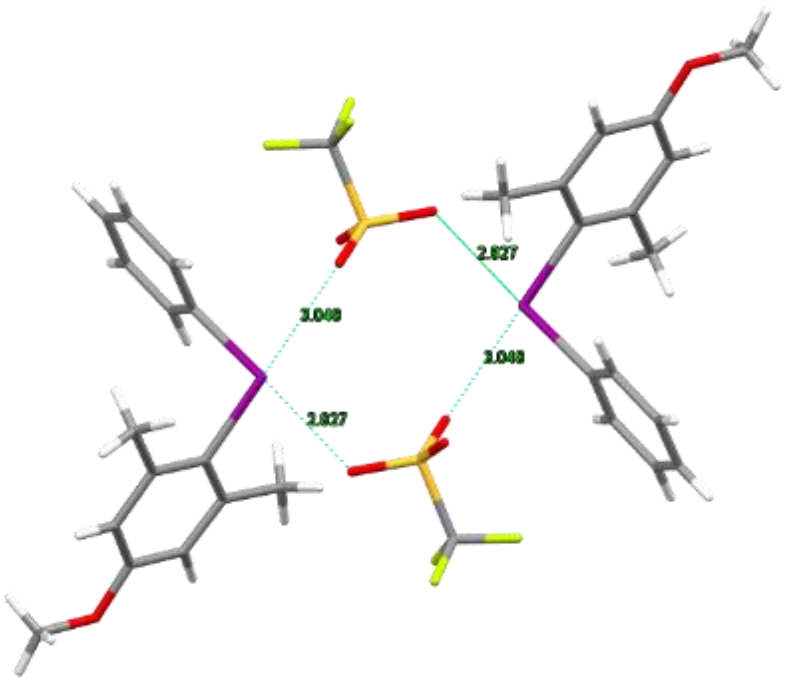


**183**

**Figure 21. Structure of diaryliodonium triflate**

When diaryliodonium trifluoroacetate salt **144** was mixed with copper (II) triflate, it did not form the same type of complex in the solid-state, crystal structure analysis indicated that the diaryliodonium salt only underwent counter-ion exchange to form the diaryliodonium triflate salt **183** rather than adopting the arrangement seen when the copper salt and the diaryliodonium salt had the same counter-ion: trifluoroacetate.

### *2.2.3 The EPR Study of Diaryliodonium Copper Complexes*

EPR (electron paramagnetic resonance) also named ESR (electron spin resonance) is a method for studying compounds with unpaired electrons. It is a magnetic resonance phenomenon in which spin electrons under a static magnetic field which is similar to the phenomenon of spin nuclear (NMR).[177, 178]

Since most of the electrons in the molecule exist in pairs, according to the Pauli exclusion principle, the two electrons in each electron pair must have one spin upward and the other spin downward, so the magnetic properties cancel each other out. Therefore, only particles with unpaired electrons (such as heavy metal atoms or free radicals) can express magnetic resonance. [174]

Although the principle of electron spin resonance is similar to that of nuclear magnetic resonance, since electrons are much lighter than the mass of the nucleus, electrons have a large magnetic moment.

According to the EPR spectroscopy, the electronic state of metal atoms can be determined, and this method could analyse the material both in solution or in the solid state.

Thus, EPR can be used for analysis of these copper complexes. The complexes were sent to Cardiff University and the analysis was carried out by Dr Emma Richards.

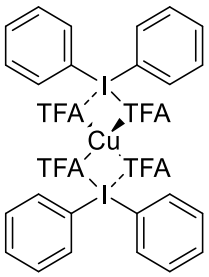


**167**

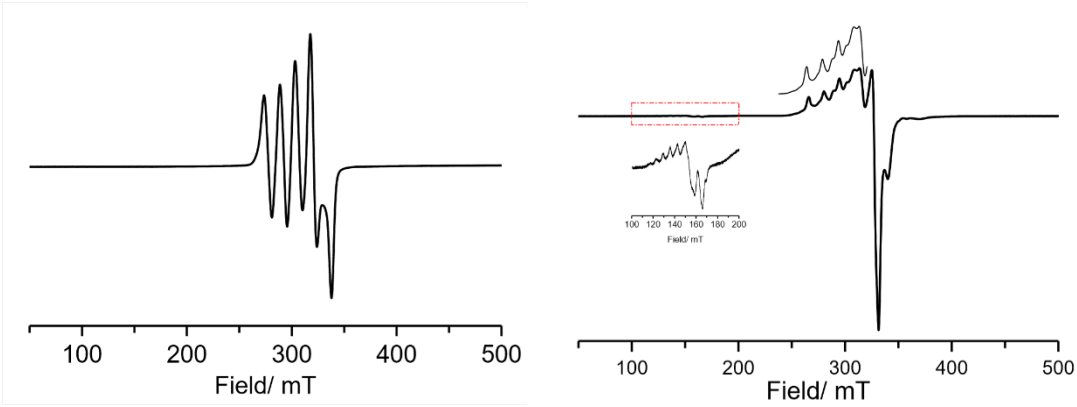


**Figure 22. EPR data for 148 in solid state and in solution**

The signal between 250-400 mT arises due to a single isolated $Cu^{2+}$ species, with predominantly axial symmetry (although there is some rhombic distortion, which must arise from the symmetry of the complexes). The copper hyperfine structure is clearly resolved in one orientation, but unfortunately, there is no resolution of any superhyperfine structure originating from any coordinating ligand nucleus (i.e. the iodine).

The features between 100-200 mT are characteristic of a "half-field" transition, which arises due to a formally forbidden $\Delta ms = \Delta 2$ transition. This is typically characteristic of spin-exchange, which might be due to the formation of dimers or stacking.

This data suggests that the complex **167** might not contain the Cu-I bond.

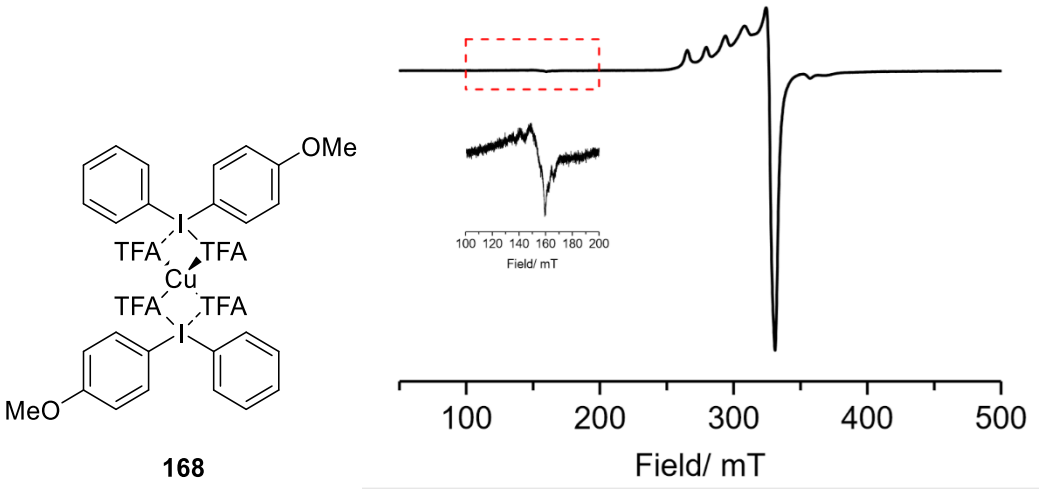


**Figure 23. EPR data for 149 in solution**

The data for **168** is similar to the data for **167**, which also suggests there may be no Cu-I bond. The complex **169** was also sent to Cardiff University but unfortunately, the data proved complex and has not yet been resolved.

### *2.2.4 The Computational Study of Diaryliodonium Copper Complexes*

Recently, a Pb-I non-covalent interaction was reported, they suggested there was an interaction due to that the Pb-I distance was shorter than the Bondi's van der Waals radii (3.885 Å vs. 4 Å). The authors also provided an electrostatic potential data to support it.[179]

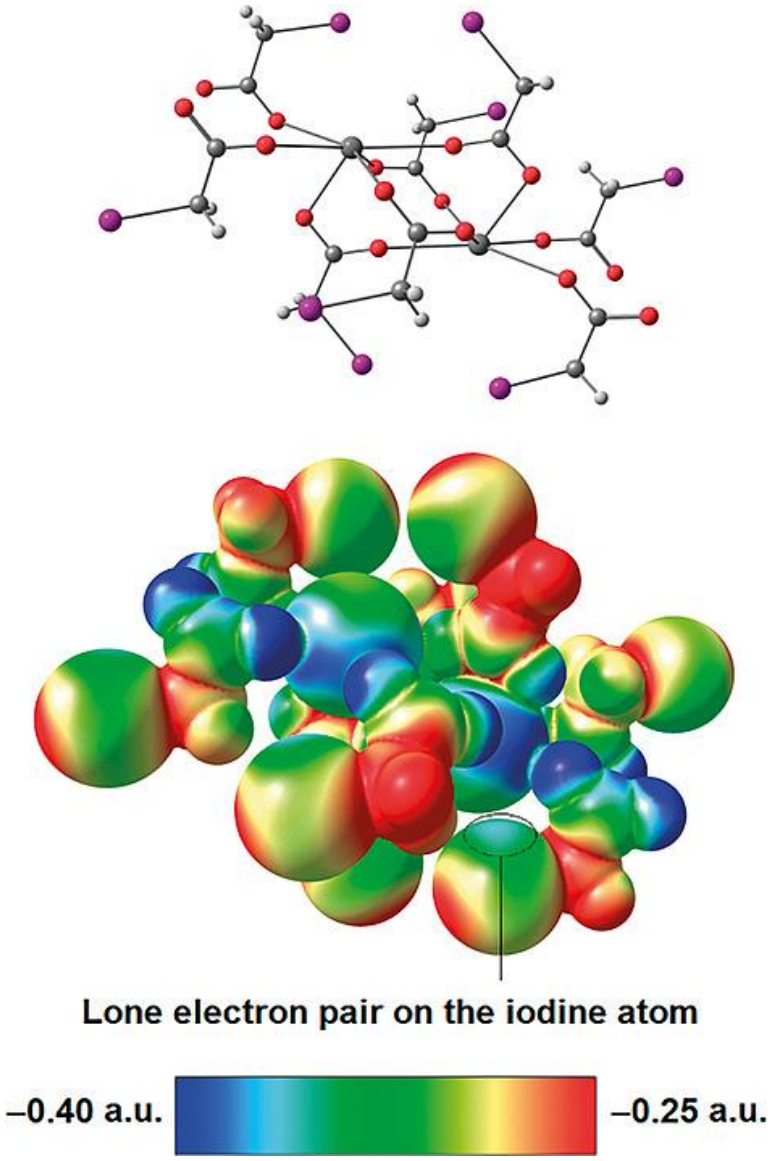


**Figure 24. The Distribution of electrostatic potential calculated on the molecule surface**

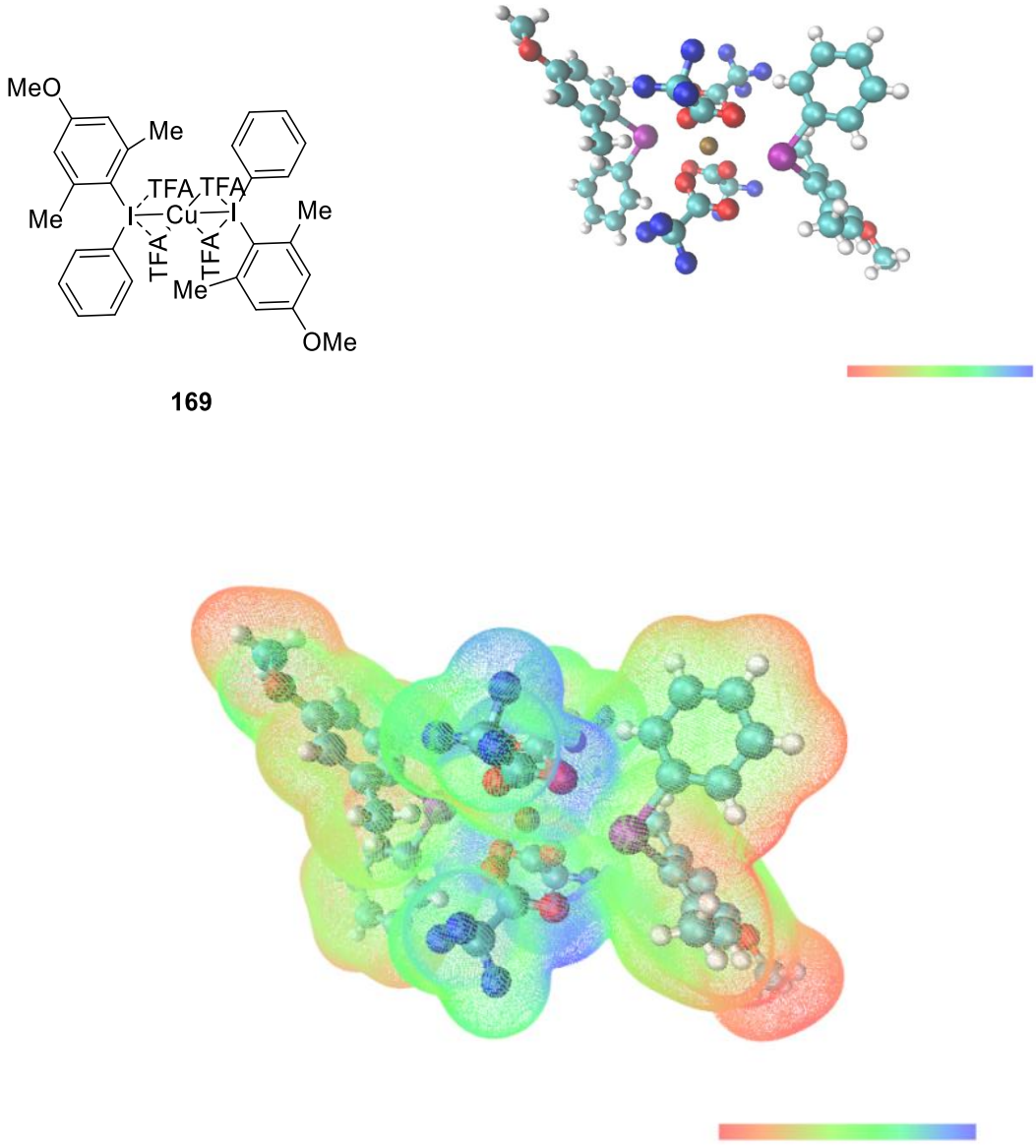


**169**

**Figure 25. Distribution of electrostatic potential calculated on the complex (169) surface**

For the complex **169**, the Cu-I distance was also shorter than the Bondi's van der Waals radii, thus we used the same method to do the calculation. Calculations used the DFT method on the B3LYP density functional level in Gaussian 09. The basis set was MIDIX[180] which has provided good results in the study of hypervalent iodine compounds and 6-31G* for Cu. The electrostatic potential was calculated by Multiwfn.

As the centre of diaryliodonium complexes is crowded, it is hard to determine the electronic density between Cu and I, but it is clear that between the oxygen and iodine there is a strong interaction, which suggests the centre of diaryliodonium complex is a result of the interaction of oxygen and iodine. It could explain why the centre of diaryliodonium complexes is similar in these three complexes but the distance of Cu-I is different, and also provide an explanation of why the 2,6-disubstitution is more effective than only 2-substitution.

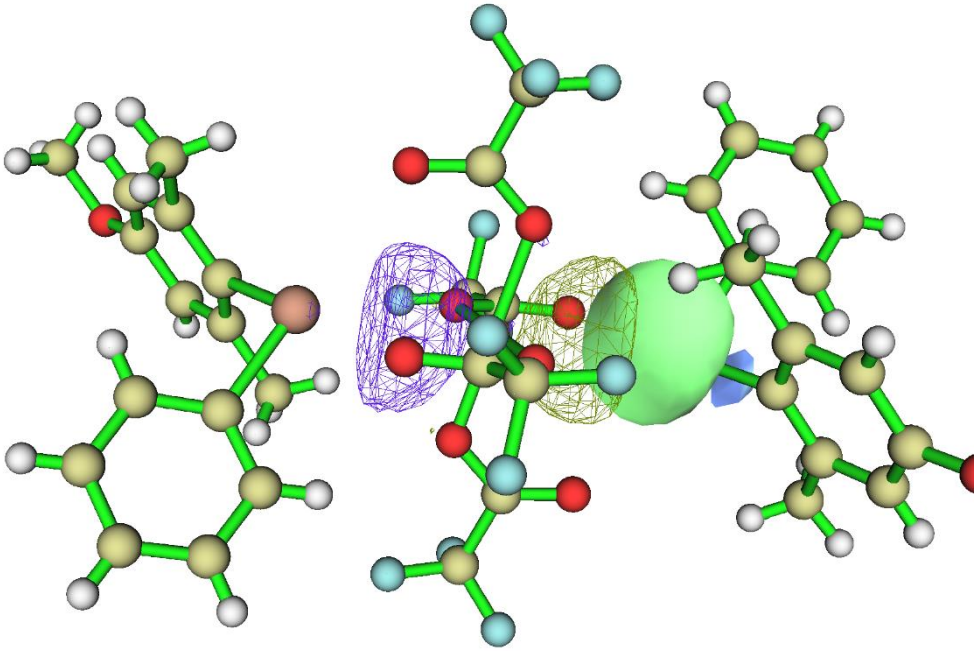

**Figure 25. NBO data for complex 169**

According to the natural bond orbitals (NBO) analysis, there is a weak interaction between copper d anti-bonding orbital and iodine lone pair as shown in Figure 25. But it still has no evidence that there is a real bond between copper and iodine.

## 2.3 Thermal Stability of Diaryliodonium Salts

Diaryliodonium salts are widely used in different reactions and often under mild conditions, but when the reaction temperature is increased, unwanted by-products such as biphenyl[181] are generated. Much of the work on proposed reaction intermediates has assumed thermal stability of the diaryliodonium salt and this has been based on melting points, however, decomposition of the diaryliodonium salt appears to take place rather than the sample just melting. To address this fundamental issue, we have explored DSC-TGA data and computational studies to provide evidence of the effect of structure on the thermal stability of diaryliodonium salts.

### *2.3.1 Computational Study of Diphenyliodonium Salts*

Understanding the possible processes of diaryliodonium salt decomposition is critical to understand the thermal stability of the diaryliodonium salt, and how and why the by-products may be generated in the reactions of diaryliodonium salts. Computational studies were investigated to help understand these processes.

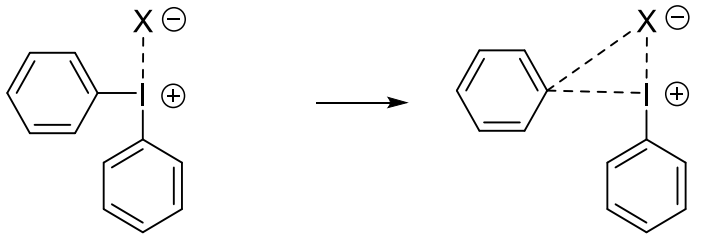


**14** **184**

X=TFA, TfO, TsO, $PF_6$, Br, Cl, $NO_3$

**Scheme 52. The model process of diphenyliodonium salts decomposition reductive elimination**

In diphenyliodonium salt **14** decomposition, we suggest that the pseudo equatorial bond between carbon and hypervalent iodine is broken and then generating intermediate **184** as a

possible decomposition process, this is nucleophilic substitution process by which diaryliodonium salts act as arylating agents. Geometries of all diaryliodonium salts were initially defined using the crystal data from CCDC or Newcastle University crystal analysis database. Calculations used the DFT method on the B3LYP density functional level in Gaussian 09. The basis set was MIDIX[180] which has provided good results in the study of hypervalent iodine compounds.

The length of the bond between the pseudo equatorial carbon and the hypervalent iodine was scanned 20 steps of 0.1 angstrom each. Analysing the scan plot of total energy when the distance changed and the final step product, to determine a point at when the bond breaks and hence the decomposition process occurs.

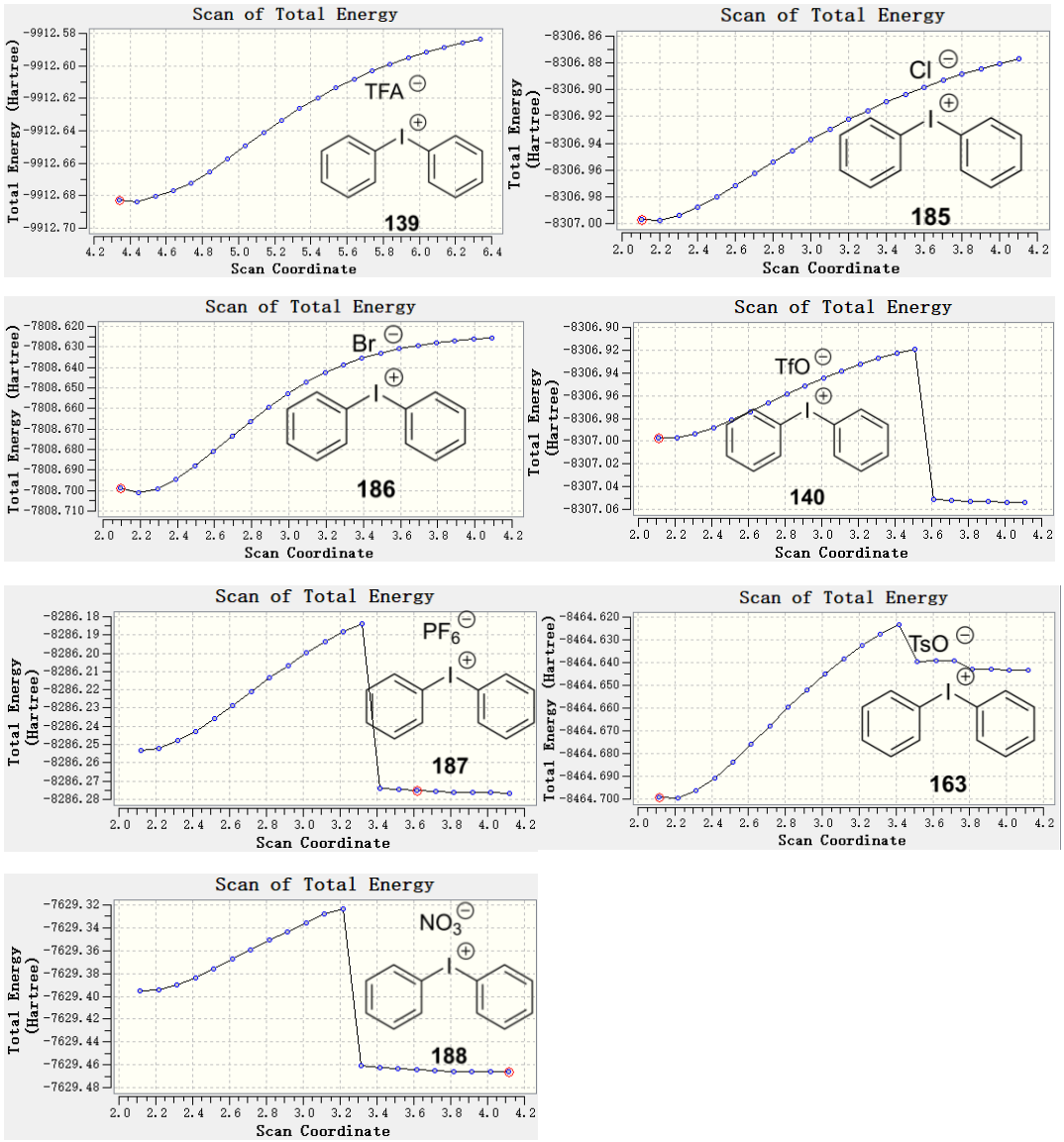


**Figure 26. The scans of total energy of diphenyliodonium salts with different counter-ions**

As the data in Figure 26 shows, the diphenyliodonium salts with the TFA (**139**), Br (**186**), Cl (**185**) counter-ions all have similar curves, as the distance increases, the total energy increases. The diphenyliodonium salts with TfO (**140**), $PF_6$ (**187**), TsO (**163**) and $NO_3$ (**188**) counter-ions would form the new compounds, and the energies would drop once the new compounds were formed.

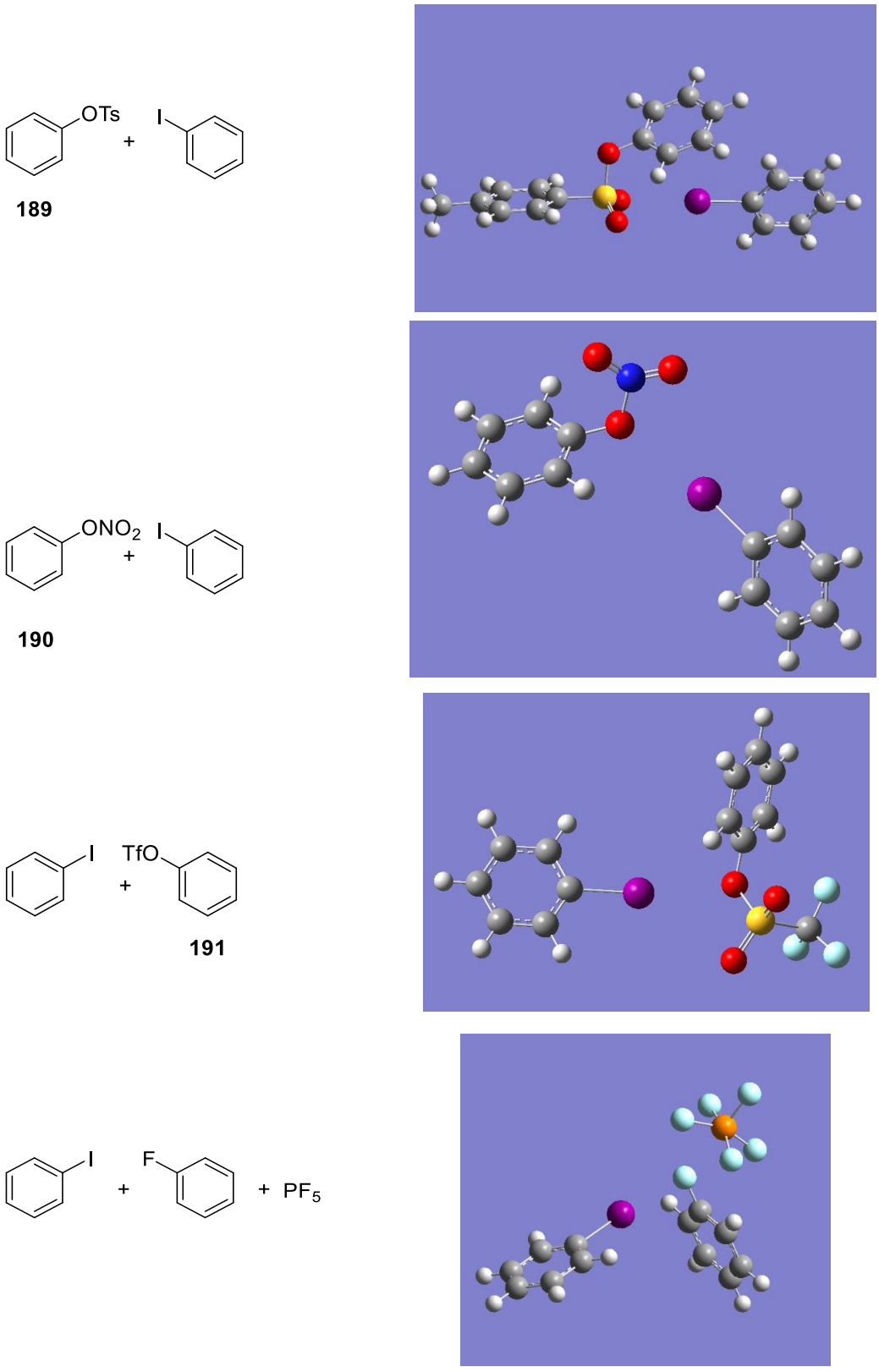


**Figure 27. The result of the final step in decomposition of diphenyliodonium salts**

The computational results for the last step in the simulation suggest the counter-ion could attack the phenyl ring and that the different counter-ions undergo different process. The diphenyliodonium salts with TFA, Br, Cl counter-ions will decompose to phenyl radical, counter-ions and iodobenzene. Whereas the results of the final step in decomposition of diphenyliodonium salts with $PF_6^{\ominus}$ (**187**), $TfO^{\ominus}$ (**140**), $TsO^{\ominus}$ (**163**) and $NO_3^{\ominus}$ (**188**) (Figure 27).

The decomposition of diphenyliodonium salts could be separated to three groups (Scheme 53).

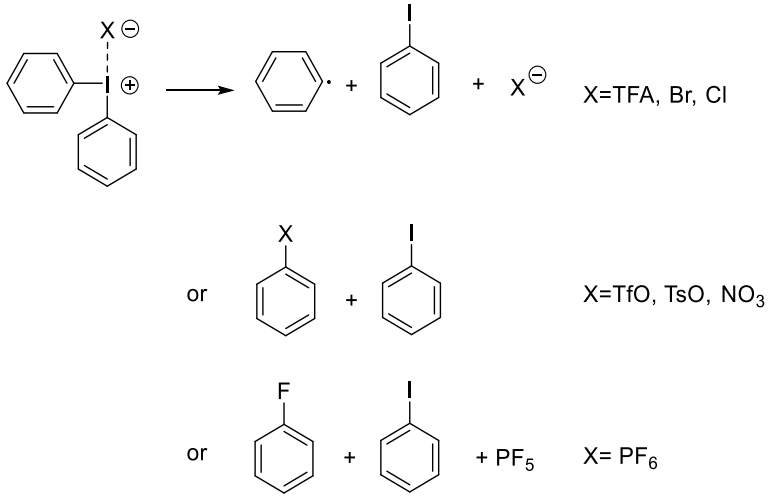


**Scheme 53. Proposed pathway of diphenyliodonium salts decomposition**

It is clear that the diphenyliodonium hexafluorophosphate would lose one fluorine atom to form fluorobenzene and stable phosphorus pentafluoride, the triflate and tosylate would attack the phenyl radical generating PhOTf and PhOTs respectively.

### *2.3.2 DSC-TGA Analysis of Diaryliodonium Salts*

Thermogravimetric analysis (TGA) is a method in which the mass of a sample is measured at different temperatures.[182] Differential scanning calorimetry (DSC) is also a thermal analysis technique, which measures the difference in the amount of heat required to increase the temperature of a sample and a reference.[183]

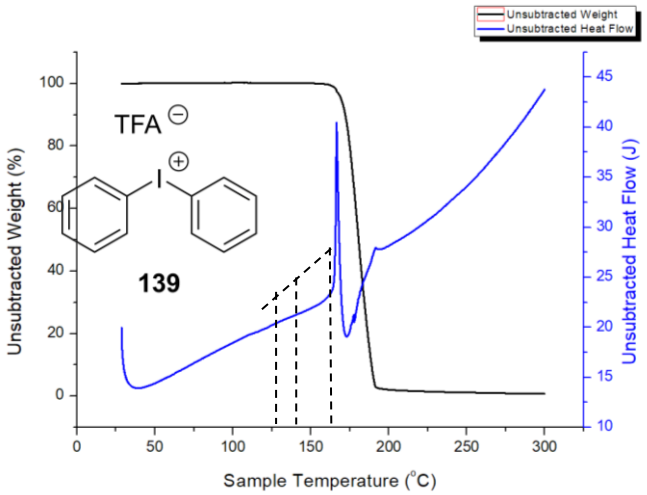


**Figure 28. An example of DSC-TGA curves for diphenyliodonium trifluoroacetate, 108**

DSC is often used in combination with TGA to determine the possible fate of the sample from the endothermic and exothermic sections of the DSC curve and the corresponding TGA curve to identify the process occurring at the transition.[184]

The DSC-TGA curve shown in Figure 28 indicates that from 164 ℃ to 169 ℃, the unsubtracted heat flow is increasing which means the whole system requires energy, which suggests the temperature is the melting point of diphenyliodonium trifluoroacetate. From 169 ℃ to 191 ℃ the curve shows the unsubtracted heat flow is decreasing which means the total system releases energy. To combine the DSC and TGA, it is clear that for diphenyliodonium trifluoroacetate the thermal decomposition started before its melting point, and the decomposition process overall releases energy.

It has been demonstrated that different counter-ions[185] and different aromatic groups[63, 186] can affect the stability of diaryliodonium salts, generally the more electron-rich the aromatic rings the less stable the diaryliodonium salt appears to be, but there is no quantitative indicator to support this. DSC-TGA provided a quantitative indicator to identify the stability of various diaryliodonium salts.

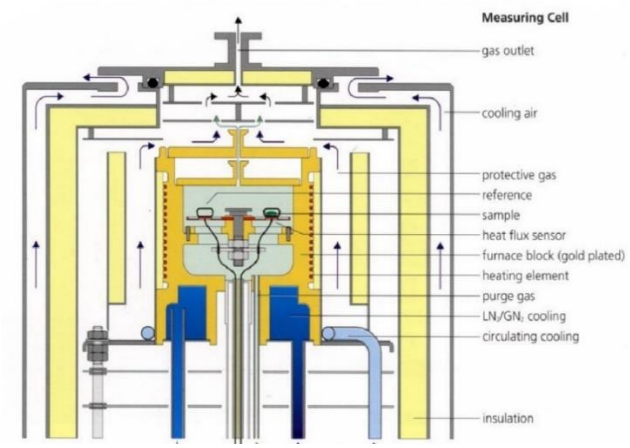


**Figure 29. DSC-TGA Measuring Cell**

Thermograms were obtained using a Perkin-Elmer Simultaneous Thermal Analyzer (STA)-6000. In this instrument, the sample is heated at a preselected rate in a controlled atmosphere. As the sample undergoes an endothermic transition, the extra power required to maintain the selected heating rate in the sample is plotted against its linearly increasing temperature, at the same time, the mass of a sample is measured and recorded. During a run, the sample chamber is continuously swept by a nitrogen flow to remove any volatiles generated in the heating process. In addition, the heating chamber was swept with nitrogen for at least 15 min prior to each run. The signal from the STA was used to plot the thermogram.

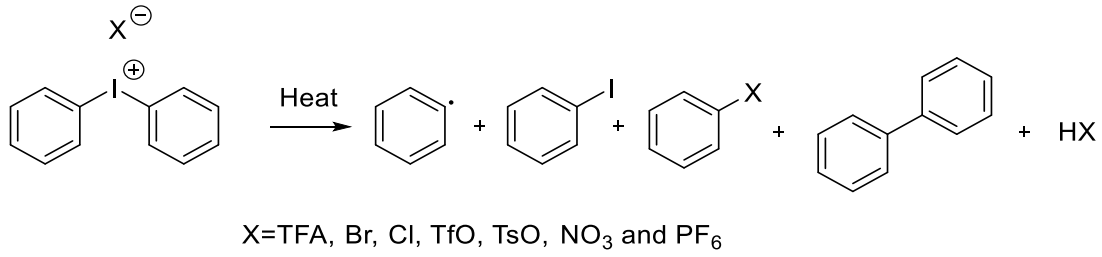


**Scheme 54. Possible decomposition products of diphenyliodonium salts**

From the calculation results, when heating diaryliodonium salts, the bond between carbon and iodine is often broken, which might generate a benzene radical, iodobenzene, biphenyl (by combination of radicals or direct elimination), and HX. Meanwhile the counter-ions may also react as a nucleophile generating PhX.

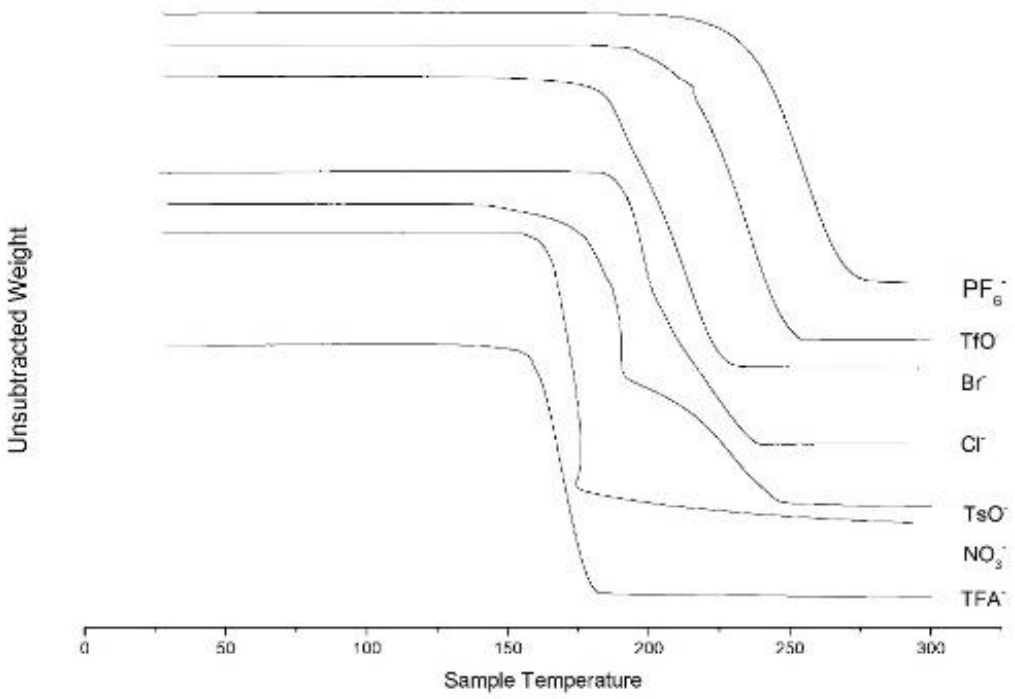


**Figure 30. TGA cuves for diaryliodonium salts**

It was found that the energies required to break the bond between carbon and iodine, and the pathway of diaryliodonium salts decomposition was dependent by the nature of the counter-ions.

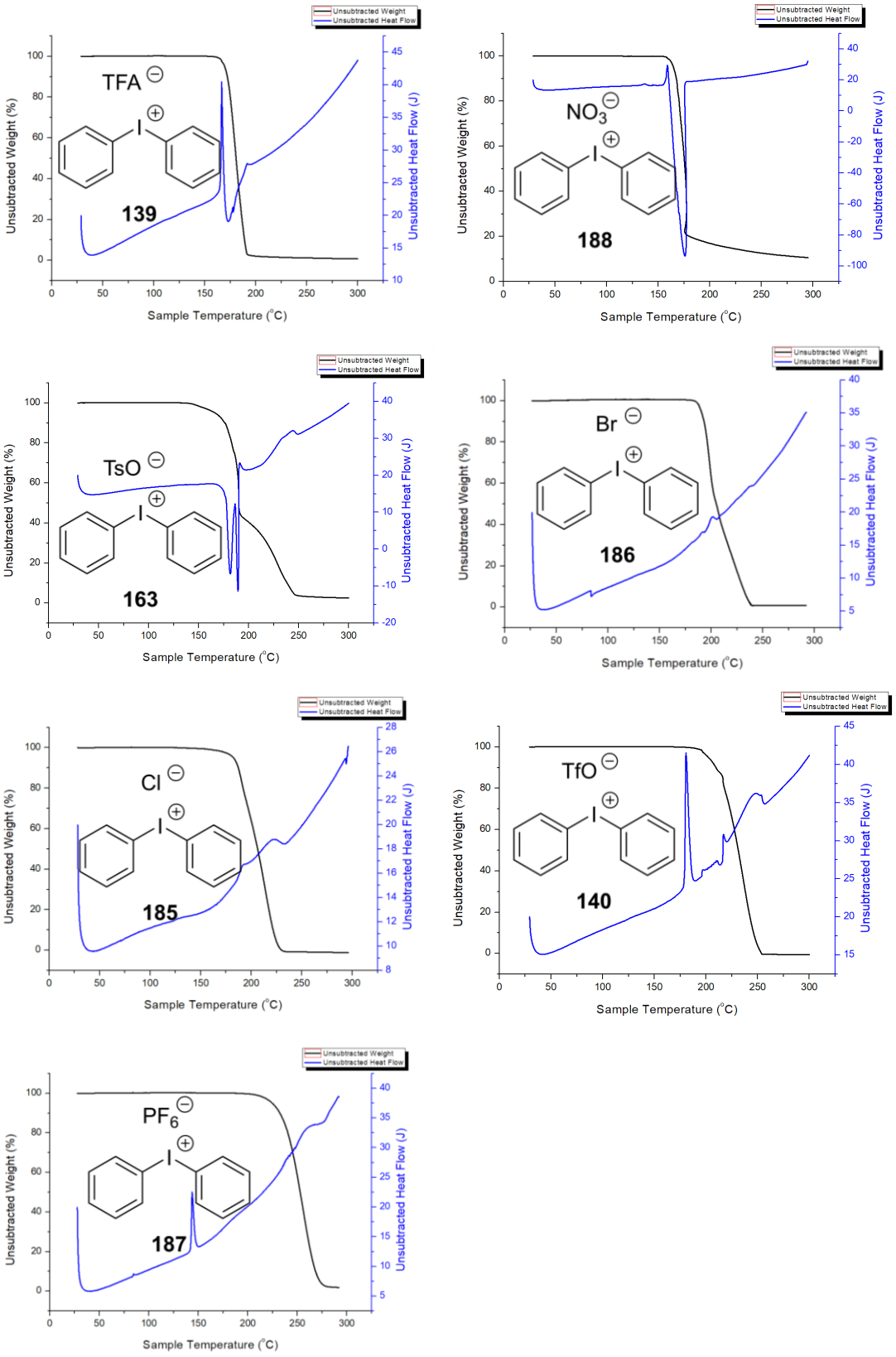


**Figure 31. DSC-TGA curves for diaryliodonium salt**

In Figure 30, the DSC curve indicated that the melting point of diphenyliodonium trifluoroacetate **139** was around 170 ℃, although the TGA curve indicated thermal decomposition before this at around 155 ℃.

The DSC-TGA curves suggested other diphenyliodonium salts with different counter-ions ($Br^{\ominus}$, $Cl^{\ominus}$, $TsO^{\ominus}$ and $NO_3^{\ominus}$) would also undergo thermal decomposition before melting except $PF_6^{\ominus}$ (**187**) and $TfO^{\ominus}$ (**140**) (Table 8). To analysis the TGA curves for various counter-ions, the shapes of TGA curves were different, thus the decomposition process would be diverse.

**Table 11. Decomposition temperature and bond length**

| **Group** | **1** | | | **2** | | | **3** |
|---|---|---|---|---|---|---|---|
| **$X^{\ominus}$** | TFA | Cl | Br | TfO | TsO | $NO_3$ | $PF_6$ |
| **Compound number** | **139** | **185** | **186** | **140** | **163** | **188** | **187** |
| **Decomposition start temperature/ ℃** | 155 | 192 | 189 | 188 | 142 | 158 | 196 |
| **Decomposition finish temperature / ℃** | 191 | 238 | 227 | 258 | 247 | 300 | 280 |
| **Melting point / ℃** | 165 | 196 | 208 | 179 | 182 | 162 | 148 |
| **The range of decomposition/ ℃** | 36 | 46 | 38 | 70 | 105 | 142 | 84 |
| **Initial mass loss /%** | 100 | 100 | 100 | 100 | 55 | 80 | 100 |
| **Bond length between counterion and iodine/Å** [a] | 2.83 | 3.06 | 3.24 | 2.88 | 2.87 | 2.76 | 3.01 |

[a] Data from CCDC.

For the trifluoroacetate salt **139**, it loses weight over a short temperature range (36 ℃). The diphenyliodonium tosylate salts **163** would decompose faster (weight loss from 100% to 45%) and then the others (weight loss from 45% to 0%) would decompose slower. From the curves and the calculation results, the diaryliodonium salts tested could be divided into three groups, Group 1 ($TFA^{\ominus}$, $Cl^{\ominus}$ and $Br^{\ominus}$) would lose weight fast, Group 2 ($TfO^{\ominus}$, $NO_3^{\ominus}$and $TsO^{\ominus}$) would

lose weight slowly and might form the new compounds, Group 3 ($PF_6^{\ominus}$) would lose weight slower than Group 1 and might form the fluorobenzene.

In Table 8, the diphenyliodonium tosylate salts **163** gave the longest range of decomposition temperature which was more than 100 ℃. From the TGA curve, **163** first loses 55% weight from 142 ℃ to 191 ℃, then loses the other 44% weight by 247 ℃. And also, the diphenyliodonium nitrate **188** first loses 80% weight fast then lose other 20% slowly. It was different to the all of the others, but the DSC-TGA result was not enough to explain what actually occurred to give the 2-stage decomposition.

The $TFA^{\ominus}$ (**139**), $TsO^{\ominus}$ (**163**) and $TfO^{\ominus}$ (**140**) salts have similar bond lengths between the counter-ion and the hypervalent iodine, and also have good solubility in organic solvents, so they are widely used in arylation reactions. They also have appropriate reactivity, and less competing side reactions such as those salts with highly nucleophilic counter-ions such as $Br^{\ominus}$ and $Cl^{\ominus}$.[186]

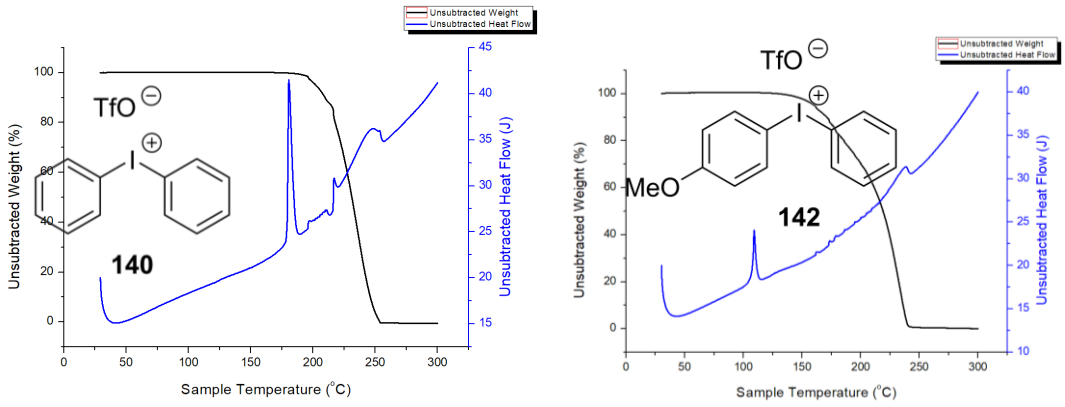


**Figure 32. TGA curves for the diaryliodonium triflate salts 140 and 142**

The thermal stability of diaryliodonium salts was also easily affected by changing the aromatic groups, introducing an electron-rich group made the diaryliodonium triflate less stable which supports the empirical observations. When introducing a 4-methoxy group into a diphenyliodonium triflate **142**, the decomposition temperature drops from 188 ℃ to 145 ℃

(Figure 32).

To combine the DSC-TGA and computational simulation results, the process of diphenyliodonium salt decomposition could be determined. The diphenyliodonium salts with TFA, Br, Cl counter-ions will decompose to low boiling point phenyl radical and iodobenzene, thus the weight loss in the TGA experiment is faster.

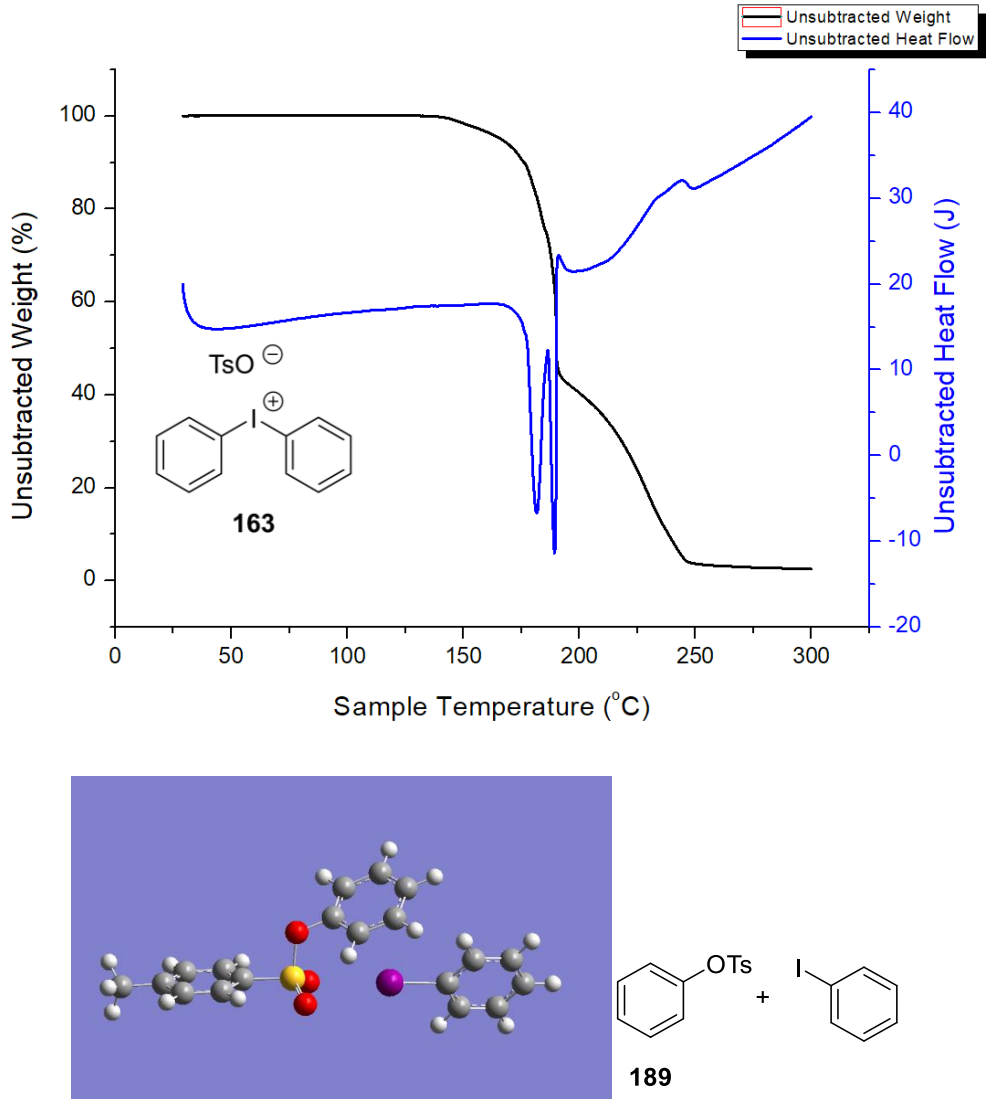


**Figure 33. The combination of DSC-TAG and computational results for the decomposition of diphenyliodonium tosyl salt**

On decomposition, the diphenyliodonium tosylate would form phenyl 4-

methylbenzenesulfonate **189** which has a boiling point of 385 °C (predicted). The DSC-TGA shows that at 191 °C, 55% weight has been lost (if only iodobenzene should be 44%), however at this point phenyl 4-methylbenzenesulfonate also started decomposition and at 250 °C all of the diphenyliodonium tosylate salt was decomposed (Figure 33).

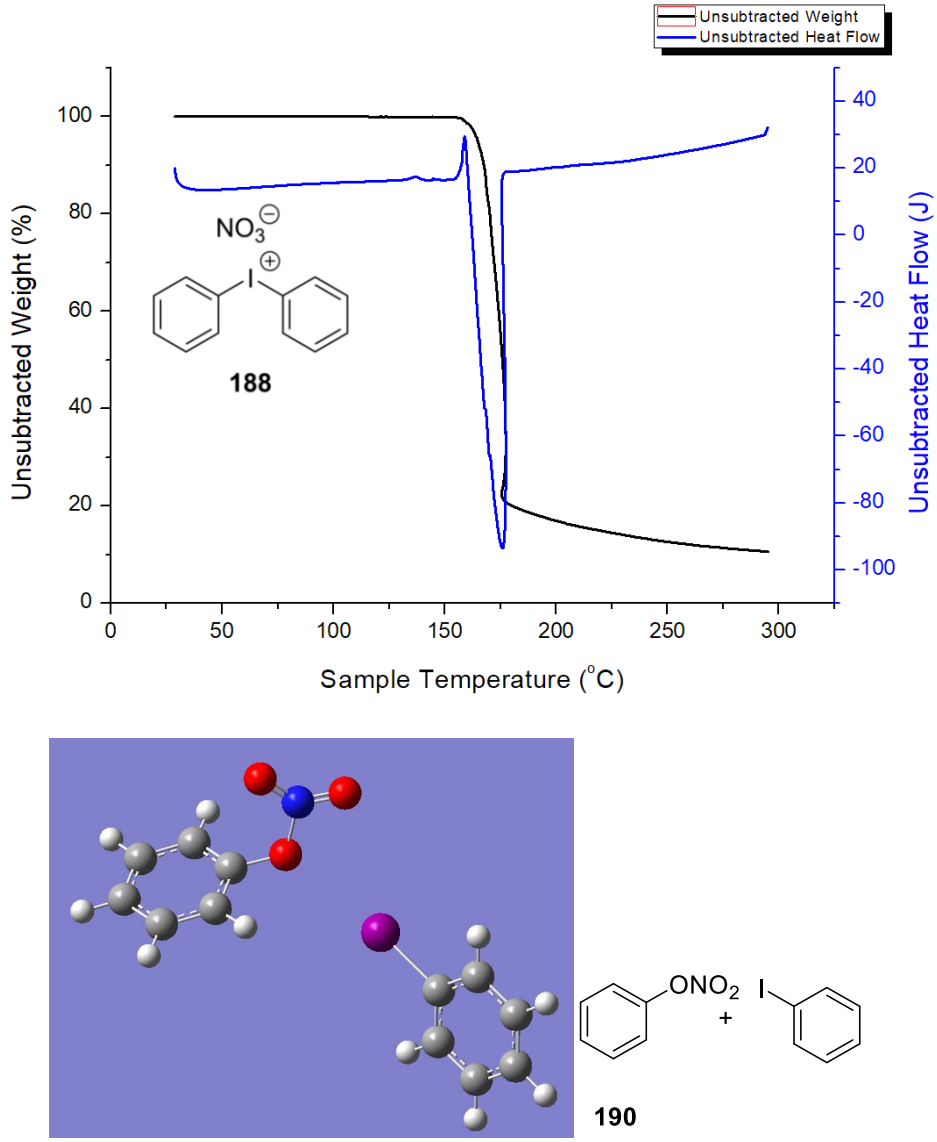


**Figure 34. The combination of DSC-TAG and computational results for the decomposition of diphenyliodonium nitrate salt**

The diphenyliodonium nitrate would form phenyl nitrate **190** which has a boiling point of 207 °C (predicted). The DSC-TGA shows that at 175 °C, 80% of the weight has been lost (if only

iodobenzene was lost it should be 62%), and the remaining mass is slowly lost as the phenyl nitrate evaporates (Figure 34).

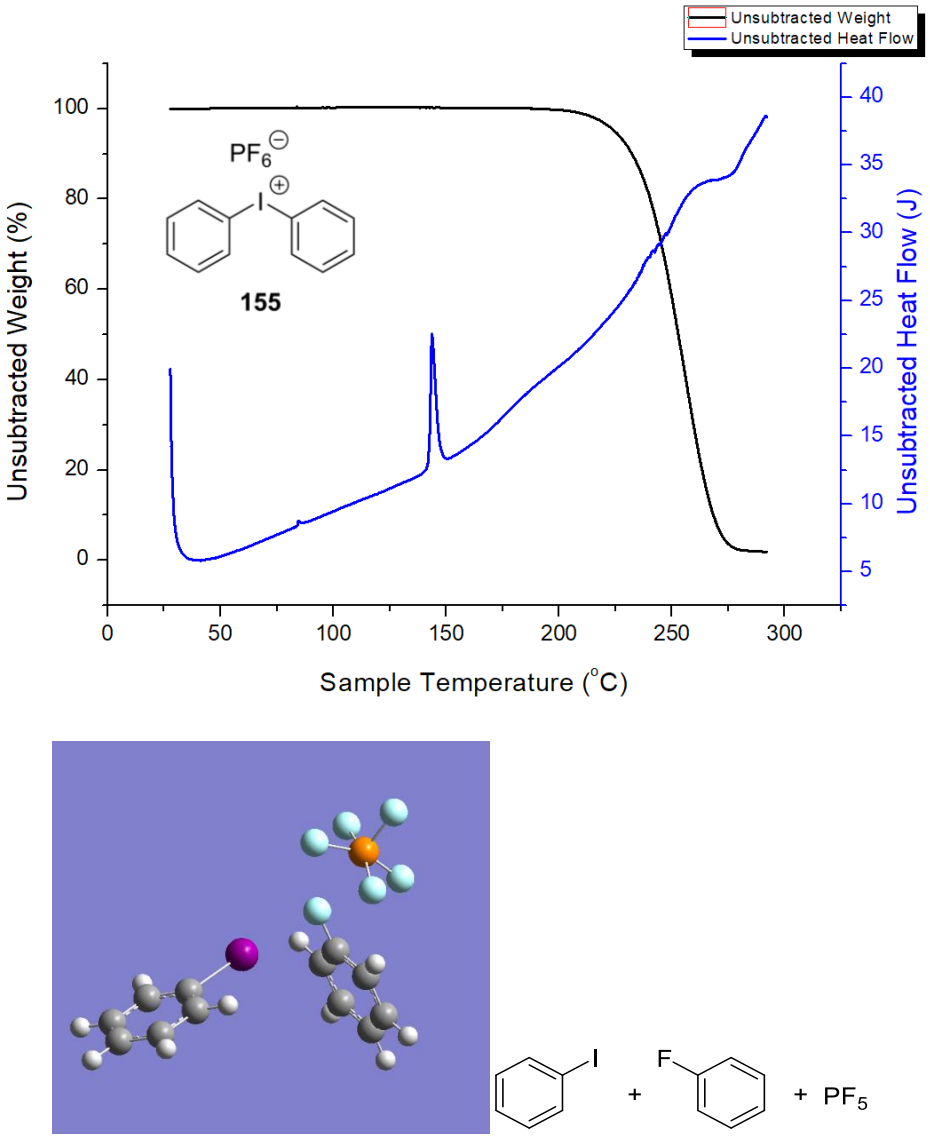


**Figure 35. The combination of DSC-TAG and computational results for the decomposition of diphenyliodonium hexafluorophosphate salt**

The diphenyliodonium hexafluorophosphate would form fluorobenzene which has a lower boiling point than the decomposition temperature and is therefore very volatile and is lost rapidly and the DSC-TGA indicates this mass loss. The change of the DSC curve after 200 °C might be the formation of fluorobenzene, but due to the low boiling point of this material the

TGA curve does not change (Figure 35).

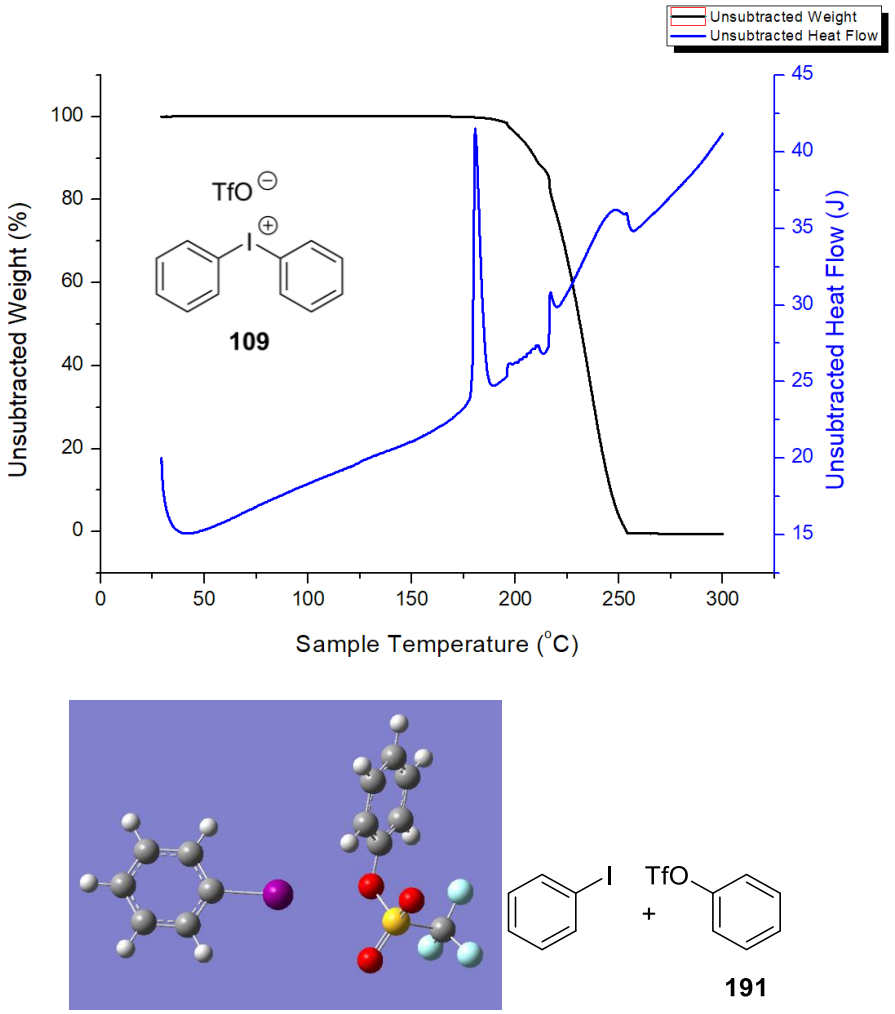


**Figure 36. The combination of DSC-TGA and computational results for the decomposition of diphenyliodonium triflate salt**

In a similar manner to diphenyliodonium hexafluorophosphate, diphenyliodonium triflate also forms a lower boiling point product: probably phenyl triflate **191**, which has a boiling point of 175 ℃ (predicted). The reason for the TGA curve change is that when the decomposition occurs, the phenyl triflate formation requires some energy.

According to the combination of the DSC-TGA results and computational study the thermal stability of some diphenyliodonium salts has been determined. The presence of different

counter-ions results in different decomposition processes. This suggests that the term 'melting point' is misleading. The introduction of an electronic-rich ring into the diaryliodonium salt causes the decomposition temperature to drop, thus reactions using diaryliodonium salts should preferentially be carried out at lower temperatures to reduce the amount of by-products and other decomposition products.

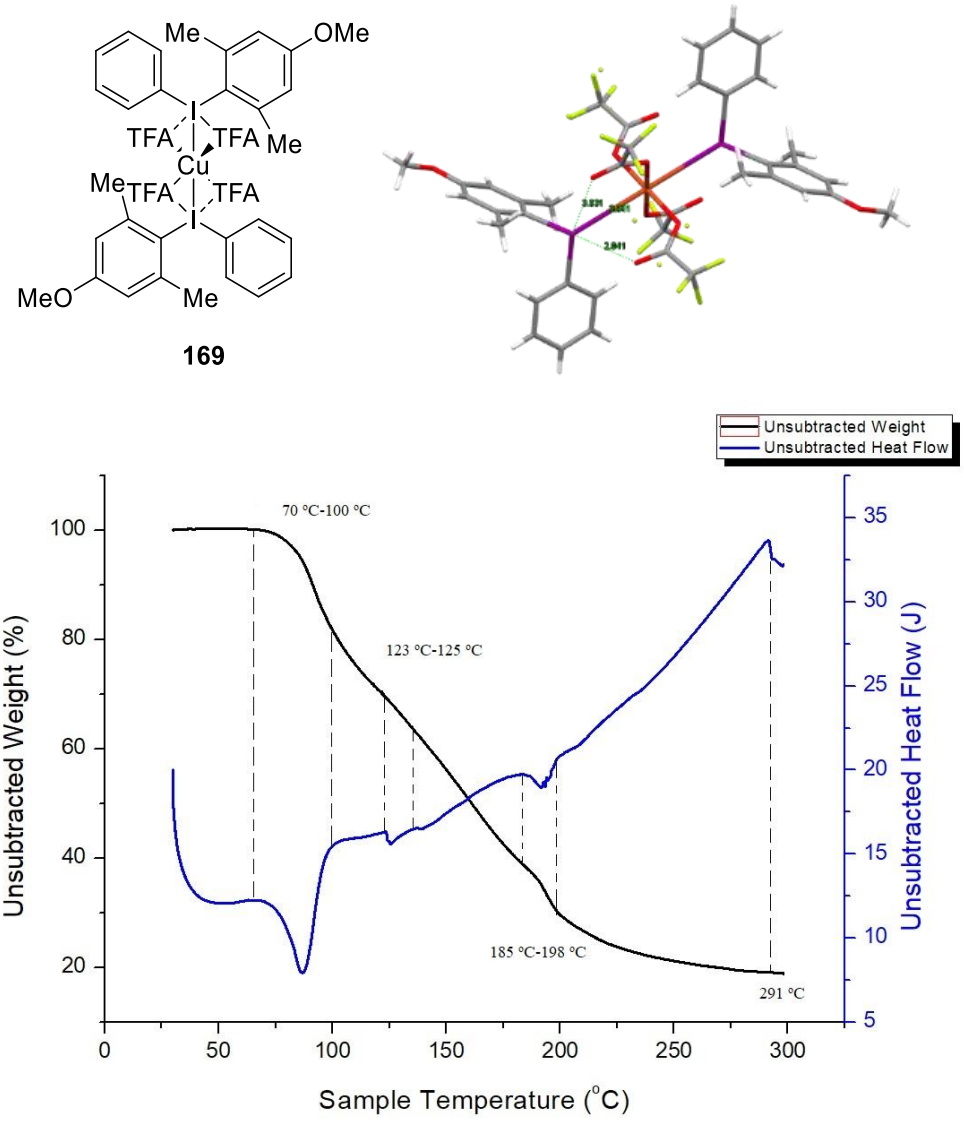


169

**Figure 37. DSC-TGA curves for diphenyliodonium copper tetratrifluoroacetate complex 169**

The bis(diphenyliodonium) copper tetratrifluoroacetate complex **169** was also investigated by DSC-TGA analysis. The DSC curve shows there are four energy changes in this process, and

the decomposition started from only 70 ℃, which was much lower than the diphenyliodonium salts.

**Table 12. TGA data for Cu-TFA decomposition from article**

| **Compound** | **Hydrolysis Temperature/** ℃ | **Decomposition Temperature/**℃ | **Second Decomposition Temperature/** ℃ |
|---|---|---|---|
| $Cu(CF_3COO)_2$ with $H_2O$ | 69 $[Cu_2(CF_3COO)_3(OH)]$ | 133 $[Cu(CF_3COO)_2CuO]$ | 268 [CuO] |

According to a study of copper(II) trifluoroacetate, which reported on the decomposition process of copper(II) trifluoroacetate.[187] The decomposition energy changes are similar to those observed in Figure 37, which suggests the energy changes are mostly due to the decomposition of copper tetratrifuoroacetate complex.

Thus from 70 ℃ to 100 ℃, the TGA curve shows that the copper complex lost one TFA counter-ion and also that the diaryliodonium salt also starts decomposition. At around 123 ℃, the copper complex lost another TFA counter-ion, and maybe form the $[Cu(CF_3COO)_2CuO]$, later at around 185 ℃ and 291 ℃, the last two counter-ions were lost.

## 2.4 Nucleophilic Substitution of Diaryliodonium Salts

As discussed in the introduction, diaryliodonium salts are suitable substrates for various nucleophilic substitution arylation reactions, however, the unwanted products usually are difficult to separate, thus figuring out the effects on selectivity of diaryliodonium salts substitution reactions is important.

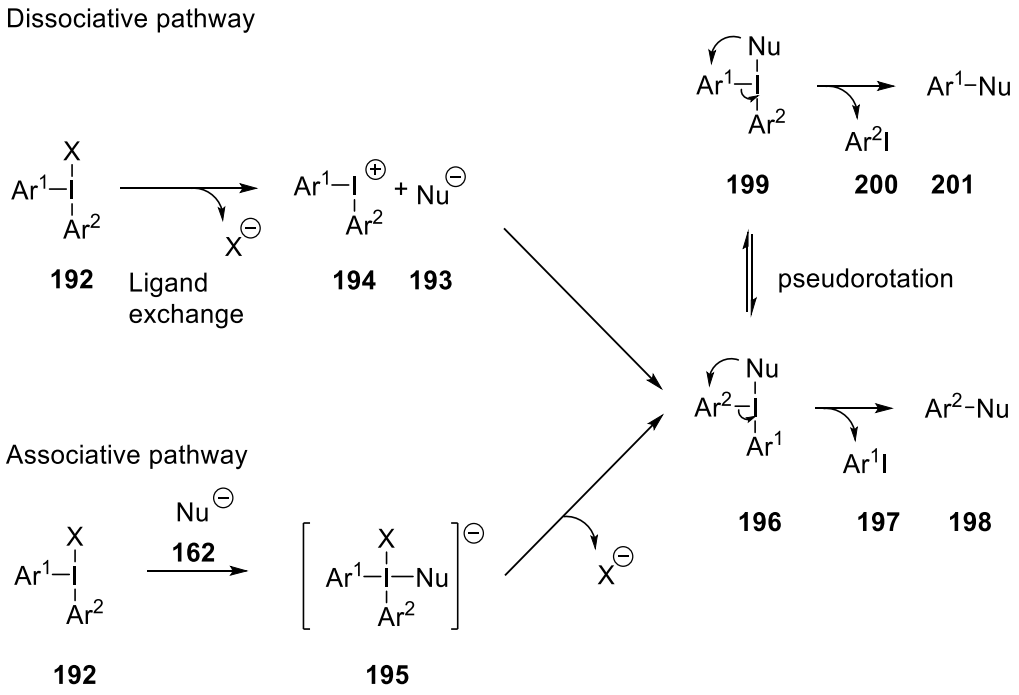


**Scheme 55. General scheme for the nucleophilic substitution of diaryliodonium salts**

For nucleophilic substitution of diaryliodonium salts, there are two possible pathways, the dissociative pathway and the associative pathway. For the dissociative pathway, the counter-ion leaves first, and the nucleophile **193** (such as nitrogen, oxygen and fluoride) connects to the central iodine, to form **196**, meanwhile in the associative pathway, the nucleophile attacks the central iodine first to form intermediate **195**, following by the counter-ion leaving to form **196**.

Compound **196** can then easily interconvert to **199** by pseudorotation, followed by nucleophilic attack on the aromatic ring, which releases the iodoarene and generates the target ArNu. It is

clear that when the intermediate is **196**, the substitution product would be **198**, while when it is **199**, the substitution product would be **201**. Thus, the control of pseudorotation is the key point to control the selectivity.

### *2.4.1 N-Arylation of Diaryliodonium Salts*

There are many studies info the selectivity of diaryliodonium salts in the *N*-arylation reaction, and usually the ratio of desired product and unwanted product is determined either by the isolation of the compounds, analysis of the reaction mixture by HPLC or GC, however a lot of time is required, for HPLC and GC, as the calibration curves are necessary, could lead to an error. For example, we found that benzene and fluorobenzene would not show when the wavelength was 230 nm, thus the reaction should be monitored by 205 nm wavelength in HPLC. And the concentration should be lower than 0.002 mol/L.

4-Fluoroaniline was chosen as the nucleophile and the ratio of desired product and unwanted product was determined by $^{19}F$ NMR, NMR is a rapid option and in this case as it yields sharp signals, covers a wide chemical shift range which allows closely related compounds to be distinguished and thus provides the best method to monitor the reaction and calculate the ratio between the desired product and any alternative products.

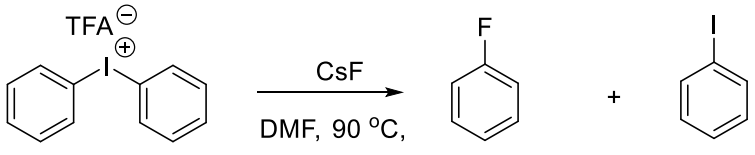


**139** **102** **36**

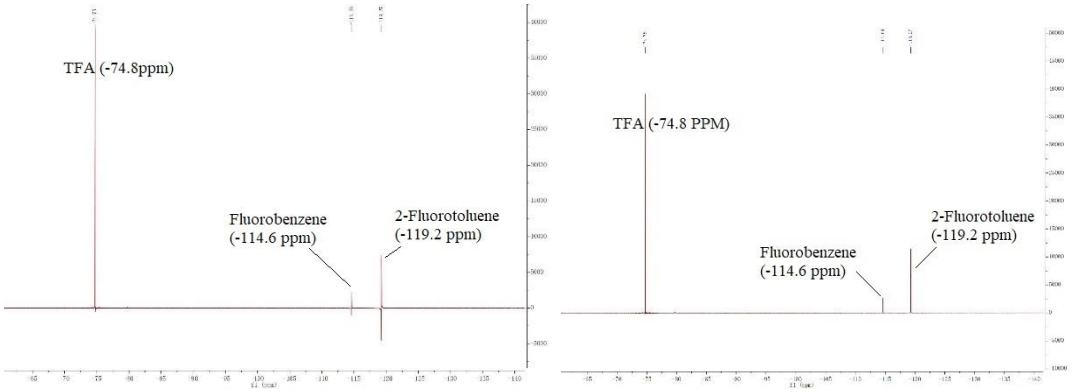


**Figure 38. An Example of $^{19}$F NMR Spectrum of Metal-Free Fluorination Reaction**

Unfortunately, the $^{19}$F NMR still has limitation, the signals, sometimes after Fourier transform, would have a part under the baseline (such as -119.2 ppm peak) which can course the main observational error (shown in Figure 37). And after the phase correction, the peaks are same as observed in normal spectrums.

The reaction yield can be calculated directly by the integration of the fluorine peaks with an internal standard. In this case, 2-fluorotoluene was selected as the internal standard because of its stability, no reaction with diaryliodonium salts and the $^{19}$F NMR signal (-119.2 ppm) is separate from the expected products, starting materials and by-products (-74.8 ppm is TFA peak, -114.6 ppm is fluorobenzene peak) (Figure 38).

The $^{19}$F NMR peaks of the *N*-arylation products were confirmed by comparison with literature studies and from experimental data (Table 13).

**Table 13. The $^{19}$F NMR peaks of *N*-arylation products in DCM**

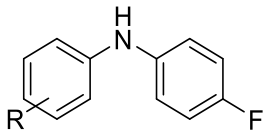


**202** R = H
**203** R = 4-OMe
**204** R = 2-Me
**205** R = 2-Me,4-OMe
**206** R = 2-*n*-Butyl, 4-OMe
**207** R = 2,6-$Me_2$, 4-OMe

| **Compound** | **R** | **$^{19}$F NMR/ppm** |
|---|---|---|
| **202** | H | -124.6 |
| **203** | 4-OMe | -126.7 |
| **204** | 2-Me | -125.7 |
| **205** | 2-Me, 4-OMe | -128.3 |
| **206** | 2-*n*-Butyl, 4-OMe | -128.8 |
| **207** | 2,6-$Me_2$, 4-OMe | -130.1 |

### 2.4.1.1 Metal-Free *N*-Arylation

It has been demonstrated by Carroll and Wood[1] that diarylamines can be successfully prepared using diaryliodonium salts under copper-free conditions. The reaction is carried out in DMF at 130 ℃ for 24 h resulting in a good yield of the desired product, it was noted that reaction selectivity was determined by electronic control.

Hence, we examined the selectivity of different diaryliodonium salts, which covered both electronic and steric control to determine the most effective one in metal-free *N*-arylation: 4-anisyl (**141**), 2-methylphenyl (**143**), 2-methyl-4-anisyl (**157**), 2-*n*-Butyl-4-anisyl (**158**), and 2,6-dimethyl-4-anisyl (**159**) phenyliodonium trifluoroacetates.

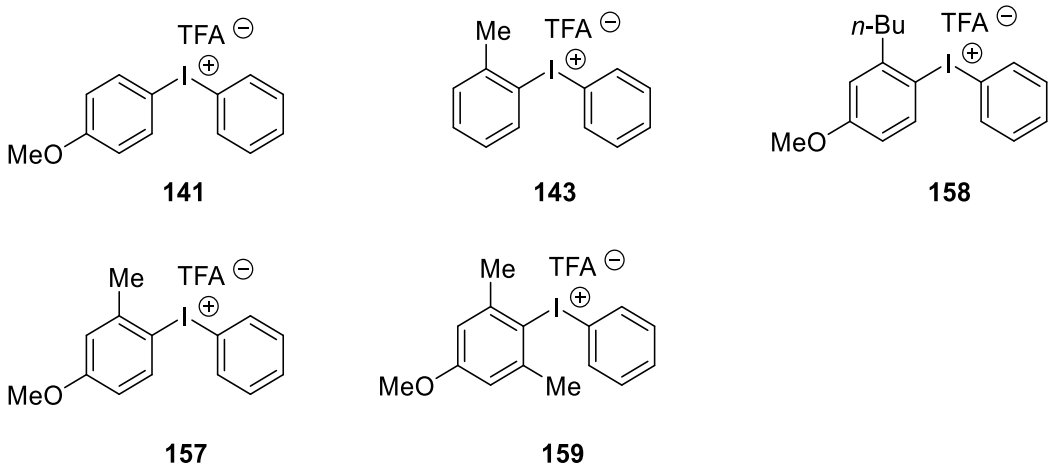


**Figure 39. The different diaryliodonium salts substrates used in the nucleophilic substitution**

**Table 14. Metal-free *N*-arylation**

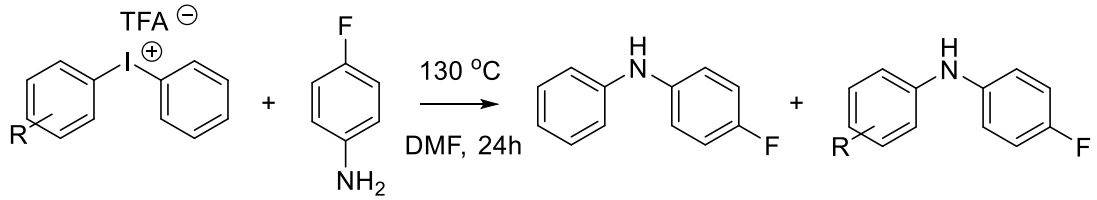


**141** R = 4-OMe
**143** R = 2-Me
**157** R = 2-Me,4-OMe
**158** R = 2-*n*-Butyl, 4-OMe
**159** R = 2,6-$Me_2$, 4-OMe

**208**

**202**

**203** R = 4-OMe
**204** R = 2-Me
**205** R = 2-Me,4-OMe
**206** R = 2-*n*-Butyl, 4-OMe
**207** R = 2,6-$Me_2$, 4-OMe

| Entry | R | Ratio[a] 202 : 203-207 | Yield[a] (combined) | Yield[a] (202) |
|---|---|---|---|---|
| **1** | 4-OMe | 2.7 : 1 | 16% | 12% |
| **2** | 2-Me | 2.3 : 1 | 65% | 45% |
| **3** | 2-Me, 4-OMe | 4.1 : 1 | 61% | 49% |
| **4** | 2-*n*-Butyl, 4-OMe | 6.0 : 1 | 86% | 72% |
| **5** | 2,6-$Me_2$, 4-OMe | 28 : 1 | 86% | 84% |

[a] Yield and ratio were the average values of reactions and calculated by $^{19}F$ NMR

Standard reaction conditions: diaryliodonium salt (0.5 mmol), 4-fluoroanline (0.5 mmol), 2-fluorotoluene (0.5 mmol internal standard) were dissolved in DMF (0.6 mL) in an NMR tube

Usually in metal-free *N*-arylation reactions, the most electron-deficient ring is reacted with a nucleophile to generate the product. As shown in Table 11, both steric and electronic control are important in the metal-free *N*-arylation. From Entry **1** and Entry **2**, 4-anisyl results in slightly better selectivity than 2-methylphenyl, the more electron-rich ring tended to provide more of the desired product but in the case of the diaryliodonium salt **143** in this reaction, due to the steric hindrance, the phenyl ring was transferred in preference. However, this selectivity can be overruled by significant steric hindrance in the *ortho*-positions due to the *ortho*-effect when the nucleophile is small, such as fluoride and chloride, the *ortho*-effect in diaryliodonium salts seems less effective with aniline. When the steric and electronic elements were combined, the selectivity was improved, and 2,6-dimethyl-4-anisyl resulted in the best selectivity in these five diaryliodonium salts which provided 96% of the desired product and 4% of the unwanted product in the reaction mixture. The steric hindrance contribution from both *ortho*-positions was more effective than when only in the 2-position, the more steric hindrance the better selectivity.

But in the Table 11 the diaryliodonium salt with only an electron-rich ring as the control element (Entry **1**) provided low yields. Entries **2** and **3** provided the products in 60% combine yields and Entries **4** and **5** provided good yields, but Entry **1** only resulted in a 16% yield.

Unfortunately, due to the high temperature, the metal-free *N*-arylation reaction still generated a by-product which was monitored by $^{19}F$ NMR at -119 ppm, however we were not able to identify this by-product. To reduce the by-product and decrease the reaction temperature, copper catalysed *N*-arylation was developed as it proceeds at lower temperatures.

### 2.4.1.2 Copper Catalysed *N*-Arylation

In order to find out the best conditions for the copper catalysed *N*-arylation reaction, we investigated different counter-ions of diaryliodonium salts, different copper catalysts, solvents, temperature and the use of additives such as a base.

### 2.4.1.3 The Effect of Solvent in *N*-Arylation

The solvents DCM, DMF and MeCN were chosen, as they have different polarity and boiling points and have been used widely as solvents for diaryliodonium salt reactions. Six different copper catalysts were chosen which included Cu(I) and Cu(II) salts.

**Table 15. Copper catalysed *N*-arylation in DCM**

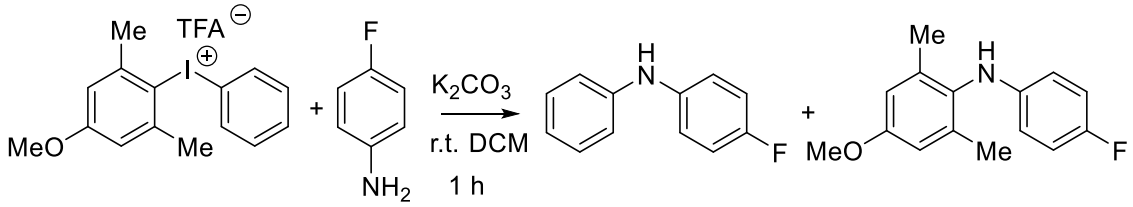


**159** **208** **202** **207**

| Entry | [Cu] | Ratio[a] 202 : 207 | Yield[a] (202) |
|---|---|---|---|
| **1** | $Cu(OTf)_2$ | 1 : 0 | 2% |
| **2** | $CuF_2$ | 1 : 0 | 21% |
| **3** | $Cu(OAc)_2$ | 1 : 0 | 18% |
| **4** | CuCl | 1 : 0 | 10% |
| **5** | CuI | 1 : 0 | 72% |
| **6** | $Cu(TFA)_2$ | 1 : 0 | 3% |

[a] Yield and ratio were the average values of reactions and calculated by $^{19}F$ NMR

Standard reaction conditions: diaryliodonium salt (0.5 mmol), 4-fluoroanline (0.5 mmol), 2-fluorotoluene (0.5 mmol internal standard), [Cu] (20% mol) and $K_2CO_3$ (1.0 mmol) were

dissolved in solvent (0.6 mL) in an NMR tube

In the reaction using DCM as the solvent, it is clear that CuI is the best copper catalyst (Table 15). All the copper catalysts produced good selectivity in this reaction, but only CuI also generated a good yield of the desired product.

All the organic copper salts produced a low yield in this reaction and only copper(II) triflate and copper(II) acetate were soluble in DCM and the reactions were therefore homogeneous, all others were heterogeneous. When using DCM as the solvent in the *N*-arylation reaction, it appears that some of the heterogeneous reactions seemed to be more effective (such as $CuF_2$, CuI).

The reaction in DCM could provide a process under mild conditions which is suitable for thermally sensitive amines, and because of the low boiling point of the solvent, it is easily removed.

**Table 16. Copper-catalysed *N*-arylation in DMF**

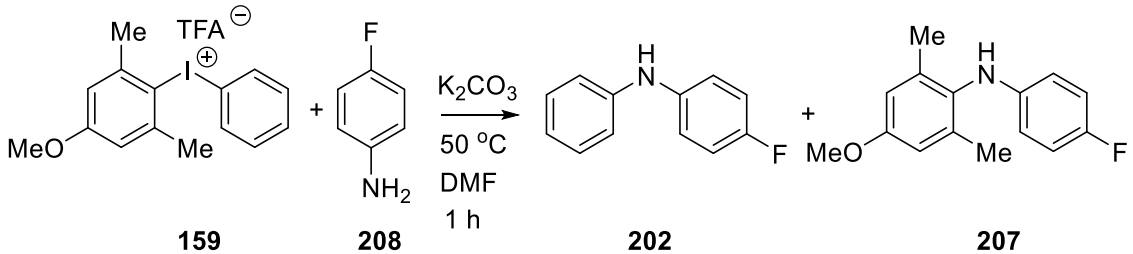


**159** **208** **202** **207**

| Entry | [Cu] | Ratio [a] 202 : 207 | Yield [a] (202) |
|---|---|---|---|
| **1** | $Cu(OTf)_2$ | 1 : 0 | 32% |
| **2** | $CuF_2$ | 1 : 0 | 87% |
| **3** | $Cu(OAc)_2$ | 40 : 1 | 39% |
| **4** | CuCl | 24 : 1 | 53% |
| **5** | CuI | 1 : 0 | 51% |
| **6** | $Cu(TFA)_2$ | 1 : 0 | 44% |

[a] Yield and ratio were the average values of reactions and calculated by $^{19}F$ NMR

Standard reaction conditions: diaryliodonium salt (0.5 mmol), 4-fluoroanline (0.5 mmol), 2-fluorotoluene (0.5 mmol internal standard), [Cu] (20% mol) and $K_2CO_3$ (1.0 mmol) were dissolved in DMF (0.6 mL) in an NMR tube

When the reaction used DMF as the solvent and the higher temperature, all the copper catalysts provided reasonable yields, the CuI still provided a suitable yield but not as good as that observed in DCM. Homogenous reactions were still not as good as heterogeneous ones, but better than in DCM, $Cu(OTf)_2$ and $Cu(OAc)_2$ all provided <40% product, unfortunately, $Cu(OAc)_2$ and CuCl did not give good selectivity with some of the alternative diarylamine being detected by $^{19}F$ NMR. When $CuF_2$ was used as the catalyst in the reaction, the yield is about 87% a little bit higher than CuI in DCM (72%) and much higher than $CuF_2$ in DCM (21%).

**Table 17. Copper catalysed *N*-Arylation in MeCN**

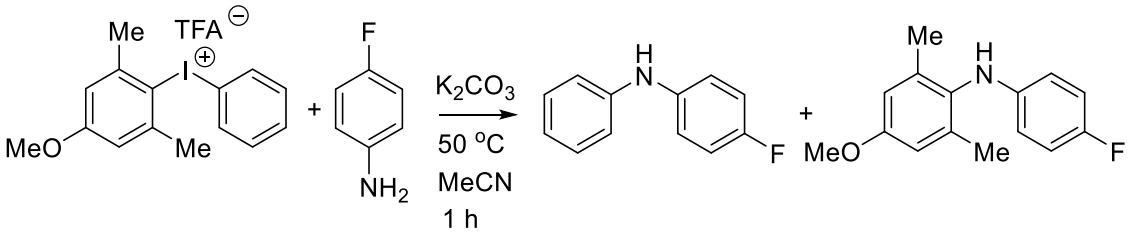


**128** **177** **171** **176**

| Entry | [Cu] | Ratio[a] 161 : 166 | Yield[a] (161) |
|---|---|---|---|
| **1** | $Cu(OTf)_2$ | 1 : 0 | 13% |
| **2** | $CuF_2$ | 0 : 1 | 5% |
| **3** | $Cu(OAc)_2$ | 3.4 : 1 | 13% |
| **4** | CuCl | 1 : 1.8 | 7% |
| **5** | CuI | 1 : 0 | 0.7% |
| **6** | $Cu(TFA)_2$ | 1 : 0 | 60% |

[a] Yield and ratio were calculated by $^{19}F$ NMR

Standard reaction conditions: diaryliodonium salt (0.5 mmol), 4-fluoroanline (0.5 mmol), 2-fluorotoluene (0.5 mmol internal standard), [Cu] (20% mol) and $K_2CO_3$ (1.0 mmol) were dissolved in MeCN (0.6 mL) in an NMR tube

In acetonitrile, these six copper catalysts seem to be less effective, even $CuF_2$ and CuCl provided the reverse selectivity which might because the halide counter-ions ($Cl^-$ and $F^-$) could also react with diaryliodonium salts so that the selectivity was changed. $Cu(OAc)_2$ did not provide a good selectivity. The yields of these reactions were lower than in DMF and DCM except $Cu(TFA)_2$. This situation might be because the copper catalysts could easily form different complexes in acetonitrile to the other solvents and enable the alternative reaction pathway thus giving a different outcome.

### 2.4.1.4 The Effect of Base in *N*-Arylation

DMF as the solvent provided a good yield of the product in the presence of $CuF_2$ and as the base could also influence the product yields, a range of such additives were investigated.

**Table 18. Copper catalysed *N*-arylation with different bases**

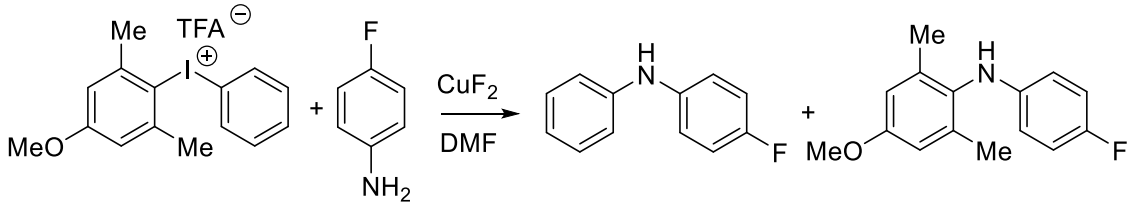


**159** **208** **202** **207**

| Entry | Base | Ratio[a] 202 : 207 | Temperature | Time | Yield [a] |
|---|---|---|---|---|---|
| **1** | N/A | 1 : 0 | r.t. | 18 h | 60% |
| **2** | $K_2CO_3$ | 1 : 0 | r.t. | 18 h | 40% |
| **3** | $Et_3N$ | N/A | r.t. | 18 h | 0% |
| **4** | Pyridine | N/A | r.t. | 18 h | 0% |
| **5** | N/A | 1 : 0 | 50 ℃ | 1 h | 30% |
| **6** | $K_2CO_3$ | 1 : 0 | 50 ℃ | 1 h | 87% |
| **7** | $Et_3N$ | 1 : 0 | 50 ℃ | 1 h | 18% |
| **8** | Pyridine | 1 : 0 | 50 ℃ | 1 h | 16% |

[a] Yield and ratio were calculated by $^{19}F$ NMR

Standard reaction conditions: diaryliodonium salt (0.5 mmol), 4-fluoroanline (0.5 mmol), 2-fluorotoluene (0.5 mmol internal standard), $CuF_2$ (20% mol) and base (1.0 mmol) were dissolved in DMF (0.6 mL) in an NMR tube

When carried out at room temperature, the reaction without base produced 60% of product and with $K_2CO_3$ this dropped to 40%, meanwhile organic bases resulted in less than 1% of the product. Increasing the temperature to 50 ℃, the reaction without base was less efficient now

with only 30% product being formed (room temperature 68%). $K_2CO_3$ provided the best result (87%), while the organic base only generated <20% product and at the same time in this reaction might produce the by-product bis(4-fluorophenyl)diazene[188] ($^{19}F$ NMR = -109.1 ppm in DMF). It was found that under the same conditions without the diaryliodonium salt, 4-fluoroaniline **208** was easily be converted to bis(4-fluorophenyl) diazene, and according to the $^{19}F$ NMR, the yield was 89% after 24 h.

In summary, the copper catalysed *N*-arylation with $K_2CO_3$ provided the best result and did not produce the by-product bis(4-fluorophenyl) diazene, organic bases such as pyridine are not suitable for this reaction.

### 2.4.1.5 The Effect of Counter-Ions in *N*-Arylation

As the different ligands in diaryliodonium salts have been shown to affect their chemical properties, TFA salts in the copper catalysed reaction usually provide high yields compared to the TfO salts. But it was noted that the TFA peak in the $^{19}F$ NMR disappeared when a copper catalyst, such as $CuF_2$, $Cu(TFA)_2$, $Cu(OAc)_2$ and $CuF_2$, was added to the solution, however the TfO peak in $^{19}F$ NMR did not change. It is still unclear why the TFA peak disappeared, but this suggested that when an added copper catalyst is present, the TFA salts and the TfO salts may present different results.

To monitor the reaction, (4-fluorophenyl)(phenyl)iodonium trifluoroacetate (**150**) and triflate (**151**) were both synthesised. $Cu(OTf)_2$ was chosen as the catalyst because the signal of triflate peak is clearly visible in the $^{19}F$ NMR. Due to the fluorine in the diaryliodonium salts, the reaction could easily be monitored by $^{19}F$ NMR; all the possible compounds could be monitored in the two possible product pairs could be monitored **A** (**202** and **211**) and **B** (**210** and **36**) (Table 19).

When the $Cu(OTf)_2$ was added to the solution of 4-fluoroaniline and the diaryliodonium trifluoroacetate **150**, the 4-fluorophenyl peak in $^{19}F$ NMR changed from -107.75 ppm to -103.87 ppm which was the same as the diaryliodonium triflate salt. It suggested that when the $Cu(OTf)_2$ was added, the diaryliodonium trifluoroacetate salt underwent ligand exchange first to form the diaryliodonium triflate salt.

**Table 19. Yields of different ligands in copper catalyst *N*-arylation**

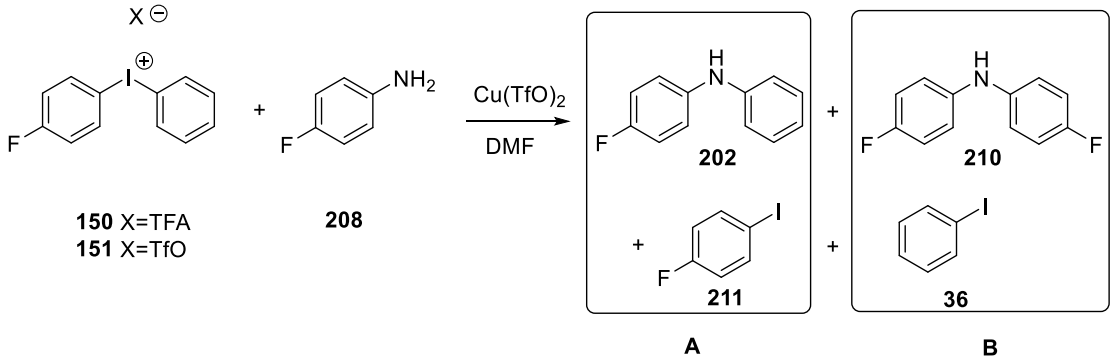


**150** X=TFA
**151** X=TfO

**208**

| | | Yields[a] (combine 202 and 210) | | | | | | Ratio |
|---|---|---|---|---|---|---|---|---|
| | | **0.5 h** | **1 h** | **1.5 h** | **2 h** | **3 h** | **4 h** | **202:210** |
| **TFA salt (119)** | r.t. with $K_2CO_3$ | 5.6% | 7.3% | 11% | 12% | 14% | 15% | 1.5 : 1 |
| | r.t. | 8.0% | 11% | 13% | 14% | 17% | 21% | 1.5 : 1 |
| | 60 °C | 71% | 74% | 81% | 79% | 75% | | 1.5 : 1 |
| | 60 °C with $K_2CO_3$ | 65% | 86% | 94% | 95% | 95% | | 1.5 : 1 |
| **TfO salt (120)** | r.t. with $K_2CO_3$ | 0.0% | 0.0% | 0.0% | 0.5% | 1.1% | 1.8% | 1.5 : 1 |
| | r.t. | 0.0% | 0.0% | 0.0% | 0.6% | 1.4% | 1.9% | 1.5 : 1 |
| | 60 °C | 14% | 24% | 32% | 34% | 38% | 42% | 1.5 : 1 |
| | 60 °C with $K_2CO_3$ | 22% | 34% | 52% | 44% | 55% | 63% | 1.5 : 1 |

[a] Yield and ratio were calculated by $^{19}F$ NMR

Standard reaction conditions: diaryliodonium salt (0.5 mmol), 4-fluoroanline (0.5 mmol), 2-fluorotoluene (0.5 mmol internal standard), $Cu(OTf)_2$ (20% mol) and $K_2CO_3$ (1.0 mmol) or no base were dissolved in DMF (0.6 mL) in an NMR tube

From the $^{19}F$ NMR, 4-fluorodiphenylamine **202** and 4-fluoroiodobenzene **211** were present in the same amounts, which suggested there were no side reactions under these conditions. The product ratio between **202** and **210** was 1.5 : 1 in all the reactions, suggesting that the counter-

ions only effect the reaction rate and not the selectivity of the process.

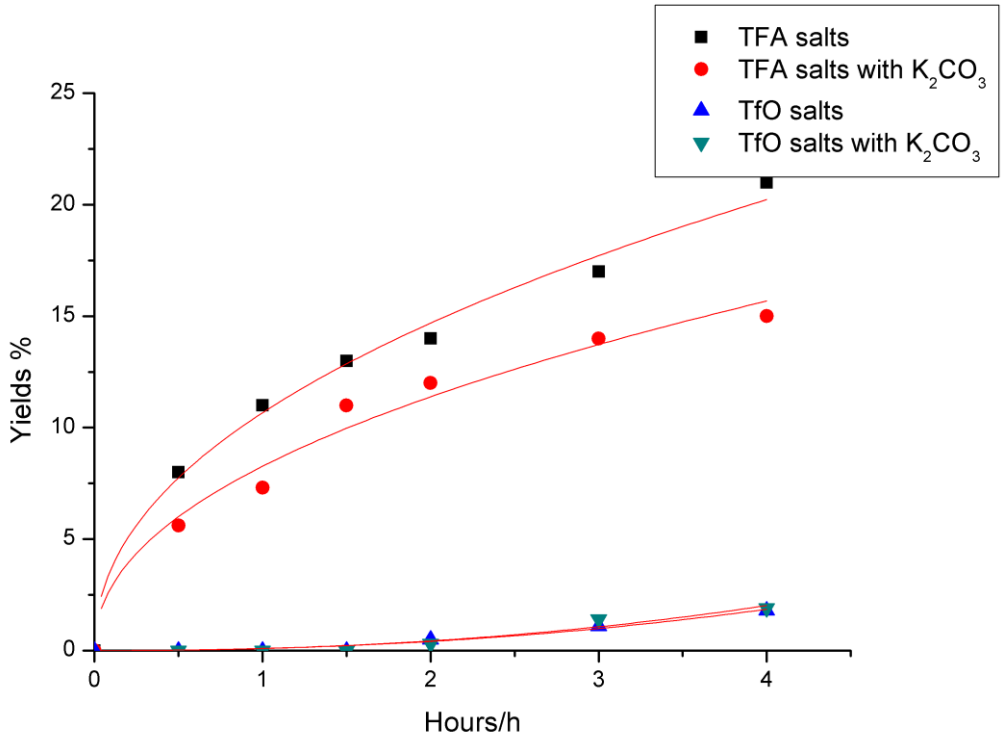


**Figure 40. Copper catalysed *N*-arylation product (202 and 210) yields with time at room temperature**

The curves were fitted with $y = ax^b$ by OriginPro 8.

As the Figure 40 shows, when the reaction was at room temperature, the TFA salts always gave a greater yield and also achieved this at a faster rate than the TfO salts. When the reaction was under base ($K_2CO_3$) conditions the reaction rate was slower.

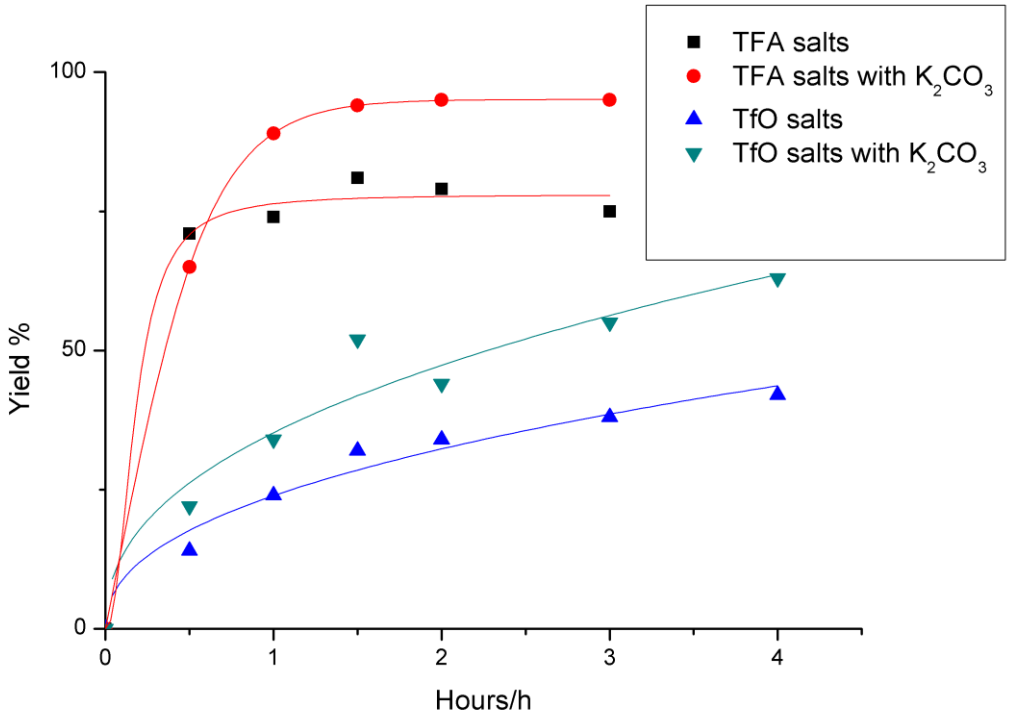


**Figure 41. Copper catalysed *N*-arylation product (202 and 210) yield with time at 60 °C**

The curves of triflate salts were fitted with $y = ax^b$, and the curves of trifluoroacetate salts were fitted with $y = y_0 + A_1e^{-x/t_1} + A_2e^{-x/t_2}$ by OriginPro 8.

However, when the temperature was raised to 60 °C, the outcome was reversed with the reaction using $K_2CO_3$ generating 95% of the combined product, and within 1 hour 86%. The TFA salts gave a faster reaction rate and higher product yields than TfO salts under all conditions.

In summary, diaryliodonium trifluoroacetate salts could provide the same selectivity but at a faster reaction rate than the triflate salts. When the reaction had added $K_2CO_3$, the product yields increased to 95% at 60 °C, whereas at room temperature the addition of base decreased the product yield. Monitoring the reaction showed that there were no side reactions when the reaction was conducted in the presence of a copper catalyst.

### 2.4.1.6 The Selectivity of Copper Catalysed *N*-arylation

**Table 20. Copper catalysed *N*-arylation**

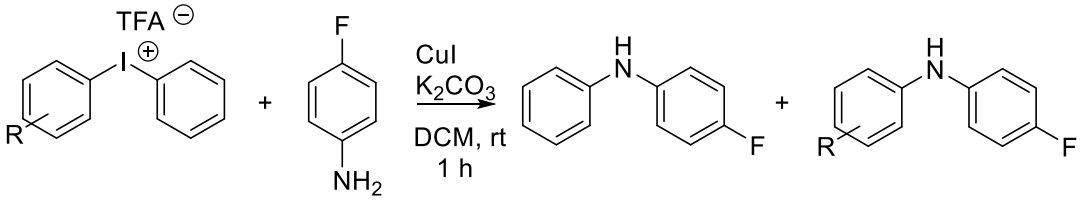


**141** R = 4-OMe
**143** R = 2-Me
**157** R = 2-Me,4-OMe
**158** R = 2-*n*-Butyl, 4-OMe
**159** R = 2,6-$Me_2$, 4-OMe

**208**

**202**

**203** R = 4-OMe
**204** R = 2-Me
**205** R = 2-Me,4-OMe
**206** R = 2-*n*-Butyl, 4-OMe
**207** R = 2,6-$Me_2$, 4-OMe

| Entry | R | Ratio [a] 202 : 203-207 | Yield[a] (combined) | Yield[a] (202) |
|---|---|---|---|---|
| **1** | 4-OMe | 1.7 : 1 | 38% | 24% |
| **2** | 2-Me | 3.7 : 1 | 72% | 56% |
| **3** | 2-Me, 4-OMe | 6.9 : 1 | 63% | 55% |
| **4** | 2-*n*-Butyl, 4-OMe | 9.3 : 1 | 82% | 74% |
| **5** | 2,6-$Me_2$, 4-OMe | 1 : 0 | 72% | 72% |

[a] Yield and ratio were the average values of reactions and calculated by $^{19}F$ NMR

Standard reaction conditions: diaryliodonium salt (0.5 mmol), 4-fluoroanline (0.5 mmol), 2-fluorotoluene (0.5 mmol internal standard), CuI (20% mol) and $K_2CO_3$ (1.0 mmol) were dissolved in DCM (0.6 mL) in an NMR tube

As previously demonstrated, the selectivity of *N*-arylation is mostly determined by the electronic nature of the relevant groups, and steric control is also evident when the arylation reaction is conducted metal-free. To determine the effect of influencing the selectivity of *N*-arylation when the reaction was conducted in the presence of a copper catalyst, five different substituent patterns of the diaryliodonium salt substrate were again investigated.

As Table 20 shows, the selectivity was mostly influenced by extreme steric factors (the least hindered arene was preferentially transferred) although electronic control was still visible but less pronounced when the reaction was conducted in the presence of a copper catalyst.

Comparison of Entries **1** and **2**, under copper catalysed conditions, show that electronic control was less effective than steric control. According to Entries **2** and **3**, when the steric hindrance was the same in the reaction, aniline preferred to react with the electron-poor ring rather than the electron-rich ring, in other words, electronic control still contributed to the selectivity. From Entries **4** and **5**, 2,6-dimethyl substitution provided more steric hindrance than a single 2-*n*-Butyl substituent, in this reaction 4-fluoroaniline prefers to react with less sterically demanding arene.

Comparing Entry **1** with others, the product yield also was affected by electronic control. It was the same as in the metal-free *N*-arylation reaction that diaryliodonium salts with electron-rich rings provided lower yields of desired product.

However the selectivity of *N*-arylation was changed with an added copper catalyst. The resulting ratio of the product and the unwanted product are shown in Table 21.

**Table 21. Selectivity of metal-free and copper catalyst *N*-arylation**

| Entry | R | Ratio 171 : 172-176 | Ratio 171 : 172-176 (with [Cu]) |
|---|---|---|---|
| **1** | 4-OMe | 2.7: 1 | 1.7 : 1 |
| **2** | 2-Me | 2.3: 1 | 3.7 : 1 |
| **3** | 2-Me, 4-OMe | 4.1:1 | 6.9 : 1 |
| **4** | 2-n-Butyl, 4-OMe | 6.0:1 | 9.3 : 1 |
| **5** | 2,6-$Me_2$, 4-OMe | 28:1 | 1 : 0 |

Addition of a copper catalyst improved the selectivity except for Entry **1**, but the electron-deficient ring was still transferred. Due to the 2,6-disubstitution pattern providing steric hindrance, Entry **5** only produced the desired product.

This suggests that when the reaction was carried out with a copper catalyst, the selectivity was primarily influenced by steric hindrance, although electronic control was still evident, the extent of the reaction was also less than for the metal-free reaction. It is still unclear why the ratio was lower for Entry **1** with an added copper catalyst.

**Table 22. The summary of copper catalysed *N*-Arylation**

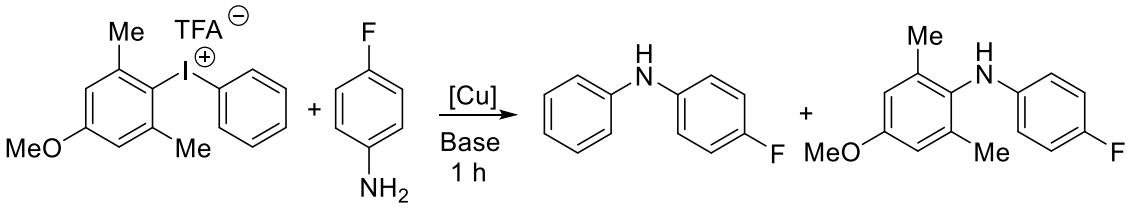


**159** **208** **202** **207**

| Entry | Solvent | Base | [Cu] | Temperature | Ratio[a] 202 : 207 | Yield[a] (202) |
|---|---|---|---|---|---|---|
| **1** | MeCN | $K_2CO_3$ | $Cu(OTf)_2$ | 50 °C | 1 : 0 | 13% |
| **2** | MeCN | $K_2CO_3$ | $CuF_2$ | 50 °C | 0 : 1 | 5% |
| **3** | MeCN | $K_2CO_3$ | $Cu(OAc)_2$ | 50 °C | 3.4 : 1 | 13% |
| **4** | MeCN | $K_2CO_3$ | CuCl | 50 °C | 1 : 1.8 | 7% |
| **5** | MeCN | $K_2CO_3$ | CuI | 50 °C | 1 : 0 | 0.7% |
| **6** | MeCN | $K_2CO_3$ | $Cu(TFA)_2$ | 50 °C | 1 : 0 | 60% |
| **7** | DMF | $K_2CO_3$ | $Cu(OTf)_2$ | 50 °C | 1 : 0 | 32% |
| **8** | DMF | $K_2CO_3$ | $CuF_2$ | 50 °C | 1 : 0 | 87% |
| **9** | DMF | $K_2CO_3$ | $Cu(OAc)_2$ | 50 °C | 40 : 1 | 39% |
| **10** | DMF | $K_2CO_3$ | CuCl | 50 °C | 24 : 1 | 53% |
| **11** | DMF | $K_2CO_3$ | CuI | 50 °C | 1 : 0 | 51% |
| **12** | DMF | $K_2CO_3$ | $Cu(TFA)_2$ | 50 °C | 1 : 0 | 44% |
| **13** | DCM | $K_2CO_3$ | $Cu(OTf)_2$ | r.t. | 1 : 0 | 2% |
| **14** | DCM | $K_2CO_3$ | $CuF_2$ | r.t. | 1 : 0 | 21% |
| **15** | DCM | $K_2CO_3$ | $Cu(OAc)_2$ | r.t. | 1 : 0 | 18% |
| **16** | DCM | $K_2CO_3$ | CuCl | r.t. | 1 : 0 | 10% |
| **17** | DCM | $K_2CO_3$ | CuI | r.t. | 1 : 0 | 72% |
| **18** | DCM | $K_2CO_3$ | $Cu(TFA)_2$ | r.t. | 1 : 0 | 3% |
| **19** | DMF | N/A | $CuF_2$ | r.t. (18 h) | 1 : 0 | 60% |
| **20** | DMF | $K_2CO_3$ | $CuF_2$ | r.t. (18 h) | 1 : 0 | 40% |

| | | | | | | |
|---|---|---|---|---|---|---|
| **21** | DMF | $Et_3N$ | $CuF_2$ | r.t. (18 h) | 1 : 0 | 0% |
| **22** | DMF | Pyridine | $CuF_2$ | r.t. (18 h) | 1 : 0 | 0% |
| **23** | DMF | N/A | $CuF_2$ | 50 ℃ | 1 : 0 | 30% |
| **24** | DMF | $Et_3N$ | $CuF_2$ | 50 ℃ | 1 : 0 | 18% |
| **25** | DMF | Pyridine | $CuF_2$ | 50 ℃ | 1 : 0 | 16% |
| **26** | DCM | N/A | $Cu(TFA)_2$ | r.t. | 1 : 0 | 36% |
| **27** | MeCN | N/A | $Cu(TFA)_2$ | 50 ℃ | 1 : 0 | 55% |
| **28** | DMF | N/A | $Cu(TFA)_2$ | 50 ℃ | 1 : 0 | 41% |

[a] Yield and ratio were calculated by $^{19}F$ NMR

Standard reaction conditions: diaryliodonium salt (0.5 mmol), 4-fluoroanline (0.5 mmol), 2-fluorotoluene (0.5 mmol internal standard), [Cu] (20% mol) and $K_2CO_3$ (1.0 mmol) were dissolved in solvent (0.6 mL) in an NMR tube

In summary, it was shown that when the *N*-arylation reaction was conducted metal-free, the selectivity was mostly controlled by the electronic nature of the relevant groups but steric factors also improved the selectivity, whereas when the reaction was conducted in the presence of a copper catalyst, the selectivity was mostly influenced by extreme steric factors although electronic control was still evident but to a lesser extent.

The best conditions for the *N*-arylation reaction was DMF as the solvent, copper (II) fluoride as the catalyst with potassium carbonate at 50 ℃ for 1 h. Meanwhile, the reaction in DCM provides mild conditions which is suitable for thermal sensitive amines.

### *2.4.2 O-Arylation of Diaryliodonium Salts*

Similar to the *N*-arylation study, 4-fluorophenol was used as the *O*-arylation nucleophile to give a fast method to monitor the reaction yields and the selectivity.

**Table 23. The $^{19}$F NMR peaks of *O*-arylation products in MeCN**

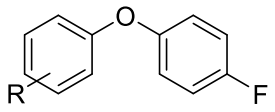


**212** R = H
**213** R = 4-OMe
**214** R = 2-Me
**215** R = 2-Me,4-OMe
**216** R = 2-n-Butyl, 4-OMe
**217** R = 2,6-$Me_2$, 4-OMe

| **Compound** | **R** | **$^{19}$F NMR/ppm** |
|---|---|---|
| **212** | H | -120.8 |
| **213** | 4-OMe | -122.1 |
| **214** | 2-Me | -122.2 |
| **215** | 2-Me, 4-OMe | -123.2 |
| **216** | 2-*n*-Butyl, 4-OMe | -123.3 |
| **217** | 2,6-$Me_2$, 4-OMe | -124.3 |

#### 2.4.2.1 Metal-Free *O*-Arylation

Initially, and like the *N*-arylation reaction we chose five different diaryliodonium salts as the substrate and 4-fluorophenol as the nucleophile, and the reactions were investigated with $K_2CO_3$ as base in MeCN.

**Table 24. Metal-free *O*-arylation**

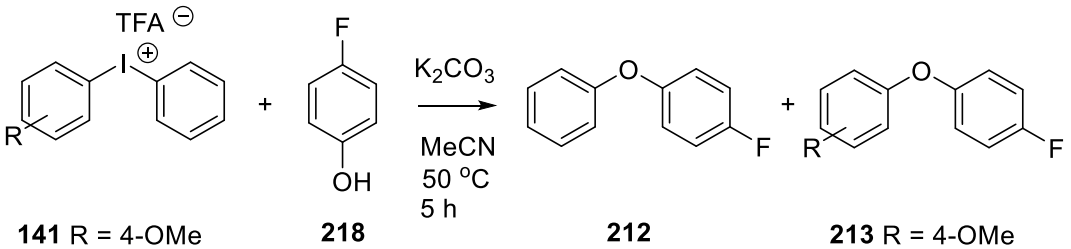


**141** R = 4-OMe
**143** R = 2-Me
**157** R = 2-Me,4-OMe
**158** R = 2-*n*-Butyl, 4-OMe
**159** R = 2,6-$Me_2$, 4-OMe

**218**

**212**

**213** R = 4-OMe
**214** R = 2-Me
**215** R = 2-Me,4-OMe
**216** R = 2-*n*-Butyl, 4-OMe
**217** R = 2,6-$Me_2$, 4-OMe

| Entry | Ar | Ratio[a] 212 : (213-217) | Yield[a] (combined) | Yield[a] (212) |
|---|---|---|---|---|
| **1** | 4-OMe | 24 : 1 | 96% | 93% |
| **2** | 2-Me | 1 : 2.4 | 98% | 32% |
| **3** | 2-Me, 4-OMe | 16 : 1 | 99% | 95% |
| **4** | 2-*n*-Butyl, 4-OMe | 29 : 1 | 98% | 96% |
| **5** | 2,6-$Me_2$, 4-OMe | 5 : 1 | 99% | 79% |

[a] Yield and ratio were the average values of reactions and calculated by $^{19}F$ NMR

Standard reaction conditions: diaryliodonium salt (0.5 mmol), 4-fluorophenol (0.5 mmol), 2-fluorotoluene (0.5 mmol internal standard) and $K_2CO_3$ (1.0 mmol) were dissolved in MeCN (0.6 mL) in an NMR tube

These five different diaryliodonium salts gave all good yields of almost 100% by $^{19}F$ NMR. In Entry **1**, when the diaryliodonium salt **141** reacted with 4-fluorophenol, the nucleophile preferred to react with the electron-deficient ring, whereas in Entry **2** the preference was less for the electronic deficient-ring due to the *ortho*-effect.[65] Unlike in *N*-arylation, the *ortho*-effect in *O*-arylation was more effective. [104, 105]

From Entries **3** and **5**, 2,6-dimethyl substitution did change the selectivity, which suggested that the *ortho*-effect still influenced the reaction, and that 2,6-dimethyl substitution provided a more

pronounced *ortho*-effect than only 2-methyl substitution. However, when a larger single substituent was introduced into the ring (Entry **4**), more of the desired product was generated, that might because the linear structure of **187** (in the structure chapter) made **187** more likely exist in the monomeric form in the reaction which could influence the selectivity.

To compare Entries **1**, **3** to **5**, the electronic effect played the most important role, for Entry **2**, due to the *ortho*-effect, the nucleophile reacted with the hindered ring, however, when the introducing the 4-methoxy group (Entry **3**), the *ortho*-effect was overtaken by the electronic effect. This suggests that when the reaction is under metal-free conditions, the selectivity is primarily influenced by electronic control.

For the metal-free *O*-arylation reaction using diaryliodonium salts, compounds **110** and **117** both exhibited good selectivity and generated more than 93% of the desired product, which suggested that metal-free *O*-arylation reactions provided good yields compared to metal-free *N*-arylation reactions. However, due to the *ortho*-effect in *O*-arylation, compound **159** did not provide as good selectivity as it did in *N*-arylation reaction suggesting that the steric effect is more important for *N*-arylation.

For both *N*-arylation and *O*-arylation reaction, the selectivity is primarily influenced by electronic control.

#### 2.4.2.2 Copper Catalysed *O*-Arylation

As diaryliodonium salts successfully demonstrated the selectivity in the *N*-arylation reaction in the presence of a copper catalyst, it was valuable to investigate whether this would also be the case for the *O*-arylation reaction. As a result, these five different diaryliodonium salts were reacted with 4-fluorophenol and $K_2CO_3$ and CuI in MeCN.

**Table 25. Copper catalysed *O*-arylation**

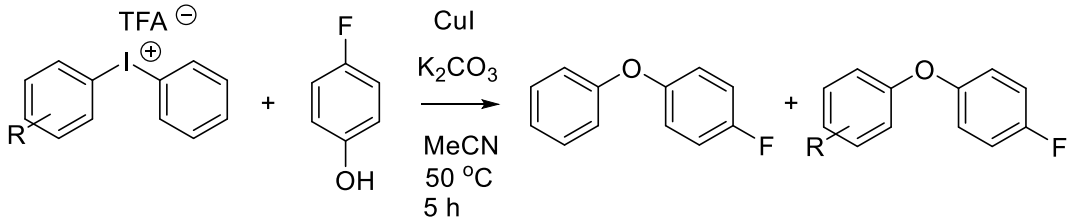


**141** R = 4-OMe
**143** R = 2-Me
**157** R = 2-Me,4-OMe
**158** R = 2-*n*-Butyl, 4-OMe
**159** R = 2,6-$Me_2$, 4-OMe

**218**

**212**

**213** R = 4-OMe
**214** R = 2-Me
**215** R = 2-Me,4-OMe
**216** R = 2-*n*-Butyl, 4-OMe
**217** R = 2,6-$Me_2$, 4-OMe

| Entry | Ar | Ratio[a] 212 : (213-217) | Yield[a] (combined) | Yield[a] (212) |
|---|---|---|---|---|
| **1** | 4-OMe | 2.6 : 1 | 5.4% | 4% |
| **2** | 2-Me | 2 : 1 | 4.5% | 3% |
| **3** | 2-Me, 4-OMe | 5.8 : 1 | 9.3% | 7.9% |
| **4** | 2-*n*-Butyl, 4-OMe | 7.3 : 1 | 5.4% | 4.8% |
| **5** | 2,6-$Me_2$, 4-OMe | 1 : 0 | 4% | 4% |

[a] Yield and ratio were the average values of reactions and calculated by $^{19}F$ NMR

Standard reaction conditions: diaryliodonium salt (0.5 mmol), 4-fluorophenol (0.5 mmol), 2-fluorotoluene (0.5 mmol internal standard), CuI (20% mol) and $K_2CO_3$ (1.0 mmol) were dissolved in MeCN (0.6 mL) in an NMR tube

As Table 22 shows, the reaction yields were all low with only about 5% of product being formed. From the ratio between **212** and **213** to **217**, it was shown that when a copper catalyst was used in the reaction, steric control had greater influence in the selectivity, although the selectivity in Entry **2** was reversed when compared with the result obtained under metal-free conditions.

From Entries **2** and **3**, electronic control still influenced the ratio of products, with similar steric hindrance, oxygen nucleophiles still preferred to react with the electron-deficient ring, but the ratio of Entry **1** was not as good as that obtained under metal-free conditions. From the Entries

**3**, **4**, and **5**, increasing the steric hindrance just made this reaction more selective and 2,6-substitution was more effective than just 2-substitution. According to the structure of the diaryliodonium salt copper complex **169** (in the structure chapter), even a large group such as the n-butyl group, does not change the outcome whereas 2,6-disubstitution does with the one substituent in the middle of the two counter-ions.

Entry **5** provided a method to get the pure product, but unfortunately, the yield was too low to be a practical method for accessing diarylethers.

To compare with the *N*-arylation reaction, the ratios of products obtained between the two reactions are similar, except that the ratio for Entry **1** is higher than Entry **2** in *O*-arylation (Table 25) but lower in *N*-arylation (Table 20), which suggests in the copper catalysed reactions, steric control is more important in *N*-arylation, and in the *O*-arylation reaction electronic control has a greater contribution than in *N*-arylation.

In order to find out the best conditions for *O*-arylation with a copper catalyst, we also investigated different copper catalysts, solvents and temperatures.

### 2.4.2.3 The Effect of Solvent in *O*-Arylation

**Table 26. Copper catalysed *O*-arylation in DCM**

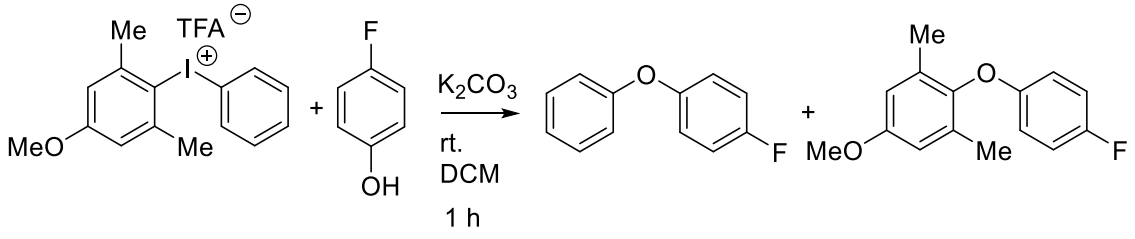


**159** **218** **212** **217**

| Entry | [Cu] | Ratio[a] 212 : 217 | Yield[a] (212) |
|---|---|---|---|
| **1** | $Cu(OTf)_2$ | 1 : 0 | 18% |
| **2** | $CuF_2$ | 4.6 : 1 | 9% |
| **3** | $Cu(OAc)_2$ | 1 : 0 | 30% |
| **4** | CuCl | 15 : 1 | 22% |
| **5** | CuI | 6.8 : 1 | 16% |
| **6** | $Cu(TFA)_2$ | 4.8 : 1 | 8% |

[a] Yield and ratio were calculated by $^{19}F$ NMR

Standard reaction conditions: diaryliodonium salt (0.5 mmol), 4-fluorophenol (0.5 mmol), 2-fluorotoluene (0.5 mmol internal standard), [Cu] (20% mol) and $K_2CO_3$ (1.0 mmol) were dissolved in DCM (0.6 mL) in an NMR tube.

The reaction was carried out in DCM at room temperature and five different copper catalysts were tested in the *O*-arylation reaction. $Cu(OTf)_2$ and $Cu(OAc)_2$ generated only compound **212** without any **217,** this might be because that in DCM the homogenous catalysts could generate the complex with iodonium salts. Meanwhile, the other three heterogeneous catalysts did not provide complete selectivity, $CuF_2$ and CuI gave similar ratios to those without the copper catalyst, although CuCl increased the ratio between **212** and **217.** Unfortunately, the $Cu(TFA)_2$ resulted in the same ratio as the reaction under metal-free conditions.

**Table 27. Copper-catalysed *O*-Arylation in DCM for 10 h**

| Entry | [Cu] | Ratio[a] 212 : 217 | Yield[a] (212) |
|---|---|---|---|
| **1** | $Cu(OTf)_2$ | 1 : 0 | 73% |
| **2** | $CuF_2$ | 10 : 1 | 66% |
| **3** | $Cu(OAc)_2$ | 1 : 0 | 46% |
| **4** | CuCl | 28 : 1 | 68% |
| **5** | CuI | 7.1 : 1 | 53% |
| **6** | $Cu(TFA)_2$ | 5.0 : 1 | 48% |

[a] Yield and ratio were calculated by $^{19}F$ NMR

Standard reaction conditions: diaryliodonium salt (0.5 mmol), 4-fluorophenol (0.5 mmol), 2-fluorotoluene (0.5 mmol internal standard), [Cu] (20% mol) and $K_2CO_3$ (1.0 mmol) were dissolved in DCM (0.6 mL) in an NMR tube.

Allowing the reaction to proceed at room temperature for 10 h, all the reaction yields increased, $Cu(OTf)_2$ gave 73% yield as the best. All the heterogeneous catalysts gave an increased the ratio of **212** and **217**, suggesting heterogeneous catalysts need a longer reaction time than homogenous catalysts. However, only $Cu(OTf)_2$ and $Cu(OAc)_2$ provided complete selectivity.

**Table 28. Copper-catalysed *O*-Arylation in MeCN**

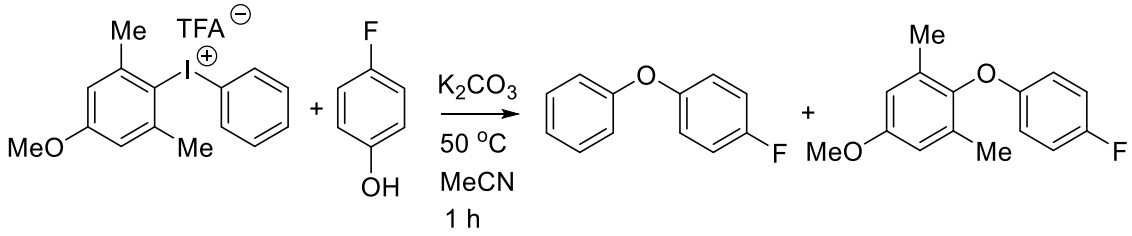


**159** **218** **212** **217**

| Entry | [Cu] | Ratio[a] 212 : 217 | Yield[a] (212) |
|---|---|---|---|
| **1** | $Cu(OTf)_2$ | 1 : 0 | 10% |
| **2** | $CuF_2$ | 4.6 : 1 | 51% |
| **3** | $Cu(OAc)_2$ | 1 : 0 | 7% |
| **4** | CuCl | N/A | N/A |
| **5** | CuI | 1 : 0 | 4% |
| **6** | $Cu(TFA)_2$ | 1 : 0 | 45% |

[a] Yield and ratio were calculated by $^{19}F$ NMR

Standard reaction conditions: diaryliodonium salt (0.5 mmol), 4-fluorophenol (0.5 mmol), 2-fluorotoluene (0.5 mmol internal standard), [Cu] (20% mol) and $K_2CO_3$ (1.0 mmol) were dissolved in MeCN (0.6 mL) in an NMR tube.

As the Table 28 shows, $Cu(OTf)_2$ and $Cu(OAc)_2$, as the homogenous catalysts provide good selectivity but the yields are much lower than the copper free process. CuI was the only heterogeneous catalyst in this set of results and provided **212** only, CuCl did not generate any product at all, the result with $CuF_2$ was just the same as the reaction without the copper catalyst, the ratio was similar but the yield dropped. That might be because heterogeneous catalyst could not form the copper complex with diaryliodonium salts and the metal free process took place. CuI might could dissolve in MeCN, thus this reaction provided a good selectivity. However, $CuF_2$ and CuCl contained strong nucleophilic atoms (F and Cl), which might react directly with the diaryliodonium salt thus the reaction ratio changed due to the formation of alternative products.

**Table 29. Copper catalysed *O*-arylation in DMF**

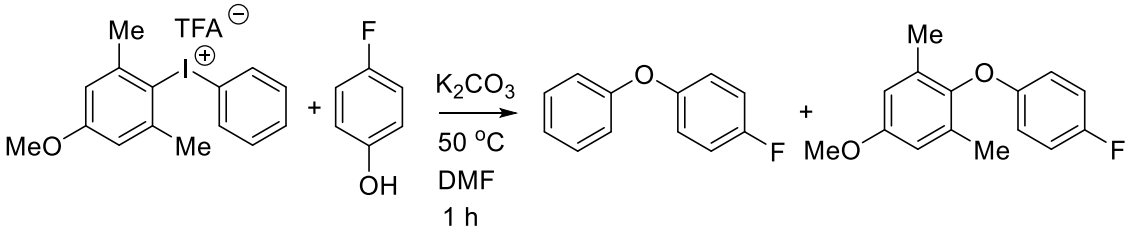


**159** **218** **212** **217**

| Entry | [Cu] | Ratio[a] 212 : 217 | Yield[a] (212) |
|---|---|---|---|
| **1** | $Cu(OTf)_2$ | 1 : 0 | 5% |
| **2** | $CuF_2$ | 1: 0 | 3% |
| **3** | $Cu(OAc)_2$ | 1 : 0 | 1% |
| **4** | CuCl | 1: 0 | 2% |
| **5** | CuI | 1 : 0 | 6% |
| **6** | $Cu(TFA)_2$ | 4.6 : 1 | 56% |

[a] Yield and ratio were calculated by $^{19}F$ NMR

Standard reaction conditions: diaryliodonium salt (0.5 mmol), 4-fluorophenol (0.5 mmol), 2-fluorotoluene (0.5 mmol internal standard), [Cu] (20% mol) and $K_2CO_3$ (1.0 mmol) were dissolved in DMF (0.6 mL) in an NMR tube.

When the solvent was DMF, all the copper catalysts, except $Cu(TFA)_2$, provided good selectivity, but the yield was still less than 10%. Comparing the $CuF_2$ in DMF to both DCM and MeCN, showed that $CuF_2$ did not change the reaction ratio in MeCN but could in DMF. One reason might be that the polarity of DMF is higher than MeCN so that the diaryliodonium salts copper complex could dissolve in the solvent changing a heterogeneous catalyst to a homogeneous one.

In summary, it was shown that when the *O*-arylation reaction was conducted metal-free, the selectivity is primarily influenced by electronic control, steric control only influenced the reaction when the substitution group is large enough (*n*-Butyl group, Entry **4**, Table 23) which stops the free interchange of the aromatic rings, and the *ortho*-effect also influenced the reaction,

which is a little different from *N*-arylation. When the reaction was conducted in the presence of a copper catalyst, the selectivity was mostly influenced by extreme steric factors although electronic control was still evident. Unlike *N*-arylation, the yields were lower when a copper catalyst was added. The best conditions for *O*-arylation were using MeCN as solvent, $K_2CO_3$ as a base at 50 ℃ for 5 h.

### *2.4.3 Fluorination of Diaryliodonium Salts*

Fluorination of diaryliodonium salts has become a focused area, especially, for the preparation of $^{18}F$ radiopharmaceuticals. As diaryliodonium salts have two aromatic rings which can both react with fluoride, it is important to improve the chemical selectivity of this process. The reaction is the same as for *N*-arylation, the diaryliodonium salt loses the counter-ion and fluoride adds to the hypervalent iodine species, following pseudorotation, the product could result from two different possible pairs of iodoarene and fluoroarene. Improving the selectivity and yields were an important part in this research.

The $^{19}F$ NMR peaks have been shown in Table 27.

**Table 30. $^{19}F$ NMR data for the possible fluorination products in DMF**

**102** R = H
**219** R = 2-Me
**220** R = 4-OMe
**221** R = 2-Me,4-OMe
**222** R = 2-n-Butyl, 4-OMe
**223** R = 2,6-$Me_2$, 4-OMe
**224** R = 4-F
**226** R = 2,4,6-$Me_3$

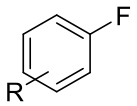


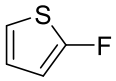


**225**

| Compound | R | $^{19}F$ NMR/ppm |
|---|---|---|
| **102** | H | -113.8 |
| **219** | 2-Me | -118.5 |
| **220** | 4-OMe | -125.0 |
| **221** | 2-Me, 4-OMe | -129.6 |
| **222** | 2-n-Butyl, 4-OMe | -130.8 |
| **223** | 2,6-$Me_2$, 4-OMe | -133.7 |
| **224** | 4-F | -115.4 |
| **225** | 2-thienyl | -135.2 |
| **226** | 2,4,6-$Me_3$ | -127.5 |

### 2.4.3.1 Metal-Free Fluorination

As mentioned in the sections on *N*- and *O*-arylation, the selectivity of metal-free nucleophilic substitution using diaryliodonium salts mostly depends on electronic control and steric control.

The different substitution patterns of the diaryliodonium salts were used to prove the importance of these effects for different fluorination reagents. Due to the large size of caesium atom, caesium fluoride was commonly used as the fluorinating agent as it was soluble in DMF

**Table 31. Metal-free fluorination using CsF**

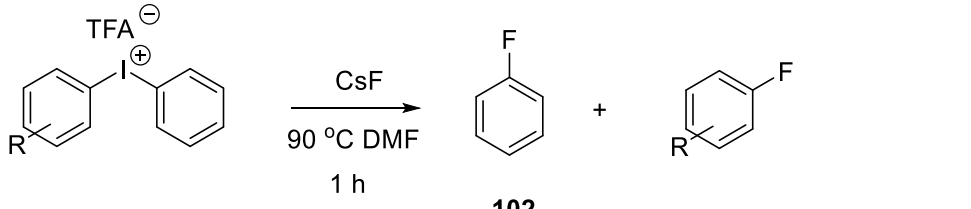


**141** R = 4-OMe
**142** R = 4-OMe ($TfO^{\ominus}$)
**157** R = 2-Me,4-OMe
**158** R = 2-*n*-Butyl, 4-OMe
**159** R = 2,6-$Me_2$, 4-OMe
**150** R = 4-F

**102**

**220** R = 4-OMe
**221** R = 2-Me,4-OMe
**222** R = 2-*n*-Butyl, 4-OMe
**223** R = 2,6-$Me_2$, 4-OMe
**224** R = 4-F

| | Ar | Ratio[a] 102: (220-224) | Yields[a] (102) |
|---|---|---|---|
| **1** | 4-OMe | 43 : 1 | 25% |
| **2** | 4-OMe ($TfO^{\ominus}$) | 44 : 1 | 31% |
| **3** | 2-n-Bu, 4-OMe | 19 : 1 | 95% |
| **4** | 2-Me, 4-OMe | 8 : 1 | 24% |
| **5** | 2,6-Me, 4-OMe | 2.2 : 1 | 11% |
| **6** | 4-F | 1 : 7 | 3% |

[a] Yield and ratio were calculated by $^{19}F$ NMR

Standard reaction conditions: diaryliodonium salt (0.5 mmol), CsF (1.0 mmol), 2-fluorotoluene (0.5 mmol internal standard) were dissolved in DMF (0.6 mL) in an NMR tube.

The reaction was carried out using DMF as solvent and caesium fluoride as the fluorination reagent. All of the reactions used 2-fluoroutoluene as an internal standard and were monitored by $^{19}F$ NMR. From this Table, the selectivity of fluorination was more dependent on electronic control than steric control. The introduction of an *ortho* substituent (Entries **3** to **5)** resulted in lower selectivity than Entry **1**, which was similar to *O*-arylation. The *ortho*-effect was also present in the fluorination reaction and that di-*ortho* substitution (Entry **5**) had a stronger *ortho*-effect than only 2-methyl substitution.

However the result was the same as *O*-arylation, when the diaryliodonium salt contained a large substituent such as the n-butyl group (Entry **3**), the selectivity was improved. The unique linear structure of diaryliodonium salt **158** may make monomer formation easier, thus the product yield was higher than others. As expected, e.g. Entry **6**, the fluoride preferred to react with electron-deficient ring 4-fluorophenyl to more **224**.

**Table 32. Metal-free fluorination using $Et_4NF$**

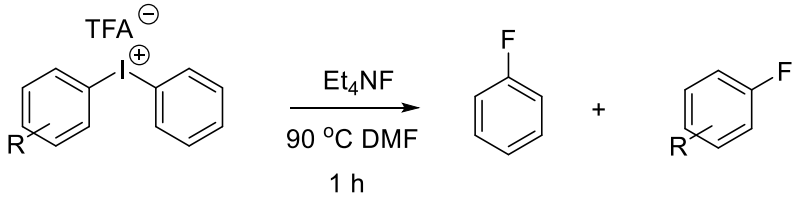


**102**

**141** R = 4-OMe
**142** R = 4-OMe ($TfO^{\ominus}$)
**157** R = 2-Me,4-OMe
**158** R = 2-*n*-Butyl, 4-OMe
**159** R = 2,6-$Me_2$, 4-OMe
**150** R = 4-F

**220** R = 4-OMe
**221** R = 2-Me,4-OMe
**222** R = 2-*n*-Butyl, 4-OMe
**223** R = 2,6-$Me_2$, 4-OMe
**224** R = 4-F

| | Ar | Ratio[a] 102: (220-224) | Yields[a] (102) |
|---|---|---|---|
| **1** | 4-OMe | 1 : 0 | 10% |
| **2** | 4-OMe ($TfO^{\ominus}$) | 1 : 0 | 9.6% |
| **3** | 2-n-Butyl, 4-OMe | 10 : 1 | 16% |
| **4** | 2-Me, 4-OMe | 13 : 1 | 20% |
| **5** | 2,6-Me, 4-OMe | 3.5 : 1 | 8.9% |
| **6** | 4-F | 1 : 2 | 7% |

[a] Yield and ratio were calculated by $^{19}F$ NMR

Standard reaction conditions: diaryliodonium salt (0.5 mmol), $Et_4NF$ (1.0 mmol), 2-fluorotoluene (0.5 mmol internal standard) were dissolved in DMF (0.6 mL) in an NMR tube

When the reaction used tetraethylammonium fluoride as the fluorination reagent, the yields dropped and the ratios between fluorobenzene and the unwanted products were also changed. In this reaction, Entries **1**, **2** provided good selectivity but in only 10% yield. The selectivity of all the reactions is similar to the results in Table 28, except Entry **3**.

To compare with Table 31, Entry **3** did not give as selective a reaction as when caesium fluoride was used as the reagent, it even provided more of the unwanted product than Entry **4**. However, using tetraethylammonium fluoride as the fluorination agent, electronic control was still the most important controlling factor in determining the selectivity of the reaction.

### 2.4.3.2 Fluorination in Flow

Flow systems have been widely used for organic synthesis, compared to batch reactions flow chemistry provides excellent mixing and improved heat transfer. It also allows solvents to be used beyond their usual boiling points to extend the range of reaction conditions. Thus, the fluorination reactions of diaryliodonium salts were also investigated in a flow system.


**Figure 42. Flow reactor configuration**

The flow system could be established by connecting two pumps to a reactor such as a coil. The solutions of the reagents are then pumped into the tube, where the reaction will take place, a solution of the product is then obtained from output of the reactor. Flow chemistry can be applied on both laboratory scales and on large scales with only limited changes to the conditions required.

It is the small diameter coil of the reactor, that provides excellent heat transfer and mixing, and the pressure can also be controlled, so that the reaction temperature can be raised above the reagents and solvent's boiling point extending the reaction parameters beyond these used in batch reactions. Using a copper coil as the reactor may negate the use of a copper catalyst as the reaction may take place on the surface of copper or via nanoparticles leached into the reaction mixture.

**Table 33. Fluorination in flow using a PTFE coil**

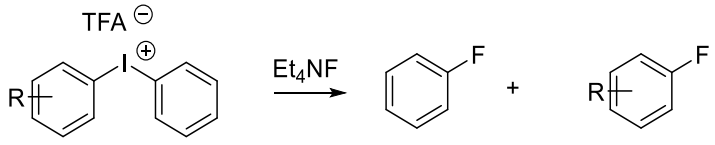


**102**

**141** R = 4-OMe
**157** R = 2-Me,4-OMe
**158** R = 2-*n*-Butyl, 4-OMe
**159** R = 2,6-$Me_2$, 4-OMe
**144** R = 2,4,6-$Me_3$

**220** R = 4-OMe
**221** R = 2-Me,4-OMe
**222** R = 2-*n*-Butyl, 4-OMe
**223** R = 2,6-$Me_2$, 4-OMe
**226** R = 2,4,6-$Me_3$

[a] Ratio were calculated by $^{19}F$ NMR

| R | Ratio: (Flow 90 °C) 102 : (220-223, 226) | Ratio: (Flow 150 °C) 102 : (220-223, 226) |
|---|---|---|
| **1** 4-OMe | 20 : 1 | 1 : 7.3 |
| **2** 2-Me, 4-OMe | 13 : 1 | 13 : 1 |
| **3** 2-n-Butyl, 4-OMe | 10 : 1 | 10 : 1 |
| **4** 2,6-$Me_2$, 4-OMe | 2.6 : 1 | 2.6 : 1 |
| **5** 2,4,6-$Me_3$ | 3.6 : 1 | 3.6 : 1 |

Standard reaction conditions: diaryliodonium salt (1 eq.), tetraethylammonium fluoride (1 eq.) were dissolved in DMF, flow rate: 0.33 mL/min, PTFE coil (20 mL).

When the reaction was carried out under flow conditions, the ratios of desired product and the unwanted product were similar to that obtained in the batch reaction except for Entry **1** when the temperature was 90 °C which was less selective. However, when the reaction temperature was increased to 150 °C, the ratio was reversed, however the outcome for other diaryliodonium salts was the same for both temperatures.

It might be that when the temperature was increased to 150 °C, compound **141** started to decompose (suggested by the TGA-DSC data) and generated both benzene and anisyl radical (from computational studies) which then reacted with fluoride thus it lost the selectivity due to

a mechanism change, this suggested the diaryliodonium salts containing electron-rich arene may be unsuitable for reactions at elevated temperatures.

**Table 34. Fluorination using aryl-2-thienyl iodonium salts in flow using a PTFE coil**

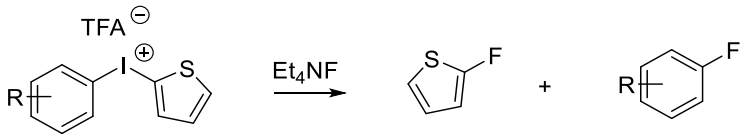


**194**

**145** R = H
**147** R = 4-OMe
**160** R = 2-Me,4-OMe
**161** R = 2,6-$Me_2$, 4-OMe
**149** R = 2,4,6-$Me_3$

**102** R = H
**220** R = 4-OMe
**221** R = 2-Me,4-OMe
**223** R = 2,6-$Me_2$, 4-OMe
**226** R = 2,4,6-$Me_3$

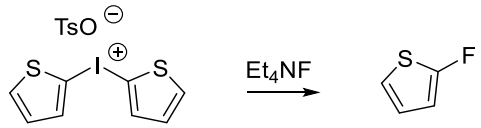


**165** **225**

[a] Ratio were calculated by $^{19}F$ NMR

| | Ar | Ratio[a]: (Flow 90 °C) (102, 220-223, 226) : (225) | Ratio[a]: (Flow 150 °C) (102, 220-223, 226) : (225) |
|---|---|---|---|
| **1** | H | 1 : 0 | 1 : 0 |
| **2** | 4-OMe | No reaction | 1 : 0 |
| **3** | 2-Me, 4-OMe | No reaction | 1 : 0 |
| **4** | 2,6-Me, 4-OMe | No reaction | 1 : 0 |
| **5** | 2,4,6-Me | 1 : 0 | 1 : 0 |
| **6** | **135** | No reaction | 1 : 0 |

Standard reaction conditions: diaryliodonium salt (1 eq.), tetraethylammonium fluoride (1 eq.) were dissolved in DMF, flow rate: 0.33 mL/min, PTFE coil (20 mL).

Due to the 2-thienyl group being a small size it will often act as the non-participating group, as a result aryl-2-thienyliodonium salts have received much attention in organic synthesis. In the batch reactions, the volatile 2-fluorothiophene may be lost, but this is not possible in the heated flow system as it is sealed. It has been shown in Table 31, all of the diaryliodonium salts provided good selectivity in the fluorination reaction, but only when the temperature was raised to 150 °C Entries **2**, **3**, **4** and **6** could generate the product. That suggested the reactions required a higher reaction temperature. Unfortunately, all the aryl-2-thienyliodonium salts reactions generated a lot of by-products again suggesting they are unstable under these reaction conditions.

**Table 35. HPLC chromatogram of the fluorination reaction mixture under the 205 nm wavelength**

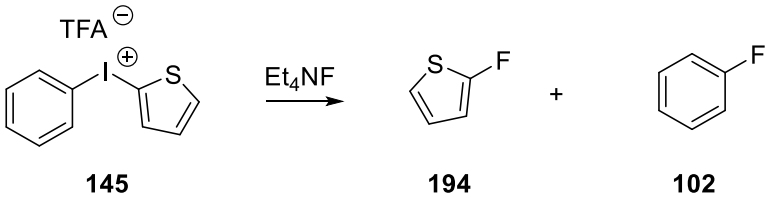


**145** **194** **102**

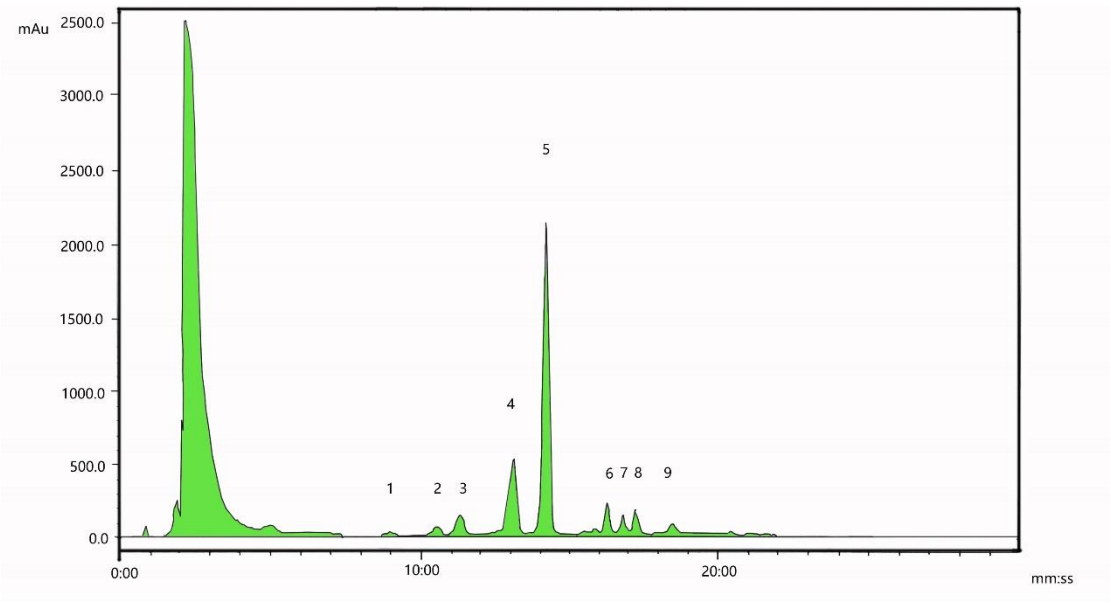


| | Number | Start (mm:ss) | End (mm:ss) | Retention (mm:ss) | Area (mAu) | Mole Ratio[a] |
|---|---|---|---|---|---|---|
| Iodobenzene | 1 | 8:36 | 9:17 | 8:55 | 354 | 1 |
| 2-Iodothiophene | 2 | 10:08 | 10:53 | 10:29 | 989 | 1.2 |

| | | | | | | |
|---|---|---|---|---|---|---|
| Fluorobenzene | 3 | 10:54 | 11:43 | 11:16 | 2313 | 0.8 |
| Benzene | 4 | 12:17 | 13:29 | 13:04 | 8761 | 0.2 |
| Thiophene | 5 | 13:36 | 14:38 | 14:09 | 29439 | 0.1 |
| Unknown | 6 | 16:02 | 16:32 | 16:15 | 2214 | |
| Unknown | 7 | 16:35 | 17:01 | 16:47 | 1129 | |
| Unknown | 8 | 17:03 | 17:41 | 17:12 | 1700 | |
| Unknown | 9 | 18:11 | 18:48 | 18:24 | 884 | |

[a]The mole of iodobenzene was set as 1

To understand the reason of low yields in the aryl-2-thienyliodonium salts reactions, HPLC was used to analysis the reaction mixture. For example, the reaction mixture of Entry **1** (90 ℃) was analysed by HPLC, the chromatogram shows that the reaction generated seven by-products: iodobenzene, benzene, thiophene and several unknown by-products.

Although the peak 5 (thiophene) had the biggest area (29439 mAu), according to the calibration curves, it was only 0.1 eq. to compare with iodobenzene. The ratio of the identified compound was also calculated from the calibration curves (provided in Appendices). This suggested that aryl-2-thienyliodonium salts are not stable even when the temperature was only 90 ℃.

### 2.4.3.3 Copper Catalysed Fluorination

As mentioned before, a copper catalyst was useful in both *N*- and *O*-arylation reactions, but unfortunately, the methods we used were not suitable for copper catalysed fluorination. Several copper catalysts ($Cu(TfO)_2$, CuI, $Cu(OAc)_2$, $CuF_2$) and different fluorination reagents (KF with 18-crown-6 or $K_{222}$, CsF, $Et_4NF$) were investigated for fluorination, but only when the reaction was carried out under flow conditions with a copper coil was the product generated.

**Table 36. Copper catalysed fluorination in flow**

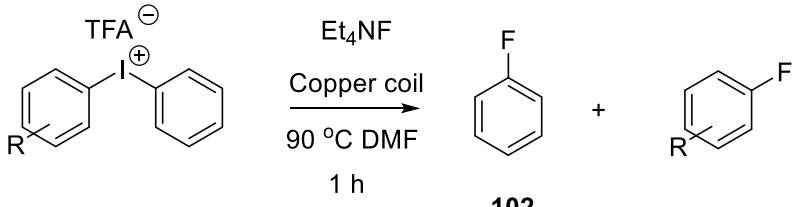


**141** R = 4-OMe
**142** R = 4-OMe (TfO$^{\ominus}$)
**157** R = 2-Me,4-OMe
**158** R = 2-*n*-Butyl, 4-OMe
**159** R = 2,6-$Me_2$, 4-OMe
**150** R = 4-F

**220** R = 4-OMe
**221** R = 2-Me,4-OMe
**222** R = 2-*n*-Butyl, 4-OMe
**223** R = 2,6-$Me_2$, 4-OMe
**224** R = 4-F

| | Ar | Ratio[a] 102: (220-224) | Yields[a] (102) |
|---|---|---|---|
| **1** | 4-OMe | 1 : 0 | 6.8% |
| **2** | 4-OMe (TfO$^{\ominus}$) | 1 : 0 | 3.8% |
| **3** | 2-*n*-Butyl, 4-OMe | 20 : 1 | 30% |
| **4** | 2-Me, 4-OMe | 13 : 1 | 16% |
| **5** | 2,6-$Me_2$, 4-OMe | 1 : 0 | 4.6% |
| **6** | 4-F | 1 : 3 | 10% |

[a] Yield and ratio were calculated by $^{19}$F NMR

Standard reaction conditions: diaryliodonium salt (1 eq.), tetraethylammonium fluoride (1 eq.), and 2-fluorotoluene (1 eq. internal standard) were dissolved in DMF, flow rate: 0.33 mL/min, copper coil (20 mL).

When the reaction was transferred to the flow system with a copper coil reactor, the steric control elements started to have a more prominent effect on the reaction, this was greater than observed with the batch reaction. Entry **5** provided good selectivity in the reaction, suggesting that when the reaction used a copper catalyst, steric control had a greater contribution than under metal-free conditions. But the yield was only 4.6% so this may influence the outcome. From Entry **1** and **2**, TFA salts usually generated more product than the TfO salts although both yields were low. Also higher yields for Entry **3** again suggested that linear structure of diaryliodonium salt **158** may make monomer formation easier and hence facilitate the reaction.

To compare with Table 33, Entry **3** improved a little bit on selectivity, but Entry **4** did not change, that might be because the steric hindrance was not enough to cause the change under these conditions.

Copper catalysed fluorination using diaryliodonium salts is similar to *O*-arylation, in that the yields drop when adding a copper catalyst. In this fluorination reaction steric and electronic control combine together to give the best selectivity.

## 2.5 Application of Fluorous Solid-Phase Extraction

It has been demonstrated that the *N*-, *O*-arylations and fluorination using diaryliodonium salts provided a good selectivity when using **141** or **159**.

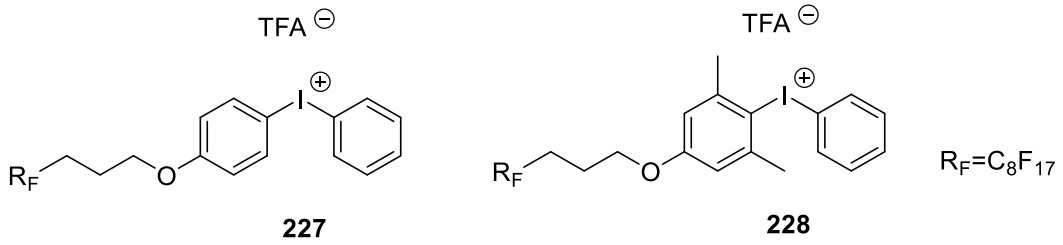


**Figure 43. The fluorous diaryliodonium salts**

As we have demonstrated the selectivity (in the chapters on *N*- and *O*-arylations) the nucleophilic substitution reaction of diaryliodonium salts is controlled by both electronic and steric factors. The two fluorous diaryliodonium salts were designed with an electron-rich group (oxygen) **227** and/or steric hindrance caused by alkyl groups in the two *ortho*- positions, **228**. The compound **227** could be used for metal-free *O*-arylation and metal free fluorination, **228** could be used with a copper catalyst for *N*-arylation and fluorination in a copper coil using a flow system.

Thus, the compounds **227** and **228** were designed as the fluorous diaryliodonium salts to investigate using the fluorous groups as a means to facilitate purification. Adding a three-carbon chain between the oxygen and the long fluorous chain reduces the inductive effect of the latter on the aromatic rings, so the selectivity should be the same as **141** and **159.**

### *2.5.1 Synthesis of* O-*Fluorous Diaryliodonium Salts*

A possible way to introduce fluorous chains into aromatic systems is the Williamson[189] ether synthesis, followed by oxidation of any iodoarene **232**, **233** to the aryliodobis(acetate) **234**, **235** by sodium perborate tetrahydrate, then diaryliodonium salt generation, finally giving the *O*-fluorous diaryliodonium salts **227** and **228**(Scheme 57).

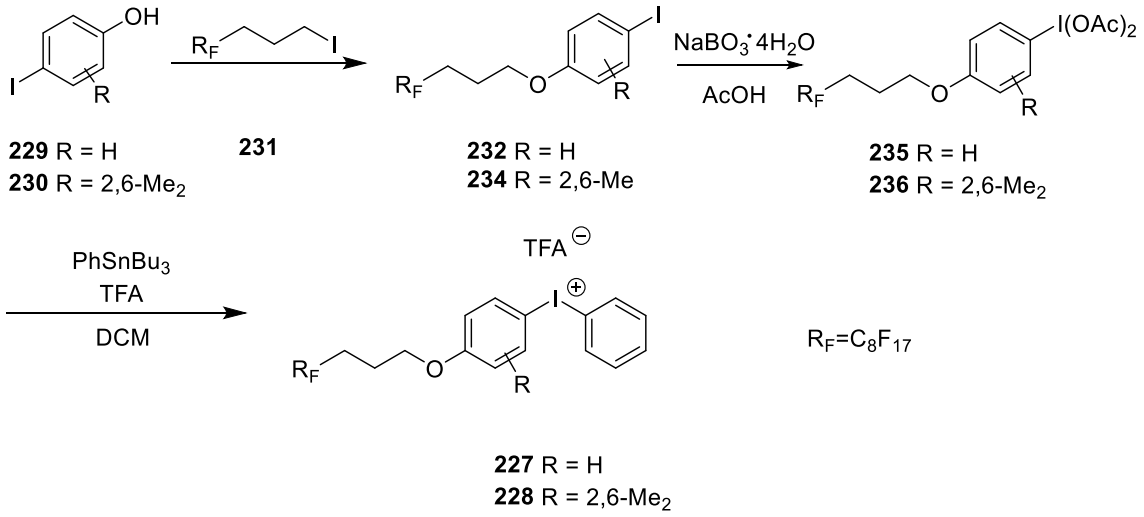


**Scheme 56. General route for *O*-fluorous diaryliodonium salts**

In the Williamson[189] ether synthesis, 4-iodophenol **231** was first converted into its caesium salt, and then it was reacted with 3-(perfluorooctyl)propyl iodide **232**. The yield of this product was 93% and it was pure enough to be used directly in the next reaction. For 4-iodo-3,5-dimethylphenol **230**, this reaction also provided the product in 92% yield, which means the steric hinderance did not affect the Williamson[189] ether synthesis.

Using the same method as before, sodium perborate tetrahydrate was used as the oxidizing agent, and provided a high yield of the iodine (III) species (such as **234**, 64%).

However, the steric hinderance did influence this reaction, as **235** was only produced in a 35% yield, this is because the two-methyl groups provide additional steric hindrance around the iodine centre. This steric effect may reduce the reactivity and therefore an intermediate $ArI(TFA)_2$ which is more reactive may be required to form the diaryliodonium salt.

The crude diaryliodonium salt (**227**, **228**) contained unwanted tributylphenylstannane **133**, because the polarity difference between the product and starting materials was wide and the product was insoluble in petroleum ether, it was easy to get the pure product just by recrystallization from DCM and petroleum ether.

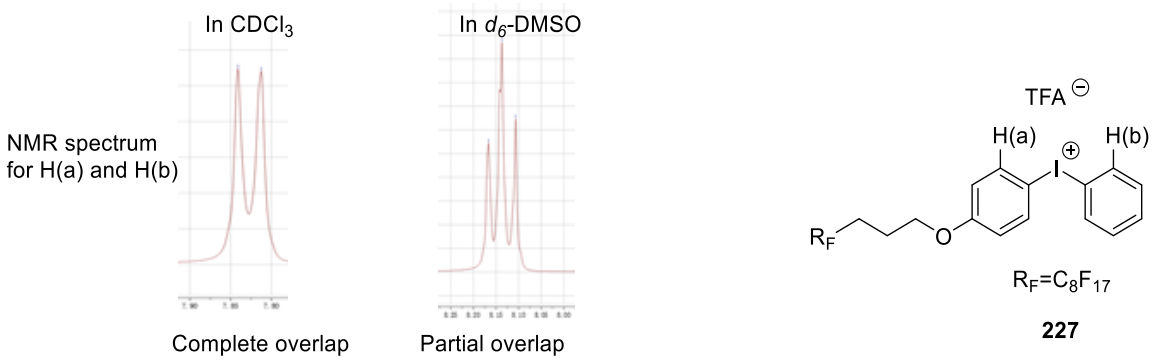


**Figure 44. The $^1$H NMR overlapping for 227**

It is interesting that the product had differences in $^1$H NMR chemical shifts which were observed on changing the solvent from $CDCl_3$ to $d_6$-DMSO, especially if the solvent is $CDCl_3$, the chemical shifts are exactly the same for H(a) and H(b). In $d_6$-DMSO the overlapping is reduced and appear as three peaks (overlapped doublets).

The use of the sterically hindered aryliodobis(acetate) **235** resulted in only 42% of the diaryliodonium salts **228**, which is similar to the production of the mesitylene(phenyl)iodonium salt **144** (45%).

### *2.5.2 Arylation Reactions Using Fluorous Diaryliodonium Salts*

As it has been shown that **141** and **159** could result in good selectivity in different reactions using diaryliodonium salts, the fluorous diaryliodonium salts **227** and **228** were tested in these reactions.

#### 2.5.2.1 *N*-Arylation Reaction

As compound **159** provided good selectivity in the copper catalysed *N*-arylation reaction, fluorous diaryliodonium salt **228** which should exhibit the same steric control was used for this process. As the data in *N*-arylation reaction chapter, both DMF and DCM as a solvent resulted good selectivity. DMF could be direct used directly with the F-SPE method, e.g. loading the reaction mixture onto the fluorous silica, then washing with 90% DMF and 10% water, should separate the product. Unwanted by-products and unreacted diaryliodonium salt could then be collected by methanol washing. However, the product would need to be extracted again due to the high boiling point of DMF, thus DCM maybe the best solvent.

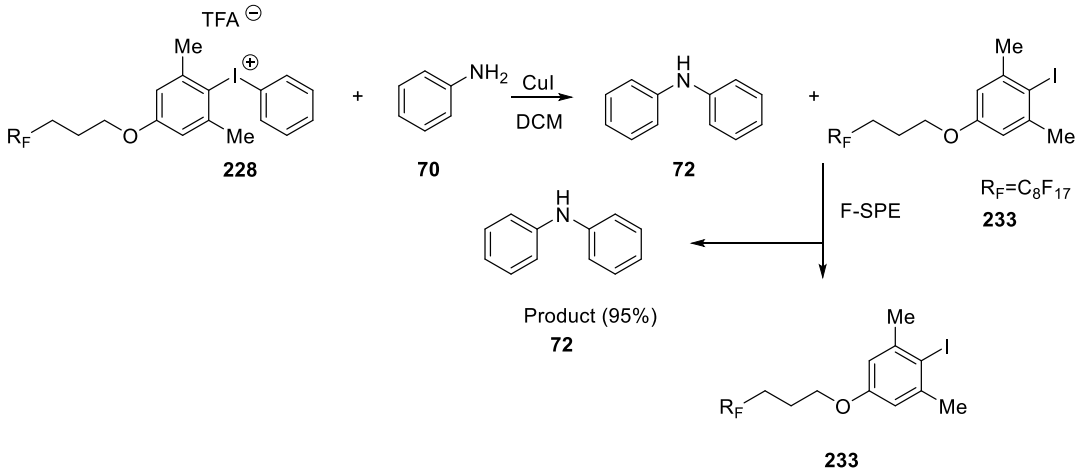


**Scheme 57. The process of F-SPE in *N*-arylation**

The reaction conditions we used for the fluorous diaryliodonium salt **228** is reaction of aniline

in the presence of CuI in DCM at room temperature for 1 h, and by using dry loading method, the product diarylamine **72**, by-product **233** and unreacted diaryliodonium salt were loaded into the fluorous silica, due to the fluorous solid-phase extraction, the mixture was easily separated by washing with 80% methanol and 20% water to get the product diarylamine, then the by-product and unreacted starting material were removed by washing with methanol.

For this reaction, we got 95% yield of the product **72** and 97% recovery of the fluorous iodobenzene **233** without any unreacted diaryliodonium salt **228** and aniline **70**.

### 2.5.2.2 *O*-Arylation Reaction

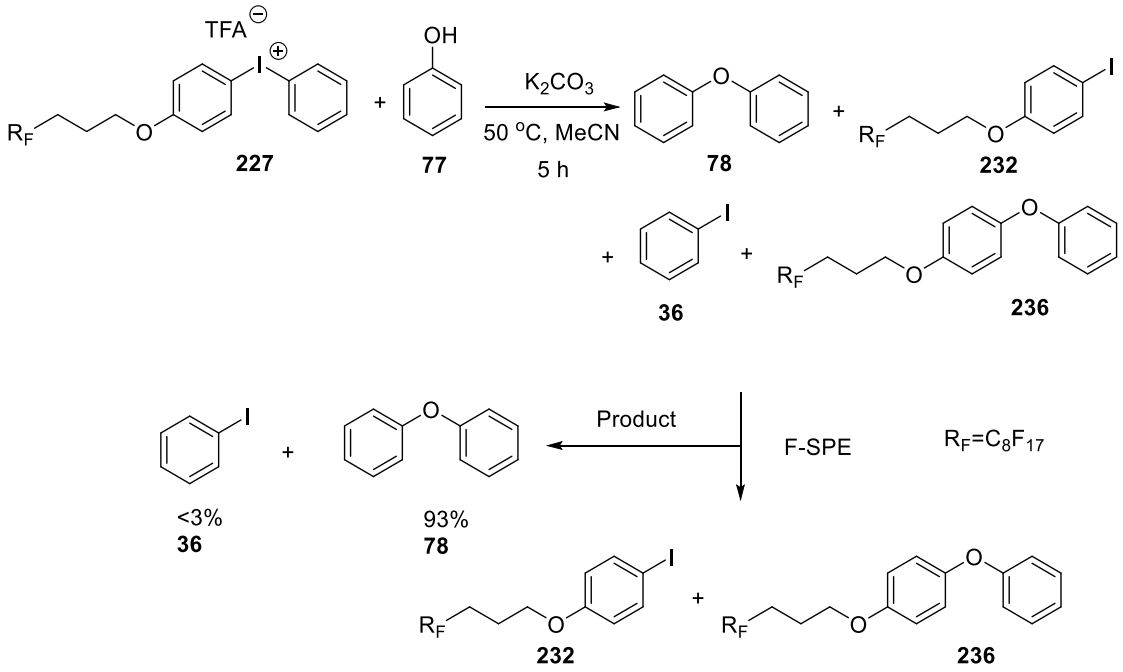


**Figure 45. The process of F-SPE in *O*-arylation**

By introducing a fluorous chain into the diaryliodonium salt, and by using the F-SPE method the diphenylether **78** and iodobenzene **36** in the mixture could easily be separated. We did a demonstration for this reaction and got 93% isolated yield of desired product **78** with less than

3% iodobenzene **36** in the $^{1}$H NMR. This is because the reaction was not 100% selective (ratio of **78**:**236** is 31:1).

### 2.5.2.3 Fluorination

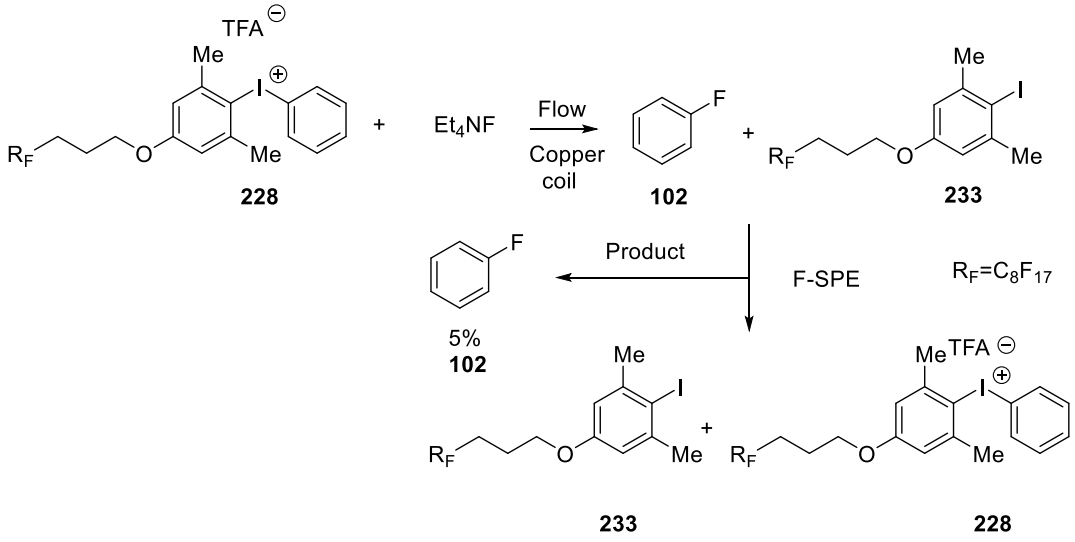


**Figure 46. The process of F-SPE in fluorination**

As used for the *N*- and *O*-arylation reactions, fluorination can also use F-SPE method to readily separate the product, but due to the low boiling point of fluorobenzene, the product yield was determined by $^{19}$F NMR. Using the F-SPE method, the product fluorobenzene **102** was separated easily from the unreacted diaryliodonium salt **228** and the fluorous iodobenzene **233** which were collected by washing with methanol, and the yield of fluorobenzene **102** was 5% by $^{19}$F NMR (no by-product was shown in $^{19}$F NMR).

# Chapter 3. Summary and Future Work

## 3.1 Summary

It has been concluded from the work presented here, that the reactions of diaryliodonium salts are usually influenced by the electronic control, and the more electron-rich system the lower the yields of product. The solid-state structures of the diaryliodonium salts were determined and it was found that the diaryliodonium salt **158** was organised as a linear structure whereas most of others were dimers. The diaryliodonium salt copper complexes were prepared and confirmed by XRD. It was shown that the prominent influence in the copper catalysed reaction was steric control and that 2,6-disubsititution was more effective than just 2-subsititution. It was noted that the more steric hindrance present results in a shorter distance between the copper and iodine suggested a novel Cu-I bond in one case.

The thermal stability of diaryliodonium salts has also been investigated and that it was influenced by both the counter-ion and the electronic nature of the arenes, the more electronic-rich the less stable. Most of the diaryliodonium salts start to decompose before the 'melting point'. The combination of DSC-TGA data and computational results suggested that for some diphenyliodonium salts i.e. with counter-ions $TfO^{\ominus}$, $TsO^{\ominus}$ and $NO_3^{\ominus}$, as the temperature increases, they would form the by-product PhX. Suggesting that the reaction using these diaryliodonium salts should be carried out at a temperature lower than 150 °C

Nucleophilic substitution of diaryliodonium salts has also been demonstrated resulting in *N*-, *O*-arylation and fluorination under different conditions some of which gave good selectivity and generated the desired product in good yield. For all of these reactions the major influence on selectivity is the electronic effect under the metal-free conditions and the diaryliodonium salt **141** shows good selectivity. However, the *ortho*-effect is also present in both *O*-arylation and fluorination reactions where the nucleophiles prefer to react with the sterically demanding

ring, in *N*-arylation, the *ortho*-effect is less important, and the nucleophiles still prefer to react with less steric hindrance ring.

While in the copper catalysed reaction, steric control is the most important factor for influencing the selectivity, although electronic control also had some effect. In all three of these reactions, diaryliodonium salt **159** provides good selectivity, however only in the *N*-arylation reaction, the product obtained in a good yield. Copper catalysed fluorination would generate the desired product only when the reaction was carried out using a copper coil in the flow system,

After introducing a long fluorous chain and using the F-SPE method, all the desired products could be easily separated demonstrating the power of this technique.

### 3.2 Future Work

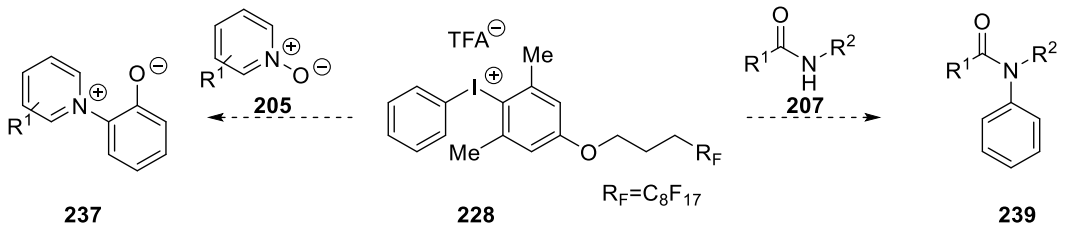


**Scheme 58. The proposed *N*-arylation using fluorous diaryliodonium salts under copper catalysed conditions**

A large amount of the research has been reported with *N*-, *O*-arylations and fluorinations using diaryliodonium salts, and the use of asymmetric diaryliodonium salts has also been developed. The compound **237** is an important synthetic intermediate, in valuable optical materials, and as components of natural products.[190-192] Aryl amides are found in a range of natural and synthetic products, including peptidomimetics, polymers, and anti-inflammatory compounds. Compound **228** is suitable for copper catalysed *N*-arylation so it may be used in these two reactions to

generate the desired products (**237** and **239**) in good yield coupled with rapid purification using the F-SPE method.

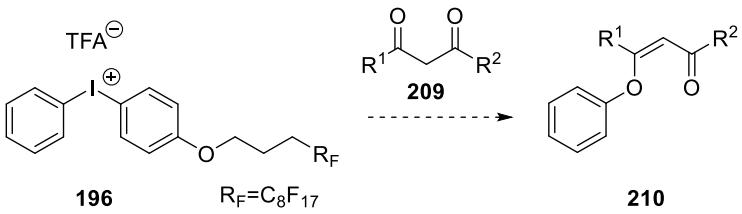


**Scheme 59. The proposed *O*-arylation using fluorous diaryliodonium salts under metal-free conditions**

*O*-Arylation using fluorous diaryliodonium salts has been found that when the reaction is carried out under metal-free conditions, it can result in a good yield with good selectivity. Considering the importance of aryl ethers, especially the existence of β-aryloxy carbonyl moiety in many useful molecules,[193] the reaction using diaryliodonium salts and ketones may also be worth optimising (Scheme 60).

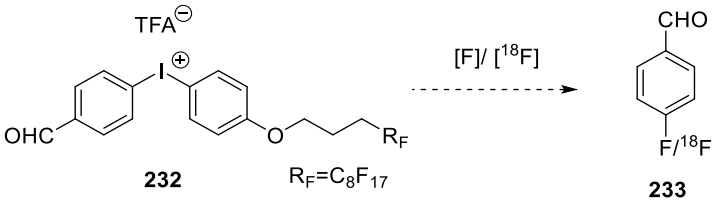


**Scheme 60. Fluorination of fluorous diaryliodonium salts under metal-free conditions**

The fluorination process is influenced mostly by electronic control under metal-free conditions, thus, when the aldehyde group is introduced, the electronic control is more prominent and 4-fluorobenzaldehyde (FBA) is the product .This is especially important as [$^{18}$F]FBA is a valuable prosthetic group in the production of PET radiopharmaceuticals. The fluorous diaryliodonium salt **232** can be synthesised and used as the substrate in fluorination reaction. Due to the short half-life of fluorine-18, rapid separation is required, and **232** can provide this.

# Chapter 4. Experimental Section

## General Experimental Section:

Reactions requiring anhydrous conditions were performed using oven- or flame-dried glassware and conducted under a positive pressure of nitrogen. Anhydrous solvent was prepared as follows: THF were heated at reflux over sodium/benzophenone.$^{1}$H, $^{13}$C and $^{19}$F spectra were recorded on a Bruker Advance 300 MHz spectrometer with tetramethylsilane solvent as the external reference for $^{1}$H and $^{13}$C. $^{19}$F spectra were relative to $CFCl_3$ as the external reference. Mass spectra were obtained using an Agilent 6550 i-Funnel QTOF-LC-MS/MS (2-digit decimals) and/or carried out at the EPSRC mass spectrometry service, Swansea (4-digit decimals). Melting points are recorded on a Gallenkamp MF-370 melting point apparatus and are uncorrected. Automated flash chromatography was carried out with Varian Intelliflash 971-FP flash purification system. The flow reactions were carried out using Uniqsis FlowSyn system. And an Agilent 1200 HPLC system was using for HPLC analysis.

DSC-TGA was obtained using a Perkin-Elmer Simultaneous Thermal Analyzer (STA)-6000. In this instrument, the sample is heated at a preselected rate in a controlled atmosphere. As the sample undergoes an endothermic transition, the extra power required to maintain the selected heating rate in the sample is plotted against its linearly increasing temperature, at the same time, the mass of a sample is measured and recorded. During a run, the sample chamber is continuously swept by a nitrogen flow to remove any volatiles generated in the heating process. In addition, the heating chamber was swept with nitrogen for at least 15 min prior to each run. The signal from the STA was used to plot the thermogram.

The calculations of copper complexes used the DFT method on the B3LYP density functional level in Gaussian 09. The basis set was MIDIX[180] which has provided good results in the study of hypervalent iodine compounds and 6-31G* for Cu. The electrostatic potential was calculated by Multiwfn.

Geometries of all diaryliodonium salts were initially defined using the crystal data from CCDC or Newcastle University crystal analysis database. Calculations of decompositions used the DFT method on the B3LYP density functional level in Gaussian 09. The basis set was MIDIX[180].

## 4.1 Phenyliodobis(acetate) (121) [194]

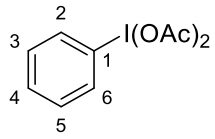


Iodobenzene (6.10 g, 30 mmol) was added to a solution of acetic acid (200 mL) at 45 °C. Sodium perborate tetrahydrate (46.2 g, 300 mmol) was added over 30 min. The solution was stirred at this temperature for 4-5 hours before the addition of water (800 mL). The product was extracted by DCM (3 × 200 mL) and the solvent was removed in *vacuo* to give a yellow solid. Subsequent crystallisation was induced though addition of DCM/ether/petrol to give the product as a white crystalline solid (7.32 g, 22.4 mmol, 76%). Mp 148-151 °C (lit.,[194] mp 162-165 °C); IR $\nu_{max}/cm^{-1}$ (neat): 1644, 1576, 1493, 1366, 1287, 1255, 1188; $^{1}H$ NMR (300 MHz, $CDCl_3$) δ: 8.10 (2H, d, H2/H6, *J*=8.0 Hz), 7.63 (1H, t, H4, *J*=7.4 Hz), 7.52 (2H, t, H3/H5, *J*=7.7 Hz), 2.10 (6H, s, $2COOCH_3$). $^{13}C$ NMR (75 MHz, $CDCl_3$) δ: 176.7 (*C*O), 135.4 (C2/C6), 132.3 (C4), 131.1 (C3/C5), 122.3 (C1), 21.1 ($COOCH_3$).

## 4.2 4-Methoxyphenyliodobis(acetate) (122)

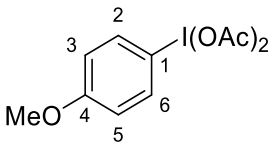


Product prepared according to the procedure outlined for **121**. Crystallisation afforded **122** as a white crystalline solid (3.52 g, 10.4 mmol, 52%). Mp 96-99 °C; IR $\nu_{max}/cm^{-1}$ (neat): 1630, 1602, 1582, 1487, 1359, 1291, 1254, 1178, 815; $^{1}H$ NMR (300 MHz, $CDCl_3$) δ: 8.05 (2H, d, H2/H6, *J*=8.0 Hz), 6.98 (2H, d, H3/H5, *J*=8.0 Hz), 3.87 (3H, s, $OCH_3$), 1.96 (6H, s, $2COOCH_3$). $^{13}C$ NMR (75 MHz, $CDCl_3$) δ: 176.5 (CO), 162.3 (C4), 137.4 (C2/C6), 117.1 (C3/C5), 110.3 (C1),55.7 ($OCH_3$), 20.1 ($COOCH_3$).

### 4.3 2-Methylphenyliodobis(acetate) (123)

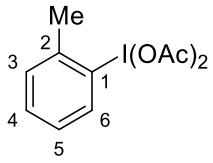


Product prepared according to the procedure outlined for **121**. Crystallisation afforded **123** as a white crystalline solid (2.11 g, 6.3 mmol, 63%). Mp 108-111 °C; IR $\nu_{max}/cm^{-1}$ (neat): 2921, 1630, 1473, 1365, 1290, 1271, 1213, 762; $^{1}H$ NMR (300 MHz, $CDCl_3$) δ: 8.19 (1H, d, H6, *J*=8.0 Hz), 7.52 (2H, m, H3/H5), 7.26 (1H, m, H4), 2.74 (3H, s, $CH_3$), 1.97 (6H, s, $2COOCH_3$); $^{13}C$ NMR (75 MHz, $CDCl_3$) δ: 176.6(CO), 140.8 (C2), 137.6 (C6), 132.4 (C5), 131.2 (C4), 128.4 (C3), 127.2 (C1) , 25.5 ($CH_3$), 20.4 ($COOCH_3$).

### 4.4 2,4,6-trimethylphenyliodobis(acetate) (124) [195]

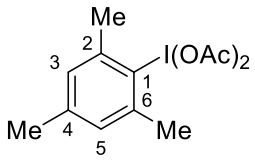


Product prepared according to the procedure outlined for **121**. Crystallisation afforded **124** as a white crystalline solid (1.93g, 5.3 mmol, 53%). Mp 159-164 °C (lit.,[195] mp 160-163 °C); IR $\nu_{max}/cm^{-1}$ (neat): 2927, 1644, 1455, 1367, 1267, 1255, 1010; $^{1}H$ NMR (300 MHz, $CDCl_3$) δ: 7.13 (2H, s, H3/H5), 2.74 (6H, s, *o*-$CH_3$), 2.38 (3H, s, *p*-$CH_3$),1.99 (6H, s, 2$COOCH_3$); $^{13}C$ NMR (75 MHz, $CDCl_3$) δ: 176.8(CO), 143.5 (C4), 141.4 (C2/C6), 129.7 (C1), 129.1 (C3/C5) , 26.8 (*o*-$CH_3$) 21.1 (*p*-$CH_3$), 20.4 (COO*C*$H_3$).

### 4.5 2-(Diacetoxyiodo)thiophene (125) [196]

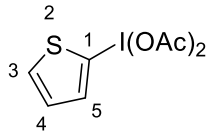


Product prepared according to the procedure outlined for **121**. Crystallisation afforded **125** as a yellow crystalline solid (1.64 g, 5.0 mmol, 23%). Mp 118-122 °C (lit.,[196] mp 120-122 °C); IR $\nu_{max}/cm^{-1}$ (neat): 3106, 1647, 1386, 1366, 1272, 1221, 1051, 1011; $^{1}H$ NMR (300 MHz, $CDCl_3$) δ: 7.70 (1H, dd, H3, *J*= 3.8 Hz, 1.2 Hz), 7.57 (1H, dd, H5, *J*= 3.8 Hz, 1.2 Hz), 7.07 (1H, dd, H4, *J*= 5.4 Hz, 1.3 Hz), 1.97 (6H, s, 2$COOCH_3$); $^{13}C$ NMR (75 MHz, $CDCl_3$) δ: 177.1(CO), 139.0 (C3), 135.9 (C5), 128.9 (C4), 106.2 (C1), 20.4 (COO*C*$H_3$).

### 4.6 Tributylphenyltin (133) [197]

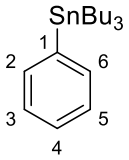


To a solution of iodobenzene (2.024g, 10.0 mmol) in dry THF (30 mL) at -78 °C was slowly added n-butyllithium solution (5.0 mL, 12.5 mmol, 2.5M in THF). The reaction mixture was stirred for 1 hour at -78 °C, then tributyltin chloride added, and the mixture stirred for a further 1 hour at -78 °C. The mixture was allowed to warm to room temperature overnight, then quenched with ammonium chloride solution. The product was extracted by ether (3 × 100 mL) and the solution was dried over $Na_2SO_4$, the solvent was removed in *vacuo* to give a colourless liquid. Purification by column chromatography on $SiO_2$ (ether:petrol 10:90) afforded a colourless liquid (3.42 g, 9.3 mmol, 93%).$^1$H NMR (300 MHz, $CDCl_3$) δ: 7.57-7.43 (2H, m), 7.39-7.29 (3H, m), 1.67-1.47 (6H, m), 1.37 (6H, m), 1.27-1.14 (6H, m), 0.93 (9H, t, *J*= 7.4 Hz). $^{13}$C NMR (75 MHz, $CDCl_3$) δ: 139.4, 132.2, 128.2, 29.4 ($CH_2CH_2CH_3$), 27.5 ($CH_2CH_3$), 13.8 (Sn-$CH_2$), 9.5 ($CH_3$)

## 4.7 Tributyl(2-thienyl)tin (134) [198]

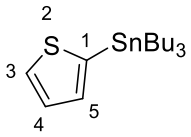


To a solution of thiophene (4.20 g, 50.0 mmol) in dry THF (150 mL) at -78 °C was slowly added n-butyllithium solution (22.0 mL, 55.0 mmol, 2.5M in THF). The reaction mixture was stirred for 1 hour at -78 °C, then tributyltin chloride (13.5 mL, 50.0 mmol) added, and the mixture stirred for a further 1 hour at -78 °C. The mixture was allowed to warm to room temperature overnight, then quenched with ammonium chloride solution. The product was extracted by ether (3 × 200 mL) and the solution was dried over $NaSO_4$, removed in *vacuo* to give a colourless liquid. Purification by column chromatography on $SiO_2$ (ether:petrol 10:90)

afforded a colourless liquid (17.7 g, 47.5 mmol, 95%). $^{1}$H NMR (300 MHz, $CDCl_3$) δ = 7.66 (1H, dd, H3, *J*= 3.8 Hz, 1.2 Hz), 7.27 (1H, dd, H5, *J*= 3.8 Hz, 1.2 Hz), 7.20 (1H, dd, H4, *J*= 5.4 Hz, 1.3 Hz), 1.74-1.58 (6H, m), 1.51-1.35 (6H, m), 1.29-1.13 (6H, m), 0.97 (9H, t, *J*= 7.4 Hz). $^{13}$C NMR (75 MHz, $CDCl_3$) δ: 142.4 (C2/C6), 136.3 (C1), 137.1 (C3/C4/C5), 29.2 ($CH_2CH_2CH_3$), 26.4 ($CH_2CH_3$), 14.7 (Sn-$CH_2$), 11.5 ($CH_3$)

**General method for the synthesis of diaryliodonium salts**

**Method A**

Dropwise addition of acid (20 mmol of TFA, TfOH) to a solution of the aryliodobis(acetate) (10 mmol) in DCM (50 mL) at -30 ℃, and the mixture stirred for half an hour which was then allowed to warm to room temperature for 1 hour. After 1 hour the solution was cooled down to -30 ℃ and arylstannane (10 mmol) was then added. The reaction mixture was allowed to warm to room temperature again and stirred overnight. The solvent was removed in *vacuo* to give the crude product and subsequent crystallisation was induced through addition of DCM/ether/petrol to give the product.

**Method B**

Dropwise addition of acid (20 mmol of TFA, TfOH) to a solution of the phenyliodobis(acetate) (10 mmol) in DCM (50 mL) at -30 ℃, and the mixture stirred for half an hour which was then allowed to warm to room temperature for 1 hour. After 1 hour the solution was cooled down to -30 ℃ and 4-fluorobenzene boronic acid (10 mmol) was added. The reaction mixture was allowed to warm to room temperature again and stirred overnight. The solvent was removed in *vacuo* to give the crude product and subsequent crystallisation was induced through addition of DCM/ether/petrol to give the product.

**Method C**

Dropwise addition of acid (20 mmol of TFA, TfOH) to a solution of the aryliodobis(acetate) (10 mmol) in DCM (50 mL) at -30 ℃, and the mixture stirred for half an hour which was then allowed to warm to room temperature for 1 hour. After 1 hour the solution was cooled down to -30 ℃ and anisole (10 mmol) was then added. The reaction mixture was allowed to warm to room temperature again and stirred overnight. The solvent was removed in *vacuo* to give the crude product and subsequent crystallisation was induced through addition of DCM/ether/petrol to give the product.

**Method D**

p-Toluenesulfonic acid was added at 60 °C to a stirred suspension of aryliodobis(acetate) (10 mmol) in acetonitrile (100 mL) and at the same temperature stirred for 30 min, the solution was allowed to cool to room temperature and the precipitate was removed by filtration. The precipitate was directly dissolved in DCM (100 mL) and the solution was cooled to -30 ℃ and arylstannane (10 mmol) was added. This mixture was allowed to warm to room temperature overnight, when the solvent was removed in *vacuo* to give the crude product. Recrystallization by ether, DCM and petrol gave the product.

### 4.8 Diphenyliodonium trifluoroacetate (139) [197]

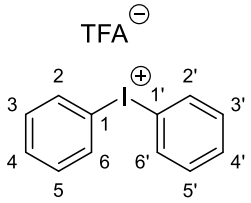


The product prepared according to **Method A**. White crystalline solid (2.54 g, 6.7 mmol, 67%). Mp 189-193 °C (lit.,[197] mp 197-198 °C); IR $\nu_{max}/cm^{-1}$ (neat): 3051, 1664, 1477, 1439, 1165, 1123; $^{1}H$ NMR (300 MHz, $CDCl_3$) δ: 7.92 (4H, d, H2/H6, *J*=7.4 Hz), 7.59 (2H, t, H4, *J*=7.4 Hz), 7.44 (4H, t, H3/H5, *J*=7.7 Hz) $^{13}C$ NMR (75 MHz, $CDCl_3$) δ: 136.5 (C2/C6), 133.1 (C4), 131.9 (C3/C5).

### 4.9 Diphenyliodonium triflate (140) [197]

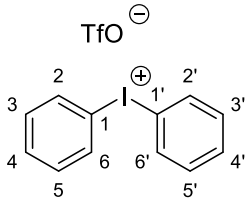


The product prepared according to **Method A**. White crystalline solid (3.22 g, 7.5 mmol, 75%). Mp 177-179 °C (lit.,[197] mp 177-178 °C); IR $\nu_{max}/cm^{-1}$ (neat): 3059, 1648, 1444, 1165, 1113; $^{1}H$ NMR (300 MHz, $CDCl_3$) δ: 7.95 (4H, d, H2/H6/H2'/H6', *J*=7.4 Hz), 7.68 (2H, t, H4/H4', *J*=7.4 Hz), 7.49 (4H, t, H3/H5/H3'/H5', *J*=7.7 Hz) $^{13}C$ NMR (75 MHz, $CDCl_3$) δ: 136.7 (C2/C6/C2'/C6'), 133.8 (C4/C4'), 132.1 (C3/C5/C3/C5).

## 4.10 4-Methoxyphenyl(phenyl)iodonium trifluoroacetate (141) [199]

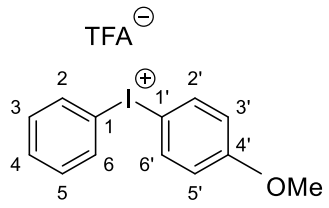


The product prepared according to **Method A**. White crystalline solid (1.84 g, 4.5 mmol, 45%). **Method C**. White crystalline solid (2.37 g, 5.8 mmol, 58%). Mp 151-153 ℃ (lit.,[199] mp 146-148℃); IR $\nu_{max}/cm^{-1}$ (neat): 3081, 1576, 1483, 1291, 1252, 1178, 1128; $^{1}H$ NMR (300 MHz, $CDCl_3$) δ: 7.88 (4H, d, H2/H6/H2'/H6', *J*=7.7 Hz), 7.46 (1H, t, H4, *J*=7.4 Hz), 7.32 (2H, t, H3/H5, *J*=7.7 Hz), 6.83 (2H, d, H3'/H5', *J*=7.4 Hz), 3.75 (3H, s, $OCH_3$). $^{13}C$ NMR (75 MHz, $CDCl_3$) δ: 162.4 (C4'), 136.9 (C2'/C6'), 134.1 (C2/C6), 131.7 (C3/C5), 131.6 (C4), 117.6 (C3'/C5'), 116.9 (C1), 104.9 (C1'), 55.6 ($OCH_3$); *m/z* (ESI): $[M\text{-}TFA]^+$ 310.99. 311($[M\text{-}TFA]^+$, 100%), 184 (40).

## 4.11 4-Methoxyphenyl(phenyl)iodonium triflate (142)[61]

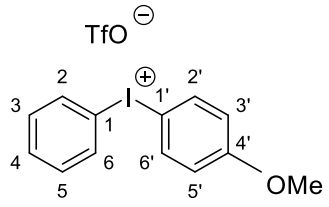


The product prepared according to **Method A**. White crystalline solid (2.22 g, 5.0mmol, 50%). Mp 137-141 ℃ ; IR $\nu_{max}/cm^{-1}$ (neat): 3082, 1572, 1483, 1301, 1253, 1168; $^{1}H$ NMR (300 MHz, $CDCl_3$) δ: 7.95 (4H, d, H2/H6/H2'/H6', *J*=7.7 Hz), 7.66 (1H, t, H4, *J*=7.4 Hz), 7.53 (2H, t, H3/H5, *J*=7.7 Hz), 6.96 (2H, d, H3'/H5', *J*=7.4 Hz), 3.79 (3H, s, $OCH_3$). $^{13}C$ NMR (75 MHz, $CDCl_3$) δ: 162.8 (C4'), 137.2 (C2'/C6'), 134.1 (C2/C6), 131.9 (C3/C5), 131.2 (C4), 118.6 (C3'/C5'), 116.8 (C1), 104.7 (C1'), 55.8 ($OCH_3$). *m/z* (ESI): $[M\text{-}TfO]^+$ 310.99. 311($[M\text{-}TfO]^+$, 100%), 184 (40).

## 4.12 2-Methylphenyl(phenyl)iodonium trifluoroacetate (143) [61]

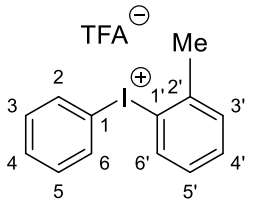


The product prepared according to **Method A**. White crystalline solid (1.69 g, 4.3 mmol, 43%). Mp 158-161 °C; IR $\nu_{max}/cm^{-1}$ (neat): 2980, 1648, 1469, 1174, 1128; $^{1}H$ NMR (300 MHz, $CDCl_3$) δ: 8.10 (1H, d, H6', *J*=7.7 Hz) 7.88 (2H, d, H2/H6, *J*=7.7 Hz), 7.54 (2H, m, H4/H3'), 7.42 (3H, m, H3/H5/H5', *J*=7.7 Hz), 7.24 (1H, t, H4', *J*=7.4 Hz), 2.63 (3H, s, $CH_3$). $^{13}C$ NMR (75 MHz, $CDCl_3$) δ: 141.1 (C2'), 137.7 (C6'), 134.3 (C2/C6), 133.9 (C3'), 131.7 (C3/C5), 131.5 (C5'), 129.2 (C4), 121.2 (C1'), 115.7 (C1), 25.55 ($CH_3$); *m/z* (ESI): $[M\text{-}TFA]^+$ 295.00. 295 ($[M\text{-}TFA]^+$, 100%), 168 (55).

## 4.13 Phenyl(mesityl)iodonium trifluoroacetate (144) [200]

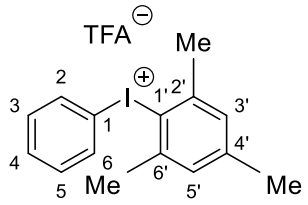


The product prepared according to **Method A**. White crystalline solid (1.89 g, 4.5 mmol, 45%). **Method B**. White crystalline solid (0.42 g, 1.0 mmol, 10%). Mp 129-131 °C (lit.,[200] mp 132-135 °C); IR $\nu_{max}/cm^{-1}$ (neat): 2983, 1654, 1596, 1473, 1386, 1277, 1235, 1178, 1124; $^{1}H$ NMR (300 MHz, $CDCl_3$) δ: 7.61 (2H, d, H2/H6, *J*=8.0 Hz), 7.43 (1H, t, H4, *J*=7.4 Hz), 7.32 (2H, t, H3/H5, *J*=7.7 Hz), 7.01 (2H, s, H3'/H5'), 2.56 (6H, s, *o*-$CH_3$), 2.27 (3H, s, *p*-$CH_3$). $^{13}C$ NMR

(75 MHz, $CDCl_3$) δ: 143.8 (C4'), 142.1 (C2'/C6'), 132.7 (C2/C6), 131.8 (C3/C5), 131.3 (C4), 130.1 (C3'/C5'), 122.3 (C1'), 114.33 (C1), 27.0 (*o*-$CH_3$), 21.1 (*p*-$CH_3$).

### 4.14 Phenyl(2-thienyl)iodonium trifluoroacetate (145)

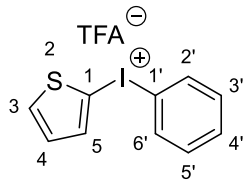


The product prepared according to **Method A**. White crystalline solid (0.87 g, 2.3 mmol, 23%). Mp 139-142 °C; IR $\nu_{max}/cm^{-1}$ (neat): 3071, 1646, 1582, 1419, 1386, 1181, 1137; $^1$H NMR (300 MHz, $CDCl_3$) δ: 8.02 (2H, d, H2'/H6', *J*= 7.8 Hz), 7.76 (1H, dd, H3, *J*= 3.8 Hz, 1.2 Hz), 7.66 (1H, dd, H5, *J*= 5.4 Hz, 1.3 Hz), 7.57 (1H, t, H4', *J*= 7.4 Hz), 7.44 (2H, t, H3'/H5' , *J*= 7.5 Hz), 7.12 (1H, dd, H4, *J* = 5.3, 3.4 Hz). $^{13}$C NMR (75 MHz, $CDCl_3$) δ: 137.5 (C3), 136.9 (C5), 135.9 (C4), 131.4 (C2'/C6'), 130.2 (C3'/C5'), 129.7 (C1), 119.4 (C1'); *m/z* (ESI): $[M\text{-}TFA]^+$ 286.85. 287 ($[M\text{-}TFA]^+$, 100%), 223 (85).

### 4.15 Phenyl(2-thienyl)iodonium triflate (146) [201]

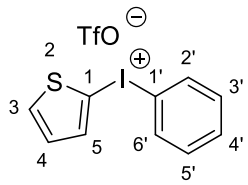


The product prepared according to **Method A**. White crystalline solid (1.42 g, 3.3 mmol, 30%). Mp 132-136 °C (lit.,[201] mp 137-139 °C); IR $\nu_{max}/cm^{-1}$ (neat): 3101, 1646, 1585, 1419, 1386, 1168; $^1$H NMR (300 MHz, $CDCl_3$) δ: 7.99 (2H, d, H2'/H6', *J*= 7.8 Hz), 7.90 (1H, dd, H3, *J*=

3.8 Hz, 1.2 Hz), 7.73 (1H, dd, H5, *J*= 5.4 Hz, 1.3 Hz), 7.63 (1H, t, H4', *J*= 7.4 Hz), 7.49 (2H, t, H3'/H5' , *J*= 7.5 Hz), 7.18 (1H, dd, H4, *J* = 5.3, 3.4 Hz). $^{13}$C NMR (75 MHz, $CDCl_3$) δ: 141.1 (C3), 137.6 (C5), 133.9 (C2'/C6'), 132.4 (C4), 132.3 (C3'/C5'), 130.2 (C1), 125.1 (C1'); *m/z* (ESI): $[M\text{-}TFA]^+$ 286.84. 287 ($[M\text{-}TFA]^+$, 100%), 223 (40).

### 4.16 4-Methoxyphenyl(2-thienyl)iodonium trifluoroacetate (147)

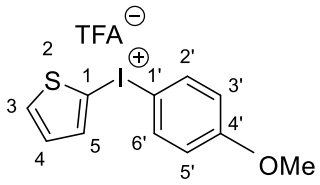


The product prepared according to **Method A**. White crystalline solid (0.74 g, 1.8 mmol, 18%). **Method C.** White crystalline solid (1.86 g, 4.5 mmol, 45%). Mp 89-94 °C; IR $\nu_{max}/cm^{-1}$ (neat): 3081, 1576, 1483, 1419, 1383, 1291, 1252, 1181, 1138; $^1$H NMR (300 MHz, $CDCl_3$) δ: 7.83 (2H, d, H3'/H5', *J* = 8.9 Hz), 7.65 – 7.49 (2H, m, H3/H5), 7.00 (1H, ddd, H4, *J* = 5.1, 3.7, 1.0 Hz), 6.81 (2H, d, H2'/H6', *J* = 7.9 Hz), 3.74 (3H, s, $CH_3$). $^{13}$C NMR (75 MHz, $CDCl_3$) δ: 165.9 (C4'),139.3 (C3), 135.8 (C5), 135.6 (C2'/C6'), 134.9(C4), 129.5 (C1), 117.4 (C1'), 114.9 (C3'/C5'), 55.7 ($OCH_3$); *m/z* (ESI): $[M\text{-}TFA]^+$ 316.83. 317 ($[M\text{-}TFA]^+$, 100%), 223 (100).

### 4.17 2-Methylphenyl(2-thienyl)iodonium trifluoroacetate (148)

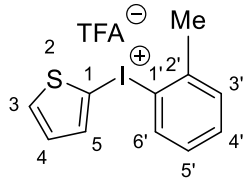


The product prepared according to **Method A**. White crystalline solid (0.76 g, 1.9 mmol, 19%). Mp 101-104 °C; IR $\nu_{max}$/cm$^{-1}$ (neat): 3080, 2983, 1648, 1469, 1419, 1174, 1128; $^{1}$H NMR (300 MHz, $CDCl_3$) δ: 8.07 (1H, d, H6, *J=7.7*), 7.53 (2H, ddd, H3'/H5', *J* = 18.8, 4.6, 1.2 Hz), 7.46 – 7.28 (2H, H3/H5, m), 7.17 – 7.05 (1H, H4, m), 6.97 (1H, dd, H4', *J* = 5.3, 3.7 Hz), 2.66 (3H, s, $CH_3$). $^{13}$C NMR (75 MHz, $CDCl_3$) δ: 142.1 (C2'), 138.6 (C6'), 137.5 (C3), 136.9 (C5), 135.9 (C4), 134.8 (C3'), 132.8 (C5'),130.2 (C3'/C5'), 129.7 (C1), 122.2 (C1'), 25.6 ($CH_3$). *m/z* (ESI): $[M\text{-}TFA]^+$ 300.86. 301 ($[M\text{-}TFA]^+$, 100%), 223 (66).

### 4.18 Mesityl(2-thienyl)iodonium trifluoroacetate (149)

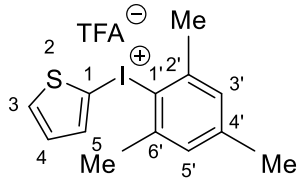


The product prepared according to **Method A**. White crystalline solid (0.27 g, 0.63 mmol, 26%). Mp 98-101 °C; IR $\nu_{max}$/cm$^{-1}$ (neat): 3082, 2983, 1654, 1596, 1473, 1441, 1383, 1277, 1235, 1178, 1124; $^{1}$H NMR (300 MHz, $CDCl_3$) δ: 7.50 – 7.41 (2H, m, H3/H5), 7.00 – 6.91 (3H, m, H4/H3'/H5'), 2.68 (6H, s, *o*-$CH_3$), 2.25 (3H, s, *p*-$CH_3$). $^{13}$C NMR (75 MHz, $CDCl_3$) δ: 145.3 (C4'), 143.4 (C2'/C6'),137.5 (C3), 136.9 (C5), 135.9 (C4), 132.0 (C3'/C5'), 129.7 (C1), 122.8 (C1') 114.33 (C1), 27.0 (*o*-$CH_3$), 21.1 (*p*-$CH_3$). *m/z* (ESI): $[M\text{-}TFA]^+$ 328.85. 329 ($[M\text{-}TFA]^+$, 100%), 223 (80).

## 4.19 Phenyl(4-fluorophenyl)iodonium trifluoroacetate (150)

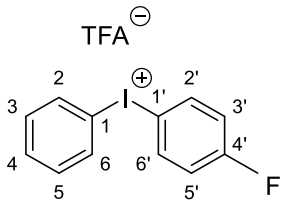


The product prepared according to **Method B**. White crystalline solid (2.65 g, 6.7 mmol, 67%). Mp 143-146 °C; IR $\nu_{max}/cm^{-1}$ (neat): 3055, 2980, 1648, 1580, 1483, 1177, 1128; $^{1}H$ NMR (300 MHz, $CDCl_3$) δ: 7.87 (4H, m, H2/H6/H2'/H6'), 7.50 (1H, t, H4, *J*=7.4 Hz), 7.35 (2H, t, H3/H5, *J*=7.7 Hz), 7.03 (2H, d, H3'/H5', *J*=7.4 Hz), 3.79 (3H, s, $OCH_3$). $^{13}C$ NMR (75 MHz, $CDCl_3$) δ: 137.2, 137.1 (C2'/C6'), 134.6 (C2/C6), 131.9 (C3/C5), 119.5, 119.2 (C3'/C5'). $^{19}F$ NMR (282 MHz, $CDCl_3$) δ: -75.4, -105.5. *m/z* (ESI): $[M\text{-}TFA]^+$ 298.88. 299 ($[M\text{-}TFA]^+$, 100%), 223 (50).

## 4.20 Phenyl(4-fluorophenyl)iodonium triflate (151) [202]

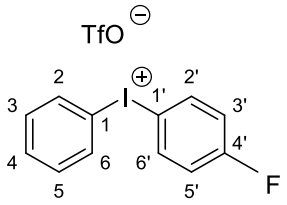


The product prepared according to **Method B**. White crystalline solid (3.22 g, 7.3 mmol, 73%). Mp 137-141 °C (lit.,[202] mp 133-134 °C); IR $\nu_{max}/cm^{-1}$ (neat): 3093, 2980, 1646, 1574, 1473, 1168; $^{1}H$ NMR (300 MHz, $CDCl_3$) δ: 7.95 (4H, d, H2/H6/H2'/H6', *J*=7.7 Hz), 7.66 (1H, t, H4, *J*=7.4 Hz), 7.53 (2H, t, H3/H5, *J*=7.7 Hz), 6.96 (2H, d, H3'/H5', *J*=7.4 Hz), 3.79 (3H, s, $OCH_3$). $^{13}C$ NMR (75 MHz, $CDCl_3$) δ: 137.9, 137.8 (C2'/C6'), 135.1 (C2/C6), 132.4 (C3/C5), 120.1,

119.8 (C3'/C5'). $^{19}$F NMR (282 MHz, $CDCl_3$) δ: -78.4, -103.8. *m/z* (ESI): $[M\text{-}TfO]^+$ 298.88. 299 ($[M\text{-}TfO]^+$, 100%), 223 (66).

### 4.21 2-Methyl-4-methoxyphenyl(phenyl)iodonium trifluoroacetate (157)

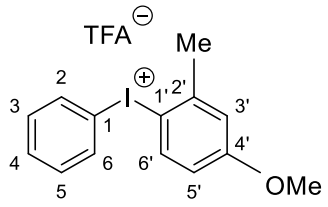


The product prepared according to **Method C**. White crystalline solid (2.83 g, 6.7 mmol, 67%). Mp 138-141 °C; IR $\nu_{max}/cm^{-1}$ (neat): 2980, 1656, 1566, 1470, 1245, 1175, 1126; $^1$H NMR (300 MHz, $CDCl_3$) δ: 7.99 (1H, d, H6', *J*=8.8 Hz), 7.82 (2H, d, H2/H6, *J*=7.4 Hz), 7.49 (1H, t, H4, *J*=7.7 Hz), 7.37 (2H, t, H3/H5, *J*=7.7 Hz), 6.91 (1H, d, H3', *J*=3.0 Hz), 6.74 (1H, dd, H4', *J*=8.8 Hz, *J*=3.0 Hz), 3.82 (3H, s, $OCH_3$), 2.55 (3H, s, $CH_3$). $^{13}$C NMR (75 MHz, $CDCl_3$) δ: 163.0 (C4'), 143.2 (C2'), 139.1 (C6'), 133.5 (C2/C6), 131.6 (C3/C5), 131.2 (C4), 117.4 (C3'), 116.2 (C1), 114.7 (C5'), 109.9 (C1'), 55.6 ($OCH_3$), 25.63 ($CH_3$); *m/z* (ESI): $[M\text{-}TFA]^+$ 325.15. 325 ($[M\text{-}TFA]^+$, 100%), 326 (50).

### 4.22 2-*n*-Butyl-4-methoxyphenyl(phenyl)iodonium trifluoroacetate (158)

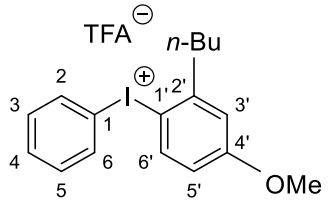


The product prepared according to **Method C**. White crystalline solid (0.65 g, 1.5 mmol, 15%). Mp 144-148 °C; IR $\nu_{max}/cm^{-1}$ (neat): 2958, 2865, 1657, 1588, 1463, 1396, 1248, 1169, 1124; $^1$H NMR (300 MHz, $CDCl_3$) δ: 7.90 (1H, d, H6', *J*=8.8 Hz), 7.74 (2H, d, H2/H6, *J*=7.4 Hz), 7.40 (1H, t, H4, *J*=7.7 Hz), 7.33 (2H, t, H3/H5, *J*=7.7 Hz), 6.83 (1H, d, H3', *J*=3.0 Hz), 6.70

(1H, dd, H5', *J*=8.8 Hz, *J*=3.0 Hz), 3.77 (3H, s, $OCH_3$), 2.71 (2H, t, $CH_2CH_2CH_2CH_3$, *J*=7.4) 1.46-1.34 (2H, m, $CH_2CH_2CH_2CH_3$) 1.34-1.18 (2H, m, $CH_2CH_2CH_2CH_3$) 0.81 (3H, t, $CH_2CH_2CH_2CH_3$, *J*=7.4). $^{13}C$ NMR (75 MHz, $CDCl_3$) δ: 163.2 (C4'), 147.6 (C2'), 139.5 (C6'), 133.2 (C2/C6), 131.7 (C3/C5), 131.4 (C4), 116.9 (C3'), 116.6 (C1), 114.8 (C5'), 109.1 (C1'), 55.6 ($OCH_3$), 38.8 ($CH_2CH_2CH_2CH_3$), 32.9 ($CH_2CH_2CH_2CH_3$), 22.4 ($CH_2CH_2CH_2CH_3$), 13.8 ($CH_2CH_2CH_2CH_3$); *m/z* (ESI): $[M\text{-}TFA]^+$ 366.92. 367 ($[M\text{-}TFA]^+$, 100%).

### 4.23 2,6-Dimethyl-4-methoxyphenyl(phenyl)iodonium trifluoroacetate (159)

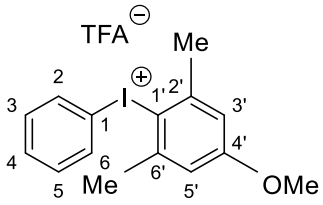


The product prepared according to **Method C**. White crystalline solid (2.54 g, 5.8 mmol, 82%). Mp 148-151 °C; IR $\nu_{max}/cm^{-1}$ (neat): 2980, 2946, 2849, 1656, 1579, 1439, 1322, 1285, 1166, 1126; $^1H$ NMR (300 MHz, $CDCl_3$) δ: 7.82 (2H, d, H2/H6, *J*= 7.4 Hz), 7.50 (1H, t, H4, *J*= 7.7 Hz), 7.38 (2H, t, H3/H5, *J*= 7.7 Hz), 6.79 (1H, s, H3'/H5'), 3.82 (3H, s, $OCH_3$), 2.64 (6H, s, $CH_3$). $^{13}C$ NMR (75 MHz, $CDCl_3$) δ: 162.8 (C4'), 144.3 (C2'/C6'), 133.8 (C2/C6), 132.5 (C3/C5), 131.2 (C4), 114.7 (C1/C1'/C3'/C5'), 55.5 ($OCH_3$), 27.2 ($CH_3$); *m/z* (ESI): $[M\text{-}TFA]^+$ 338.83. 339 ($[M\text{-}TFA]^+$, 100%).

### 4.24 2-Methyl-4-methoxyphenyl(2-thienyl)iodonium trifluoroacetate (160)

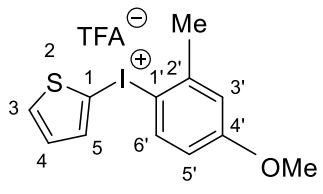

The product prepared according to **Method C**. White crystalline solid (0.66 g, 1.5 mmol, 55%). Mp 144-146 °C; IR $\nu_{max}/cm^{-1}$ (neat): 3066, 2980, 1655, 1566, 1467, 1419, 1245, 1179, 1132; $^{1}H$ NMR (300 MHz, $CDCl_3$) δ: 7.96 (1H, d, H6', *J* = 9.0 Hz), 7.51 (2H, ddd, H3/H5, *J* = 15.8, 4.5, 1.2 Hz), 6.96 (1H, dd, H4, *J* = 5.3, 3.7 Hz), 6.82 (1H, d, H5', *J* = 3.1 Hz), 6.64 (1H, dd, H3', *J* = 9.0, 3.1 Hz), 3.74 (3H, s, $OCH_3$), 2.62 (3H, s, $CH_3$). $^{13}C$ NMR (75 MHz, $CDCl_3$) δ:162.9 (C4'),142.2 (C5), 138.2 (C2'/C6'), 137.9 (C3), 134.9(C4), 129.4(C1), 117.28 (C1'), 114.9 (C3'/C5'), 56.6 ($OCH_3$), 25.8 ($CH_3$). *m/z* (ESI): $[M\text{-}TFA]^+$ 330.83. 331 ($[M\text{-}TFA]^+$, 100%).

## 4.25 2,6-Dimethyl-4-methoxyphenyl(2-thienyl)iodonium trifluoroacetate (161)

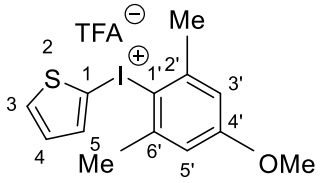


The product prepared according to **Method C**. White crystalline solid (0.60 g, 1.4 mmol, 48%). Mp 137-142 °C; IR $\nu_{max}/cm^{-1}$ (neat): 3066, 2980, 2946, 1655, 1566, 1447, 1419, 1245, 1177, 1131; $^{1}H$ NMR (300 MHz, $CDCl_3$) δ: 7.60 – 7.33 (2H, m, H3/H5), 6.96 (1H, dd, H4, *J* = 5.2, 3.9 Hz), 6.67 (2H, s, H3'/H5'), 3.73 (3H, s, $OCH_3$), 2.69 (6H, s, $CH_3$). $^{13}C$ NMR (75 MHz, $CDCl_3$) δ: 163.8 (C4'), 144.2 (C2'/C6'), 143.1(C5), 138.1(C3), 134.9(C4), 129.4(C1), 122.8(C1'), 115.7 (C3'/C5'), 56.6 ($OCH_3$), 27.8 ($CH_3$). *m/z* (ESI): $[M\text{-}TFA]^+$ 344.84. 345 ($[M\text{-}TFA]^+$, 5%), 223(100).

## 4.26 Diphenyliodonium tosylate (163) [203]

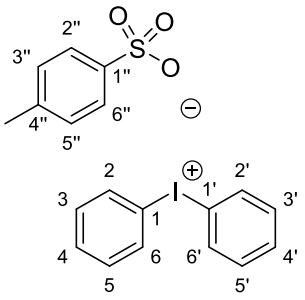

The product prepared according to **Method D**. White crystalline solid (2.66 g, 5.9 mmol, 59%). Mp 150-154 °C (lit.,[203] mp 178–179 °C); IR $\nu_{max}/cm^{-1}$ (neat): 3051, 2970, 1664, 1211, 1170, 1160; $^{1}H$ NMR (300 MHz, $CDCl_3$) δ: 7.98 (4H, d, H2/H6/H2'/H6', *J*=8.5 Hz), 7.58-7.44 (4H, m, H4/H4' /H2''/H6''), 7.49 (4H, t, H3/H5/H3'/H5', *J*=8.0 Hz), 7.05 (2H, d, H3''/H5'' , *J*=8.0 Hz). $^{13}C$ NMR (75 MHz, $CDCl_3$) δ: 140.7 (C1''), 136.7 (C2/C6/C2'/C6'), 133.8 (C4/C4'), 132.1 (C3/C5/C3'/C5'), 128.7 (C3''/C5''), 125.9 (C2''/C6''), 99.6 (C4''), 21.3 ($CH_3$).

## 4.27 Phenyl(2-thienyl)iodonium tosylate (164)

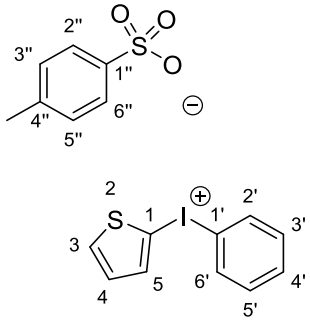

The product prepared according to **Method D**. White crystalline solid (0.69 g, 1.5 mmol, 30%). Mp 141-144 °C; IR $\nu_{max}/cm^{-1}$ (neat): 3071, 2971, 1664, 1493, 1441, 1206, 1169, 1159; $^{1}H$ NMR (300 MHz, $CDCl_3$) δ:7.92 (2H, d, H2'/H6', *J*= 7.8 Hz), 7.81 (1H, dd, H3, *J*= 3.8 Hz, 1.2 Hz), 7.56 (1H, dd, H5, *J*= 5.4 Hz, 1.3 Hz), 7.52-7.47 (3H, m, H4'/H2''/H6''), 7.33 (2H, t, H3'/H5', *J*= 7.5 Hz), 7.05-6.95 (3H, m, H4/H3''/H5''), 2.30 (3H, s, $CH_3$). $^{13}C$ NMR (75 MHz, $CDCl_3$)

δ: 142.1 (C3), 140.5 (C1''), 139.5 (C5), 135.9 (C4), 134.1 (C2'/C6'), 131.4 (C3'/C5'), 129.7 (C1), 128.5 (C3''/C5''), 125.8 (C2''/C6''), 119.1 (C1'), 99.6 (C4''), 21.3 ($CH_3$); *m/z* (ESI): $[M\text{-}TsO]^+$ 286.84. 287 ($[M\text{-}TsO]^+$, 100%).

### 4.28 Di(2-thienyl)iodonium tosylate (165) [198]

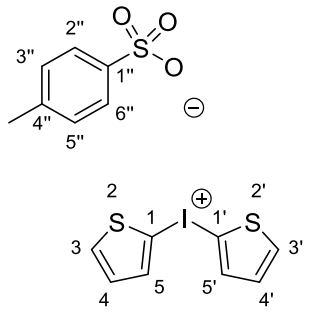


The product prepared according to **Method D**. White crystalline solid (0.36 g, 0.92 mmol, 30%). Mp 131-135 °C (lit.,[198] mp 134 °C); IR $\nu_{max}/cm^{-1}$ (neat): 3066, 2981, 1647, 1493, 1441, 1179, 1132; $^1H$ NMR (300 MHz, $CDCl_3$) δ 7.72 (2H, dd, H3/H3', *J* = 3.8, 1.2 Hz), 7.48 (2H, dd, H4/H4', *J* = 5.4, 1.3 Hz), 7.38 (2H, d, H2''/H6'', *J*= 7.8 Hz), 7.02 (2H, d, H3''/H5'' , *J*= 7.8 Hz), 6.94 (2H, dd, H5/H5', *J* = 5.3, 3.8 Hz). $^{13}C$ NMR (75 MHz, $CDCl_3$) δ: 141.7 (C3/C3'), 139.8 (C1''), 139.3 (C5/C5'), 135.1 (C4/C4'), 129.0 (C1/C1'), 128.5 (C3''/C5''), 125.7 (C2''/C6''), 102.9 (C4''), 21.3 ($CH_3$); *m/z* (ESI): $[M\text{-}TsO]^+$ 292.80. 293($[M\text{-}TsO]^+$, 100%).

### 4.29 1-Iodo-4-(perfluorooctyl)propoxy benzene (232)

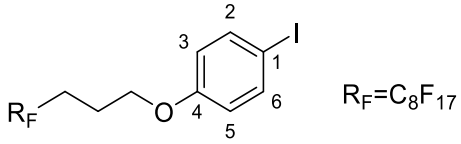


To the solution of 4-iodophenol (0.55 g, 2.5 mmol) and $Cs_2CO_3$ (1.63 g, 5.0 mmol) in DMF (40 mL) was added 3-(perfluorooctyl)propyl iodide (1.47 g, 2.5 mmol). The solution was stirred at

room temperature for 6 hours. The reaction was quenched by addition of water (50 mL) and the mixture was extracted with diethyl ether (3 × 30 mL). The organic layer was washed with brine and dried over $MgSO_4$. The solution was removed in *vacuo* to yield the title compound as a white powder (1.58 g, 2.3 mmol, 93%). Mp 88-90 °C; IR $\nu_{max}/cm^{-1}$ (neat): 1644, 1576, 1493, 1366, 1287, 1255, 1188; $^1H$ NMR (300 MHz, $CDCl_3$) δ: 7.59 (2H, d, H2/H6, *J*=8.8 Hz), 6.71 (2H, d, H3/H5, *J*=8.8 Hz), 4.02 (2H, t, $OCH_2$, *J*= 5.8 Hz), 2.40-2.19 (2H, m, $CH_2CH_2CF_2$), 2.14-2.05 (2H, m, $CH_2CH_2CF_2$). $^{13}C$ NMR (300MHz, $CDCl_3$) δ: 158.4 (C4), 138.3 (C2/C6), 116.8 (C3/C5), 83.1 (C4), 66.3 ($CH_2O$), 27.9 ($CH_2CF_2$), 20.6 ($OCH_2CH_2$); *m/z* (ASAP) 680($[M+H]^+$, 100%). Found $[M+H]^+$ 679.9529. $C_{17}H_{10}F_{17}IO$ requires 679.9505.

### 4.30 4-Iodo-3, 5-dimethyl-1-(perfluorooctyl)propoxybenzene (233)

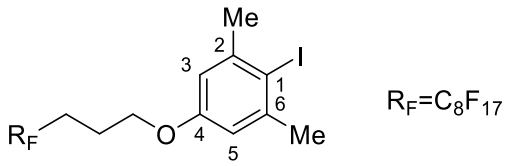


Using 4-iodo-3,5-dimethyl-phenol (0.42 g, 5.0 mmol), 3-(perfluorooctyl)propyl iodide (1.47 g, 2.5 mmol), $Cs_2CO_3$ (1.63 g, 5.0 mmol) and DMF (80 mL). White crystalline solid (1.65 g, 2.3 mmol, 93%). Mp 128-130 °C; IR $\nu_{max}/cm^{-1}$ (neat): 1644, 1576, 1493, 1366, 1287, 1255, 1188; $^1H$ NMR (300 MHz, $CDCl_3$) δ: 6.60 (2H, s, H2/H6), 3.92 (2H, t, $OCH_2$, *J*= 5.8 Hz), 2.37(6H, s, $CH_3$) 2.40-2.19 (2H, m, $CH_2CH_2CF_2$), 2.10-1.96 (2H, m, $CH_2CH_2CF_2$). $^{13}C$ NMR (75 MHz, $CDCl_3$) δ: 158.4 (C4), 143.0 (C2/C6), 113.4 (C3/C5), 97.5 (C4), 66.3 ($CH_2O$), 29.71 ($CH_3$), 27.9 ($CH_2CF_2$), 20.6 ($OCH_2CH_2$); *m/z* (ASAP) 708 ($[M+H]^+$, 100%). Found $[M+H]^+$ 707.9816. $C_{19}H_{14}F_{17}IO$ requires 707.9818.

### 4.31 Diacetoxyiodo-4-(perfluorooctyl)propoxybenzene (234)

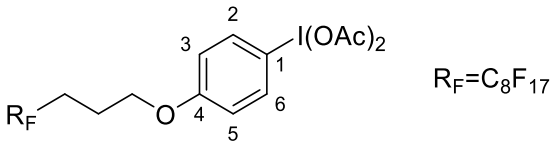


To the solution of **232** (1.58 g, 2.32 mmol) in acetic acid (45 mL) was added sodium perborate tetrahydrate (3.57 g, 23.2 mmol) portion wise at 45 °C under nitrogen over 30 min. The mixture was stirred at this temperature for another 6 hours. The reaction was quenched by addition of water (100 mL) and the mixture was extracted with dichloromethane (2 × 50 mL). The solution was removed in *vacuo* to give a yellow solid and subsequent crystallisation was induced though addition of DCM/ether/petrol to give the white crystalline solid (1.28 g, 1.5 mmol, 64%). Mp 132-136 °C; IR $\nu_{max}/cm^{-1}$ (neat): 1586, 1486, 1376, 1287, 1238, 1196; $^{1}H$ NMR (300 MHz, $CDCl_3$) δ: 7.96 (2H, d, H2/H6, *J*=8.8 Hz), 6.90 (2H, d, H3/H5, *J*=8.8 Hz), 4.02 (2H, t, $OCH_2$, *J*= 5.8 Hz), 2.33-2.16 (2H, m, $CH_2CH_2CF_2$), 2.14-2.05 (8H, m, $CH_2CH_2CF_2$, $2COOCH_3$). $^{13}C$ NMR (300MHz, $CDCl_3$) δ: 176.5 (COO), 161.1 (C4), 138.3 (C2/C6), 137.2 (C3/C5), 112.1 (C4), 66.7 ($CH_2O$), 27.8 ($CH_2CF_2$), 20.7 ($OCH_2CH_2$), 20.3 ($COOCH_3$).

### 4.32 Diacetoxyiodo-2, 6-dimethyl-4-(perfluorooctyl)propoxybenzene (235)

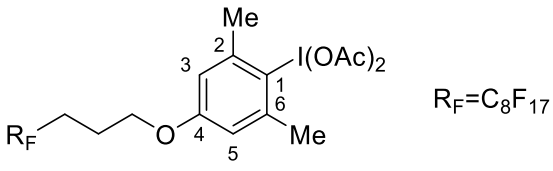


The product prepared according to **234**. White crystalline solid (0.87 g, 1.06 mmol, 35%). Mp 130-134 °C; IR $\nu_{max}/cm^{-1}$ (neat): 1654, 1582, 1452, 1323, 1196, 1152; $^{1}H$ NMR (300 MHz, $CDCl_3$) δ: 6.73 (2H, s, H2/H6), 4.01 (2H, t, $OCH_2$, *J*= 5.8 Hz), 2.64 (6H, s, $CH_3$), 2.40-2.19

(2H, m, C$H_2$CH$_2$CF$_2$), 2.10-1.96 (8H, m, CH$_2$C$H_2$CF$_2$, 2COOCH$_3$). $^{13}$C NMR (75 MHz, CDCl$_3$) δ: 176.7 (COO), 161.4 (C4), 143.0 (C2/C6), 113.4 (C3/C5), 97.5 (C4), 66.3 (CH$_2$O), 29.71 (CH$_3$), 27.9 (*C*H$_2$CF$_2$), 20.6 (OCH$_2$*C*H$_2$), 20.4 (COO*C*H$_3$);

### 4.33 (4-(Perfluorooctyl)propoxy phenyl)phenyliodonium trifluoroacetate (227)

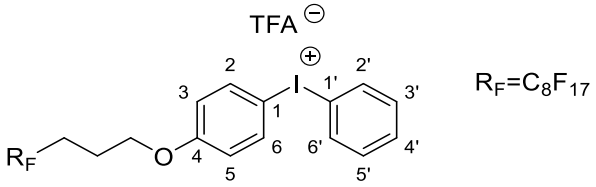


To the solution of **234** (0.81 g, 1.02 mmol) in anhydrous dichloromethane (10 mL) was added trifluoroacetic acid (0.16 mL, 2.04 mmol) portion wise at –30 °C under nitrogen. After 30 minutes, the solution was warmed to room temperature and stirred for another hour. When the solution was recooled to –30 °C, tributyltin benzene was added (0.19 g, 1.02 mmol). The solution was warmed to room temperature overnight. The solvent was removed in *vacuo* and subsequent crystallisation was induced though addition of DCM/ether/petrol to give the white crystalline solid (0.42 g, 0.49 mmol, 48%). Mp 168-172 °C; IR $\nu_{max}$/cm$^{-1}$ (neat): 1644, 1576, 1493, 1366, 1287, 1255, 1188; $^1$H NMR (300 MHz, CDCl$_3$) δ: 7.90 (4H, t, H2/H2′/H6/H6′, *J*= 7.4 Hz), 7.58 (1H, t, H4′, *J*=7.4 Hz), 7.44 (2H, t, H3′/H5′, *J*=7,4 Hz), 6.95 (2H, d, H3/H5, *J*=8.8 Hz), 4.02 (2H, t, OCH$_2$, *J*= 5.8 Hz), 2.40-2.17 (2H, m, C$H_2$CH$_2$CF$_2$), 2.14-2.05 (2H, m, CH$_2$C*H*-$_2$CF$_2$). $^{13}$C NMR (75 MHz, CDCl$_3$) δ: 161.4 (C4), 138.7 (C2/C6), 133.1 (C2’/C6’), 131.4 (C3’/C5’), 131.6 (C4’), 117.8 (C3/C5), 116.9 (C1’), 104.9 (C1), 66.5 (CH$_2$O), 27.9 (*C*H$_2$CF$_2$), 20.6 (OCH$_2$*C*H$_2$); *m/z* (NSI) 757 ([M-TFA]$^+$, 100%). Found [M-TFA]$^+$ 756.9871. C$_{23}$H$_{15}$F$_{17}$IO requires 756.9891.

## 4.34 (2,6-Dimethyl-4-(perfluorooctyl)propoxy phenyl)phenyliodonium trifluoroacetate (228)

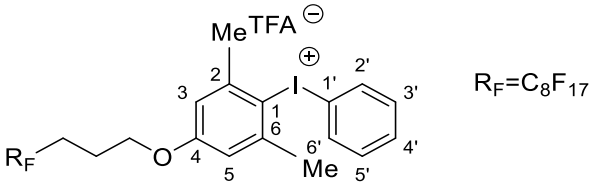


The product prepared according to the method for **227**. White crystalline solid (0.42 g, 0.47 mmol, 42%). Mp 172-176 ℃; IR $\nu_{max}/cm^{-1}$ (neat): 1654, 1582, 1451, 1323, 1196,1152; $^1$H NMR (300 MHz, $CDCl_3$) δ: 7.68 (2H, d, H2'/H6', *J*= 7.8 Hz), 7.52 (1H, t, H4', *J*= 7.4 Hz), 7.40 (2H, t, H3/H5, *J*= 7.7 Hz), 6.81 (1H, s, H3'/H5'), 4.08 (2H, t, $OCH_2$, *J*= 5.8 Hz), 2.67 (6H, s, $CH_3$), 2.47-2.24 (2H, m, C*H*$_2$$CH_2CF_2$), 2.22-1.99 (2H, m, $CH_2$C*H*$_2$$CF_2$). $^{13}$C NMR (75 MHz, $CDCl_3$) δ: 161.7 (C4), 144.4 (C2/C6), 132.4 (C2'/C6'), 131.8 (C3'/C5'), 131.2 (C4), 115.0 (C1/C1'/C3/C5), 66.6 ($CH_2O$), 27.3 ($CH_3$), 27.9 (*C*$H_2CF_2$), 20.6 ($OCH_2$*C*$H_2$); *m/z* (ESI): [M-TFA]$^+$ 785.76. 786 ([M-TFA]$^+$, 100%).

## HPLC Method

The HPLC methods were carried out by using an Agilent 1200 HPLC system and using both 230 nm and 205 nm as the wavelength (benzene and fluorobenzene would not show when the wavelength was 230 nm). The fluorophase PFP column (5 μm of particle, 150 mm × 4.6 mm) was used to separate the reaction mixture. The elution method was using water/acetonitrile as the mobile phase, the eluted rate was 1.0 mL/min. The gradient started at 20% acetonitrile over 5 min, when the acetonitrile was increased linearly to 80% over 20 min and 80% acetonitrile for 5 min.

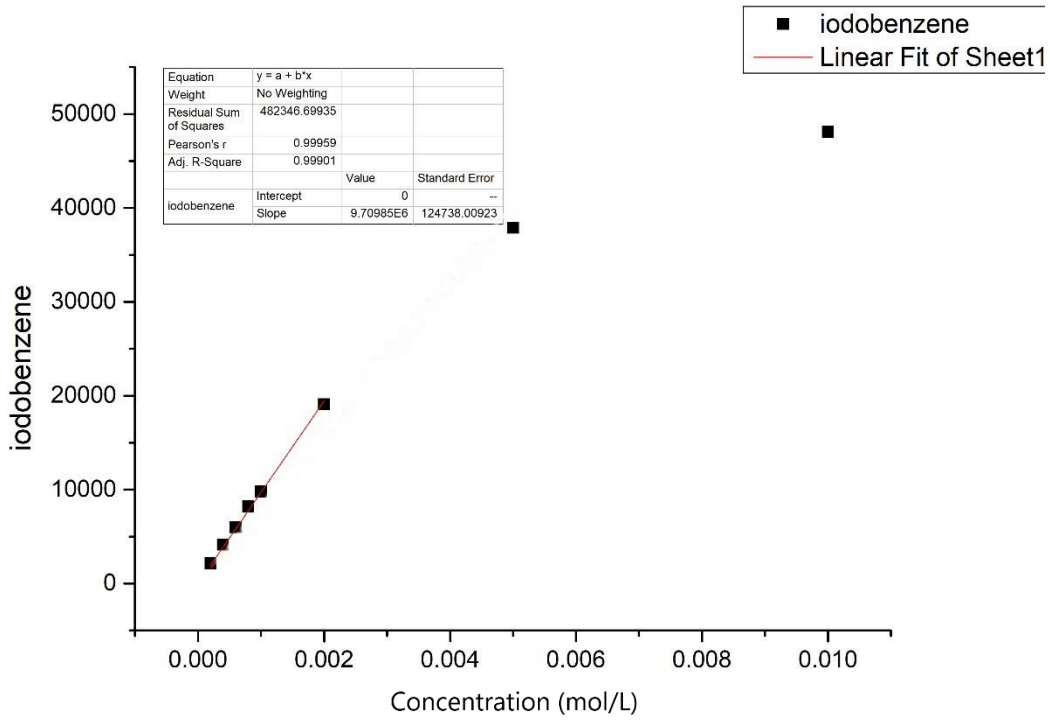


**Figure 47. Calibration curve of iodobenzene at 230 nm**

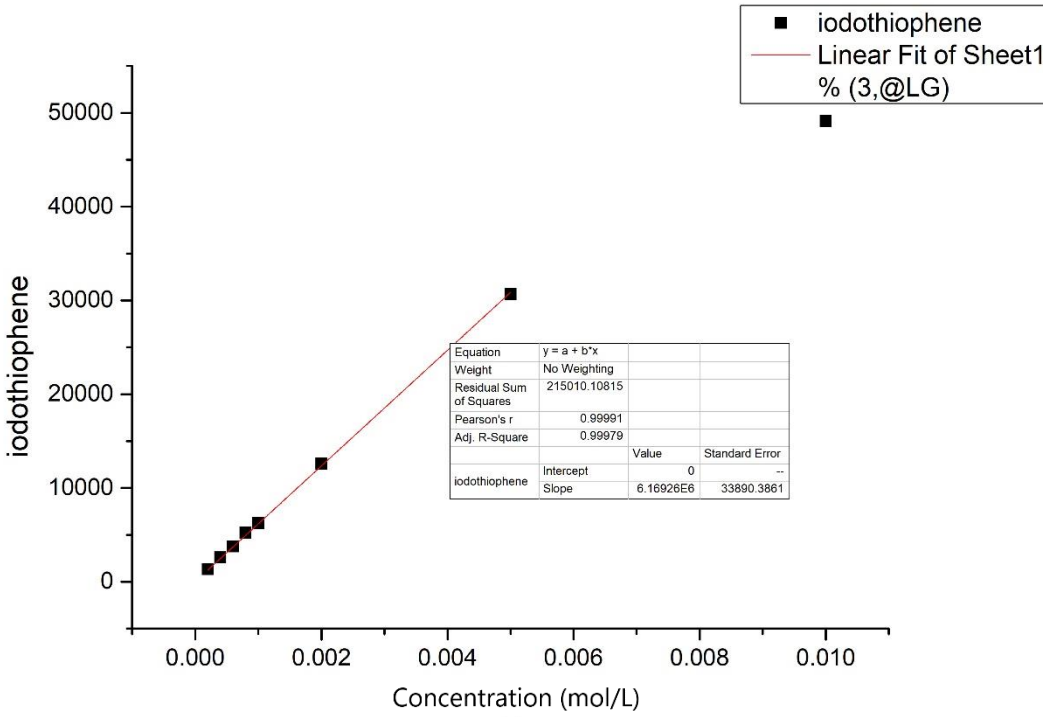


**Figure 48. Calibration curve of iodothiophene at 230 nm**

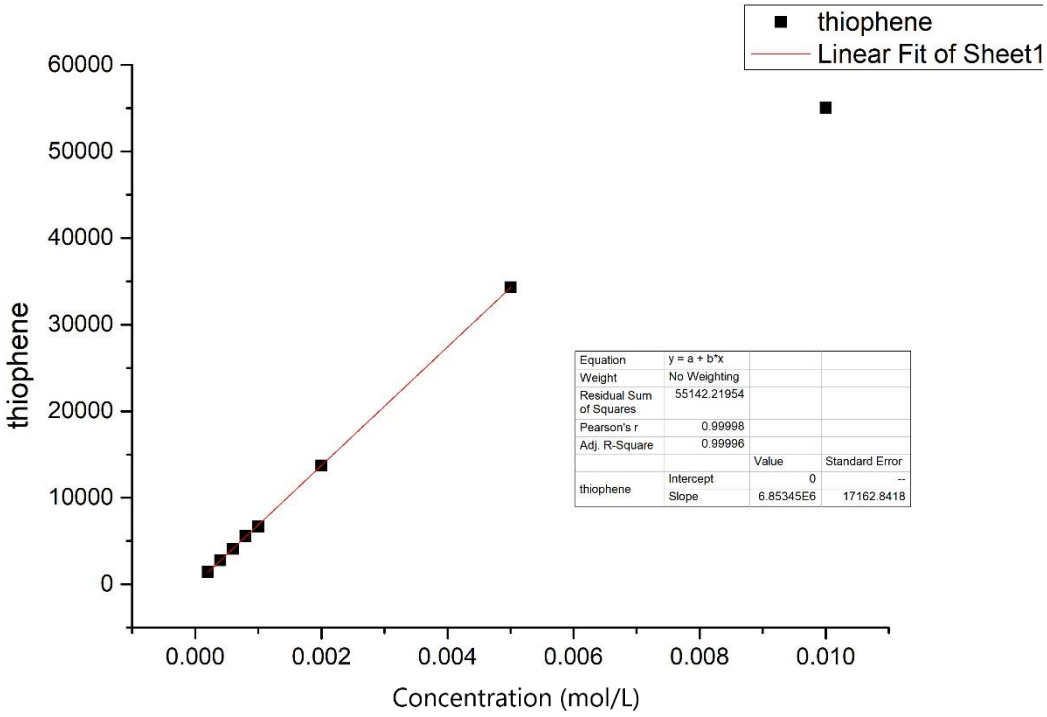


**Figure 49. Calibration curve of thiophene at 230 nm**

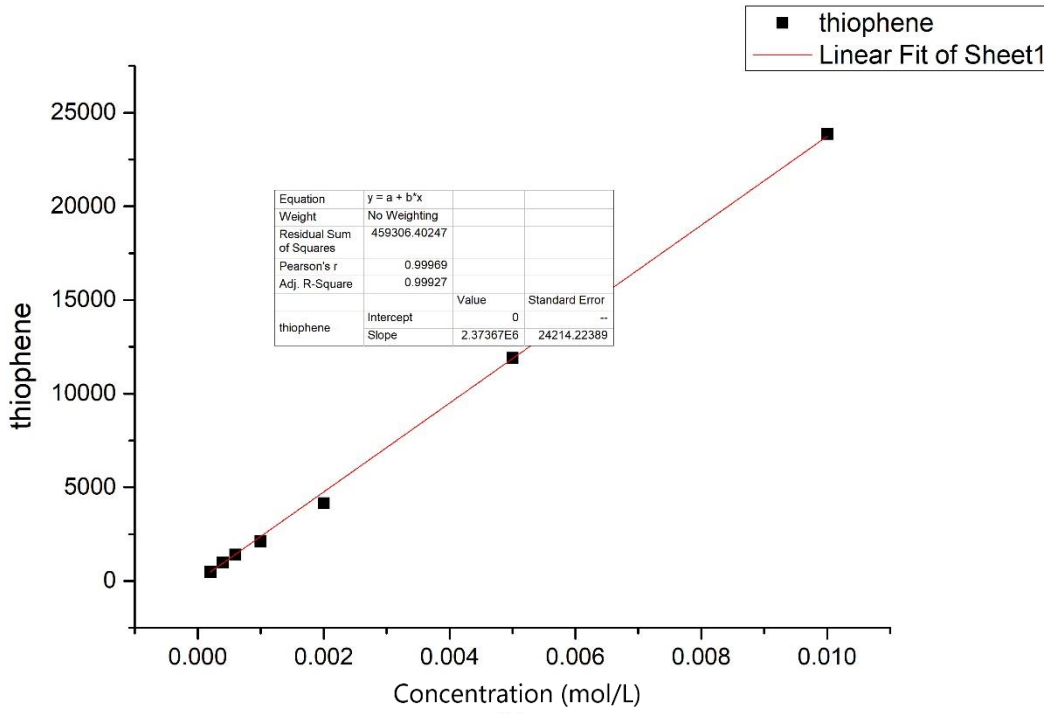


**Figure 50. Calibration curve of thiophene at 205 nm**

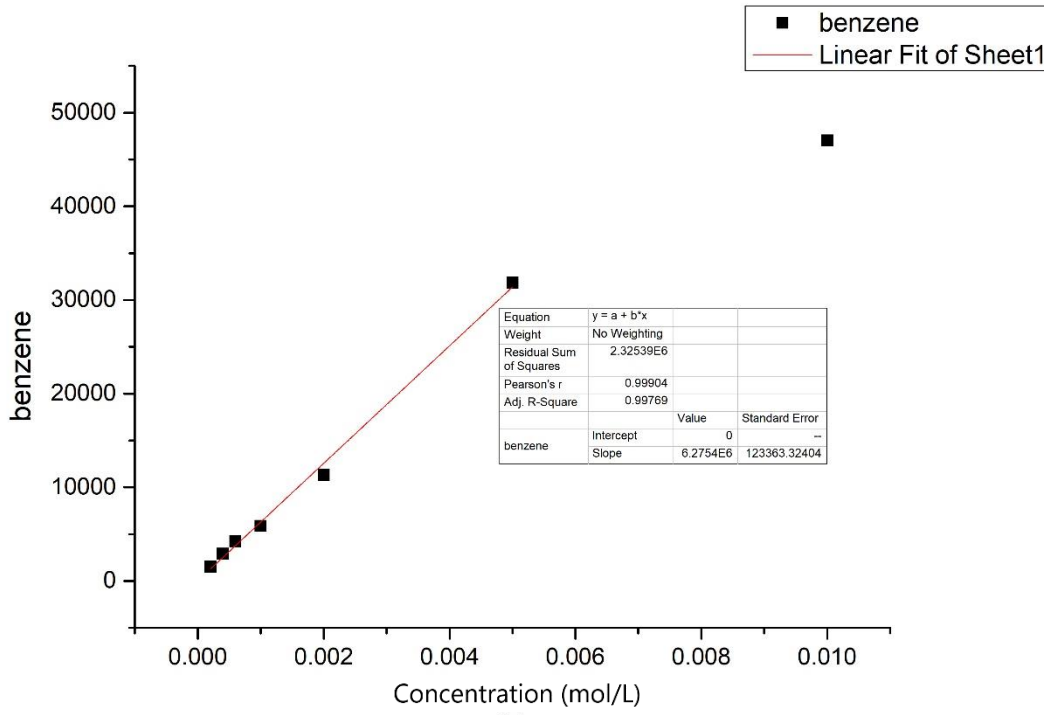


**Figure 51. Calibration curve of benzene at 205 nm**

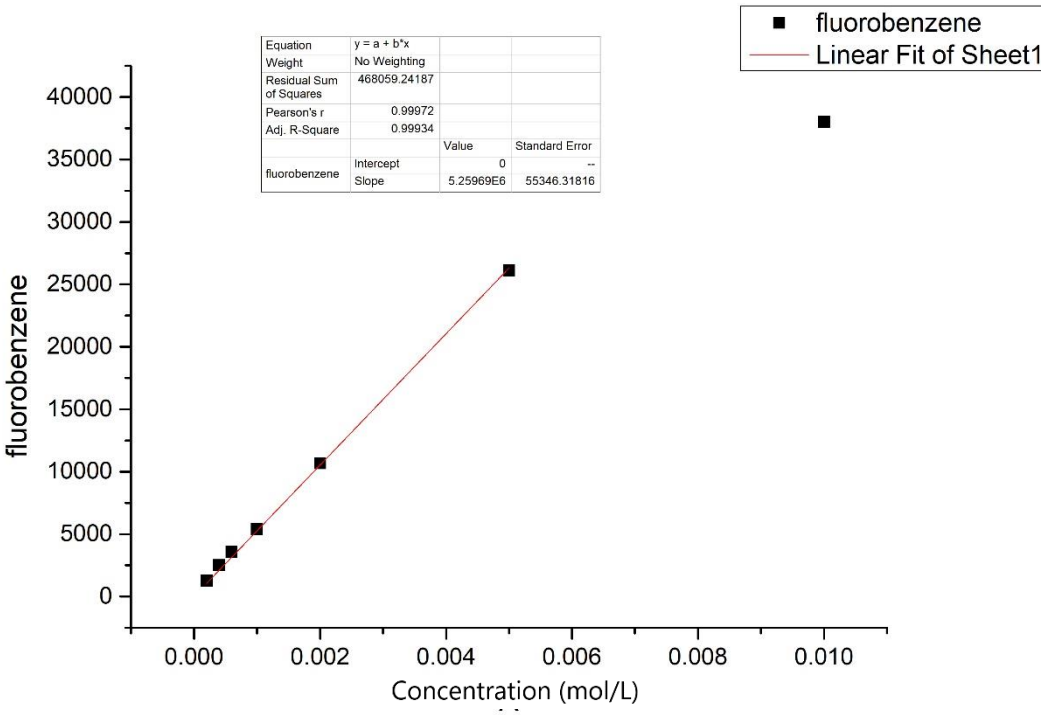


**Figure 52. Calibration curve of fluorobenzene at 205 nm**

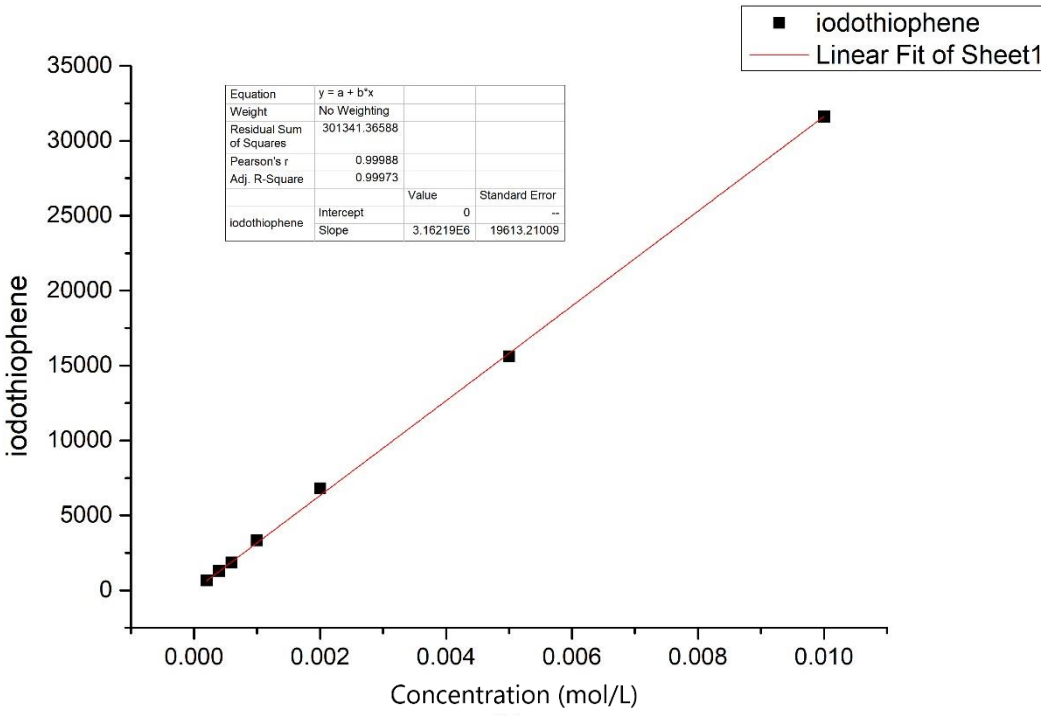


**Figure 53. Calibration curve of iodothiophene at 205 nm**

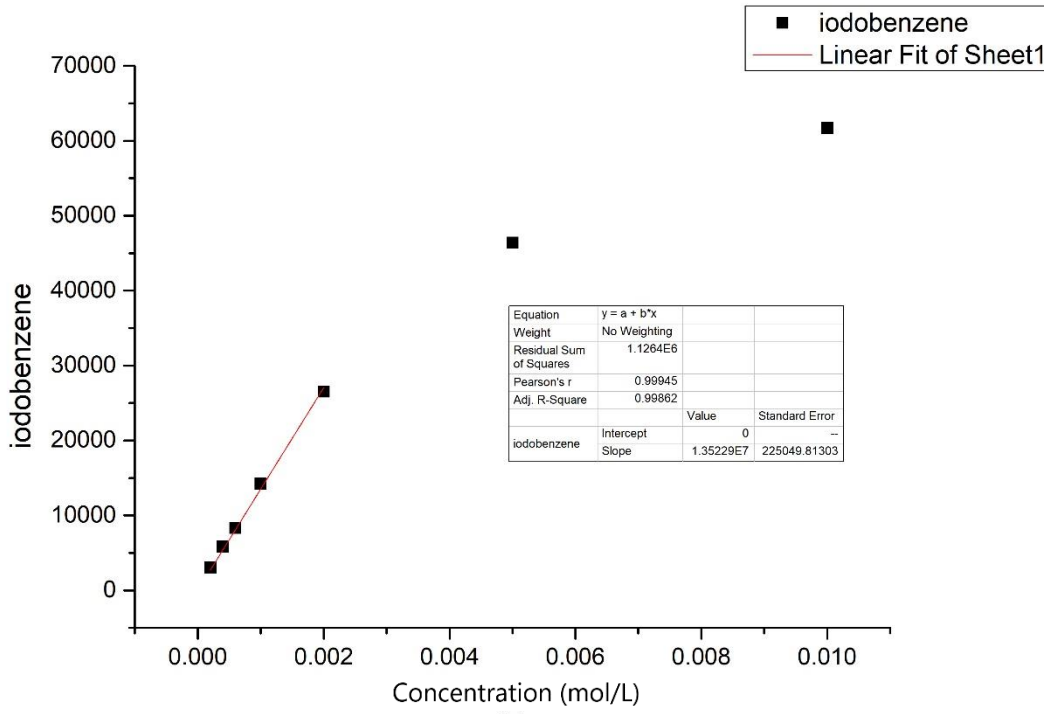


**Figure 54. Calibration curve of iodobenzene at 205 nm**

1. C. Willgerodt, . *J. Prakt. Chem.*, 1885, **33**, 154-160.
2. C. Willgerodt, *Ber. Dtsch. Chem. Ges.*, 1892, **25**, 3494-3502.
3. C. Hartmann and V. Meyer, *Ber. Dtsch. Chem. Ges.*, 1893, **26**, 1727-1732.
4. C. Hartmann and V. Meyer, *Ber. Dtsch. Chem. Ges.*, 1894, **27**, 426-432.
5. O. J. Curnow, *J. Chem. Educ.*, 1998, **75**, 910.
6. P. J. Stang and V. V. Zhdankin, *Chem. Rev.*, 1996, **96**, 1123-1178.
7. E. M. Archer and T. G. van Schalkwyk, *Acta Crystallogr.*, 1953, **6**, 88-92.
8. G. C. Pimentel, *J. Chem. Phys.*, 1951, **19**, 446-448.
9. D. B. Dess and J. C. Martin, *J. Org. Chem.*, 1983, **48**, 4155-4156.
10. D. B. Dess and J. C. Martin, *J. Am. Chem. Soc.*, 1991, **113**, 7277-7287.
11. H. Peters, *J. Chem. Soc., Trans.*, 1902, **81**, 1350-1361.
12. M. Frigerio, M. Santagostino, S. Sputore and G. Palmisano, *J. Org. Chem.*, 1995, **60**, 7272-7276.
13. R. Jafari motlagh and S. Zakavi, *New J. Chem.*, 2018, **42**, 19137-19143.
14. S. Zakavi and R. J. Motlagh, *Chemistryselect*, 2016, **1**, 5008-5013.
15. T. Wirth, in *Hypervalent Iodine Chemistry*, Springer, 2003, pp. 185-208.
16. N. Soldatova, P. Postnikov, A. A. Troyan, A. Yoshimura, M. S. Yusubov and V. V. Zhdankin, *Tetrahedron Lett.*, 2016, **57**, 4254-4256.
17. A. Maity, S. M. Hyun, A. K. Wortman and D. C. Powers, *Angew. Chem. Int. Ed. Engl.*, 2018, **57**, 7205-7209.
18. I. M. Geraskin, O. Pavlova, H. M. Neu, M. S. Yusubov, V. N. Nemykin and V. V. Zhdankin, *Adv. Synth. Catal.*, 2009, **351**, 733-737.
19. N. Jalalian, T. B. Petersen and B. Olofsson, *Chem. Eur. J.*, 2012, **18**, 14140-14149.
20. S.-K. Kang, S.-H. Lee and D. Lee, *Synlett*, 2000, **2000**, 1022-1024.
21. J. L. Dektar and N. P. Hacker, *J. Org. Chem.*, 1990, **55**, 639-647.
22. N. Lewis and P. Wallbank, *Synthesis*, 1987, **1987**, 1103-1106.
23. P. K. Sajith and C. H. Suresh, *Inorg. Chem.*, 2012, **51**, 967-977.
24. D. H. R. Barton, J. C. Jaszberenyi, K. Lessmann and T. Timar, *Tetrahedron*, 1992, **48**, 8881-8890.
25. T. L. Macdonald and N. Narasimhan, *J. Org. Chem.*, 1985, **50**, 5000-5001.
26. A. Podgorsek and J. Iskra, *Molecules*, 2010, **15**, 2857-2871.
27. A. Podgorsek, M. Jurisch, S. Stavber, M. Zupan, J. Iskra and J. A. Gladysz, *J. Org. Chem.*, 2009, **74**, 3133-3140.
28. K. C. Nicolaou, N. L. Simmons, Y. Ying, P. M. Heretsch and J. S. Chen, *J. Am. Chem. Soc.*, 2011, **133**, 8134-8137.
29. W. Zhong, J. Yang, X. Meng and Z. Li, *J. Org. Chem.*, 2011, **76**, 9997-10004.
30. C. Willgerodt, *Ber. Dtsch. Chem. Ges.*, 1892, **25**, 3494-3502.
31. L. Emmanuvel, T. M. Shaikh and A. Sudalai, *Org. Lett.*, 2005, **7**, 5071-5074.
32. F. M. Beringer, M. Drexler, E. M. Gindler and C. C. Lumpkin, *J. Am. Chem. Soc.*, 1953, **75**, 2705-2708.
33. J. Yan, Z. Zhou and M. Zhu, *Synth. Commun.*, 2006, **36**, 1495-1502.
34. A. E. Allen and D. W. MacMillan, *J. Am. Chem. Soc.*, 2011, **133**, 4260-4263.
35. M. Ochiai and T. Wirth, *by Wirth T., Top. Curr. Chem*, 2003, **224**, 5-68.
36. S. Martín-Santamaría, M. A. Carroll, V. W. Pike, H. S. Rzepa and D. A. Widdowson, *J. Chem. Soc., Perkin Trans.2*, 2000, 2158-2161.
37. T. Dohi, M. Ito, N. Yamaoka, K. Morimoto, H. Fujioka and Y. Kita, *Angew. Chem. Int. Ed. Engl.*, 2010, **49**, 3334-3337.

38. E. A. Merritt and B. Olofsson, *Angew. Chem. Int. Ed. Engl.*, 2009, **48**, 9052-9070.
39. M. Bielawski, M. Zhu and B. Olofsson, *Adv. Synth. Catal.*, 2007, **349**, 2610-2618.
40. M. Bielawski, D. Aili and B. Olofsson, *J. Org. Chem.*, 2008, **73**, 4602-4607.
41. G. F. Koser, R. H. Wettach and C. S. Smith, *J. Org. Chem.*, 1980, **45**, 1543-1544.
42. V. W. Pike, F. Butt, A. Shah and D. A. Widdowson, *J. Chem. Soc., Perkin Trans.1*, 1999, 245-248.
43. M. A. Carroll, V. W. Pike and D. A. Widdowson, *Tetrahedron Lett.*, 2000, **41**, 5393-5396.
44. T. Kitamura, J. Matsuyuki and H. Taniguchi, *Synthesis-Stuttgart*, 1994, **1994**, 147-148.
45. A. McKillop and D. Kemp, *Tetrahedron*, 1989, **45**, 3299-3306.
46. A. Shah, V. W. Pike and D. A. Widdowson, *J. Chem. Soc., Perkin Trans.1*, 1997, DOI: Doi 10.1039/A704062h, 2463-2465.
47. A. Kryska and L. Skulski, *Molecules*, 2001, **6**, 875-880.
48. A. McKillop and W. R. Sanderson, *Tetrahedron*, 1995, **51**, 6145-6166.
49. M. D. Hossain, Y. Ikegami and T. Kitamura, *J. Org. Chem.*, 2006, **71**, 9903-9905.
50. J. V. Crivello and J. H. Lam, *J. Org. Chem.*, 1978, **43**, 3055-3058.
51. M. J. Peacock and D. Pletcher, *Tetrahedron Lett.*, 2000, **41**, 8995-8998.
52. E. A. Merritt, J. Malmgren, F. J. Klinke and B. Olofsson, *Synlett*, 2009, **2009**, 2277-2280.
53. F. M. Beringer, H. E. Bachofner, R. A. Falk and M. Leff, *J. Am. Chem. Soc.*, 1958, **80**, 4279-4281.
54. F. Marshall Beringer, P. S. Forgione and M. D. Yudis, *Tetrahedron*, 1960, **8**, 49-63.
55. F. M. Beringer, A. Brierley, M. Drexler, E. M. Gindler and C. C. Lumpkin, *J. Am. Chem. Soc.*, 1953, **75**, 2708-2712.
56. J. J. Lubinkowski, J. W. Knapczyk, J. L. Calderon, L. R. Petit and W. E. Mcewen, *J. Org. Chem.*, 1975, **40**, 3010-3015.
57. J. J. Lubinkowski, M. Gomez, J. L. Calderon and W. E. Mcewen, *J. Org. Chem.*, 1978, **43**, 2432-2435.
58. J. V. Crivello and J. H. Lam, *J. Org. Chem.*, 1978, **43**, 3055-3058.
59. J. J. Lubinkowski, C. Gimenezarrieche and W. E. Mcewen, *J. Org. Chem.*, 1980, **45**, 2076-2079.
60. T. Okuyama, T. Takino, T. Sueda and M. Ochiai, *J. Am. Chem. Soc.*, 1995, **117**, 3360-3367.
61. J. Malmgren, S. Santoro, N. Jalalian, F. Himo and B. Olofsson, *Chem. Eur. J.*, 2013, **19**, 10334-10342.
62. J. Wen, R. Y. Zhang, S. Y. Chen, J. Zhang and X. Q. Yu, *J. Org. Chem.*, 2012, **77**, 766-771.
63. M. A. Carroll and R. A. Wood, *Tetrahedron*, 2007, **63**, 11349-11354.
64. Z. Gonda and Z. Novak, *Chem. Eur. J.*, 2015, **21**, 16801-16806.
65. K. M. Lancer and G. H. Wiegand, *J. Org. Chem.*, 1976, **41**, 3360-3364.
66. K. Aradi, A. Meszaros, B. L. Toth, Z. Vincze and Z. Novak, *J. Org. Chem.*, 2017, **82**, 11752-11764.
67. N. Ichiishi, A. J. Canty, B. F. Yates and M. S. Sanford, *Org. Lett.*, 2013, **15**, 5134-5137.
68. Y. Wang, C. Chen, J. Peng and M. Li, *Angew. Chem. Int. Ed. Engl.*, 2013, **52**, 5323-5327.
69. P. Li, G. Cheng, H. Zhang, X. Xu, J. Gao and X. Cui, *J. Org. Chem.*, 2014, **79**, 8156-8162.
70. S. Rousseaux, E. Vrancken and J. M. Campagne, *Angew. Chem. Int. Ed. Engl.*, 2012, **51**, 10934-10935.
71. T. Wiglenda and R. Gust, *J. Med. Chem.*, 2007, **50**, 1475-1484.
72. K. Kamiya and Y. Shigeta, *Biochim. Biophys. Acta*, 2011, **1807**, 1328-1335.
73. J. C. Antilla, J. M. Baskin, T. E. Barder and S. L. Buchwald, *J. Org. Chem.*, 2004, **69**, 5578-5587.
74. D. M. T. Chan, K. L. Monaco, R. P. Wang and M. P. Winters, *Tetrahedron Lett.*, 1998, **39**, 2933-2936.
75. D. A. Evans, J. L. Katz and T. R. West, *Tetrahedron Lett.*, 1998, **39**, 2937-2940.
76. P. Y. S. Lam, C. G. Clark, S. Saubern, J. Adams, M. P. Winters, D. M. T. Chan and A. Combs, *Tetrahedron Lett.*, 1998, **39**, 2941-2944.
77. V. Hardouin Duparc, G. L. Bano and F. Schaper, *ACS Catalysis*, 2018, **8**, 7308-7325.

78. T. D. Quach and R. A. Batey, *Org. Lett.*, 2003, **5**, 4397-4400.
79. J. C. Vantourout, H. N. Miras, A. Isidro-Llobet, S. Sproules and A. J. Watson, *J. Am. Chem. Soc.*, 2017, **139**, 4769-4779.
80. S. Schafer and T. Wirth, *Angew. Chem. Int. Ed. Engl.*, 2010, **49**, 2786-2789.
81. J. Li and L. Liu, *Rsc Advances*, 2012, **2**, 10485-10487.
82. F. Tinnis, E. Stridfeldt, H. Lundberg, H. Adolfsson and B. Olofsson, *Org. Lett.*, 2015, **17**, 2688-2691.
83. F. L. Guo, L. M. Wang, P. Q. Wang, J. J. Yu and J. W. Han, *Asian J. Org. Chem.*, 2012, **1**, 218-221.
84. J. Peng, C. Chen, Y. Wang, Z. Lou, M. Li, C. Xi and H. Chen, *Angew. Chem. Int. Ed. Engl.*, 2013, **52**, 7574-7578.
85. N. Asao, T. Nogami, K. Takahashi and Y. Yamamoto, *J. Am. Chem. Soc.*, 2002, **124**, 764-765.
86. T. Ikariya and A. J. Blacker, *Acc. Chem. Res.*, 2007, **40**, 1300-1308.
87. A. T. Ashcroft, A. K. Cheetham, J. S. Foord, M. L. H. Green, C. P. Grey, A. J. Murrell and P. D. F. Vernon, *Nature*, 1990, **344**, 319-321.
88. S. K. Kang, H. W. Lee, W. K. Choi, R. K. Hong and J. S. Kim, *Synth. Commun.*, 1996, **26**, 4219-4224.
89. S. K. Kang, S. H. Lee and D. Lee, *Synlett*, 2000, **2000**, 1022-1024.
90. K. Matsuzaki, K. Okuyama, E. Tokunaga, N. Saito, M. Shiro and N. Shibata, *Org. Lett.*, 2015, **17**, 3038-3041.
91. S. Li, H. Lv, Y. Yu, X. Ye, B. Li, S. Yang, Y. Mo and X. Kong, *Chem Commun (Camb)*, 2019, **55**, 11267-11270.
92. T. Lv, Z. Wang, J. You, J. Lan and G. Gao, *J. Org. Chem.*, 2013, **78**, 5723-5730.
93. D. Zhu, M. Chen, M. Li, B. Luo, Y. Zhao, P. Huang, F. Xue, S. Rapposelli, R. Pi and S. Wen, *Eur. J. Med. Chem.*, 2013, **68**, 81-88.
94. D. Zhu, Q. Liu, B. Luo, M. Chen, R. Pi, P. Huang and S. Wen, *Adv. Synth. Catal.*, 2013, **355**, 2172-2178.
95. Y. Wu, X. Peng, B. Luo, F. Wu, B. Liu, F. Song, P. Huang and S. Wen, *Org Biomol Chem*, 2014, **12**, 9777-9780.
96. S. Riedmuller and B. J. Nachtsheim, *Beilstein J Org Chem*, 2013, **9**, 1202-1209.
97. Y. Wang, M. Li, L. Wen, P. Jing, X. Su and C. Chen, *Org Biomol Chem*, 2015, **13**, 751-763.
98. F. Theil, *Angewandte Chemie-International Edition*, 1999, **38**, 2345-2347.
99. J. P. Zhu, *Synlett*, 1997, **1997**, 133-&.
100. M. A. Franklin, S. G. Penn, C. B. Lebrilla, T. H. Lam, I. N. Pessah and T. F. Molinski, *J. Nat. Prod.*, 1996, **59**, 1121-1127.
101. J. Lindley, T. J. Mason and J. P. Lorimer, *Ultrasonics*, 1987, **25**, 45-48.
102. Q. Zhang, D. Wang, X. Wang and K. Ding, *J. Org. Chem.*, 2009, **74**, 7187-7190.
103. M. Rovira, M. Soler, I. Guell, M. Z. Wang, L. Gomez and X. Ribas, *J. Org. Chem.*, 2016, **81**, 7315-7325.
104. L. Ramezani, A. Yahyazadeh and M. Sheykhan, *Chemcatchem*, 2018, **10**, 4636-4651.
105. K. Bahrami and M. Khodamorady, *Catal. Lett.*, 2019, **149**, 688-698.
106. M. Hosseini-Sarvari and Z. Razmi, *Rsc Advances*, 2014, **4**, 44105-44116.
107. R. Arundhathi, D. Damodara, P. R. Likhar, M. L. Kantam, P. Saravanan, T. Magdaleno and S. H. Kwon, *Adv. Synth. Catal.*, 2011, **353**, 1591-1600.
108. E. C. Jorgensen and R. A. Wiley, *J Med Pharm Chem*, 1962, **91**, 1307-1315.
109. N. Jalalian, E. E. Ishikawa, L. F. Silva Jr and B. Olofsson, *Org. Lett.*, 2011, **13**, 1552-1555.
110. H. Gao, Q. L. Xu, C. Keene and L. Kurti, *Chem. Eur. J.*, 2014, **20**, 8883-8887.
111. Y. Yang, X. S. Wu, J. W. Han, S. Mao, X. F. Qian and L. M. Wang, *Eur. J. Org. Chem.*, 2014, **2014**, 6854-6857.

112. B. Q. Xiong, X. F. Feng, L. Z. Zhu, T. Q. Chen, Y. B. Zhou, C. T. Au and S. F. Yin, *Acs Catalysis*, 2015, **5**, 537-543.
113. S. A. Jacobsen, S. Rødbotten and T. Benneche, *J. Chem. Soc., Perkin Trans. 1*, 1999, 3265-3268.
114. T. Zhou, T. C. Li and Z. C. Chen, *Helv. Chim. Acta*, 2005, **88**, 290-296.
115. P. B. Thorat, N. A. Waghmode and N. N. Karade, *Tetrahedron Lett.*, 2014, **55**, 5718-5721.
116. W. Xiong, C. Qi, Y. Peng, T. Guo, M. Zhang and H. Jiang, *Chem. Eur. J.*, 2015, **21**, 14314-14318.
117. M. Rajabi, T. Sudha, N. H. Darwish, P. J. Davis and S. A. Mousa, *Bioorg. Med. Chem. Lett.*, 2016, **26**, 4112-4116.
118. B. Bhattarai, J. H. Tay and P. Nagorny, *Chem Commun (Camb)*, 2015, **51**, 5398-5401.
119. D. W. Lin, T. Masuda, M. B. Biskup, J. D. Nelson and P. S. Baran, *J. Org. Chem.*, 2011, **76**, 1013-1030.
120. S. M. Johnson, H. M. Petrassi, S. K. Palaninathan, N. N. Mohamedmohaideen, H. E. Purkey, C. Nichols, K. P. Chiang, T. Walkup, J. C. Sacchettini, K. B. Sharpless and J. W. Kelly, *J. Med. Chem.*, 2005, **48**, 1576-1587.
121. M. Fananas-Mastral and B. L. Feringa, *J. Am. Chem. Soc.*, 2014, **136**, 9894-9897.
122. Z. F. Xu, C. X. Cai, M. Jiang and J. T. Liu, *Org. Lett.*, 2014, **16**, 3436-3439.
123. M. E. Phelps, E. J. Hoffman, N. A. Mullani and M. M. Ter-Pogossian, *J Nucl Med*, 1975, **16**, 210-224.
124. S. D. Schimler, S. J. Ryan, D. C. Bland, J. E. Anderson and M. S. Sanford, *J. Org. Chem.*, 2015, **80**, 12137-12145.
125. M. V. Der Puy, *J. Fluorine Chem.*, 1982, **21**, 385-392.
126. M. A. Carroll, J. Nairne and J. L. Woodcraft, *J. Labelled Compd. Radiopharm.*, 2007, **50**, 452-454.
127. M. A. Carroll, J. Nairne, G. Smith and D. A. Widdowson, *J. Fluorine Chem.*, 2007, **128**, 127-132.
128. M.-S. S. Carroll, *Widdowson DA. Chem. Commun*, 2000, **649**.
129. T. L. Ross, J. Ermert, C. Hocke and H. H. Coenen, *J. Am. Chem. Soc.*, 2007, **129**, 8018-8025.
130. Y. Yamada and M. Okawara, *Bull. Chem. Soc. Jpn.*, 1972, **45**, 1860-1863.
131. K. M. Lancer and G. Wiegand, *J. Org. Chem.*, 1976, **41**, 3360-3364.
132. R. Richarz, P. Krapf, F. Zarrad, E. A. Urusova, B. Neumaier and B. D. Zlatopolskiy, *Organic & biomolecular chemistry*, 2014, **12**, 8094-8099.
133. B. D. Zlatopolskiy, J. Zischler, P. Krapf, F. Zarrad, E. A. Urusova, E. Kordys, H. Endepols and B. Neumaier, *Chem. Eur. J.* 2015, **21**, 5972-5979.
134. D. O'Hagan, *Chem. Soc. Rev.*, 2008, **37**, 308-319.
135. T. Liang, C. N. Neumann and T. Ritter, *Angew. Chem. Int. Ed. Engl.*, 2013, **52**, 8214-8264.
136. G. E. Berendsen and L. d. Galan, *J. Liq. Chromatogr.*, 1978, **1**, 403-426.
137. A. P. Dobbs and M. R. Kimberley, *J. Fluorine Chem.*, 2002, **118**, 3-17.
138. N. J. Simpson, *Solid-phase extraction: principles, techniques, and applications*, CRC Press, 2000.
139. M. C. Hennion, *J. Chromatogr. A*, 1999, **856**, 3-54.
140. D. P. Curran, S. Hadida and M. He, *J. Org. Chem.*, 1997, **62**, 6714-6715.
141. W. Zhang and D. P. Curran, *Tetrahedron*, 2006, **62**, 11837-11865.
142. M. Matsugi and D. P. Curran, *Org. Lett.*, 2004, **6**, 2717-2720.
143. K. Von Werner, *J. Fluorine Chem.*, 1985, **28**, 229-233.
144. G.-S. Yang, X.-j. Xie, G. Zhao and Y. Ding, *J. Fluorine Chem.*, 1999, **98**, 159-161.
145. C. Rocaboy and J. A. Gladysz, *Chem. Eur. J.*, 2003, **9**, 88-95.
146. P. C. Hartmann, A. Collet, M. Viguier and C. Blanc, *J. Fluorine Chem.*, 2004, **125**, 1909-1918.
147. M. Iizuka and M. Yoshida, *J. Fluorine Chem.*, 2009, **130**, 926-932.
148. M. Khrizanforov, T. Gryaznova, O. Sinyashin and Y. Budnikova, *J. Organomet. Chem.*, 2012, **718**, 101-

104.
149. D. Mikhaylov, T. Gryaznova, Y. Dudkina, M. Khrizanphorov, S. Latypov, O. Kataeva, D. A. Vicic, O. G. Sinyashin and Y. Budnikova, *Dalton Trans*, 2012, **41**, 165-172.
150. H. Sawada, M. Nakayama, M. Yoshida, T. Yoshida and N. Kamigata, *J. Fluorine Chem.*, 1990, **46**, 423-431.
151. K. J. L. Paciorek, R. H. Kratzer, J. H. Nakahara and H. M. Atkins, *J. Fluorine Chem.*, 1991, **53**, 355-367.
152. J. C. Xiao, C. Ye and J. M. Shreeve, *Org. Lett.*, 2005, **7**, 1963-1965.
153. X.-C. Guo and Q.-Y. Chen, *J. Fluorine Chem.*, 1999, **93**, 81-86.
154. J. Ignatowska and W. Dmowski, *J. Fluorine Chem.*, 2007, **128**, 997-1006.
155. S. Barata-Vallejo and A. Postigo, *J. Org. Chem.*, 2010, **75**, 6141-6148.
156. T. Takagi and T. Kanamori, *J. Fluorine Chem.*, 2011, **132**, 427-429.
157. S. Choi, Y. J. Kim, S. M. Kim, J. W. Yang, S. W. Kim and E. J. Cho, *Nat Commun*, 2014, **5**, 4881.
158. Y. Li, Q. Guo, X. F. Li, H. Zhang, F. H. Yu, W. J. Yu, G. Q. Xia, M. Y. Fu, Z. G. Yang and Z. X. Jiang, *Tetrahedron Lett.*, 2014, **55**, 2110-2113.
159. Q. Qi, Q. Shen and L. Lu, *J. Am. Chem. Soc.*, 2012, **134**, 6548-6551.
160. R. Shimizu, E. Yoneda and T. Fuchikami, *Tetrahedron Lett.*, 1996, **37**, 5557-5560.
161. M. Wende, F. Seidel and J. A. Gladysz, *J. Fluorine Chem.*, 2003, **124**, 45-54.
162. H. S. J. G. Sharefkin, *Org. Synth.*, 1963, **43**, 62.
163. A. McKillop and W. R. Sanderson, *J. Chem. Soc., Perkin Trans. 1*, 2000, 471-476.
164. B. C. Lee, K. C. Lee, H. Lee, R. H. Mach and J. A. Katzenellenbogen, *Bioconjugate Chem.*, 2007, **18**, 514-523.
165. M. Ochiai, K. Miyamoto, Y. Yokota, T. Suefuji and M. Shiro, *Angew. Chem. Int. Ed.*, 2005, **44**, 75-78.
166. M. Ochiai, M. Toyonari, T. Nagaoka, D.-W. Chen and M. Kida, *Tetrahedron Lett.*, 1997, **38**, 6709-6712.
167. V. W. Pike, F. Butt, A. Shah and D. A. Widdowson, *J. Chem. Soc., Perkin Trans. 1*, 1999, 245-248.
168. A. Shah, V. W. Pike and D. A. Widdowson, *J. Chem. Soc., Perkin Trans. 1*, 1997, 2463-2466.
169. N. W. Alcock and R. M. Countryman, *J. Chem. Soc., Dalton Trans.*, 1977, 217-219.
170. T. Khotsyanova, T. Babushkina, V. Saatsazov, T. Tolstaya and G. Semin, *Doklady Akademii Nauk SSSR*, 1975, **222**, 403-405.
171. D. I. Bugaenko, M. A. Yurovskaya and A. V. Karchava, *Org. Lett.*, 2018, **20**, 6389-6393.
172. G. Cavallo, J. S. Murray, P. Politzer, T. Pilati, M. Ursini and G. Resnati, *IUCrJ*, 2017, **4**, 411-419.
173. R.W. Harrington and W. Clegg, *CSD Communication*, 2020.
174. D. D. DesMarteau, W. T. Pennington, V. Montanari and B. H. Thomas, *J. Fluorine Chem.*, 2003, **122**, 57-61.
175. J. L. Woodcraft, PhD Thesis, Newcastle University, 2006.
176. R. J. Phipps, L. McMurray, S. Ritter, H. A. Duong and M. J. Gaunt, *J. Am. Chem. Soc.*, 2012, **134**, 10773-10776.
177. B. Odom, D. Hanneke, B. D'Urso and G. Gabrielse, *Phys. Rev. Lett.*, 2006, **97**, 030801.
178. A. L. Barra, L. C. Brunel and J. B. Robert, *Chem. Phys. Lett.*, 1990, **165**, 107-109.
179. S. A. Adonin, A. S. Novikov and M. N. Sokolov, *Eur. J. Inorg. Chem.*, 2019, **2019**, 4221-4223.
180. M. A. Carroll, S. Martín-Santamaría, V. W. Pike, H. S. Rzepa and D. A. Widdowson, *J. Chem. Soc., Perkin Trans. 2*, 1999, 2707-2714.
181. M. Uchiyama, T. Suzuki and Y. Yamazaki, *Chem. Lett.*, 1983, **12**, 1201-1202.
182. P. Zhu, S. Sui, B. Wang, K. Sun and G. Sun, *J. Anal. Appl. Pyrolysis*, 2004, **71**, 645-655.
183. E. F. Rothgery, D. E. Audette, R. C. Wedlich and D. A. Csejka, *Thermochimica Acta*, 1991, **185**, 235-243.

184. A. C. Y. Wong and F. Lam, *Polymer Testing*, 2002, **21**, 691-696.
185. E. Lindstedt, M. Reitti and B. Olofsson, *J. Org. Chem.*, 2017, **82**, 11909-11914.
186. M. Ochiai, T. Suefuji, K. Miyamoto, N. Tada, S. Goto, M. Shiro, S. Sakamoto and K. Yamaguchi, *J. Am. Chem. Soc.,* 2003, **125**, 769-773.
187. M. Mosiadz, K. L. Juda, S. C. Hopkins, J. Soloducho and B. A. Glowacki, *J. Fluorine Chem.*, 2012, **135**, 59-67.
188. J. Jiang and J. Li, *ChemistrySelect*, 2020, **5**, 542-548.
189. A. Williamson, *Philosophical Magazine Series 3*, 1850, **37**, 350-356.
190. J. V. Crivello and J. L. Lee, *J. Polym. Sci., Part A: Polym. Chem.*, 2010, **48**, 4484-4495.
191. T. Morofuji, A. Shimizu and J.-i. Yoshida, *J. Am. Chem. Soc.*, 2013, **135**, 5000-5003.
192. N. L. Segraves, S. J. Robinson, D. Garcia, S. A. Said, X. Fu, F. J. Schmitz, H. Pietraszkiewicz, F. A. Valeriote and P. Crews, *J. Nat. Prod.*, 2004, **67**, 783-792.
193. J. Dai, K. Krohn, S. Draeger and B. Schulz, *Eur. J. Org. Chem.*, 2009, **2009**, 1564-1569.
194. M. D. Hossain and T. Kitamura, *J. Org. Chem.*, 2005, **70**, 6984-6986.
195. C. Ye, B. Twamley and J. n. M. Shreeve, *Org. Lett.*, 2005, **7**, 3961-3964.
196. H. Togo, T. Nabana and K. Yamaguchi, *J. Org. Chem.*, 2000, **65**, 8391-8394.
197. M. D. Hossain, Y. Ikegami and T. Kitamura, *J. Org. Chem.*, 2006, **71**, 9903-9905.
198. M. Zhu, N. Jalalian and B. Olofsson, *Synlett*, 2008, **2008**, 592-596.
199. M. C. Caserio, D. L. Glusker and J. D. Roberts, *J. Am. Chem. Soc.*, 1959, **81**, 336-342.
200. T. Dohi, M. Ito, K. Morimoto, Y. Minamitsuji, N. Takenaga and Y. Kita, *Chem. Commun.*, 2007, 4152-4154.
201. V. V. Zhdankin, *Science of Synthesis*, Thieme Chemistry, 2007.
202. M. D. Hossain and T. Kitamura, *Tetrahedron*, 2006, **62**, 6955-6960.
203. T. B. Petersen, R. Khan and B. Olofsson, *Org. Lett.*, 2011, **13**, 3462-3465.

# Appendices

## XRD of 2-Butyl-4-methoxyphenyl(phenyl)iodonium trifluoroacetate (158)

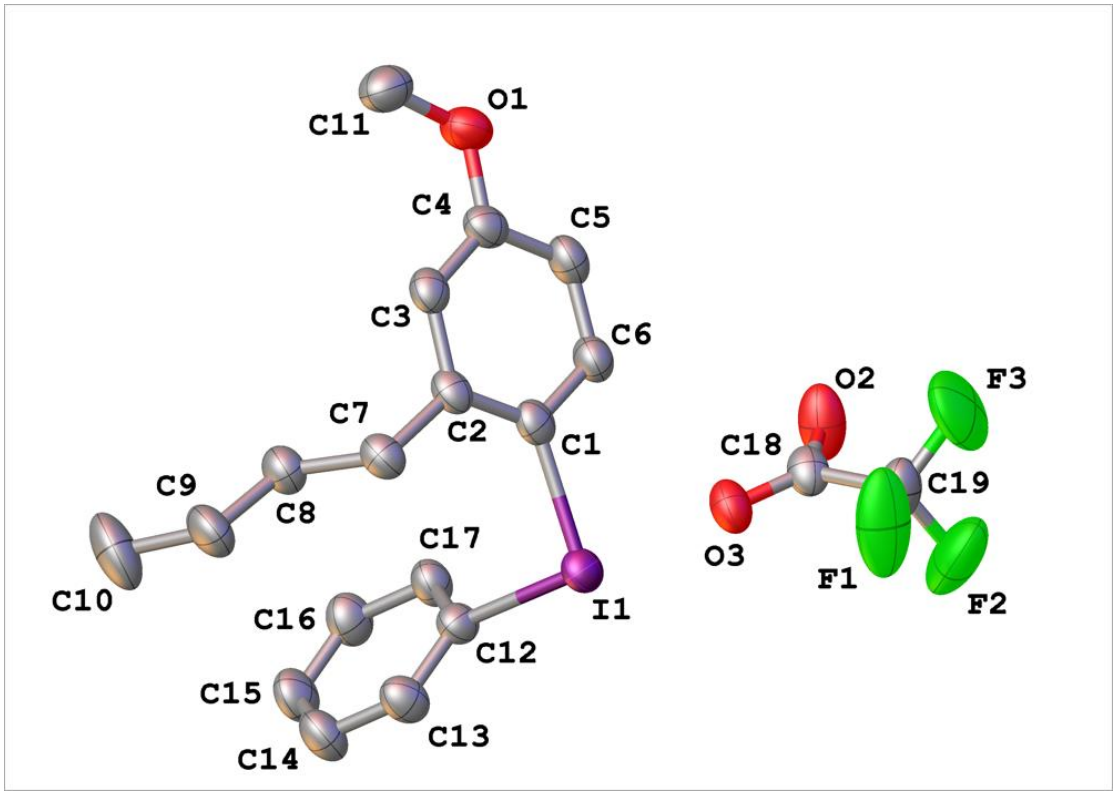

Table 1 : Crystal data and structure refinement for mac190011.

| | |
|---|---|
| Identification code | mac190011 |
| Empirical formula | C19H20F3IO3 |
| Formula weight | 480.25 |
| Temperature/K | 150.0(2) |
| Crystal system | monoclinic |
| Space group | P21/c |
| a/Å | 9.4825(5) |
| b/Å | 19.8080(10) |
| c/Å | 10.4968(5) |
| α/° | 90 |
| β/° | 95.376(4) |
| γ/° | 90 |
| Volume/Å3 | 1962.93(17) |
| Z | 4 |
| ρcalcg/cm3 | 1.625 |
| μ/mm-1 | 13.210 |
| F(000) | 952.0 |
| Crystal size/mm3 | 0.22 × 0.14 × 0.03 |
| Radiation | CuKα (λ = 1.54184) |
| 2Θ range for data collection/° | 8.928 to 134.062 |
| Index ranges | -10 ≤ h ≤ 11, -23 ≤ k ≤ 23, -12 ≤ l ≤ 12 |
| Reflections collected | 14443 |
| Independent reflections | 3482 [Rint = 0.0609, Rsigma = 0.0478] |
| Data/restraints/parameters | 3482/0/237 |
| Goodness-of-fit on F2 | 1.046 |
| Final R indexes [I>=2σ (I)] | R1 = 0.0361, wR2 = 0.0797 |
| Final R indexes [all data] | R1 = 0.0514, wR2 = 0.0888 |
| Largest diff. peak/hole / e Å-3 | 0.83/-0.66 |

**Table 2 Fractional Atomic Coordinates ($\times 10^4$) and Equivalent Isotropic Displacement Parameters ($Å^2 \times 10^3$) for mac190011. $U_{eq}$ is defined as 1/3 of of the trace of the orthogonalised $U_{IJ}$ tensor.**

| Atom | *x* | *y* | *z* | U(eq) |
|---|---|---|---|---|
| I1 | 4857.2(3) | 6723.4(2) | 3666.4(3) | 39.28(12) |
| F1 | 9155(4) | 6753(3) | 7174(6) | 122(2) |
| F2 | 8419(5) | 7746(3) | 7334(6) | 113.3(18) |
| F3 | 8025(5) | 7060(3) | 8757(4) | 111.7(17) |
| O1 | 1026(4) | 4888(2) | 6677(3) | 51.6(9) |
| O2 | 5626(4) | 7170(2) | 7216(4) | 70.0(12) |
| O3 | 6740(4) | 6597.7(18) | 5774(3) | 48.6(8) |
| C1 | 3605(5) | 6041(2) | 4614(4) | 38.0(10) |
| C2 | 3414(5) | 5370(2) | 4227(4) | 37.0(10) |
| C3 | 2550(5) | 4974(2) | 4948(4) | 38.9(10) |
| C4 | 1903(5) | 5240(3) | 5966(4) | 41.7(11) |
| C5 | 2130(6) | 5908(3) | 6322(5) | 45.1(12) |
| C6 | 2987(5) | 6310(3) | 5642(4) | 41.8(11) |
| C7 | 3979(5) | 5054(3) | 3087(4) | 41.3(11) |
| C8 | 2815(6) | 4934(3) | 1993(5) | 47.0(12) |
| C9 | 3345(7) | 4578(3) | 852(5) | 60.0(15) |
| C10 | 2221(10) | 4506(4) | -273(6) | 88(2) |
| C11 | 828(6) | 4187(3) | 6404(6) | 56.7(14) |
| C12 | 3513(5) | 6731(2) | 1940(4) | 37.5(10) |
| C13 | 4103(5) | 6578(3) | 822(5) | 46.1(12) |
| C14 | 3250(6) | 6582(3) | -312(5) | 53.7(14) |
| C15 | 1833(6) | 6733(3) | -319(5) | 52.7(13) |
| C16 | 1249(6) | 6885(3) | 799(5) | 50.5(13) |
| C17 | 2098(5) | 6886(3) | 1950(5) | 42.5(11) |
| C18 | 6674(5) | 6942(2) | 6750(5) | 41.2(11) |
| C19 | 8064(6) | 7108(3) | 7499(6) | 58.6(15) |

**Table 3 Anisotropic Displacement Parameters ($Å^2×10^3$) for mac190011. The Anisotropic displacement factor exponent takes the form: $-2\pi^2[h^2a^{*2}U_{11}+2hka^*b^*U_{12}+\ldots]$.**

| Atom | $U_{11}$ | $U_{22}$ | $U_{33}$ | $U_{23}$ | $U_{13}$ | $U_{12}$ |
|---|---|---|---|---|---|---|
| I1 | 40.48(17) | 44.30(18) | 31.80(16) | 2.45(13) | -3.26(11) | -1.24(14) |
| F1 | 50(2) | 152(5) | 155(5) | -84(4) | -33(2) | 29(3) |
| F2 | 97(3) | 87(3) | 161(5) | -48(3) | 38(3) | -47(3) |
| F3 | 98(3) | 177(5) | 53(2) | -10(3) | -33(2) | -10(3) |
| O1 | 51(2) | 63(2) | 42.7(18) | 4.1(17) | 11.0(15) | -4.5(17) |
| O2 | 49(2) | 81(3) | 78(3) | -35(2) | -9(2) | 15(2) |
| O3 | 58(2) | 50(2) | 36.5(18) | -6.5(16) | -5.5(15) | 2.8(16) |
| C1 | 36(2) | 47(3) | 29(2) | -1(2) | -5.3(18) | 2(2) |
| C2 | 43(3) | 39(3) | 28(2) | 1.2(19) | -2.7(19) | 6(2) |
| C3 | 44(3) | 39(3) | 31(2) | 1.2(19) | -6.4(19) | 0(2) |
| C4 | 40(3) | 52(3) | 32(2) | 4(2) | -0.4(19) | -1(2) |
| C5 | 48(3) | 54(3) | 33(2) | -10(2) | 2(2) | 2(2) |
| C6 | 50(3) | 43(3) | 32(2) | -5(2) | 1(2) | -1(2) |
| C7 | 47(3) | 44(3) | 33(2) | 0(2) | 3(2) | 5(2) |
| C8 | 53(3) | 51(3) | 36(2) | -5(2) | 3(2) | -1(2) |
| C9 | 79(4) | 68(4) | 34(3) | -10(3) | 8(3) | -3(3) |
| C10 | 116(6) | 100(6) | 46(3) | -25(4) | -15(4) | 18(5) |
| C11 | 54(3) | 60(4) | 56(3) | 11(3) | 4(3) | -11(3) |
| C12 | 39(2) | 41(2) | 32(2) | 4(2) | -0.4(18) | -2(2) |
| C13 | 39(3) | 61(3) | 38(3) | 3(2) | 2(2) | 5(2) |
| C14 | 59(3) | 70(4) | 32(2) | -6(2) | 3(2) | 3(3) |
| C15 | 52(3) | 69(4) | 35(3) | -1(2) | -10(2) | 0(3) |
| C16 | 46(3) | 61(3) | 43(3) | -3(2) | -4(2) | 2(2) |
| C17 | 43(3) | 51(3) | 33(2) | -4(2) | -1(2) | -1(2) |
| C18 | 49(3) | 35(2) | 38(3) | 0(2) | -7(2) | 5(2) |
| C19 | 48(3) | 63(4) | 62(4) | -15(3) | -9(3) | -6(3) |

**Table 4 Bond Lengths for mac190011.**

| Atom | Atom | Length/Å | Atom | Atom | Length/Å |
|---|---|---|---|---|---|
| I1 | C1 | 2.108(5) | C3 | C4 | 1.385(7) |
| I1 | C12 | 2.116(4) | C4 | C5 | 1.386(8) |
| F1 | C19 | 1.323(8) | C5 | C6 | 1.382(7) |
| F2 | C19 | 1.323(8) | C7 | C8 | 1.535(7) |
| F3 | C19 | 1.328(7) | C8 | C9 | 1.515(7) |
| O1 | C4 | 1.361(6) | C9 | C10 | 1.521(9) |
| O1 | C11 | 1.427(7) | C12 | C13 | 1.381(7) |
| O2 | C18 | 1.234(7) | C12 | C17 | 1.377(7) |
| O3 | C18 | 1.237(6) | C13 | C14 | 1.376(7) |
| C1 | C2 | 1.397(7) | C14 | C15 | 1.376(8) |
| C1 | C6 | 1.383(7) | C15 | C16 | 1.377(8) |
| C2 | C3 | 1.405(7) | C16 | C17 | 1.388(7) |
| C2 | C7 | 1.495(7) | C18 | C19 | 1.507(7) |

**Table 5 Bond Angles for mac190011.**

| Atom | Atom | Atom | Angle/° | Atom | Atom | Atom | Angle/° |
|---|---|---|---|---|---|---|---|
| C1 | I1 | C12 | 95.04(17) | C13 | C12 | I1 | 117.8(3) |
| C4 | O1 | C11 | 117.7(4) | C17 | C12 | I1 | 120.3(3) |
| C2 | C1 | I1 | 122.5(3) | C17 | C12 | C13 | 121.9(4) |
| C6 | C1 | I1 | 114.9(4) | C14 | C13 | C12 | 118.8(5) |
| C6 | C1 | C2 | 122.7(5) | C13 | C14 | C15 | 120.0(5) |
| C1 | C2 | C3 | 116.2(4) | C14 | C15 | C16 | 120.9(5) |
| C1 | C2 | C7 | 125.8(4) | C15 | C16 | C17 | 119.7(5) |
| C3 | C2 | C7 | 117.9(4) | C12 | C17 | C16 | 118.7(5) |
| C4 | C3 | C2 | 121.7(4) | O2 | C18 | O3 | 129.4(5) |
| O1 | C4 | C3 | 124.4(5) | O2 | C18 | C19 | 114.2(5) |
| O1 | C4 | C5 | 115.4(4) | O3 | C18 | C19 | 116.3(5) |
| C3 | C4 | C5 | 120.2(5) | F1 | C19 | F2 | 105.0(6) |
| C6 | C5 | C4 | 119.6(5) | F1 | C19 | F3 | 108.3(6) |
| C5 | C6 | C1 | 119.6(5) | F1 | C19 | C18 | 114.6(5) |
| C2 | C7 | C8 | 112.2(4) | F2 | C19 | F3 | 103.4(5) |
| C9 | C8 | C7 | 113.3(5) | F2 | C19 | C18 | 111.2(5) |
| C8 | C9 | C10 | 113.4(6) | F3 | C19 | C18 | 113.5(5) |

**Table 6 Hydrogen Atom Coordinates (Å×10$^4$) and Isotropic Displacement Parameters (Å$^2$×10$^3$) for mac190011.**

| Atom | *x* | *y* | *z* | U(eq) |
|---|---|---|---|---|
| H3 | 2409 | 4522 | 4737 | 47 |
| H5 | 1707 | 6085 | 7014 | 54 |
| H6 | 3147 | 6758 | 5876 | 50 |
| H7A | 4420 | 4626 | 3336 | 50 |
| H7B | 4701 | 5345 | 2786 | 50 |
| H8A | 2068 | 4665 | 2311 | 56 |
| H8B | 2410 | 5365 | 1716 | 56 |
| H9A | 3683 | 4133 | 1114 | 72 |
| H9B | 4141 | 4829 | 575 | 72 |
| H10A | 2607 | 4261 | -949 | 133 |
| H10B | 1926 | 4946 | -576 | 133 |
| H10C | 1421 | 4266 | -4 | 133 |
| H11A | 431 | 4132 | 5535 | 85 |
| H11B | 195 | 3998 | 6971 | 85 |
| H11C | 1724 | 3959 | 6523 | 85 |
| H13 | 5061 | 6474 | 836 | 55 |
| H14 | 3631 | 6482 | -1075 | 64 |
| H15 | 1262 | 6734 | -1089 | 63 |
| H16 | 289 | 6986 | 783 | 61 |
| H17 | 1719 | 6989 | 2712 | 51 |

**XRD of copper complex 167**

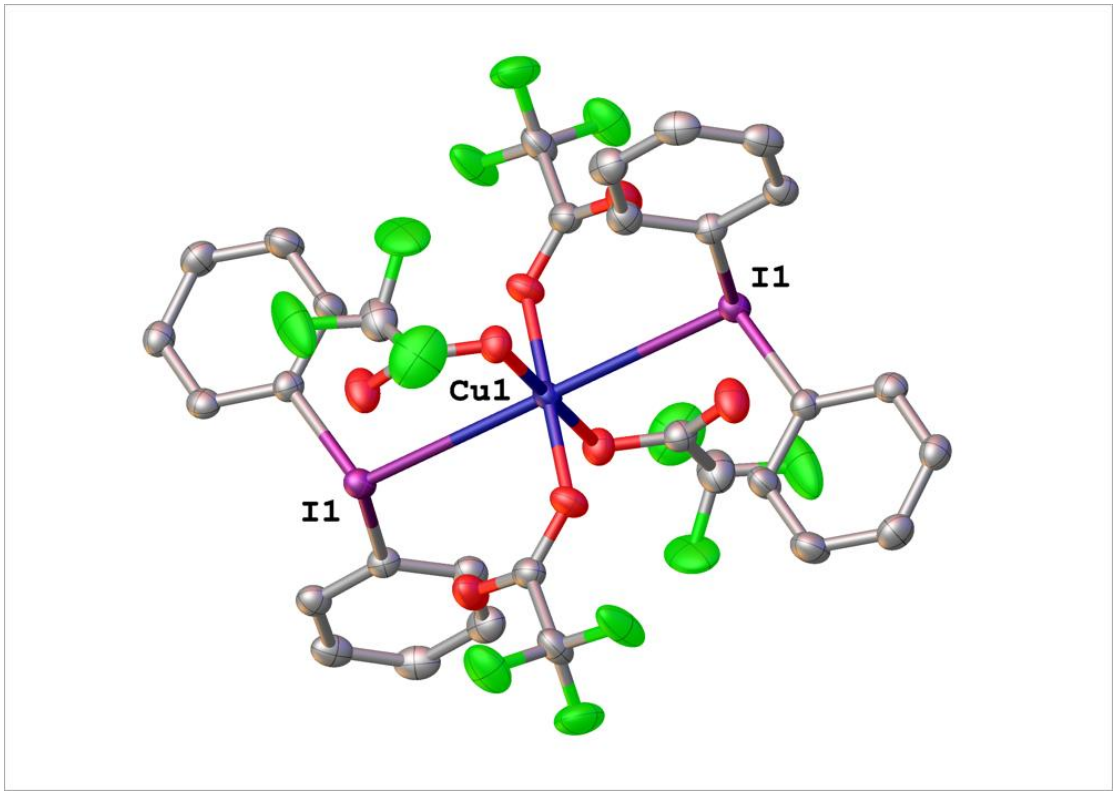

## Table 1 : Crystal data and structure refinement for mac190017.

| | |
|---|---|
| Identification code | mac190017 |
| Empirical formula | $C_{32}H_{20}CuF_{12}I_2O_8$ |
| Formula weight | 1077.82 |
| Temperature/K | 150.0(2) |
| Crystal system | triclinic |
| Space group | P-1 |
| a/Å | 9.3632(3) |
| b/Å | 9.8158(3) |
| c/Å | 10.4334(3) |
| α/° | 84.659(3) |
| β/° | 77.340(3) |
| γ/° | 78.671(3) |
| Volume/Å$^3$ | 916.10(5) |
| Z | 1 |
| $\rho_{calc}$g/cm$^3$ | 1.954 |
| μ/mm$^{-1}$ | 15.082 |
| F(000) | 519.0 |
| Crystal size/mm$^3$ | 0.31 × 0.12 × 0.07 |
| Radiation | CuKα (λ = 1.54184) |
| 2Θ range for data collection/° | 8.698 to 133.954 |
| Index ranges | $-11 \leq h \leq 11$, $-11 \leq k \leq 11$, $-12 \leq l \leq 11$ |
| Reflections collected | 25038 |
| Independent reflections | 3225 [$R_{int}$ = 0.0690, $R_{sigma}$ = 0.0319] |
| Data/restraints/parameters | 3225/51/277 |
| Goodness-of-fit on F$^2$ | 1.046 |
| Final R indexes [I>=2σ (I)] | $R_1$ = 0.0257, $wR_2$ = 0.0644 |
| Final R indexes [all data] | $R_1$ = 0.0289, $wR_2$ = 0.0664 |
| Largest diff. peak/hole / e Å$^{-3}$ | 0.92/-0.89 |

**Table 2 Fractional Atomic Coordinates ($\times 10^4$) and Equivalent Isotropic Displacement Parameters ($Å^2 \times 10^3$) for mac190017. $U_{eq}$ is defined as 1/3 of of the trace of the orthogonalised $U_{IJ}$ tensor.**

| Atom | *x* | *y* | *z* | U(eq) |
|---|---|---|---|---|
| I1 | 4191.9(2) | 4305.6(2) | 3432.6(2) | 24.37(9) |
| Cu1 | 5000 | 5000 | 0 | 23.17(15) |
| F4 | 9678(2) | 5917(3) | 1260(3) | 52.8(6) |
| F5 | 8887(3) | 7226(3) | -301(2) | 57.1(7) |
| F6 | 8066(3) | 7773(2) | 1692(2) | 53.5(6) |
| O1 | 3794(3) | 6835(2) | -142(2) | 31.3(5) |
| O2 | 3004(3) | 6821(3) | 2049(3) | 41.8(6) |
| O3 | 6668(3) | 5878(2) | 77(2) | 31.2(5) |
| O4 | 6831(3) | 5356(3) | 2202(3) | 38.1(6) |
| C1 | 2124(3) | 3645(3) | 4052(3) | 24.3(7) |
| C2 | 1457(3) | 3644(3) | 5373(4) | 26.8(7) |
| C3 | 114(4) | 3177(3) | 5749(4) | 29.0(7) |
| C4 | -537(4) | 2765(4) | 4812(4) | 33.1(8) |
| C5 | 155(4) | 2791(4) | 3491(4) | 36.5(8) |
| C6 | 1516(4) | 3239(4) | 3100(4) | 31.0(8) |
| C7 | 5475(3) | 2486(3) | 4134(3) | 24.3(7) |
| C8 | 5244(4) | 2149(3) | 5473(4) | 28.5(7) |
| C9 | 6090(4) | 929(4) | 5894(4) | 33.1(8) |
| C10 | 7142(4) | 123(3) | 5002(4) | 35.7(9) |
| C11 | 7365(4) | 503(4) | 3665(4) | 36.6(9) |
| C12 | 6523(4) | 1703(4) | 3210(4) | 31.0(8) |
| C13 | 3084(4) | 7342(3) | 930(4) | 28.8(7) |
| C14 | 2249(4) | 8843(4) | 766(4) | 42.3(9) |
| C15 | 7196(4) | 5880(3) | 1089(4) | 28.6(7) |
| C16 | 8469(4) | 6705(4) | 913(4) | 35.0(8) |
| F1A | 1430(30) | 9400(30) | 1832(17) | 77(6) |
| F2A | 1390(20) | 8880(30) | -100(19) | 63(5) |
| F3A | 3178(18) | 9681(17) | 175(13) | 73(4) |
| F1B | 1170(20) | 9150(20) | 1786(16) | 68(5) |
| F2B | 1660(20) | 9120(30) | -282(17) | 72(6) |
| F3B | 3174(19) | 9724(15) | 735(12) | 68(3) |

**Table 3 Anisotropic Displacement Parameters ($Å^2×10^3$) for mac190017. The Anisotropic displacement factor exponent takes the form: $-2\pi^2[h^2a^{*2}U_{11}+2hka^*b^*U_{12}+\ldots]$.**

| Atom | $U_{11}$ | $U_{22}$ | $U_{33}$ | $U_{23}$ | $U_{13}$ | $U_{12}$ |
|---|---|---|---|---|---|---|
| I1 | 27.04(12) | 24.64(12) | 22.91(14) | 2.41(8) | -6.43(9) | -8.50(8) |
| Cu1 | 25.9(3) | 25.7(3) | 19.1(4) | -1.6(3) | -6.0(3) | -5.9(3) |
| F4 | 33.2(11) | 71.4(16) | 60.6(17) | 1.2(13) | -19.5(11) | -16.9(11) |
| F5 | 75.6(16) | 87.7(18) | 25.8(13) | 10.0(12) | -14.8(12) | -58.4(15) |
| F6 | 79.1(17) | 44.9(13) | 45.7(15) | -8.9(11) | -16.3(13) | -26.7(12) |
| O1 | 33.1(12) | 29.3(12) | 28.8(14) | -2.5(10) | -3.9(11) | -1.6(10) |
| O2 | 49.2(15) | 42.4(14) | 26.4(15) | 3.5(12) | -5.8(12) | 4.7(12) |
| O3 | 36.5(12) | 33.3(12) | 29.3(14) | -1.5(10) | -13.6(11) | -11.7(10) |
| O4 | 39.2(13) | 53.9(15) | 25.5(15) | 0.5(12) | -5.4(11) | -21.1(12) |
| C1 | 24.2(15) | 25.1(15) | 23.1(18) | 2.6(13) | -4.2(13) | -6.0(12) |
| C2 | 26.5(16) | 26.0(16) | 28.2(19) | 0.0(13) | -9.3(14) | -2.1(13) |
| C3 | 28.4(16) | 29.5(16) | 26.5(19) | 2.4(14) | -2.2(14) | -4.2(13) |
| C4 | 27.9(16) | 32.7(18) | 39(2) | 0.8(15) | -3.8(15) | -10.1(14) |
| C5 | 38.5(19) | 44(2) | 34(2) | -4.0(16) | -14.7(17) | -13.2(16) |
| C6 | 34.9(18) | 39.1(19) | 22.3(19) | -1.9(15) | -7.5(15) | -12.9(15) |
| C7 | 25.0(15) | 20.7(14) | 27.8(19) | 0.6(13) | -6.4(13) | -5.4(12) |
| C8 | 28.8(16) | 29.8(16) | 30(2) | -0.1(14) | -8.1(14) | -10.7(13) |
| C9 | 37.9(18) | 32.5(18) | 35(2) | 8.5(15) | -14.3(16) | -16.8(15) |
| C10 | 38.1(19) | 21.4(16) | 53(3) | 2.0(16) | -20.0(18) | -6.9(14) |
| C11 | 34.4(18) | 30.0(18) | 46(3) | -9.4(16) | -9.1(17) | -2.9(15) |
| C12 | 32.8(17) | 31.2(17) | 31(2) | -1.1(14) | -6.9(15) | -10.7(14) |
| C13 | 26.7(16) | 29.6(17) | 30(2) | 0.5(15) | -7.3(15) | -5.0(13) |
| C14 | 48(2) | 37(2) | 38(2) | -1.8(18) | -8.3(19) | 2.9(17) |
| C15 | 26.3(16) | 30.1(17) | 31(2) | -4.9(14) | -7.6(14) | -4.5(13) |
| C16 | 46(2) | 40.8(19) | 23(2) | -1.6(15) | -9.2(16) | -17.1(16) |
| F1A | 124(13) | 48(8) | 44(7) | -19(5) | -23(7) | 33(7) |
| F2A | 54(5) | 62(8) | 72(10) | -3(6) | -40(7) | 22(5) |
| F3A | 76(6) | 39(4) | 95(10) | 15(7) | -5(7) | -9(3) |
| F1B | 74(5) | 46(7) | 47(7) | -1(4) | 29(6) | 29(5) |
| F2B | 98(12) | 61(8) | 37(4) | -2(5) | -20(5) | 36(8) |
| F3B | 91(6) | 29(3) | 93(9) | 10(6) | -37(7) | -18(3) |

**Table 4 Bond Lengths for mac190017.**

| Atom | Atom | Length/Å | Atom | Atom | Length/Å |
|---|---|---|---|---|---|
| I1 | Cu1 | 3.5247(2) | C3 | C4 | 1.387(5) |
| I1 | C1 | 2.110(3) | C4 | C5 | 1.388(6) |
| I1 | C7 | 2.114(3) | C5 | C6 | 1.393(5) |
| Cu1 | O1 | 1.940(2) | C7 | C8 | 1.385(5) |
| Cu1 | $O1^{1}$ | 1.940(2) | C7 | C12 | 1.383(5) |
| Cu1 | O3 | 1.945(2) | C8 | C9 | 1.391(5) |
| Cu1 | $O3^{1}$ | 1.945(2) | C9 | C10 | 1.375(6) |
| F4 | C16 | 1.339(4) | C10 | C11 | 1.392(6) |
| F5 | C16 | 1.327(4) | C11 | C12 | 1.389(5) |
| F6 | C16 | 1.332(4) | C13 | C14 | 1.539(5) |
| O1 | C13 | 1.260(4) | C14 | F1A | 1.305(12) |
| O2 | C13 | 1.223(4) | C14 | F2A | 1.326(11) |
| O3 | C15 | 1.261(4) | C14 | F3A | 1.328(11) |
| O4 | C15 | 1.230(4) | C14 | F1B | 1.310(10) |
| C1 | C2 | 1.383(5) | C14 | F2B | 1.313(11) |
| C1 | C6 | 1.372(5) | C14 | F3B | 1.333(10) |
| C2 | C3 | 1.386(5) | C15 | C16 | 1.537(5) |

**Table 5 Bond Angles for mac190017.**

| Atom | Atom | Atom | Angle/° | Atom | Atom | Atom | Angle/° |
|---|---|---|---|---|---|---|---|
| C1 | I1 | Cu1 | 111.22(9) | C9 | C10 | C11 | 120.6(3) |
| C1 | I1 | C7 | 95.94(12) | C12 | C11 | C10 | 120.4(3) |
| C7 | I1 | Cu1 | 115.56(9) | C7 | C12 | C11 | 117.4(3) |
| O1 | Cu1 | I1 | 100.71(7) | O1 | C13 | C14 | 113.5(3) |
| O1[1] | Cu1 | I1 | 79.29(7) | O2 | C13 | O1 | 129.1(3) |
| O1 | Cu1 | O1[1] | 180.0 | O2 | C13 | C14 | 117.4(3) |
| O1 | Cu1 | O3[1] | 91.04(10) | F1A | C14 | C13 | 116.5(12) |
| O1[1] | Cu1 | O3 | 91.04(10) | F1A | C14 | F2A | 108.6(16) |
| O1 | Cu1 | O3 | 88.96(10) | F1A | C14 | F3A | 108.8(14) |
| O1[1] | Cu1 | O3[1] | 88.96(10) | F2A | C14 | C13 | 108.7(12) |
| O3 | Cu1 | I1 | 92.71(7) | F2A | C14 | F3A | 102.1(13) |
| O3[1] | Cu1 | I1 | 87.29(7) | F3A | C14 | C13 | 111.1(9) |
| O3 | Cu1 | O3[1] | 180.0 | F1B | C14 | C13 | 110.5(10) |
| C13 | O1 | Cu1 | 115.8(2) | F1B | C14 | F2B | 106.8(15) |
| C15 | O3 | Cu1 | 124.8(2) | F1B | C14 | F3B | 106.1(14) |
| C2 | C1 | I1 | 119.3(2) | F2B | C14 | C13 | 115.5(11) |
| C6 | C1 | I1 | 117.2(2) | F2B | C14 | F3B | 108.3(13) |
| C6 | C1 | C2 | 123.6(3) | F3B | C14 | C13 | 109.2(8) |
| C1 | C2 | C3 | 117.8(3) | O3 | C15 | C16 | 114.8(3) |
| C2 | C3 | C4 | 120.2(3) | O4 | C15 | O3 | 130.3(3) |
| C3 | C4 | C5 | 120.7(3) | O4 | C15 | C16 | 114.9(3) |
| C4 | C5 | C6 | 119.8(3) | F4 | C16 | C15 | 111.2(3) |
| C1 | C6 | C5 | 118.0(3) | F5 | C16 | F4 | 107.4(3) |
| C8 | C7 | I1 | 119.3(2) | F5 | C16 | F6 | 106.7(3) |
| C12 | C7 | I1 | 117.1(2) | F5 | C16 | C15 | 114.5(3) |
| C12 | C7 | C8 | 123.6(3) | F6 | C16 | F4 | 106.4(3) |
| C7 | C8 | C9 | 117.5(3) | F6 | C16 | C15 | 110.2(3) |
| C10 | C9 | C8 | 120.5(3) | | | | |

**Table 6 Hydrogen Atom Coordinates (Å×10$^4$) and Isotropic Displacement Parameters (Å$^2$×10$^3$) for mac190017.**

| Atom | *x* | *y* | *z* | U(eq) |
|---|---|---|---|---|
| H2 | 1894 | 3946 | 5987 | 32 |
| H3 | -351 | 3140 | 6633 | 35 |
| H4 | -1446 | 2468 | 5070 | 40 |
| H5 | -288 | 2511 | 2870 | 44 |
| H6 | 1997 | 3261 | 2220 | 37 |
| H8 | 4550 | 2717 | 6069 | 34 |
| H9 | 5943 | 658 | 6784 | 40 |
| H10 | 7709 | -685 | 5296 | 43 |
| H11 | 8081 | -50 | 3072 | 44 |
| H12 | 6659 | 1968 | 2319 | 37 |

**Table 7 Atomic Occupancy for mac190017.**

| Atom | *Occupancy* | Atom | *Occupancy* | Atom | *Occupancy* |
|---|---|---|---|---|---|
| F1A | 0.488 | F2A | 0.488 | F3A | 0.488 |
| F1B | 0.512 | F2B | 0.512 | F3B | 0.512 |

**XRD of copper complex 168**

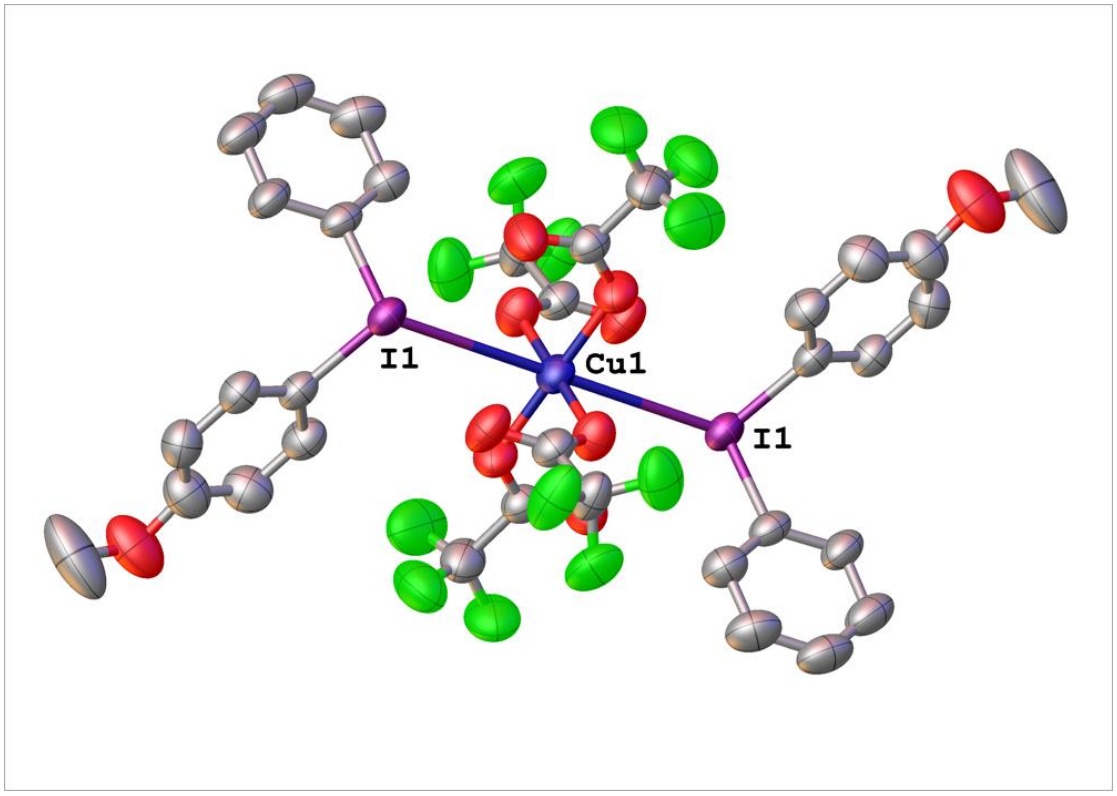

## Table 1 : Crystal data and structure refinement for mac190039.

| | |
|---|---|
| Identification code | mac190039 |
| Empirical formula | $C_{34}H_{24}CuF_{12}I_2O_{10}$ |
| Formula weight | 1137.87 |
| Temperature/K | 240.0(2) |
| Crystal system | triclinic |
| Space group | P-1 |
| a/Å | 9.4346(5) |
| b/Å | 10.6438(5) |
| c/Å | 10.7917(7) |
| α/° | 80.812(5) |
| β/° | 77.709(5) |
| γ/° | 78.410(4) |
| Volume/Å$^3$ | 1029.50(11) |
| Z | 1 |
| $\rho_{calc}$g/cm$^3$ | 1.835 |
| μ/mm$^{-1}$ | 13.498 |
| F(000) | 551.0 |
| Crystal size/mm$^3$ | 0.27 × 0.14 × 0.07 |
| Radiation | CuKα (λ = 1.54184) |
| 2Θ range for data collection/° | 8.448 to 133.544 |
| Index ranges | $-11 \leq h \leq 11$, $-12 \leq k \leq 10$, $-12 \leq l \leq 12$ |
| Reflections collected | 14450 |
| Independent reflections | 3634 [$R_{int}$ = 0.0670, $R_{sigma}$ = 0.0525] |
| Data/restraints/parameters | 3634/388/306 |
| Goodness-of-fit on $F^2$ | 1.114 |
| Final R indexes [I>=2σ (I)] | $R_1$ = 0.0433, $wR_2$ = 0.1003 |
| Final R indexes [all data] | $R_1$ = 0.0574, $wR_2$ = 0.1123 |
| Largest diff. peak/hole / e Å$^{-3}$ | 0.89/-0.85 |

**Table 2 Fractional Atomic Coordinates ($\times 10^4$) and Equivalent Isotropic Displacement Parameters ($Å^2 \times 10^3$) for mac190039. $U_{eq}$ is defined as 1/3 of of the trace of the orthogonalised $U_{IJ}$ tensor.**

| Atom | *x* | *y* | *z* | U(eq) |
|---|---|---|---|---|
| I1 | 3742.4(4) | 8275.8(3) | 4398.5(4) | 55.15(18) |
| Cu1 | 5000 | 5000 | 5000 | 53.6(3) |
| F1 | 755(5) | 6023(5) | 8796(5) | 103.4(15) |
| F2 | 2696(7) | 4798(7) | 9232(5) | 126(2) |
| F3 | 1279(6) | 4099(5) | 8341(5) | 107.5(15) |
| O1 | 7560(9) | 10750(7) | -394(6) | 115(2) |
| O2 | 3624(5) | 4691(4) | 6581(4) | 72.7(12) |
| O3 | 2550(6) | 6729(5) | 6699(5) | 87.2(15) |
| O4 | 6479(5) | 4993(4) | 5990(5) | 71.8(11) |
| O5 | 6290(5) | 7140(4) | 5671(5) | 75.2(12) |
| C1 | 4955(6) | 9164(5) | 2760(6) | 54.4(12) |
| C2 | 4995(7) | 10444(6) | 2678(6) | 59.8(13) |
| C3 | 5851(8) | 11025(7) | 1604(7) | 71.0(16) |
| C4 | 6664(9) | 10290(8) | 673(7) | 79.2(18) |
| C5 | 6586(9) | 8985(7) | 781(7) | 78.0(18) |
| C6 | 5748(7) | 8407(6) | 1825(7) | 64.2(14) |
| C7 | 7770(20) | 12054(13) | -488(11) | 166(6) |
| C8 | 1647(6) | 8734(6) | 3862(5) | 55.1(13) |
| C9 | 1137(7) | 9999(6) | 3422(6) | 67.0(15) |
| C10 | -260(8) | 10260(8) | 3094(7) | 80.1(18) |
| C11 | -1063(8) | 9291(9) | 3243(8) | 83.4(19) |
| C12 | -515(8) | 8053(8) | 3693(8) | 82.0(19) |
| C13 | 869(7) | 7756(7) | 4011(7) | 66.3(15) |
| C14 | 2751(7) | 5590(6) | 7079(6) | 57.3(13) |
| C15 | 1840(8) | 5141(7) | 8382(7) | 76.0(17) |
| C16 | 6765(7) | 6057(6) | 6145(6) | 58.0(13) |
| F4A | 7756(13) | 5058(10) | 7976(9) | 106(3) |
| F5A | 8044(13) | 7003(6) | 7311(12) | 105(3) |
| F6A | 9257(7) | 5460(9) | 6312(8) | 100(2) |
| C17 | 7925(12) | 5898(10) | 6970(11) | 72(2) |
| F4B | 8360(30) | 4838(17) | 7430(20) | 112(6) |
| F5B | 7240(30) | 6630(20) | 8020(20) | 134(6) |
| F6B | 9000(20) | 6530(30) | 6510(20) | 140(6) |
| C17B | 7810(20) | 6000(20) | 7040(20) | 102(5) |

**Table 3 Anisotropic Displacement Parameters ($Å^2×10^3$) for mac190039. The Anisotropic displacement factor exponent takes the form: $-2\pi^2[h^2a^{*2}U_{11}+2hka^*b^*U_{12}+\ldots]$.**

| Atom | $U_{11}$ | $U_{22}$ | $U_{33}$ | $U_{23}$ | $U_{13}$ | $U_{12}$ |
|---|---|---|---|---|---|---|
| I1 | 49.3(2) | 52.6(2) | 61.1(3) | -5.44(15) | -17.06(15) | 3.03(14) |
| Cu1 | 55.5(6) | 45.1(6) | 55.9(7) | -10.8(5) | -7.5(5) | 2.0(5) |
| F1 | 92(3) | 100(3) | 94(3) | -24(2) | 23(2) | 6(2) |
| F2 | 115(4) | 186(6) | 63(3) | -2(3) | -16(2) | 0(3) |
| F3 | 109(4) | 94(3) | 104(3) | -10(2) | 21(3) | -25(3) |
| O1 | 148(6) | 130(5) | 69(3) | -11(3) | 6(3) | -63(4) |
| O2 | 71(3) | 67(2) | 65(2) | -11.3(19) | 5(2) | 8(2) |
| O3 | 92(4) | 62(3) | 86(3) | -4(2) | 15(3) | -1(2) |
| O4 | 81(3) | 59(2) | 81(3) | -9(2) | -28(2) | -10(2) |
| O5 | 74(3) | 57(2) | 96(3) | -14(2) | -34(3) | 9.4(19) |
| C1 | 49(3) | 51(3) | 61(3) | -9(2) | -18(2) | 5(2) |
| C2 | 61(3) | 53(3) | 66(3) | -10(2) | -20(3) | 1(2) |
| C3 | 82(4) | 61(3) | 71(4) | -3(3) | -23(3) | -10(3) |
| C4 | 92(5) | 87(4) | 62(3) | -8(3) | -12(3) | -25(3) |
| C5 | 82(4) | 84(4) | 68(4) | -21(3) | -6(3) | -14(3) |
| C6 | 62(3) | 55(3) | 75(4) | -17(3) | -15(3) | 0(2) |
| C7 | 272(18) | 149(8) | 85(7) | -3(6) | 19(9) | -119(10) |
| C8 | 44(3) | 61(3) | 55(3) | -12(2) | -10(2) | 8(2) |
| C9 | 56(3) | 64(3) | 71(4) | -7(3) | -14(3) | 13(2) |
| C10 | 61(4) | 92(4) | 75(4) | -11(3) | -18(3) | 20(3) |
| C11 | 52(3) | 113(5) | 83(5) | -26(4) | -20(3) | 10(3) |
| C12 | 58(3) | 99(4) | 92(5) | -28(4) | -20(3) | -4(3) |
| C13 | 59(3) | 68(3) | 72(4) | -14(3) | -16(3) | -3(3) |
| C14 | 54(3) | 59(3) | 56(3) | -11(2) | -10(2) | -2(2) |
| C15 | 75(4) | 79(4) | 60(3) | -7(3) | 0(3) | 3(3) |
| C16 | 54(3) | 54(3) | 64(3) | -14(2) | -11(2) | 2(2) |
| F4A | 137(8) | 108(6) | 80(5) | 19(4) | -47(4) | -35(5) |
| F5A | 128(7) | 62(3) | 152(7) | -26(4) | -85(6) | -6(4) |
| F6A | 67(3) | 111(5) | 123(5) | -21(4) | -41(3) | 8(3) |
| C17 | 77(5) | 52(4) | 92(5) | -4(4) | -36(4) | -6(4) |
| F4B | 120(12) | 102(8) | 133(13) | -34(8) | -83(11) | 14(7) |
| F5B | 142(12) | 152(13) | 124(10) | -53(9) | -70(8) | 13(9) |
| F6B | 127(10) | 161(13) | 153(12) | -20(10) | -65(9) | -33(9) |
| C17B | 105(9) | 93(9) | 121(9) | -26(7) | -64(8) | 6(7) |

**Table 4 Bond Lengths for mac190039.**

| Atom | Atom | Length/Å | Atom | Atom | Length/Å |
|---|---|---|---|---|---|
| I1 | Cu1 | 3.4538(4) | C3 | C4 | 1.376(11) |
| I1 | C1 | 2.090(6) | C4 | C5 | 1.391(11) |
| I1 | C8 | 2.120(5) | C5 | C6 | 1.366(10) |
| Cu1 | O2 | 1.938(4) | C8 | C9 | 1.379(8) |
| Cu1 | $O2^{1}$ | 1.938(4) | C8 | C13 | 1.361(9) |
| Cu1 | $O4^{1}$ | 1.928(5) | C9 | C10 | 1.401(10) |
| Cu1 | O4 | 1.928(5) | C10 | C11 | 1.368(12) |
| F1 | C15 | 1.297(8) | C11 | C12 | 1.367(12) |
| F2 | C15 | 1.310(9) | C12 | C13 | 1.383(10) |
| F3 | C15 | 1.332(10) | C14 | C15 | 1.543(10) |
| O1 | C4 | 1.361(10) | C16 | C17 | 1.519(11) |
| O1 | C7 | 1.426(14) | C16 | C17B | 1.509(17) |
| O2 | C14 | 1.242(7) | F4A | C17 | 1.295(12) |
| O3 | C14 | 1.206(8) | F5A | C17 | 1.319(12) |
| O4 | C16 | 1.259(8) | F6A | C17 | 1.339(14) |
| O5 | C16 | 1.223(7) | F4B | C17B | 1.279(18) |
| C1 | C2 | 1.359(9) | F5B | C17B | 1.306(19) |
| C1 | C6 | 1.386(9) | F6B | C17B | 1.34(2) |
| C2 | C3 | 1.397(10) | | | |

**Table 5 Bond Angles for mac190039.**

| Atom | Atom | Atom | Angle/° | Atom | Atom | Atom | Angle/° |
|---|---|---|---|---|---|---|---|
| C1 | I1 | Cu1 | 113.41(15) | C11 | C10 | C9 | 120.2(7) |
| C1 | I1 | C8 | 98.6(2) | C12 | C11 | C10 | 121.0(7) |
| C8 | I1 | Cu1 | 113.92(17) | C11 | C12 | C13 | 120.4(8) |
| O2 | Cu1 | I1 | 96.97(13) | C8 | C13 | C12 | 117.7(6) |
| $O2^1$ | Cu1 | I1 | 83.03(13) | O2 | C14 | C15 | 113.0(6) |
| $O2^1$ | Cu1 | O2 | 180.0 | O3 | C14 | O2 | 129.4(6) |
| $O4^1$ | Cu1 | I1 | 79.07(13) | O3 | C14 | C15 | 117.6(6) |
| O4 | Cu1 | I1 | 100.93(13) | F1 | C15 | F2 | 108.7(7) |
| $O4^1$ | Cu1 | O2 | 91.2(2) | F1 | C15 | F3 | 107.5(7) |
| $O4^1$ | Cu1 | $O2^1$ | 88.8(2) | F1 | C15 | C14 | 113.1(6) |
| O4 | Cu1 | O2 | 88.8(2) | F2 | C15 | F3 | 105.8(7) |
| O4 | Cu1 | $O2^1$ | 91.2(2) | F2 | C15 | C14 | 109.5(6) |
| O4 | Cu1 | $O4^1$ | 180.0 | F3 | C15 | C14 | 112.0(6) |
| C4 | O1 | C7 | 117.3(8) | O4 | C16 | C17 | 112.7(6) |
| C14 | O2 | Cu1 | 121.6(4) | O4 | C16 | C17B | 116.3(10) |
| C16 | O4 | Cu1 | 118.8(4) | O5 | C16 | O4 | 128.2(6) |
| C2 | C1 | I1 | 118.9(5) | O5 | C16 | C17 | 119.0(6) |
| C2 | C1 | C6 | 122.5(6) | O5 | C16 | C17B | 115.5(10) |
| C6 | C1 | I1 | 118.5(4) | F4A | C17 | C16 | 114.6(9) |
| C1 | C2 | C3 | 118.8(6) | F4A | C17 | F5A | 109.2(11) |
| C4 | C3 | C2 | 119.7(6) | F4A | C17 | F6A | 104.4(9) |
| O1 | C4 | C3 | 124.5(7) | F5A | C17 | C16 | 112.6(8) |
| O1 | C4 | C5 | 115.5(7) | F5A | C17 | F6A | 105.1(10) |
| C3 | C4 | C5 | 119.9(7) | F6A | C17 | C16 | 110.2(8) |
| C6 | C5 | C4 | 120.8(7) | F4B | C17B | C16 | 112.6(16) |
| C5 | C6 | C1 | 118.2(6) | F4B | C17B | F5B | 109(2) |
| C9 | C8 | I1 | 118.6(5) | F4B | C17B | F6B | 103(2) |
| C13 | C8 | I1 | 117.3(4) | F5B | C17B | C16 | 113.9(16) |
| C13 | C8 | C9 | 124.1(6) | F5B | C17B | F6B | 103(2) |
| C8 | C9 | C10 | 116.6(7) | F6B | C17B | C16 | 113.8(16) |

**Table 6 Hydrogen Atom Coordinates (Å×10$^4$) and Isotropic Displacement Parameters (Å$^2$×10$^3$) for mac190039.**

| Atom | *x* | *y* | *z* | U(eq) |
|---|---|---|---|---|
| H2 | 4462 | 10925 | 3326 | 72 |
| H3 | 5871 | 11905 | 1519 | 85 |
| H5 | 7110 | 8499 | 134 | 94 |
| H6 | 5711 | 7531 | 1906 | 77 |
| H7A | 8398 | 12271 | -1287 | 249 |
| H7B | 8220 | 12148 | 203 | 249 |
| H7C | 6835 | 12620 | -444 | 249 |
| H9 | 1693 | 10645 | 3348 | 80 |
| H10 | -644 | 11094 | 2774 | 96 |
| H11 | -1996 | 9477 | 3034 | 100 |
| H12 | -1076 | 7407 | 3786 | 98 |
| H13 | 1255 | 6917 | 4316 | 80 |

**Table 7 Atomic Occupancy for mac190039.**

| **Atom** | ***Occupancy*** | **Atom** | ***Occupancy*** | **Atom** | ***Occupancy*** |
|---|---|---|---|---|---|
| F4A | 0.6718 | F5A | 0.6718 | F6A | 0.6718 |
| C17 | 0.6718 | F4B | 0.3282 | F5B | 0.3282 |
| F6B | 0.3282 | C17B | 0.3282 | | |

**XRD of copper complex 169**

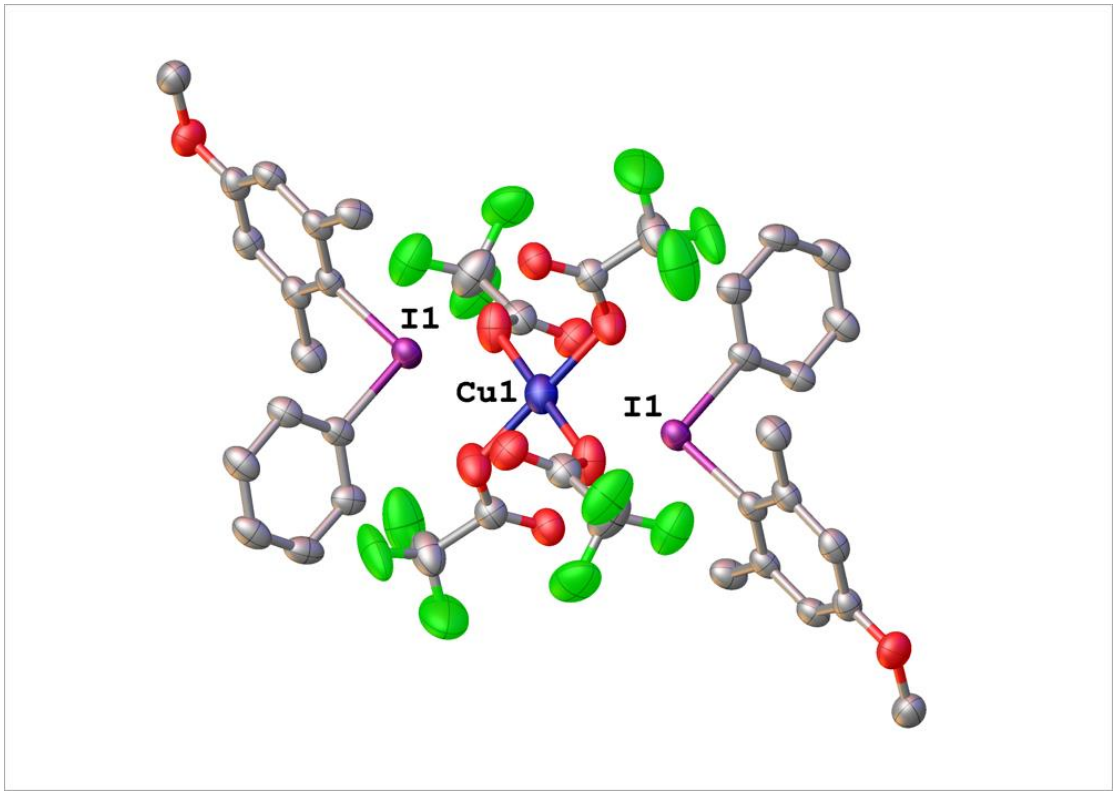

## Table 1 : Crystal data and structure refinement for mac190012_fa.

| | |
|---|---|
| Identification code | mac190012_fa |
| Empirical formula | $C_{38}H_{32}CuF_{12}I_2O_{10}$ |
| Formula weight | 1193.97 |
| Temperature/K | 150.0(2) |
| Crystal system | triclinic |
| Space group | P-1 |
| a/Å | 10.0566(3) |
| b/Å | 10.7236(4) |
| c/Å | 11.3620(4) |
| α/° | 107.865(4) |
| β/° | 100.613(3) |
| γ/° | 98.237(3) |
| Volume/Å$^3$ | 1119.84(7) |
| Z | 1 |
| $\rho_{calc}$g/cm$^3$ | 1.770 |
| μ/mm$^{-1}$ | 12.441 |
| F(000) | 583.0 |
| Crystal size/mm$^3$ | 0.26 × 0.09 × 0.05 |
| Radiation | CuKα (λ = 1.54184) |
| 2Θ range for data collection/° | 8.428 to 133.82 |
| Index ranges | $-11 \leq h \leq 11$, $-12 \leq k \leq 12$, $-13 \leq l \leq 13$ |
| Reflections collected | 30567 |
| Independent reflections | 3958 [$R_{int}$ = 0.0575, $R_{sigma}$ = 0.0286] |
| Data/restraints/parameters | 3958/411/344 |
| Goodness-of-fit on $F^2$ | 1.051 |
| Final R indexes [I>=2σ (I)] | $R_1$ = 0.0346, $wR_2$ = 0.0877 |
| Final R indexes [all data] | $R_1$ = 0.0407, $wR_2$ = 0.0919 |
| Largest diff. peak/hole / e Å$^{-3}$ | 1.03/-1.17 |

**Table 2 Fractional Atomic Coordinates ($\times 10^4$) and Equivalent Isotropic Displacement Parameters ($Å^2 \times 10^3$) for mac190012_fa. $U_{eq}$ is defined as 1/3 of of the trace of the orthogonalised $U_{IJ}$ tensor.**

| Atom | *x* | *y* | *z* | U(eq) |
|---|---|---|---|---|
| I1 | 5567.7(3) | 3343.2(3) | 6196.0(3) | 37.56(13) |
| Cu1 | 5000 | 0 | 5000 | 49.4(3) |
| F1A | 2757(15) | -755(7) | 838(16) | 89(4) |
| F2A | 1505(6) | 582(8) | 1667(8) | 91(2) |
| F3A | 3286(9) | 1348(7) | 1145(6) | 91(2) |
| O0AA | 9242(4) | 6367(4) | 11636(3) | 50.6(8) |
| O1 | 3842(5) | -269(4) | 3301(4) | 61.7(10) |
| O2 | 3917(4) | 1919(3) | 3687(3) | 53.7(9) |
| O3 | 6572(4) | -255(4) | 4257(4) | 62.6(10) |
| O4 | 7672(4) | 1913(3) | 5071(3) | 48.3(8) |
| C1 | 6777(4) | 4426(4) | 8047(4) | 33.9(9) |
| C2 | 7898(4) | 5425(5) | 8174(4) | 35.6(9) |
| C3 | 8740(4) | 6093(5) | 9396(4) | 38.4(10) |
| C4 | 8462(5) | 5777(5) | 10424(4) | 39.6(10) |
| C5 | 7311(5) | 4777(5) | 10258(4) | 40.5(10) |
| C6 | 6442(5) | 4082(4) | 9067(4) | 37.0(9) |
| C7 | 8244(5) | 5795(5) | 7076(5) | 44.6(11) |
| C8 | 10423(5) | 7390(5) | 11850(5) | 52.2(12) |
| C9 | 5207(5) | 3020(5) | 8914(5) | 46.3(11) |
| C10 | 3883(4) | 4298(5) | 6342(4) | 34.8(9) |
| C11 | 2552(5) | 3529(5) | 5952(4) | 39.8(10) |
| C12 | 1468(5) | 4203(6) | 6001(5) | 44.9(11) |
| C13 | 1727(5) | 5575(6) | 6421(5) | 46.7(11) |
| C14 | 3072(5) | 6314(5) | 6835(5) | 45.8(11) |
| C15 | 4178(5) | 5679(5) | 6794(5) | 39.5(10) |
| C16 | 3623(5) | 742(5) | 3019(5) | 45.3(11) |
| C17 | 2894(7) | 447(6) | 1629(6) | 75.2(16) |
| C18 | 7504(5) | 745(5) | 4406(4) | 40.0(10) |
| C19 | 8477(6) | 382(5) | 3539(6) | 63.5(14) |
| F4A | 8546(10) | -844(6) | 3153(10) | 89(3) |
| F5A | 9692(10) | 1156(11) | 3995(13) | 116(4) |
| F6A | 7970(12) | 579(11) | 2442(8) | 118(3) |
| F4B | 9210(14) | -449(13) | 3924(15) | 103(4) |
| F5B | 9355(14) | 1364(10) | 3530(15) | 89(4) |
| F6B | 7914(13) | -311(16) | 2353(9) | 109(4) |
| F1B | 2510(20) | -866(11) | 980(30) | 64(4) |

| | | | | |
|---|---|---|---|---|
| F3B | 3967(15) | 835(18) | 1097(14) | 109(5) |
| F2B | 1936(19) | 1048(19) | 1300(20) | 127(6) |

**Table 3 Anisotropic Displacement Parameters ($Å^2×10^3$) for mac190012_fa. The Anisotropic displacement factor exponent takes the form: $-2\pi^2[h^2a^{*2}U_{11}+2hka^*b^*U_{12}+\ldots]$.**

| Atom | $U_{11}$ | $U_{22}$ | $U_{33}$ | $U_{23}$ | $U_{13}$ | $U_{12}$ |
|---|---|---|---|---|---|---|
| I1 | 38.41(17) | 42.36(19) | 36.89(17) | 16.20(12) | 10.45(11) | 16.57(12) |
| Cu1 | 63.4(6) | 41.0(5) | 49.9(6) | 18.8(5) | 21.9(5) | 12.5(5) |
| F1A | 119(9) | 65(4) | 66(6) | 15(3) | 1(5) | 17(4) |
| F2A | 77(3) | 89(5) | 93(5) | 30(4) | -17(3) | 23(3) |
| F3A | 137(6) | 72(4) | 52(3) | 34(3) | -11(4) | -3(4) |
| O0AA | 58(2) | 56(2) | 35.8(16) | 15.9(15) | 8.0(14) | 11.3(16) |
| O1 | 101(3) | 45.0(19) | 53(2) | 24.8(17) | 29(2) | 27.3(19) |
| O2 | 66(2) | 40.2(18) | 55(2) | 21.7(16) | 8.5(17) | 5.8(16) |
| O3 | 73(2) | 47(2) | 73(3) | 16.3(18) | 41(2) | 7.6(17) |
| O4 | 55(2) | 40.0(17) | 55(2) | 19.1(15) | 17.9(16) | 14.7(15) |
| C1 | 35(2) | 41(2) | 35(2) | 18.8(18) | 12.6(16) | 18.2(17) |
| C2 | 35(2) | 44(2) | 39(2) | 22.3(18) | 15.0(17) | 19.7(18) |
| C3 | 32(2) | 46(2) | 45(2) | 22.0(19) | 12.5(17) | 15.0(18) |
| C4 | 44(2) | 45(2) | 36(2) | 16.8(18) | 13.1(17) | 18.9(19) |
| C5 | 48(2) | 47(2) | 37(2) | 21.8(19) | 16.9(18) | 19.2(19) |
| C6 | 42(2) | 37(2) | 43(2) | 20.0(18) | 18.0(18) | 18.8(18) |
| C7 | 37(2) | 63(3) | 44(2) | 29(2) | 13.8(19) | 12(2) |
| C8 | 49(3) | 54(3) | 47(3) | 10(2) | 6(2) | 13(2) |
| C9 | 50(3) | 48(3) | 50(3) | 25(2) | 21(2) | 12(2) |
| C10 | 33(2) | 46(2) | 35(2) | 24.3(18) | 10.2(16) | 13.9(17) |
| C11 | 39(2) | 49(3) | 37(2) | 23(2) | 10.0(17) | 8.2(18) |
| C12 | 30(2) | 69(3) | 44(2) | 32(2) | 9.6(18) | 9(2) |
| C13 | 41(2) | 65(3) | 54(3) | 39(2) | 19(2) | 25(2) |
| C14 | 47(2) | 49(3) | 58(3) | 33(2) | 21(2) | 23(2) |
| C15 | 37(2) | 45(2) | 48(2) | 28(2) | 15.0(19) | 13.1(18) |
| C16 | 49(3) | 42(2) | 52(2) | 23(2) | 18(2) | 8(2) |
| C17 | 102(4) | 56(3) | 58(3) | 22(2) | -3(3) | 10(3) |
| C18 | 45(2) | 40(2) | 42(2) | 19.9(19) | 12.2(18) | 11.9(18) |
| C19 | 78(3) | 47(3) | 78(3) | 22(2) | 45(3) | 16(2) |
| F4A | 116(7) | 44(3) | 133(7) | 25(4) | 91(6) | 29(3) |
| F5A | 76(4) | 109(7) | 145(9) | 13(6) | 58(4) | -8(5) |
| F6A | 196(9) | 123(7) | 84(4) | 55(5) | 81(5) | 82(7) |
| F4B | 106(8) | 94(8) | 144(10) | 54(7) | 66(7) | 52(7) |
| F5B | 114(8) | 47(4) | 137(11) | 35(5) | 98(8) | 20(5) |
| F6B | 112(8) | 117(9) | 80(5) | 3(5) | 51(5) | 2(7) |
| F1B | 72(8) | 60(5) | 47(7) | 11(4) | 7(6) | 0(5) |

| | | | | | | |
|---|---|---|---|---|---|---|
| F3B | 138(9) | 126(11) | 56(6) | 48(7) | 11(6) | -8(7) |
| F2B | 160(11) | 109(11) | 108(11) | 42(8) | -7(8) | 54(9) |

**Table 4 Bond Lengths for mac190012_fa.**

| Atom | Atom | Length/Å | Atom | Atom | Length/Å |
|---|---|---|---|---|---|
| I1 | C1 | 2.098(4) | C4 | C5 | 1.402(7) |
| I1 | C10 | 2.108(4) | C5 | C6 | 1.382(7) |
| Cu1 | O1 | 1.975(4) | C6 | C9 | 1.504(7) |
| Cu1 | $O1^{1}$ | 1.975(4) | C10 | C11 | 1.382(6) |
| Cu1 | $O3^{1}$ | 1.940(4) | C10 | C15 | 1.376(7) |
| Cu1 | O3 | 1.940(4) | C11 | C12 | 1.392(7) |
| F1A | C17 | 1.296(10) | C12 | C13 | 1.369(8) |
| F2A | C17 | 1.432(8) | C13 | C14 | 1.381(7) |
| F3A | C17 | 1.300(8) | C14 | C15 | 1.386(6) |
| O0AA | C4 | 1.356(6) | C16 | C17 | 1.527(8) |
| O0AA | C8 | 1.425(6) | C17 | F1B | 1.334(12) |
| O1 | C16 | 1.257(6) | C17 | F3B | 1.402(11) |
| O2 | C16 | 1.216(6) | C17 | F2B | 1.294(11) |
| O3 | C18 | 1.264(6) | C18 | C19 | 1.520(7) |
| O4 | C18 | 1.217(6) | C19 | F4A | 1.268(7) |
| C1 | C2 | 1.393(6) | C19 | F5A | 1.290(9) |
| C1 | C6 | 1.402(6) | C19 | F6A | 1.348(9) |
| C2 | C3 | 1.393(6) | C19 | F4B | 1.356(10) |
| C2 | C7 | 1.503(6) | C19 | F5B | 1.278(10) |
| C3 | C4 | 1.376(7) | C19 | F6B | 1.293(10) |

**Table 5 Bond Angles for mac190012_fa.**

| Atom | Atom | Atom | Angle/° | Atom | Atom | Atom | Angle/° |
|---|---|---|---|---|---|---|---|
| C1 | I1 | C10 | 96.74(16) | C10 | C15 | C14 | 117.6(4) |
| O1[1] | Cu1 | O1 | 180.0 | O1 | C16 | C17 | 115.1(5) |
| O3[1] | Cu1 | O1[1] | 89.51(18) | O2 | C16 | O1 | 129.6(5) |
| O3 | Cu1 | O1[1] | 90.49(18) | O2 | C16 | C17 | 115.3(5) |
| O3 | Cu1 | O1 | 89.51(18) | F1A | C17 | F2A | 104.4(8) |
| O3[1] | Cu1 | O1 | 90.49(18) | F1A | C17 | F3A | 111.4(9) |
| O3 | Cu1 | O3[1] | 180.0 | F1A | C17 | C16 | 117.5(10) |
| C4 | O0AA | C8 | 117.2(4) | F2A | C17 | C16 | 104.2(5) |
| C16 | O1 | Cu1 | 118.9(3) | F3A | C17 | F2A | 101.9(6) |
| C18 | O3 | Cu1 | 120.0(3) | F3A | C17 | C16 | 115.3(5) |
| C2 | C1 | I1 | 117.1(3) | F1B | C17 | C16 | 112.2(15) |
| C2 | C1 | C6 | 124.0(4) | F1B | C17 | F3B | 101.8(10) |
| C6 | C1 | I1 | 118.8(3) | F3B | C17 | C16 | 103.5(8) |
| C1 | C2 | C3 | 116.9(4) | F2B | C17 | C16 | 122.4(11) |
| C1 | C2 | C7 | 123.7(4) | F2B | C17 | F1B | 109.8(12) |
| C3 | C2 | C7 | 119.4(4) | F2B | C17 | F3B | 104.6(10) |
| C4 | C3 | C2 | 121.1(4) | O3 | C18 | C19 | 111.9(4) |
| O0AA | C4 | C3 | 124.5(4) | O4 | C18 | O3 | 129.9(5) |
| O0AA | C4 | C5 | 115.2(4) | O4 | C18 | C19 | 118.1(4) |
| C3 | C4 | C5 | 120.3(4) | F4A | C19 | C18 | 115.9(5) |
| C6 | C5 | C4 | 121.1(4) | F4A | C19 | F5A | 111.5(8) |
| C1 | C6 | C9 | 123.2(4) | F4A | C19 | F6A | 102.3(7) |
| C5 | C6 | C1 | 116.6(4) | F5A | C19 | C18 | 112.7(8) |
| C5 | C6 | C9 | 120.2(4) | F5A | C19 | F6A | 105.2(8) |
| C11 | C10 | I1 | 119.4(3) | F6A | C19 | C18 | 108.1(6) |
| C15 | C10 | I1 | 117.3(3) | F4B | C19 | C18 | 108.1(8) |
| C15 | C10 | C11 | 123.3(4) | F5B | C19 | C18 | 115.8(8) |
| C10 | C11 | C12 | 117.4(5) | F5B | C19 | F4B | 106.9(9) |
| C13 | C12 | C11 | 120.6(4) | F5B | C19 | F6B | 105.4(9) |
| C12 | C13 | C14 | 120.5(4) | F6B | C19 | C18 | 116.9(7) |
| C13 | C14 | C15 | 120.6(5) | F6B | C19 | F4B | 102.5(8) |

**Table 6 Hydrogen Atom Coordinates (Å×10$^4$) and Isotropic Displacement Parameters (Å$^2$×10$^3$) for mac190012_fa.**

| Atom | *x* | *y* | *z* | U(eq) |
|---|---|---|---|---|
| H3 | 9503 | 6763 | 9519 | 46 |
| H5 | 7129 | 4578 | 10962 | 49 |
| H7A | 8397 | 5023 | 6459 | 67 |
| H7B | 9066 | 6493 | 7380 | 67 |
| H7C | 7489 | 6106 | 6688 | 67 |
| H8A | 10130 | 8119 | 11627 | 78 |
| H8B | 11028 | 7032 | 11334 | 78 |
| H8C | 10906 | 7709 | 12733 | 78 |
| H9A | 4375 | 3282 | 8606 | 69 |
| H9B | 5198 | 2917 | 9722 | 69 |
| H9C | 5261 | 2185 | 8315 | 69 |
| H11 | 2387 | 2597 | 5667 | 48 |
| H12 | 559 | 3717 | 5746 | 54 |
| H13 | 993 | 6013 | 6427 | 56 |
| H14 | 3237 | 7246 | 7144 | 55 |
| H15 | 5087 | 6167 | 7063 | 47 |

**Table 7 Atomic Occupancy for mac190012_fa.**

| Atom | *Occupancy* | Atom | *Occupancy* | Atom | *Occupancy* |
|---|---|---|---|---|---|
| F1A | 0.6659 | F2A | 0.6659 | F3A | 0.6659 |
| F4A | 0.5952 | F5A | 0.5952 | F6A | 0.5952 |
| F4B | 0.4048 | F5B | 0.4048 | F6B | 0.4048 |
| F1B | 0.3341 | F3B | 0.3341 | F2B | 0.3341 |

**XRD of 2,6-dimethyl-4-methoxyphenyl(phenyl)iodonium triflate (144)**

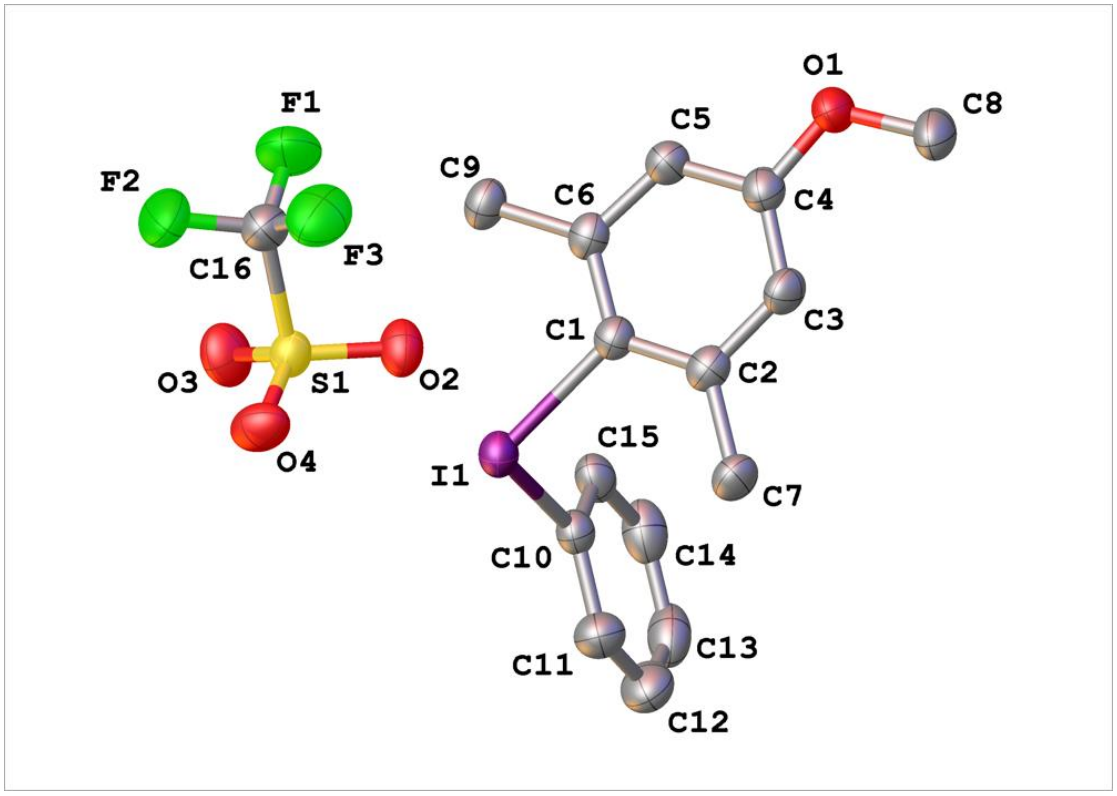

## Table 1 : Crystal data and structure refinement for mac190016_2_fa.

| | |
|---|---|
| Identification code | mac190016_2_fa |
| Empirical formula | $C_{16}H_{16}F_3IO_4S$ |
| Formula weight | 488.25 |
| Temperature/K | 150.0(2) |
| Crystal system | monoclinic |
| Space group | $P2_1/c$ |
| a/Å | 11.5339(3) |
| b/Å | 19.0051(4) |
| c/Å | 8.4730(3) |
| α/° | 90 |
| β/° | 96.622(3) |
| γ/° | 90 |
| Volume/Å$^3$ | 1844.91(8) |
| Z | 4 |
| $\rho_{calc}$g/cm$^3$ | 1.758 |
| μ/mm$^{-1}$ | 15.140 |
| F(000) | 960.0 |
| Crystal size/mm$^3$ | 0.4 × 0.15 × 0.02 |
| Radiation | CuKα (λ = 1.54184) |
| 2Θ range for data collection/° | 7.716 to 133.802 |
| Index ranges | $-13 \leq h \leq 13$, $-22 \leq k \leq 17$, $-10 \leq l \leq 9$ |
| Reflections collected | 13294 |
| Independent reflections | 3262 [$R_{int}$ = 0.0577, $R_{sigma}$ = 0.0462] |
| Data/restraints/parameters | 3262/183/229 |
| Goodness-of-fit on $F^2$ | 1.038 |
| Final R indexes [I>=2σ (I)] | $R_1$ = 0.0464, $wR_2$ = 0.1141 |
| Final R indexes [all data] | $R_1$ = 0.0618, $wR_2$ = 0.1265 |
| Largest diff. peak/hole / e Å$^{-3}$ | 2.27/-0.87 |

**Table 2 Fractional Atomic Coordinates ($\times 10^4$) and Equivalent Isotropic Displacement Parameters ($Å^2 \times 10^3$) for mac190016_2_fa. $U_{eq}$ is defined as 1/3 of of the trace of the orthogonalised $U_{IJ}$ tensor.**

| Atom | *x* | *y* | *z* | U(eq) |
|---|---|---|---|---|
| I1 | 5515.1(3) | 3962.4(2) | 2773.8(5) | 37.57(17) |
| S1 | 7066.5(13) | 4881.6(7) | 6403.2(18) | 36.5(3) |
| F1 | 9112(5) | 5308(3) | 5775(7) | 80.7(14) |
| F2 | 8647(4) | 5667(3) | 8008(7) | 81.4(15) |
| F3 | 9168(4) | 4594(3) | 7752(7) | 73.5(13) |
| O1 | 9747(4) | 2528(2) | 187(7) | 49.0(11) |
| O2 | 7200(4) | 4294(2) | 5360(6) | 48.1(11) |
| O3 | 6560(5) | 5507(3) | 5641(6) | 57.8(13) |
| O4 | 6620(4) | 4707(3) | 7852(6) | 54.8(12) |
| C1 | 6965(5) | 3453(3) | 1930(7) | 34.9(12) |
| C2 | 6977(5) | 2724(3) | 1932(7) | 37.1(13) |
| C3 | 7922(5) | 2398(3) | 1330(8) | 38.6(13) |
| C4 | 8793(5) | 2802(3) | 783(8) | 39.3(13) |
| C5 | 8750(5) | 3533(3) | 828(8) | 39.2(13) |
| C6 | 7838(5) | 3882(3) | 1430(7) | 34.4(12) |
| C7 | 6048(6) | 2263(3) | 2496(9) | 44.7(15) |
| C8 | 9819(6) | 1776(3) | 76(10) | 54.0(18) |
| C9 | 7833(6) | 4667(3) | 1502(8) | 41.8(14) |
| C10 | 4284(5) | 3689(3) | 823(8) | 35.8(12) |
| C11 | 3321(6) | 3309(4) | 1116(9) | 49.4(15) |
| C12 | 2499(6) | 3148(4) | -156(10) | 59.9(18) |
| C13 | 2656(7) | 3363(4) | -1650(10) | 58.4(17) |
| C14 | 3627(7) | 3746(4) | -1937(9) | 53.8(16) |
| C15 | 4469(6) | 3918(3) | -654(8) | 40.8(13) |
| C16 | 8583(6) | 5123(4) | 7013(9) | 50.2(15) |

**Table 3 Anisotropic Displacement Parameters ($Å^2×10^3$) for mac190016_2_fa. The Anisotropic displacement factor exponent takes the form: $-2\pi^2[h^2a^{*2}U_{11}+2hka^*b^*U_{12}+\ldots]$.**

| Atom | $U_{11}$ | $U_{22}$ | $U_{33}$ | $U_{23}$ | $U_{13}$ | $U_{12}$ |
|---|---|---|---|---|---|---|
| I1 | 38.0(2) | 32.0(2) | 42.9(3) | -6.76(15) | 5.52(16) | 0.92(14) |
| S1 | 41.4(7) | 30.9(7) | 37.6(8) | -1.8(6) | 5.9(6) | -1.1(6) |
| F1 | 71(3) | 70(3) | 109(4) | -1(3) | 47(3) | -17(2) |
| F2 | 58(3) | 70(3) | 116(4) | -45(3) | 10(3) | -15(2) |
| F3 | 52(2) | 66(3) | 98(3) | 3(2) | -12(2) | 5(2) |
| O1 | 39(2) | 36(2) | 74(3) | -11(2) | 17(2) | 0.4(17) |
| O2 | 52(2) | 42(2) | 48(3) | -12(2) | -2(2) | 6(2) |
| O3 | 67(3) | 44(2) | 63(3) | 5(2) | 9(2) | 17(2) |
| O4 | 56(3) | 64(3) | 46(3) | -1(2) | 14(2) | -17(2) |
| C1 | 35(3) | 31(2) | 39(3) | -4(2) | 4(2) | -1(2) |
| C2 | 39(3) | 33(3) | 38(3) | -1(2) | 2(2) | -4(2) |
| C3 | 40(3) | 25(3) | 50(4) | 0(2) | 5(2) | -1(2) |
| C4 | 34(3) | 36(3) | 48(3) | -6(2) | 4(2) | 1(2) |
| C5 | 39(3) | 34(3) | 46(3) | -2(2) | 9(3) | -3(2) |
| C6 | 40(3) | 30(3) | 32(3) | -2(2) | 2(2) | -1(2) |
| C7 | 48(3) | 33(3) | 55(4) | -1(3) | 13(3) | -7(3) |
| C8 | 43(3) | 38(3) | 80(5) | -16(3) | 8(3) | 3(3) |
| C9 | 51(3) | 29(3) | 45(4) | -3(2) | 5(3) | -3(2) |
| C10 | 35(3) | 31(3) | 42(3) | -6(2) | 6(2) | 3(2) |
| C11 | 42(3) | 48(4) | 59(4) | -5(3) | 10(3) | -6(3) |
| C12 | 43(3) | 59(4) | 76(4) | -19(3) | 1(3) | -7(3) |
| C13 | 54(4) | 49(4) | 68(4) | -23(3) | -9(3) | 10(3) |
| C14 | 64(4) | 47(4) | 48(4) | -8(3) | -1(3) | 15(3) |
| C15 | 44(3) | 33(3) | 47(3) | -3(2) | 12(2) | 6(2) |
| C16 | 45(3) | 42(3) | 66(4) | -8(3) | 14(3) | -5(2) |

**Table 4 Bond Lengths for mac190016_2_fa.**

| Atom | Atom | Length/Å | Atom | Atom | Length/Å |
|---|---|---|---|---|---|
| I1 | C1 | 2.127(6) | C2 | C3 | 1.400(9) |
| I1 | C10 | 2.116(6) | C2 | C7 | 1.503(9) |
| S1 | O2 | 1.443(5) | C3 | C4 | 1.386(9) |
| S1 | O3 | 1.444(5) | C4 | C5 | 1.391(9) |
| S1 | O4 | 1.425(5) | C5 | C6 | 1.389(9) |
| S1 | C16 | 1.825(7) | C6 | C9 | 1.493(8) |
| F1 | C16 | 1.321(9) | C10 | C11 | 1.371(9) |
| F2 | C16 | 1.330(8) | C10 | C15 | 1.366(9) |
| F3 | C16 | 1.326(9) | C11 | C12 | 1.385(11) |
| O1 | C4 | 1.366(8) | C12 | C13 | 1.362(12) |
| O1 | C8 | 1.437(8) | C13 | C14 | 1.381(12) |
| C1 | C2 | 1.386(8) | C14 | C15 | 1.409(11) |
| C1 | C6 | 1.398(9) | | | |

**Table 5 Bond Angles for mac190016_2_fa.**

| Atom | Atom | Atom | Angle/° | Atom | Atom | Atom | Angle/° |
|---|---|---|---|---|---|---|---|
| C10 | I1 | C1 | 96.2(2) | C6 | C5 | C4 | 121.2(6) |
| O2 | S1 | O3 | 115.4(3) | C1 | C6 | C9 | 124.3(6) |
| O2 | S1 | C16 | 101.6(3) | C5 | C6 | C1 | 115.8(5) |
| O3 | S1 | C16 | 104.2(3) | C5 | C6 | C9 | 119.9(6) |
| O4 | S1 | O2 | 115.0(3) | C11 | C10 | I1 | 118.2(5) |
| O4 | S1 | O3 | 114.2(3) | C15 | C10 | I1 | 118.4(5) |
| O4 | S1 | C16 | 104.2(3) | C15 | C10 | C11 | 123.3(6) |
| C4 | O1 | C8 | 117.3(5) | C10 | C11 | C12 | 118.2(7) |
| C2 | C1 | I1 | 117.6(4) | C13 | C12 | C11 | 120.3(7) |
| C2 | C1 | C6 | 125.2(6) | C12 | C13 | C14 | 121.3(7) |
| C6 | C1 | I1 | 117.2(4) | C13 | C14 | C15 | 119.2(7) |
| C1 | C2 | C3 | 116.7(5) | C10 | C15 | C14 | 117.8(7) |
| C1 | C2 | C7 | 125.1(6) | F1 | C16 | S1 | 110.9(5) |
| C3 | C2 | C7 | 118.1(5) | F1 | C16 | F2 | 107.5(6) |
| C4 | C3 | C2 | 120.1(5) | F1 | C16 | F3 | 108.7(6) |
| O1 | C4 | C3 | 123.9(6) | F2 | C16 | S1 | 110.9(5) |
| O1 | C4 | C5 | 115.1(6) | F3 | C16 | S1 | 111.2(5) |
| C3 | C4 | C5 | 121.0(6) | F3 | C16 | F2 | 107.6(6) |

**Table 6 Hydrogen Atom Coordinates (Å×10$^4$) and Isotropic Displacement Parameters (Å$^2$×10$^3$) for mac190016_2_fa.**

| Atom | *x* | *y* | *z* | U(eq) |
|---|---|---|---|---|
| H3 | 7966 | 1909 | 1298 | 46 |
| H5 | 9342 | 3793 | 448 | 47 |
| H7A | 5362 | 2279 | 1740 | 67 |
| H7B | 5863 | 2429 | 3507 | 67 |
| H7C | 6328 | 1788 | 2601 | 67 |
| H8A | 9157 | 1602 | -603 | 81 |
| H8B | 9824 | 1573 | 1115 | 81 |
| H8C | 10523 | 1648 | -357 | 81 |
| H9A | 8526 | 4846 | 1117 | 63 |
| H9B | 7811 | 4815 | 2582 | 63 |
| H9C | 7158 | 4844 | 855 | 63 |
| H11 | 3222 | 3164 | 2140 | 59 |
| H12 | 1837 | 2892 | 10 | 72 |
| H13 | 2099 | 3249 | -2494 | 70 |
| H14 | 3725 | 3889 | -2963 | 65 |
| H15 | 5129 | 4179 | -809 | 49 |